Scuola Internazionale Superiore di Studi Avanzati - Trieste

APPROACHES TO REGULATE NEURONAL NETWORK ACTIVITY OF HYPOGLOSSAL MOTONEURONS: nAChR AGONISTS AND RILUZOLE

Thesis submitted for the degree of "Doctor Philosophiae"

Candidate:
Dr. Nerijus Lamanauskas

Supervisor:
Prof. Andrea Nistri

SISSA - Via Beirut 2-4 - 34014 TRIESTE - ITALY

TABLE OF CONTENTS

NOTE

All work reported there comes solely from my own experiments and data analysis, unless otherwise stated. In particular, experiments concerning Western-blot technique were carried out by Dr. E. Fabbretti. Part of the data reported in the present thesis have been published in the following articles:

Quitadamo C, Fabbretti E, **Lamanauskas N** & Nistri A (2005) Activation and desensitization of neuronal nicotinic receptors modulate glutamatergic transmission on neonatal rat hypoglossal motoneurons. *Eur J Neurosci*, **22**, 2723- 2734.

Lamanauskas N & Nistri A (2006) Persistent rhythmic oscillations induced by nicotine on neonatal rat hypoglossal motoneurons in vitro. *Eur J Neurosci,* **24,** 2543-2556.

Lamanauskas N & Nistri A (2007) Riluzole blocks the persistent Na^+ current and modulates release of glutamate via PKC-dependent presynaptic NMDA receptors on neonatal rat hypoglossal motoneurons in vitro. Submitted.

ABSTRACT

Mammalian brainstem nuclei control vital functions of the body via the III-XII cranial nerves. The nucleus hypoglossus (XII nucleus) innervates the tongue musculature and, therefore, regulates several motor behaviors, including mastication, swallowing, sucking, and speech and is involved in respiration. These motor commands are generated by hypoglossal motoneuron (HM) network activity, which employs mainly glutamatergic neurotransmission. Neuronal network outputs are modulated by various factors, such as nicotinic acetylcholine receptors (nAChRs), persistent inward currents (PICs) and ambient levels of glutamate. To study the mechanism responsible for neuronal network changes induced by different drugs, I used an *in vitro* brain slice preparation from neonatal rat. I employed whole cell voltage- and current clamp recordings, nerve recording and immunohistochemical staining technique.

I found that nAChRs of XII nucleus are composed of α4, α7 and β2 subunits, which were abundantly expressed on HM somata and fibers. Presynaptic nAChRs upregulated GABAergic neurotransmission. The effect was calcium dependent. However, GABA responses of the motoneuron membrane were unchanged by nAChR activation. The nAChR agonist nicotine enhanced glutamatergic release at premotoneuronal network level. In 40 % of HMs, enhanced glutamatergic neurotransmission produced theta frequency oscillations. Nicotine-induced oscillations persisted for at least eight minutes and required sustained nAChR activation. They relied on network nAChRs, as motoneuron receptors desensitized quickly and were not involved in the oscillatory behaviour. Oscillations required both chemical and electrical transmission, since they were blocked by AMPA, mGluR1 and gap junction blockers. Synaptic inhibition and PICs were not essential for oscillatory behaviour. Oscillations made neuronal firing regular, since spikes appeared at the peak of each oscillation. Furthermore, XII nerve recording revealed that oscillations were not a local phenomenon, but were rhythmically transmitted from the XII nucleus to the effector muscles.

The neuroprotective drug riluzole depressed excitatory synaptic transmission in a frequency-dependent fashion. Riluzole also blocked the persistent sodium current (I_{NaP}), but the effect was not specific, since it also inhibited the persistent calcium current (I_{CaP}). The fast sodium current was unaffected by riluzole. Riluzole inhibited glutamatergic neurotransmission in the presence of TTX by interfering with the facilitatory role of presynaptic NMDA receptors. We propose that riluzole blocked PKC activity necessary to support presynaptic NMDA receptors.

These results outline various targets for pharmacological approaches to conditions like sleep apnea or dysphagia characterized by dysfunction of the nucleus hypoglossus.

LIST OF ABBREVIATIONS

ACh, acetylcholine;

AChE, acetylcholinesterase;

AD, Alzheimer's disease;

ADHD, Attention-deficit hyperactivity disorder;

AIDA, (RS)-1-Aminoindan-1,5-dicarboxylic acid;

ALS, Amyotrophic lateral sclerosis;

Amb, nucleus ambiguous;

AMPA, alpha-amino-3-hydroxy-5-methyl-4-isoxazolepropionic acid;

AP, action potential;

APV, D-amino-phosphonovaleriate;

β-AP, β-amyloid protein;

BK current, large conductance, calcium- and voltage-regulated calcium-activated potassium current;

CaMKII, Ca^{2+}–calmodulin-dependent protein kinase II;

CAT, choline acetyltransferase;

CC, current clamp;

Chel, chelerythrin;

CNS, central nervous system;

CNQX, 6-cyano-7-nitroquinoxaline-2,3-dione;

CTX, Gs proteins, sensitive to cholera toxin;

CV, coefficient of variation;

DA, dopamine;

DHβE, dihydro-β-erythroidine hydrobromide;

DRG, dorsal group of respiratory neurons;

DMRC,dorsal medullary reticular column;

DMX, dorsal motor nucleus of the vagus nerve;

EC, external cuneate nucleus;

EPSP, excitatory postsynaptic potential;

ER, endoplasmic reticulum;

E12, embryonic day 12;

F/I curve, plot of spike firing frequency versus injected current amplitude;

GABA, γ-aminobutyric acid;

Gr, gracile nucleus;

GTS-21, dimethoxy benzylidene anabaseine dihydrochloride;

HM, hypoglossal motoneuron;

I_{CaP}, persistent calcium current;

$I_{(CAN)}$, calcium-activated non-specific cation current;

ICP, inferior cerebellar peduncle;

I_h, hyperpolarization-activated inward current;

$I_{K(Ca)}$, calcium-activated potassium current;

$I_{K,leak}$, leak potassium current;

I_{NaP}, persistent sodium current;

IO, inferior olive;

$K_{(ATP)}$ channel, ATP activated ion channel;

Ki, knock-in;

Ko, knock-out;

LDH, lactate dehydrogenase;

LRN, lateral reticular nucleus;

nAChRs, nicotinic acetylcholine receptors

mAChR, muscarinic acetylcholine receptor;

mEPSP, miniature excitatory postsynaptic potential;

mGluR1, metabotropic glutamate subtype 1 receptor;

MLA, methyllycaconitine citrate;

MVe, medial vestibular nucleus;

NMDA, N-methyl-D-aspartate;

NTS, nucleus tractus solitarius;

py (or P), pyramidal tract;

PD, Parkinson's disease;

PIC, persistent inward current;

PKA, cAMP-dependent protein kinase A;

PKC, Ca^{2+}/ phospholipid-dependent protein kinase C;

preBotC, pre-Botzinger complex;

P0-P5, postnatal day 0-5;

QX- 314, N-(2.6-dimethylphenylcarbamoylmethyl) triethylammonium bromide;

R, correlation coefficient;

Riluzole, 2-amino-6-trifluoromethoxybenzothiazol;

Rin, cell input resistance;

RO, nucleus raphe obscurus;

sEPSP, spontaneous excitatory postsynaptic potential;

SpVe, spinal vestibular nucleus;

Sp5i, spinal trigeminal nucleus;

SK current, small conductance and voltage-independent calcium-activated potassium current;

SNV, spinal trigeminal nucleus

Sol, nucleus of the solitary tract;

stv, spinal tract of the trigeminal nucleus;

TM1-TM4, 1-4 transmembrane domains;

TTX, tetrodotoxin;

XII nucleus, hypoglossal nucleus;

VC, voltage clamp;

Vh, holding potential under voltage clamp mode;

Vj, liquid junction potential;

Vm, membrane potential under currentclamp mode;

VRG, ventral group of respiratory neurons;

5-HT_3, serotonin.

INTRODUCTION

1. Neuronal oscillations

1.1 Oscillation presence and function in the brain

The mammalian brain is a complex biological system, which in humans is estimated to contain about 10^{12} cells (neurons and glia cells) and from 10^{15} to 5 x 10^{15} synapses between neurons in the adulthood (Drachman, 2005). Anatomically and functionally interconnected neurons form neuronal networks, which exert a particular function in the brain. Although a neuronal network is based on the anatomical connections between the neurons, the participation of a neuron to the network is not fixed. On the other hand, even weakly coupled neurons could connect together due to internal and/ or external changes and fire synchronously to perform a particular function. Thus, besides the anatomical neuronal networks, functional neuronal networks exist (Faingold, 2004). The same neuron could belong to several functional neuronal networks, and the neuronal network could be composed of a set of local networks, where "local" means that axonal conductance delays can be ignored (Traub *et al.,* 2004). Further in the text I will use the term "neuronal network" referring to a local and functional neuronal network. At particular conditions, neuronal networks could generate oscillatory activity, which could also be recorded at single cell level. Oscillation is defined as a rapid, synchronous fluctuation in the membrane potential, which could be sub-threshold or above-threshold, and in the latter case it leads to synchronous spiking.

Oscillations are found in many parts of the brain, including preBotC in brainstem (Feldman Del Negro, 2006), cortex (Traub *et al.,* 1996), thalamus (Steriade & Timofeev, 2003), hypothalamus (Froy & Miskin, 2007), hippocampus (Buzsaki, 2002), inferior olivary complex (Llinas & Yarom, 1986; Long *et al.,* 2002), cerebellum (Soteropoulos & Baker, 2006), locus coeruleus (Ballantyne *et al.,* 2004), amygdale (Collins *et al.,* 2001), basal ganglia (Bevan *et al.,* 2002), external globus pallidus (Bevan *et al.,* 2002), ventral tegmental area (Shi, 2005), nucleus accumbens (Leung & Yim, 1993) and hypoglossal nucleus (Sharifullina *et al.,* 2005). Oscillations may differ in shape, frequency and synchrony, reflecting differences in neuronal signaling.

Oscillations could be observed *in vivo*, *in vitro* and in neuronal cultures, and, even their functional significance is open to question, they have been proposed to be important for many physiological and pathological functions. Oscillations control respiratory rhythm generation (Feldman & Del Negro, 2006) and mastication (Smith & Denny, 1990), regulate circadian

rhythms in mammals (Froy & Miskin, 2007), generate motor programs (Murthy & Fetz, 1996), exert locomotion in vertebrates (Grillner *et al.,* 1998), and are believed to be involved in higher cognitive functions, such as sensory processing in the olfactory system (Freeman, 1972; Laurent *et al.,* 1996), in sensory and perceptual binding (Gray *et al.,* 1989; Rodriguez *et al.,* 1999), in pattern recognition (Singer, 1999), in associative learning (Buzsaki, 2002; Miltner *et al.,* 1999), and in high cognitive and conscious processes (Llinas & Ribary, 1993). Excessive or uncontrolled oscillations produce pathological conditions, such as epilepsy (Grenier *et al.,* 2003; Traub *et al.,* 2001) or deadly bursting in the hypoglossal nucleus (Sharifullina *et al.,* 2005). It has also been proposed that oscillations provide a temporal framework, so that synchronization of them carries coded information (Singer & Gray, 1995).

1.2 Classification of neuronal oscillations

Neuronal network rhythmic activity was first recorded in the cortex with electroencephalogram (EEG) recordings in 1929 by H. Berger (Berger, 1929). Since then, five major types of rhythmic activity have been recognized in the brain: alpha, beta, gamma, delta and theta waves. Later on, more invasive recording techniques, such as single unit recordings with extracellular electrodes, intracellular recordings and local field potential recordings, revealed the presence of oscillations in other brain regions as well. Moreover, oscillations of other frequencies have been discovered. To date, the following types of oscillations are reported (Berger, 1929; Buzsaki, 2002; Traub *et al.,* 2004; Steriade, 2006):

Slow oscillations (0.5-1 Hz), recorded in all major types of neocortical neurons are made up by a prolonged depolarizing phase, followed by a long-lasting hyperpolarizing phase. They appear at the very onset of slow-wave sleep and disappear in wakefulness and REM sleep.

Delta oscillations (1-4 Hz) are found in stages 3 and 4 of sleep. They are also associated with very young brain and certain encephalopathies.

Theta oscillations (4-8 Hz) are present during REM sleep and can be seen during deep relaxed states, such as trances, hypnosis, meditation, deep day dreams, light sleep and the preconscious state just upon waking or before falling asleep. They are often associated with drowsiness and young age and can sometimes be produced by hyperventilation. These waves represent one of the most common oscillation types in the hippocampus of experimental animals and are present during diverse locomotor activities, described as "preparatory", "orienting" and "exploratory".

Alpha oscillations (Berger's wave) (8-12 Hz) are found during relaxed, alert state of consciousness when the subject keeps the eyes closed, but is still awake. The rhythm is most

evident in the occipital (visual) cortex and is thought to represent the activity of the visual cortex in an idle state. An alpha-like variation called "μ" is sometimes seen over the motor cortex (central scalp) during relaxed state, and attenuates with movement, or even with the intention to move.

Beta oscillations (12-30 Hz) usually are low in amplitude and have multiple and varying frequencies. They are associated with normal mental acitivity, active, busy or anxious thinking and active concentration. These rhythms are also found during various pathologies and drug effects.

Gamma oscillations (30-70 Hz) are involved in higher mental activity, such as perception, problem solving, fear and consciousness. Sometimes it is difficult to distinguish between beta and gamma oscillations, since neurons may pass from beta to gamma oscillations very rapidly (0.5-1 s) with slight depolarization. Therefore, these two types of oscillations could be grouped as beta/ gamma oscillations.

Very fast oscillations (VFO) (70-200 Hz) are generated in the axonal plexus via electrical coupling. They were discovered in hippocampal slices in 1998 (Draguhn *et al.,* 1998) and appear to drive persistent gamma oscillations. They represent an interesting phenomenon, since their frequency is not gated by a synaptic time constant or by a membrane kinetic time constant, as for other oscillations types. VFO frequency is determined by the axonal electrical coupling and by the topological properties of a sparsely connected network.

There are no absolute borderlines for the frequency ranges of each type of oscillations. "Pure" rhythms are generated in restricted neuronal circuits of simplified experimental preparations, while the living brain exposes a mixture of oscillations, superimposed on each other.

1.3 Methods of oscillation induction

Since many studies are done *in vitro,* knowing the experimental paradigms to induce oscillations helps one to focus on what system parameters might be relevant for the generation and structure of oscillations. The experimental paradigms in which *in vitro* oscillations have been studied are the following ones (Traub *et al.,* 2004):

1) Oscillations may occur spontaneously in normal artificial cerebrospinal fluid.

2) Oscillations may appear due to drug administration, applied either via bath solution or by puffer application. Drugs used for this purpose include activators of ionotropic and G-protein coupled receptors. In this paradigm, other types of receptors, both excitatory and inhibitory, could be pharmacologically blocked.

3) Oscillations may be produced by a repetitive electrical (tetanic) stimulation. Such stimulation activates neurons directly, which leads to neurotransmitter release. These neurotransmitters induce the oscillations after some delay, and oscillations are not locked to the electrical stimulation. The tetanic paradigm can be applied to two tissue sites at once and, thus, it is helpful for the study of oscillatory synchronization between two sites. Tetanic stimulation can also be combined with drug application.

4) Oscillations may arise as a result of altered ionic milieu, either by removing or adding certain ions, such as K^+. The paradigm is similar to a tetanic stimulation, because high K^+ solution depolarizes at least some neurons, which leads to the release of neurotransmitters.

1.4 Molecular mechanisms of oscillations

The neuronal mechanisms of oscillations are complex; they depend on both internal and external conditions, and on the state of a single neuron and the neuronal network. Computational studies showed that just eight voltage-dependent ion channel types could yield 1.8 million single-compartment model neurons with different discharge properties, including pacemaker activity (Prinz *et al.,* 2003). This is a simplified model, since the CNS contains a large diversity of ion channel types with different somatic and dendritic distribution on the same neuron (Ramirez *et al.,* 2004). Even neurons within a single anatomical category are not identical in their properties and possess different combinations of ion channels (Ramirez *et al.,* 2004). This heterogeneity is not only determined genetically. Activity- dependent and activity-independent mechanisms can regulate the ionic conductances by phosphorylation or dynamic modulation by intracellular Ca^{2+}(Ramirez *et al.,* 2004). Usually synaptic and cellular components act together to exert the common oscillatory pattern.

At cellular level, there is continuous interplay between inward (depolarizing) and outward (hyperpolarizing) currents. Typically, a neuron begins to show a rhythm with the activation of inward currents or the cessation of steady outward currents. The rhythm may be later terminated because of the inactivation of channels, responsible for the inward current, or the inward current activates calcium- or sodium-dependent potassium currents that hyperpolarize the membrane (Harris-Warrick, 2002). The next cycle can be initiated by activation of the I_h current, by voltage-independent intracellular signals, by the slow activation or inactivation properties of inward or outward currents or by other mechanisms (Harris-Warrick, 2002). There appear to be multiple ionic mechanisms in different systems to shape each phase of the

rhythmic motor pattern (Harris-Warrick, 2002). These intrinsic neuronal properties, contributing to oscillations, are the following ones:

1) The conditions for **spontaneous action potential generation**. For example, kainate can increase interneuron axon excitability in the hippocampus and could give rise to ectopic axonal spikes, which are important for the generation of VFO and certain gamma oscillations (Semyanov & Kullmann, 2001).

2) **Metabotropic receptors**, which can excite neurons by depolarizing them through blocking particular K^+ currents. For example, coincident activation of mGluRs and mAChRs can produce theta frequency oscillations in the hippocampal CA3 region (Cobb *et al.,* 2000). mGluR5 receptor activation on hypoglossal motoneurons can generate theta frequency oscillations (Sharifullina *et al.,* 2005).

3) The presence of **dendritic electrogenesis**. For instance, hippocampal pyramidal cell dendritic Ca^{2+} spikes contribute to one type of theta oscillations in vitro (Gillies *et al.,* 2002); Na^+ dendritic spikes may influence the gain of interneuron EPSPs and their tendency to fire doublets (Traub & Miles, 1995; Martina *et al.,* 2000).

4) The presence of **gap junctions** between neurons. Electrical synapses operate faster than chemical ones, and, therefore, can mediate reciprocal synchronous interactions between neurons (Gibson *et al.,* 1999; Bennett & Zukin, 2004). Electrical coupling is prominent between many types of neurons during the first week after birth and then the incidence of coupling gradually subsides (Peinado *et al.,* 1993). Synchronous activity of population of neurons is mediated by electrical coupling in many areas in the brain, including neocortex, hippocampus, inferior olive, locus coeruleus, retina, olfactory bulb, and neonatal rat spinal cord (Bennett & Zukin, 2004). Gap junctions are present between astrocytes, too (Altevogt & Paul, 2004; Schools *et al.,* 2006). Functional coupling is also present between locus coeruleus neurons and glia cells as spontaneous oscillations, generated by neurons, could be observed in a subset of glia cells (Alvarez-Maubecin *et al.,* 2000).

5) **Persistent sodium current** (I_{NaP}) can initiate and maintain tonic or burst firing and is responsible for burst generation in spinal motoneurons (Li & Bennett, 2003; Elbasiouny *et al.*, 2006; Theiss *et al.*, 2007; Zhong *et al.,* 2007), in the mammalian network of whisking rhythm generation (Cramer *et al.,* 2007) and in mouse neocortical networks (van Drongelen *et al.*, 2006), since its inhibition by riluzole disrupts rhythmic activity. I_{NaP} is, however, unnecessary for motoneuron bursting evoked by brainstem preBotzinger neurons (Pace *et al.*, 2007 a, b).

6) **Hyperpolarization-activated inward current** (I_h) activates and deactivates relatively slowly at subthreshold voltages, suggesting that it could contribute to the subthreshold inward currents that initiate tonic or burst firing. Thus, I_h acts as a depolarizing leak current, which could tonically depolarize the neurons, phase advancing the onset of firing and increasing spike frequency in the neonatal rat spinal cord and mammalian hindbrain. In the crustacean stomatogastric ganglion, the lateral pyloric neuron undergoes post-inhibitory rebound and produces oscillatory pattern. Dopamine and red pigment-concentrating hormone (Kiehn *et al.,* 2000; Butt *et al.,* 2002) phase-advance and increase neuron spiking by enhancing post-inhibitory rebound, which is driven by I_h.

7) **Calcium channels** depolarize neurons and carry calcium ions inside the cell. These processes control neurotransmitter release and activate intracellular signal cascades. Calcium imaging shows that virtually all rhythmically active motoneuron networks possess oscillations in intracellular calcium level (Harris-Warrick, 2002). Calcium mobilization into neurons may also facilitate oscillatory bursting in phasically firing cells (Leung & Yim, 1991; Li & Hatton, 1996).

Lamprey spinal motoneurons and interneurons contain all known types of Ca^{2+} channels, with N-type channels making the largest fraction (El Manira & Bussieres, 1997). Pharmacological tools show that the N-type calcium current plays a major role in shaping the lamprey spinal locomotor rhythm, while L-type contributes to the rhythm, and P/Q-type channels have no effect on it (Buschges *et al.,* 2000).

8) Study on thalamic neurons shows that neuronal T-type calcium channels can underlie membrane potential bistability, i.e. the existence of two resting membrane potentials (Williams *et al.,* 1997; Toth *et al.,* 1998). The current, generated by these channels, has been named **window current** ($I_{Twindow}$). Window current is the main mechanism for the expression of slow (<1 Hz) oscillations (Crunelli *et al.,* 2005).

9) **Calcium-activated potassium currents** ($I_{K(Ca)}$) are either small conductance and voltage-independent (SK currents) or large conductance and dually regulated by calcium and voltage (BK currents). Apamin sensitive SK currents are involved in lamprey spinal neurons and trigeminal motoneuron oscillations, since they regulate burst duration and spike frequency (Wikstrom & El Manira, 1998; Del Negro *et al.,* 1999).

10) **Calcium-activated non-specific cation current** ($I_{(CAN)}$) drives respiratory bursting in the preBötzinger complex of neonatal mice (Pace *et al.,* 2007, b). $I_{(CAN)}$ underlies robust

inspiratory drive potentials in preBötC neurons, and is fully evoked by ionotropic and metabotropic glutamatergic synaptic inputs.

11) **$K_{(ATP)}$ channels** are periodically activated in synchrony with each respiratory cycle in newborn mice brainstem (Haller *et al.,* 2001). The channel open probability reflects activity-dependent intracellular ATP fluctuations. Thus, by sensing metabotropic activity of the cell through changes in ATP concentration, channels periodically adjust neuronal excitability and continuously modulate central respiratory neurons (Haller *et al.,* 2001). Oscillations are paced by $K_{(ATP)}$ channels also on cerebellar granule cells (D'Angelo *et al.,* 2001), on thalamic neurons (Fuentealba *et al.,* 2004) and on hypoglossal motoneurons (Sharifullina *et al.,* 2005).

1.5 Synaptic mechanisms of oscillations

Besides intrinsic membrane properties of oscillating neurons, synaptic interactions also play a significant role in rhythmogenesis. Most experiments were done on mammalian locomotion and respiratory rhythms, since the rhythmicity is maintained even in a slice preparation, after their natural afferent inputs were removed. A principal kernel of respiratory drive is localized in the pre-Botzinger complex (preBotC) within the ventrolateral medulla, which contains all classes of respiratory neuron that are necessary for respiratory rhythm generation (Connelly *et al.,* 1992). The crucial role of the preBotC is demonstrated by the evidence that the rhythmic respiratory output from the brainstem disappears when the preBotC is deleted (Smith *et al.,* 1991). Several models of synaptic network organization have been proposed, which lead to a rhythmic activity. The models of respiration are summarized below.

1.5.1 Network model of respiratory rhythm generation

The network model of respiration was proposed by Ogilvie and co-authors (Ogilvie *et al.,* 1992). According to this model, the principal rhythm generating mechanism is reciprocal synaptic inhibition. It was first suggested by G. Brown (Brown, 1911) as the basis for spinal locomotor activity, where two groups of neurons are connected via synaptic inhibition and give rise to an alternating left and right stepping cycle in cats. A similar reciprocal inhibition was assumed to be responsible for swimming in Xenopus (Roberts & Tunstall, 1990), heartbeat in leaches (Peterson, 1983) and gill rhythm in tadpoles (Galante *et al.,* 1996). The model assumes that there are three phases of respiration: inspiratory, post-inspiratory and expiratory phases (Ogilvie *et al.,* 1992). All three phases are controlled by different type of neurons, inspiratory, post-inspiratory and expiratory ones, respectively. The network model does not consider

pacemaker neurons, instead the principal mechanism of the rhythm generation is assumed to be alternation between excitatory and inhibitory phases, produced by different classes of neuron (Fig. 1).

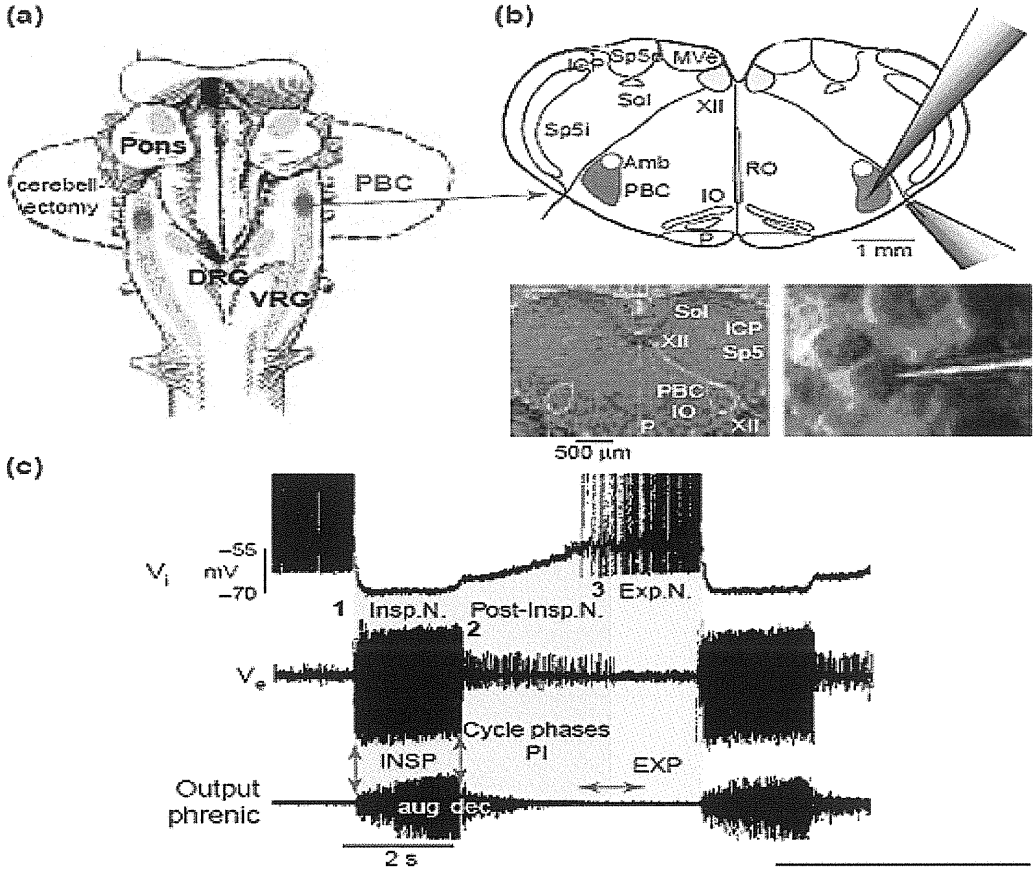

Fig. 1. Network model of respiratory rhythm generation with a three respiratory rhythm phases (a) Dorsal view of the brainstem, which contains different components of the respiratory network. Muscles, involved in respiration, are innervated by the dorsal and ventral groups of respiratory neurons (DRG, blue and VRG, orange). Only the VRG is essential for rhythm generation, where the preBotC (red) is located. The Kolliger-Fuse nucleus and the nucleus parabrachialis in the pons (blue) are involved in reflex regulation and shaping of respiratory activity patterns. (b) A scheme of *in vitro* recording from preBotC neurons (red) and from the rootlet of the hypoglossal nerve. Abbreviations: PBC, pre-Botzinger complex; Amb, nucleus ambiguus; XII, hypoglossal nucleus; RO, nucleus raphe obscurus; Sol, nucleus of the solitary tract; MVe, medial vestibular nucleus; SpVe, spinal vestibular nucleus; Sp5i, spinal trigeminal nucleus; ICP, inferior cerebellar peduncle; IO, inferior olive; P, pyramidal tract. (c) In the mature cat *in vivo*, medullary respiratory neurons show a three-phased respiratory rhythm. This is illustrated by a simultaneous triple-recording of the main populations of neurons. Two extracellular and one intracellular recordings show firing of an inspiratory neuron (1), post-inspiratory neuron (2) and expiratory neuron (3). The sequence of discharges is fixed and has an the following order: inspiration, post-inspiration and expiration. Whereas the transitions from expiration to inspiration and from inspiration to post-inspiration occur within a few milliseconds (vertical arrows), the transition from post-inspiration to expiration is quite variable (horizontal arrows). (From Richter & Spyer, 2001).

The network receives excitation from the reticular formation, and the inspiratory phase gives additional excitation through recurrent excitatory synaptic mechanisms (Ogilvie *et al.,* 1992). Synaptic inhibition between neurons sets the various stages of the respiratory rhythm. In particular, inspiratory neurons give rise to inhibition for expiratory neurons, which, therefore, discharge out of phase with respect to inspiration (Fig. 1). Post-inspiratory neurons receive an additional concurrent depolarization during inspiration and thus fire immediately following the cessation of inspiration (Fig. 1). The synaptic inhibition also regulates the excitability of glutamatergic connections and intrinsic membrane properties (Ramirez & Viemari, 2005). Thus, intrinsic voltage-regulated conductances are synaptically controlled and can only become effective during a short time window. Cellular bursting occurs only at the onset of the inspiratory and post-inspiratory phases and later activates antagonistic respiratory phases (Fig. 1). These processes have been successfully tested in computer simulations (Botros & Bruce, 1990; Ogilvie *et al.,* 1992).

However, blocking synaptic inhibition in mammalian respiratory system does not abolish rhythm generation itself, but it abolishes phase relationships between inspiration and expiration (Ramirez *et al.,* 1997; Shao & Feldman, 1997). In addition, it was demonstrated that synaptic inhibition exists not only between neurons that are rhythmically active out of phase, but also in phase with each other (Tian *et al.,* 1999). Similarly, inspiratory neurons receive synaptic inhibition concurrently during the inspiratory phase (Ramirez & Richter, 1996). Thus, mutual inhibitory connections may be involved in generating reciprocal activity or, alternatively, they may synchronize or modulate it. The above data show that synaptic inhibition, at least in some cases, is not necessarily involved in rhythm generation, compromising the basic network theory.

1.5.2 Pacemaker model of respiratory rhythm generation

Whether the neuron is a pacemaker or not is determined by the densities and dynamics of ion channels (Ramirez *et al.,* 2004). Although there are a few exceptions in which a single mammalian neuron can control a rhythmic behaviour (Brecht *et al.,* 2004), usually manipulation of a single pacemaker neuron does not alter rhythmic network activity (Ramirez *et al.,* 2004). Thus, a single neuron can only increase the probability of a network to oscillate, but a minimum number of pacemaker neurons have to burst during a specific time window to exert their action (Ramirez *et al.,* 2004). The number of pacemaker neurons also determines the

regularity of oscillations, since reducing the number of active pacemaker neuron result to an irregular rhythm (Pena & Ramirez, 2002). The role of pacemaker neurons in rhythm generation is not fixed and depends on changes in intrinsic bursting properties, inhibitory and excitatory synaptic inputs and their neuromodulatory state. Within a neuronal network, different pacemaker neurons may determine the onset of the subsequent activity state (Ramirez *et al.,* 2004). A neuron may contribute to the initiation of network activity during one cycle, but become a follower neuron in the next cycle. Therefore, neuronal networks with pacemaker neurons are plastic ones and are subject to intrinsic changes, synaptic changes and neuromodulation.

The pacemaker model of respiratory rhythm generation was developed on the basis that rhythmic discharges of respiratory neurons continue when all inhibitory synaptic transmission is blocked. Furthermore, cellular bursting was also observed when synaptic transmission was blocked by CNQX (Koshiya & Smith, 1999; Thoby-Brisson & Ramirez, 2001) or by lowering extracellular Ca^{2+} concentration (Onimaru *et al.,* 1995). The pacemaker theory postulates that a part of preBotC neurons express intrinsic bursting properties (these are called pacemaker neurons) and the remaining neurons do not have intrinsic bursting properties (these are called follower neurons) (Richter & Spyer, 2001). The respiratory rhythm originates principally from pacemaker cells, which synaptically transmit rhythmic activity to inspiratory-follower neurons and thus drive an inspiratory rhythm (Richter & Spyer, 2001). Between 5 % and 25% of neonatal rat preBotC neurons *in vitro* conditions are such pacemakers (Feldman & Del Negro, 2006). Presumed pacemaker neurons in neonatal rodents have a comparably low membrane potential of approximately –50 mV and their pacemaker properties depend on a persistent sodium current (I_{NaP}) (Richter & Spyer, 2001; Feldman & Del Negro, 2006, see Fig. 2). Another phenotype of pacemaker properties appears developmentally. Before postnatal day 4 (P4), there are less than 1 % of pacemaker neurons, and between P8 and P15 about 8 % of preBotC neurons become pacemaker ones (Pena *et al.,* 2004; Del Negro *et al.,* 2005). These pacemaker neurons are voltage-independent and their activity is suppressed by Cd^{2+} or by flufenamic acid, suggesting that bursting depends on calcium-activated nonspecific and voltage-insensitive current (I_{CAN}) (Pena *et al.,* 2004; Del Negro *et al.,* 2005). Thus, it appears that there are two types of pacemaker neuron in the preBotC.

However, presumed pacemaker cells, which are supposed to drive the rhythm, do not show any voltage control of burst frequencies (Onimaru *et al.,* 1995). Moreover, bath application of riluzole, an I_{NaP} blocker, does not suppress firing (Del Negro *et al.,* 2005). Maybe rhythm

generation depends on either or both types of pacemaker neuron? Co-application of riluzole and flufenamic acid silences the rhythm *in vitro* as well (Pena *et al.,* 2004; Del Negro *et al.,* 2005). However, these drugs hyperpolarize membrane potential and lower overall neuronal excitability, which could be the reason of the rhythm block. Indeed, AMPA or substance P can restart the rhythm after riluzole and flufenamic acid application (Del Negro *et al.,* 2005). These results challenge the obligatory rhythmogenic role of pacemaker neurons.

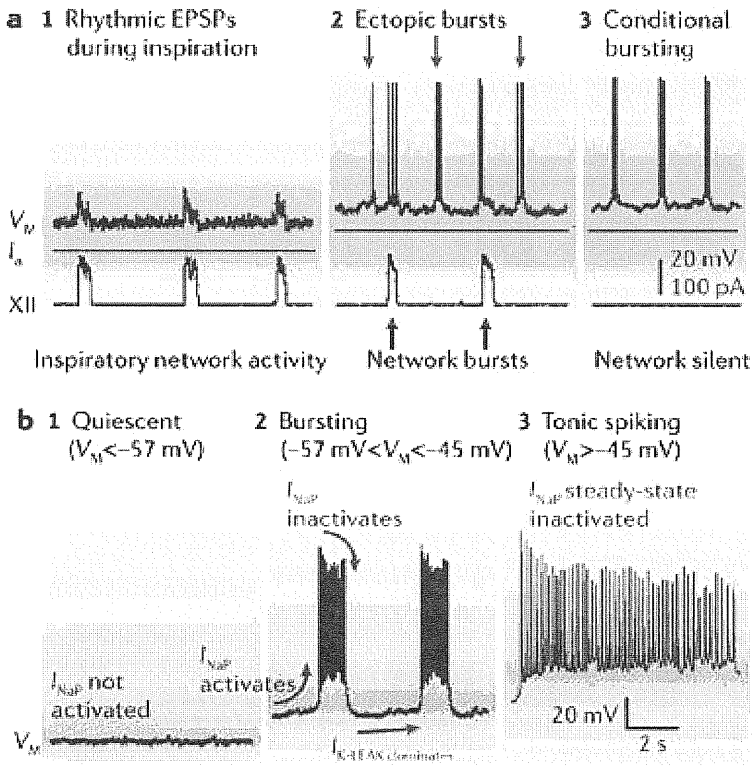

Fig. 2. Pacemaker model of respiratory rhythm generation. (a) Bursting-pacemaker neurons are capable of oscillating between spiking and quiescent phases, when synaptically isolated. PreBotC neurons exhibit EPSPs in phase with XII nerve motor output at baseline membrane potentials of –60 mV or below, but are otherwise silent (left panel). Tonic depolarization above –57 mV causes ectopic bursting during their normally silent period; the bursts are similar to those occurring during inspiration, which reflect an intrinsic burst-generating mechanism (central panel). Pacemaker neurons maintain voltage-dependent bursting in the range of –57 to –45 mV after synaptic isolation, when XII nerve does not produce motor output (right panel, bottom). Voltage-dependent bursting depends on I_{NaP} and $I_{K,leak}$. (b) Bursting is conditional because it depends on baseline membrane potential. Depolarizing the baseline membrane potential imposes steady-state inactivation that limits the amount of I_{NaP} available for subsequent bursts. By limiting I_{NaP}, baseline depolarization decreases burst duration and reduces the time needed for de-inactivation of I_{NaP} after a burst. Tonic inputs can also hyperpolarize the baseline to –57 mV or lower, which fails to activate I_{NaP} and the neuron remains quiescent (panel b1). Depolarization to –45 mV (or higher) steady state inactivates I_{NaP} to such an extent that burst cycles are no longer possible and the neuron spikes tonically (panel b3). (From Feldman & Del Negro, 2006).

1.5.3 Group-pacemaker model of respiratory rhythm generation

The group-pacemaker hypothesis of respiratory rhythm was proposed by Feldman and Del Negro and considers respiratory rhythm to be an emergent property. The rhythm is called emergent because individual agents interact following simple rules but none possesses a blueprint for the collective behaviour that results (Feldman & Del Negro, 2006). According to this hypothesis, the rhythm is a summative activity of recurrent synaptic connections and intrinsic membrane properties of individual neurons (Fig. 3). Thus, glutamatergic excitatory synapses between preBotC neurons depolarize neurons and initiate positive feedback through recurrent excitation. Depolarization activates I_{NaP}, I_{CAN} and voltage-gated Ca^{2+} channels, which serve to amplify the synaptic depolarization and then generate high-frequency spiking to form inspiratory potential. Metabotropic glutamate receptors also activate periodically during inspiration, which boosts I_{CAN} through intracellular Ca^{2+} release and might modulate channels (Feldman & Del Negro, 2006).

The preBotC neuronal network contains a small subset of pacemaker neurons which can be rhythmically active even when synaptically isolated. They participate in network activity but are not necessary for the rhythm.

Both glycinergic and GABAergic neurons contribute to controlling the membrane potential of preBotC neurons and participate in the formation of the respiratory pattern, but they are not essential *in vitro* as the rhythm persists after the removal of synaptic inhibition (Feldman & Del Negro, 2006). Instead burst termination is driven by outward currents, such as Ca^{2+}-dependent K^+ currents and electrogenic pumps (Fig. 3).

PreBotC neurons recover slowly from post-inspiratory hyperpolarization, and the recovery is dominated by subthreshold K^+ channels and tonic inputs. The new respiratory cycle begins with the most excitable neurons, which recover midway through expiration and begin spiking before the next inspiratory cycle (Fig. 8, part 2). Computer simulations show that early-onset spiking in a small fraction of neurons recruits other less excitable neurons to fire, and the process initiates a positive feedback that spreads rapidly until the majority of neurons are firing (Fig. 3, parts 3 and 4). However, the precise connectivity among respiratory neurons and the role of these connections in the rhythm orchestration remains to be determined.

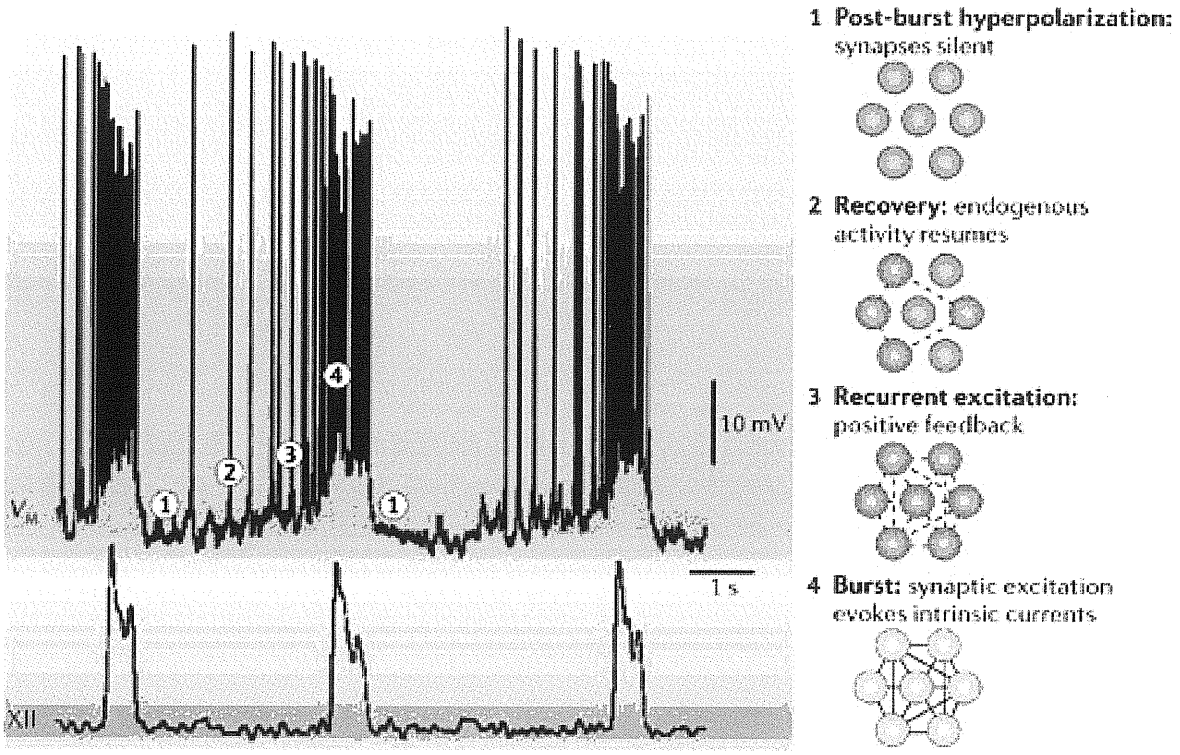

Fig. 3. Group-pacemaker model of respiratory rhythm generation. Top trace shows membrane potential of a rhythm-generating neuron and the bottom trace shows XII motor output, which represents network activity. Images to the right of the traces depict neuronal activity at different stages of the respiratory cycle. **1** is the refractory state that follows inspiration, in which activity dependent outward currents depress membrane potential, and excitatory synapses in the network are inactive. During epoch **2**, the most excitable neurons recover from post-burst hyperpolarization and begin to spike at a low rate. By **3** these highly excitable cells begin to synaptically activate other neurons, leading to aggregation of network activity itself due to recurrent synaptic excitation — a positive-feedback process. The inspiratory burst (**4**) ensues once a critical number of cells in the network are activated by recurrent excitation. In this final step, synaptic inputs recruit burst generating intrinsic currents such as I_{CAN} and I_{NaP}, which give rise to large inspiratory burst potentials with high-frequency spike activity. Inspiratory bursts terminate owing to intrinsic properties of cells that can reverse the positive feedback process, including Ca^{2+}-dependent K^+ currents and electrogenic pumps, which are recruited by cationic influx during inspiration. (From Feldman & Del Negro, 2006).

1.6 Modulation of oscillation by nAChRs

Both preclinical animal studies and a clinical study in volunteers have showed that α7 nAChR agonists enhance cognitive functions (Kitagawa *et al.*, 2003; Buccafusco *et al.*, 2005). GTS-21, an agonist of α7 nAChRs, produced statistically significant enhancement of three parameters of cognitive function, including attention, working memory and episodic secondary memory, compared to placebo (Kitagawa *et al.*, 2003). In experimental animals, nicotine or nAChR ligands improve both short- and long-term memory, and enhance cognitive performance (Buccafusco *et al.*, 2005). Some of the cellular effects of nAChR agonists overlap with the

cellular mechanisms of LTP, including long-lasting increases in intracellular concentrations of Ca^{2+}, activation of second-messenger systems and transcription factors, elevated levels of gene products and enhanced neurotransmitter release (Buccafusco *et al.*, 2005). In addition, nAChRs can exert their action by modulating brain oscillatory rhythms. However, the data on oscillation modulation by nAChR activation in different brain areas are conflicting.

Some studies have shown that nAChR activation could enhance rhythmic activity *in vitro* (Song *et al.*, 2005) and *in vivo* (Bringmann, 1997; Siok *et al.*, 2006). Nicotine reinforces the occipital theta rhythm in the pedunculopontine tegmental nucleus in rats (Bringmann, 1997). Administration of α7 nAChR agonists augments hippocampal theta oscillation induced by electrical stimulation of the brainstem reticular formation (Siok *et al.*, 2006). I*n vitro,* tetanic stimulation-induced gamma oscillations are also facilitated by activation of α7 nAChRs in rat hippocampal slices (Song *et al.*, 2005). In addition, α7 nAChR agonists enhance amphetamine-induced theta and gamma oscillations in both the hippocampal CA3 region and enthorinal cortex (Hajos *et al.*, 2005; Hoffmann *et al.*, 2005).

Other studies have reported nAChR activation to block oscillations. Theta oscillations in hippocampus have been blocked by nicotinic activation (Bland & Colom, 1988). In thalamic and cortical neurons network- and intrinsically-generated slow oscillations have been blocked by nAChR blockage as well (Steriade, 1993). In rat prefrontal cortex slices, oscillations are also reduced by nicotine (Mansvelder *et al.,* 2006). In rat EEG studies, nicotine decreases the power and frequency of both theta and delta waves (Ferger & Kuschinsky 1997). Nicotine administration *in vivo* suppresses the duration and frequency of HVS (bursts of 6–12 Hz oscillations lasting for approximately 0.5–3 s) in rodents (Radek, 1993; Riekkinen *et al.,* 1993). Human and rodent EEG recordings demonstrate that nAChR activation is able to change rhythm frequency, depressing one type of oscillation and selectively increasing a different one (Mansvelder *et al.,* 2006). Nicotine application induces an acceleration of synchronized cortical activity with an increase of the dominant frequency in the alpha band, while the power of theta and delta frequency bands decreases (Kadoya *et al.,* 1994; Lindgren *et al.,* 1999). However, other studies have indicated that nAChR activation has no effect on oscillations (Konopacki *et al.*, 1988; Konopacki & Golebiewski, 1992). Whether nicotine could induce network oscillations by itself is not settled (Mansvelder *et al.,* 2006). Several studies have reported that nicotine does not induce hippocampal oscillations recorded *in vitro* (Williams & Kauer 1997) or *in vivo* (Konopacki *et al.*, 1988). Thus, modulation of oscillation by nAChRs is unresolved yet and is open to question.

2. Nicotinic ACh receptors

2.1. Cholinergic system in the brain

Neurons, which synthesize, store and release the neurotransmitter acetylcholine (ACh), are called cholinergic neurons; an assembly of cholinergic neurons in the central and peripheral nervous system is called a cholinergic system.

Acetylcholine is an ester of acetic acid and choline with chemical formula $CH_3COOCH_2CH_2N^+(CH3)_3$. The systematic name is 2-acetoxy-N,N,N-trimethylethanaminium. It was first identified in 1914 by H.H. Dale for its actions on heart tissue. In 1921, it was confirmed as a neurotransmitter by the classical O. Loewi's experiments on the heart muscle cells of the frog. Loewi initially gave it the name *vagusstoff* because it was released from the vagus nerve. Dale and Loewi received the 1936 Nobel Prize in Physiology or Medicine for their work.

The cholinergic system is one of the most important and phylogenetically oldest nervous pathways. The brain cholinergic system is made up of a series of closely connected subsystems. A single cholinergic cell innervates its own discrete area, although many areas in the brain receive cholinergic inputs from several subsystems, and the cholinergic innervation is largely overlapping.

The major cholinergic subsystems are (see Fig. 4, Woolf, 1991; Gotti & Clementi, 2004):

1) **Magnocellular basal complex** (nucleus basalis) is the most significant group of cholinergic neurons, which provides the largest cortical and hippocampal inputs. These are large neurons (30-50 μm) that constitute 5-10 % of all of the neurons in the subsystem.

2) **Laterodorsal and peduculopontine tegmental nuclei** is the second most important cholinergic complex in the brain. They innervate deep cerebellar nuclei, tectum, medial habenula, thalamus, substantia nigra, pontine reticular formation, raphe nuclei, medullary reticular formation, vestibular nuclei and locus coeruleus.

3) **Striatum,** whose cholinergic fibres originate from the intrinsic cholinergic neurons within the caudate nucleus, putamen and nucleus accumbens, and do not project beyond the borders of the striatum. Cholinergic neurons constitute approximately 1 % of all striatal neurons.

4) **Lower brain stem**, whose cholinergic neurons from the brainstem reticular formation and the spinal intermediate grey matter innervate the superior colliculus, cerebellar nuclei and cortex.

5) Habenula-interpeduncular system. The habenula receives inputs from the thalamus and projects to the interpeduncular nucleus. Therefore, it is an important relay station through which the limbic system can influence the brainstem reticular formation.

6) Autonomic nervous system. The preganglionic neurons in both sympathetic and parasympathetic systems are cholinergic. The parasympathetic preganglionic cells, located in a number of nuclei in the encephalic trunk and segments S2-S4 in the spinal cord, project to (or near) target organs. The sympathetic preganglionic cells are located in the column of the mediolateral grey matter of the spinal cord extending from T1 to L3; they innervate paravertebral sympathetic ganglia.

Acetylcholine is synthesized in the cholinergic neurons from choline and acetyl-CoA by the enzyme choline acetyltransferase (CAT), which is found in the cytosol. Acetyl-CoA is synthesized primarily in mitochondria; choline is supplied by a high affinity active transport system from the extracellular space. After synthesis, ACh is packaged into synaptic vesicles together with ATP, where it is protected from degradation. Upon nerve activation, ACh is released by exocytosis and exerts its role. Soon after, ACh is degradated by extracellular and cytosolic acetylcholinesterases (AChEs) to choline and acetate. About half of the choline, which is transported into cholinergic axon terminals, comes from hydrolysis of ACh that has been released. Thus, the level to which ACh accumulates within the cell represents a steady state between ongoing synthesis and degradation. The 100-fold increase in the *net* synthesis of ACh during prolonged stimulation would require only twofold increase in the actual rate of ACh synthesis if intracellular degradation was blocked (Nicholls *et al.,* 1992). In the central nervous system, additional factors could influence the amount of ACh that accumulates within cholinergic nerve terminals; these factors include the supply of choline, acetyl-CoA and the activity of CAT (Tucek, 1978; Jope, 1979). On rapid release from the motor nerve ending, ACh reaches 0.1-1 mM concentration (Katz & Miledi, 1977).

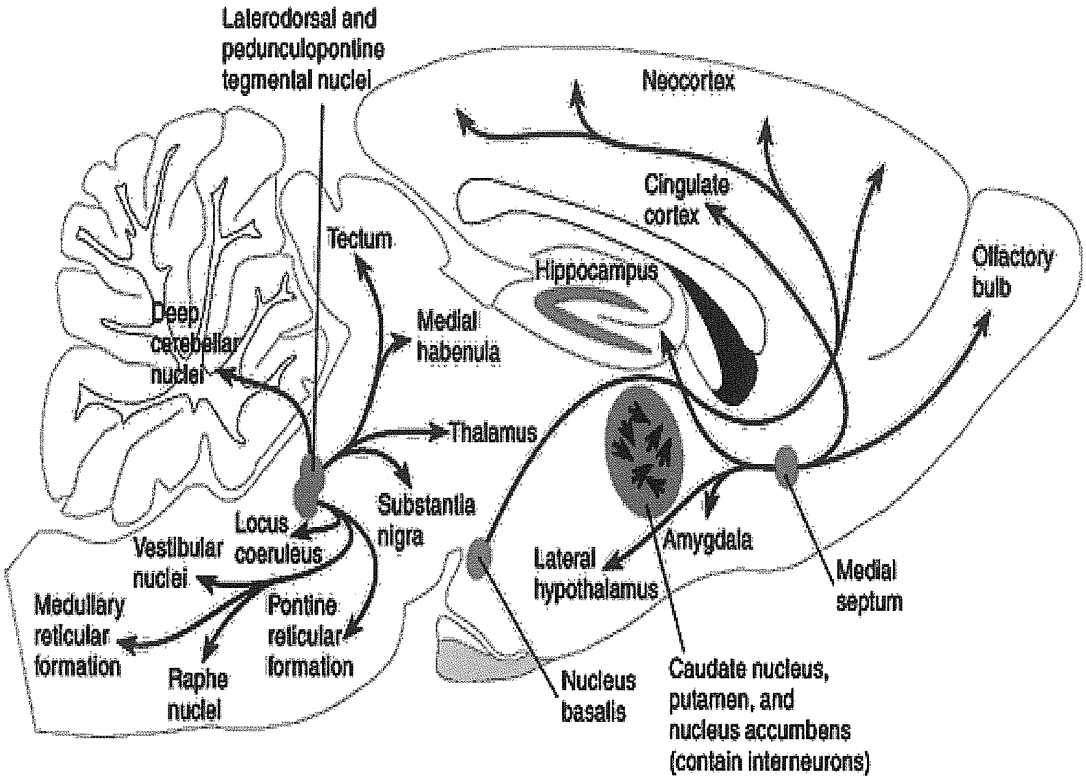

Fig. 4. Central cholinergic pathways in the brain. The main cholinergic subsystems are: magnocellular basal complex (nucleus basalis), which innervates cortex and hippocampus; laterodorsal and peduculopontine tegmental nuclei, which innervate deep cerebellar nuclei, tectum, medial habenula, thalamus, substantia nigra, pontine reticular formation, raphe nuclei, medullary reticular formation, vestibular nuclei and locus coeruleus; striatum, which intrinsic cholinergic neurons within caudate nucleus, putamen and nucleus accumbens make local connections; and Habenula-interpeduncular system, a cholinergic relay station between thalamus and the interpeduncular nucleus. The autonomic nervous system contains both the sympathetic and parasympathetic cholinergic preganglionic cells. Adapted from Woolf, 1991; Gotti & Clementi, 2004.

2.2 Nicotinic ACh receptor types

Since the discovery of ACh receptors, it was shown that cholinergic transmission in neuronal tissues could be pharmacologically separated in two groups: sensitive to nicotine and sensitive to muscarine. The observation led to the terms nicotinic acetylcholine receptors (nAChRs) and muscarinic acetylcholine receptors (mAChRs), respectively. These two classes of cholinergic receptor are members of two structurally and functionally unrelated receptor super-families: nAChRs are ligand gated ion channels, while mAChRs are G-protein coupled receptors, which exert their action via GTP-binding proteins. nAChRs are heterogenous and comprise muscle receptors, found at the skeletal neuromuscular junction, where they mediate neuromuscular transmission, and neuronal receptors, found throughout the central and peripheral nervous

system (Gotti & Clementi, 2004). However, this distinction between neuronal and non-neuronal subtypes does not always hold up, as neuronal receptors have been identified in a variety of non-neuronal tissues (Gotti and Clementi, 2004). Initial studies were made on nAChRs at the vertebrate neuromuscular junction and in the electrical eel (*Torpedo marmorata*) electrical organ, where nAChRs are abundantly expressed. For a long time, nAChR was a model of ligand gated ion channel. Neuronal nAChRs, which are less abundantly expressed, were investigated later. In this work, I will focus on neuronal nAChRs that are expressed in the central and peripheral nervous system.

2.3 nAChR genes and subunit composition

So far, twelve neuronal nAChRs genes have been cloned: nine α type (α2-α10) and three β type (β2-β4) (Sargent, 1993; Le Novere & Changeux, 1995; Lindstrom, 1997). nAChR chromosomal localization in humans is shown in Table 1.

Table 1. Chromosomal localisations of the genes coding for subunits of the human neuronal nAChRs. nAChR refers to the nicotinic acetylcholine receptor at the protein level; the genes coding for the human nAChR subunits follow the nomenclature CHRNA1-10 and CHRNB1-4. CHRNA6 has been cloned, but not localized; CHRNA8 is found only in avians. Data are taken from Anand & Lindstrom, 1992; Weiland *et al.*, 2000; Lustig & Peng, 2002; Lustig, 2006.

nAChR subunit	Chromosomal localization
CHRNA2	8p21
CHRNA3	15q24
CHRNA4	20q13.3
CHRNA5	15q24
CHRNA6	not localized
CHRNA7	15q14
CHRNA8	not present
CHRNA9	4p15.1
CHRNA10	11p15.5
CHRNB2	1q21.3
CHRNB3	8p11.22
CHRNB4	15q24

The neuronal nAChR subunits are called α according to their homology to muscle α1 subunit, when they have two adjacent cysteins at their N-terminal part (amino acid positions 192 and 193), which are thought to participate to the ACh binding site. Subunits lacking a pair of cysteins are termed β subunits (Le Novere & Changeux, 1995; Changeux & Edelstein, 1998). The diversity of nAChRs is further increased by the alternative splicing. For human nAChRs, alternative splicing was observed for CHRNA3, CHRNA4, CHRNA5 and CHRNA7 genes

(reviewed by Weiland *et al.,* 2000). nAChRs are highly conserved during evolution, and the same subunit has more than 80 % amino acid identity across vertebrate species (Le Novere & Changeux, 1995).

Neuronal nAChRs usually have pentameric structure, and can be either homomeric, composed of a single type of subunit, or heteromeric, composed of several subunit types (Fig. 5). Since minute amount of biological material rendered biochemical experiments difficult, the putative stoichiometry was derived from the assembly of converging information. First, the molecular weight of purified nAChR is always in the 300 kDa range, all subunits identified so far are less than 600 amino acid in length, and every subunit is expected to weight approximately 40-70 kDa (Lindstrom, 1997). Thus, nAChRs are expected to assemble from five subunits. Second, heteromeric nAChR activation is typically characterized by a Hill coefficient of about 1.5, which also suggests that nAChRs should have a stoichiometry of 2:3 (Sargent *et al.,* 1993). Third, homomeric α7 receptors display five binding sites for the competitive antagonist methyllicaconitine, and therefore must be pentameric (Palma *et al.,* 1996). Fourth, crystalline structure of the acetylcholine-binding protein isolated from snail further confirmed the pentameric organization of N-terminal domain (Brejc *et al.,* 2001).

The major brain nAChRs consist of heteromeric α4β2 subunits and homomeric α7 subunits (Lindstrom, 1997; Breese *et al.,* 1997), while main ganglionic receptors are composed of α3β4 subunits (Lindstrom, 1997). α7, α8 and α9 form functional homomeric receptors, α9 and α10 subunits can also compose heteromeric nAChRs, while the remaining subunits in the brain usually have a stoichiometry of $(\alpha)_2(\beta)_3$ (Itier & Bertrand, 2001; Lustig, 2006). It was shown that in heterologous expression systems α7 subunits can also co-assemble with β3 subunits (Palma *et al.*, 1996) or β2 subunits (Khiroug *et al.,* 2002). α2, α3 and α4 together with β2 and β4 can form functional nAChRs with distinct pharmacological kinetics; α5, α6 and β3 subunits are unable to form functional channels when expressed alone or in a combination with any other single subunit (Convoy & Berg, 1995; Le Novere *et al.*, 1996; Wang *et al.,* 1996). Therefore, α5, α6 and β3 subunits are so called "orphan" subunits, because natively they can form functional receptors only in combination with other α and β subunits. They are auxiliary subunits, that probably have a role in controlling either ion permeability, desensitization or receptor location. Thus, besides simple heteromeric subunits, nAChRs can be formed by multiple heteromeric subunits, expressed both natively and in heterologous expression systems (Wang *et al.,* 1996; Zwart & Vijverberg, 1998; Nelson *et al.*, 2003; Vailati *et al.,* 2003; Marritt *et al.,* 2005; Mao *et al.,* 2006).

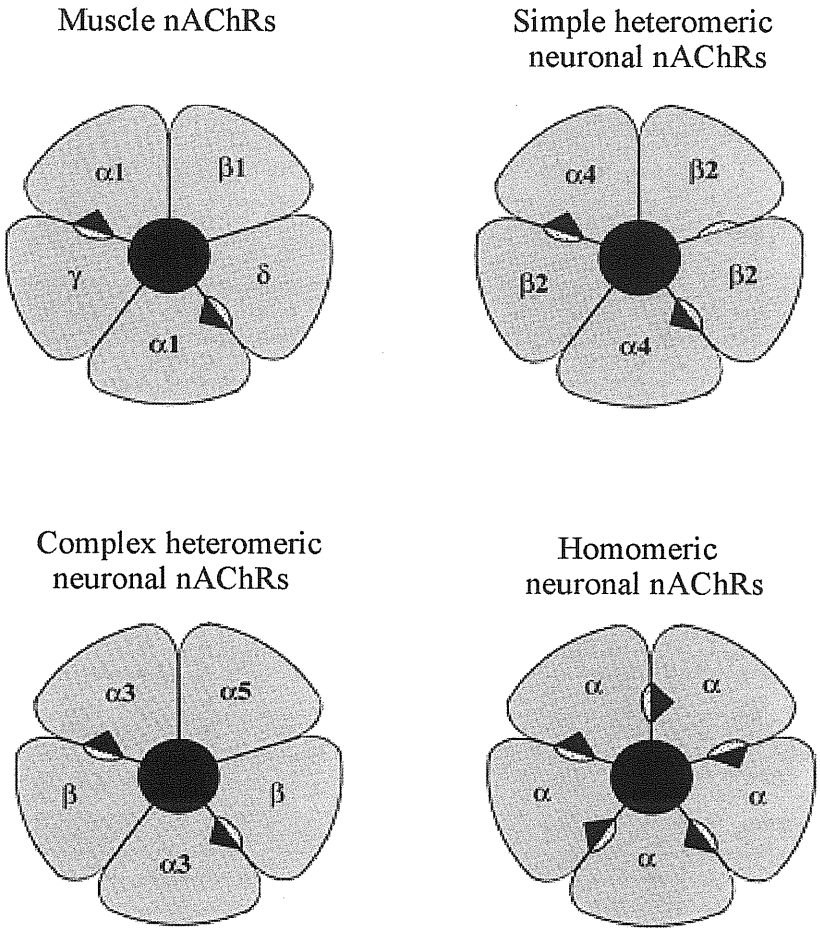

Fig. 5. Different classes of nAChRs: subunit stoichiometry and arrangement. Muscle nAChRs are composed of two α1, one β1, one γ and one γ subunits. Neuronal nAChRs are made up from either homomeric α7, α8, α9 subunits and simple or multiple heteromeric receptors, containing α and β subunits. Note that all nAChRs have a pentameric structure. Modified from Wang *et al.,* 1996.

2.4 nAChR molecular structure

nAChRs belong to the gene superfamily of ligand gated ion channels, which also includes $GABA_A$, $GABA_C$, glycine and serotonin ($5\text{-}HT_3$) receptors (reviewed by Le Novere & Changeux, 1995; Changeux & Edelstein, 1998). Each subunit is a protein, whose size ranges from 40 to 70 kDa and consists of four putative membrane-spanning domains (TM1, TM2, TM3 and TM4). Each domain is composed of hydrophobic amino acids that stabilize the domain within the hydrophobic lipid membrane. Every subunit has extracellular N- and C-terminal parts, a loop, linking TM2 with TM3, and intracellular loops, linking TM1 with TM2,

TM3 with TM4 (Fig. 6A). The N-terminal part presents glycosilation sites, while the intracellular loop between TM3 and TM4 presents phosphorylation sites (Fig. 6A).

Homomeric receptors have five identical binding sites per receptor molecule, whereas the heteromeric receptors, that contain two α subunits, have only two binding sites per receptor molecule. The ACh-binding sites reside in the extracellular domain and lie approximately 30 Å from the extracellular apex of the nAChR (Fig. 6B). When two molecules of ACh bind to the nAChR, the channel opens immediately (time constant about 20 μs) (Unwin, 1995).

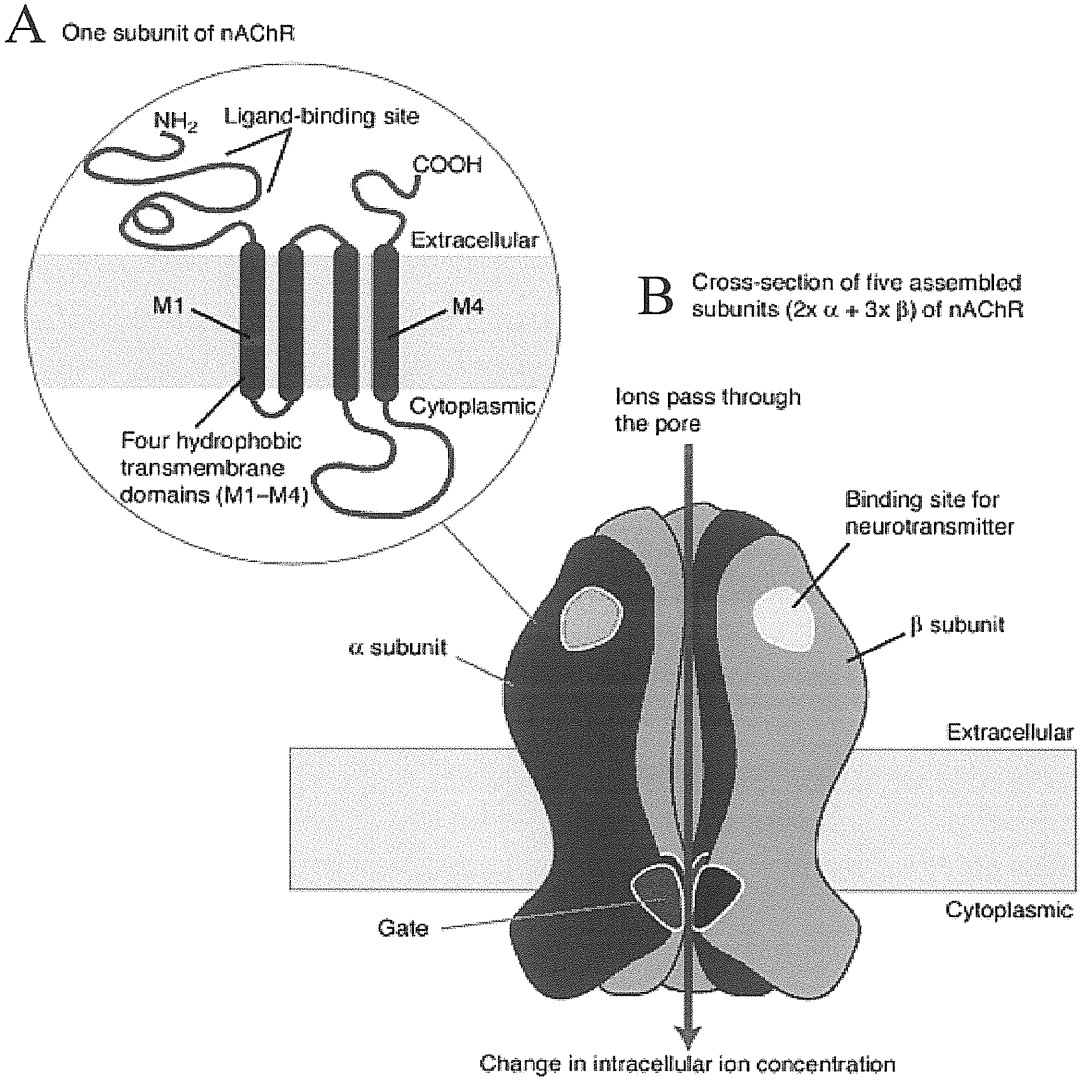

Fig. 6. Structure of neuronal nAChR and a single subunit. (A) A single subunit is composed of extracellular N- and C-termini and four transmembrane domains (TM1-TM4). Intracellular loop between TM3 and TM4 presents phosphorylation sites. (B) The most widespread nAChR type is composed of $(\alpha 4)_2(\beta 2)_3$ subunits, and has a central pore, gating region and two ACh binding sites at the contact between α and β subunits. Modified from Bate & Gardiner, 1999.

The nAChR channel has a pore of 9-10 Å in an open state, which contributes to the selectivity for particular ions (Unwin, 1995). The nAChRs are permeable to most cations, such as Na^+, K^+ and Ca^{2+}, although monovalent cations are preferred. The mechanism of selectivity is poor.
The nAChR conductance varies in the range from 5 pS to 35 pS, depending on the subunit composition (Papke *et al.,* 1989; Charnet *et al.,* 1992). The gating kinetics of nicotinic channels also depends on subunit composition. Nicotinic channels, composed of β2 and α2, α3 or α4 subunits, openings can be described by two exponential functions, with 0.1-0.5 ms and 2-7 ms, respectively (Papke *et al.,* 1989).

2.5 nAChR life cycle

nAChR subunits are initially synthesized in the endoplasmic reticulum (ER) as core-glycosylated high-mannose proteins (Fig. 7). From the ER they are moved to the Golgi complex, where, most probably, they form hetero-oligomers (Sallette *et al*., 2005; Ellgaard & Helenius, 2003). These processes generate a mixed population of pentameric oligomers and heterogeneous higher molecular weight oligomers, that probably correspond to either misfolded entities or small aggregates formed from immature subunits (Cooper & Millar, 1997). Misfolded proteins are degradated and, as a result, only pentameric nAChRs acquire complex carbohydrates that protect them against endohydrolases. Carbohydrated receptors exit from the Golgi complex and eventually reach the cell surface. The process takes around three hours (Smith *et al*, 1987; Sallette *et al.*, 2005). The most common posttranslational modification of nAChRs is phosphorylation, although the functional significance of it is not always evident. Muscle nAChRs are phosphorylated by at least three protein kinases: cAMP-dependent protein kinase A (PKA), Ca^{2+}/ phospholipid-dependent protein kinase C (PKC) and unidentified tyrosine kinase (Zigmond *et al.,* 1999). The exit from the ER to medial Golgi compartment is a relatively slow process as compared to the maturation steps. Maturation is nearly completed after 30 min, whereas trafficking and complex oligosaccharide glycosylation requires around 3 hours (Sallette *et al.*, 2005). Therefore, the exit from the ER is the limiting step within the secretory pathway, pointing to an accumulation of protein inside the cell, thus only a small part of nAChRs (around 15 %) is found at the cell surface (Arroyo-Jimenez et al., 1999; Harkness & Millar, 2002; Nashmi *et al.,* 2003; Grailhe *et al.,* 2004; Sallette *et al.*, 2005). nAChR maturation is an inefficient process, only about 30 % of the synthesized subunits eventually compose functional receptors (Merlie & Lindstrom, 1983; Arroyo-Jimenez *et al,* 1999; Morello *et al*, 2000; Christianson & Green, 2004; Sallette *et al.*, 2005). The half-life of

nAChR in the plasma membrane is estimated to be in the 10 h time range (Stollberg & Berg, 1987; Sallette *et al.*, 2005). Surface receptors are then internalized to the endosomal compartment and targeted to Lamp1 containing lysosomal compartments where they are degraded (Darsow *et al.*, 2005, Fig. 7).

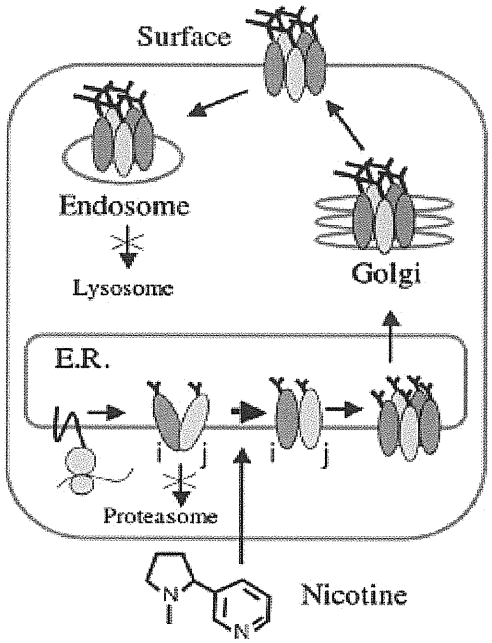

Fig. 7. Schematic representation of nAChR life cycle in the cell. Single subunits are synthesised in the ER, subunits mature and assemble into pentameric receptors; misfolded subunits being degraded by the ERAD machinery. Pentameric receptors are then relocated to the Golgi apparatus, where the sugars are trimmed, and exported to the cell surface. Surface receptors later are internalized into endosomes and eventually routed to lysosomes, where they are degradated. From Corringer *et al.*, 2006.

2.6 Neuronal nAChR expression during development and aging

During development of the rat, nAChRs could be detected as early as at embryonic day 12 (E12) (Tribollet *et al.*, 2004). Studies, performed on the developing brain, show that nAChRs gene expression is regulated developmentally and could be expressed transiently (Sargent, 1993). In the chicken optic lobe, β2 subtype expression occurs in a rostrocaudal gradient over the time when retinal afferents invade the tectum (Sargent, 1993). There is an increase in receptor heterogeneity and complexity in chick retina during the development that is also maintained in adulthood (Vailati *et al.*, 2003). nAChR expression depends both on innervation and on contact with the target tissue, both processes affect nAChR subtypes independently

(Sargent, 1993). Denervation also alters the number, distribution and size of nAChRs clusters (Sargent, 1993). In rat, nAChR expression is the highest during synapse formation. The level of mRNA for α7 increases from E13 until birth, after which it decreases during the first few days to adult expression level (Gotti & Clementi, 2004). nAChR expression depends on different brain structures: for example, in cortex and hippocampus, β2 is low at P7, but increases by P14; the expression of α4 is already high at P7 (Gotti & Clementi, 2004).

There were suggestions to correlate declined cognitive abilities in aged humans with decreased number of nAChRs. However, data show either no decrease, or only a moderate decrease in nAChRs expression during aging in humans or rats (Tribollet *et al.,* 2004). In rat, nAChR expression is slightly decreasing during aging, although with some regional specificity (Gotti & Clementi, 2004). For example, α4 mRNA decreases in the thalamus but not in the cortex; the decrease of α3 is more marked than α4 and is present in almost all brain zones (Gotti & Clementi, 2004). The fact that there is marked neurodegeneration in β2 Ko mice during aging indicates that β2 containing receptors are important for neuronal survival during aging (Gotti & Clementi, 2004).

2.7 nAChR distribution in the brain

nAChR distribution has been consistently investigated at both mRNA and protein level using *in situ* hybridization (for mRNA studies) or labeled nicotinic agents, immunohistochemistry, immunopurification and *in vivo* mapping using PET (for protein studies) (Gotti & Clementi, 2004). nAChRs are expressed in relatively low density, but their pattern of distribution is homogenous, not restricted to the brain cholinergic pathways. Often neurons express more than one type of nAChR subtype; in these cases, one class of subtypes dominates (Margiotta & Gurantz, 1989). Even neighboring neurons can have different subunit types and with different proportions (Poth *et al.,* 1997; Azam *et al.,* 2002; Marritt *et al.,* 2005). Within one neuron, the diverse nAChR subtypes are spatially segregated relative to each other and targeted to discrete synapse-associated sites (reviewed by Rosenberg *et al.,* 2002). Nicotinic receptors are mainly located in various cortical areas, the periacqueductal grey matter, the basal ganglia, the thalamus, the hippocampus, the cerebellum, and the retina (Gotti *et al.,* 1997) The α4 and β2 subunits, one of the most diffused receptor subtypes in the brain, are widely expressed throughout the brain and spinal cord, and the β2 subunit is also expressed in the autonomic ganglia (Picciotto *et al.,* 2001). The α3 and β4 subunits, which are critical for fast synaptic transmission in the autonomic nervous system, are present mostly in autonomic ganglia, but

also in pineal gland, the anteroventral nucleus of the thalamus, the subiculum of the hippocampus, the medial habenula, interpeduncular nucleus, spinal cord and retina (Picciotto *et al.*, 2001; Gotti & Clementi, 2004). They can be expressed with or without the α5 subunit. The mRNA encoding the α7 subunit is found throughout the brain, with particularly high levels in the hippocampus, cortex and very low or no expression in the thalamus (Picciotto *et al.*, 2001). The α6 containing receptors, very often in conjunction with the β3 subunit, are present in the optic pathway, the locus coeruleus and dopaminergic neurons of the mesostriatal pathways, where they control dopamine release (Picciotto *et al.*, 2001; Gotti & Clementi, 2004). The α8 subunit is found only in avians, not in mammals, and the α9/α10-containing receptors are expressed only extraneuronally, in cochlear hair cells of the inner hair, the pituitary pars tuberalis and the olfactory epithelium (Elgoyhen *et al.*, 1994; Millar, 2003; Gotti & Clementi, 2004). In summary, the brain nAChRs are chiefly composed of α4, α7 and β2 subunits, while the autonomic ganglia contain mostly α3, α5, β2 and β4 subunits (Fig. 8).

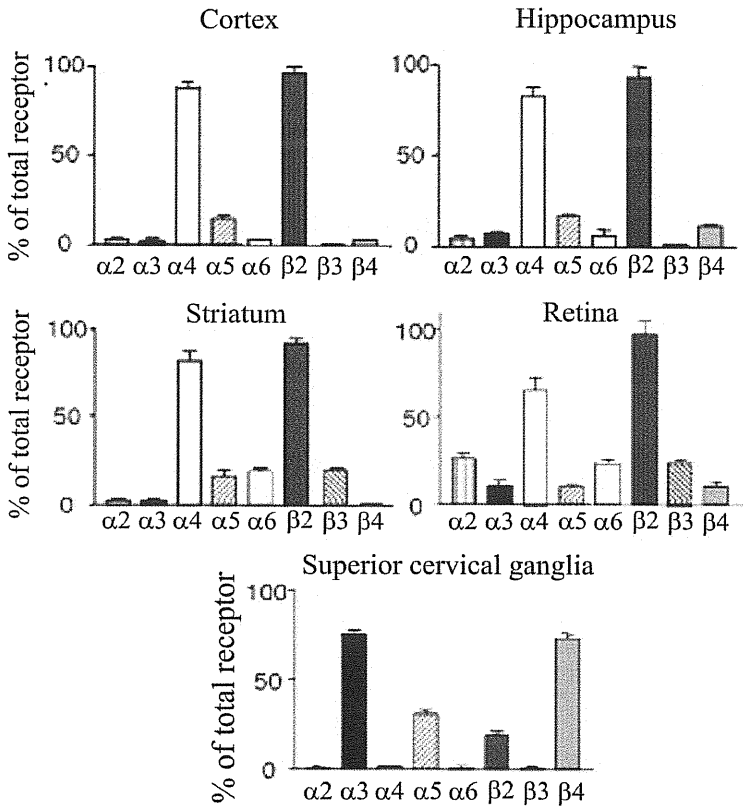

Fig. 8. The cerebral cortex contains mostly α4, α5, β2, and β4 subunits, which are unequally distributed among the different layers; the hippocampus contains α3, α4, α5, α7, β2, β3, and β4 subunits; the mesocorticolimbic system contains α2, α3, α4, α5, α6, α7, b2, b3, and b4 subunits; the auditory cortex contains α7 subunits; the optic lobe contains α2, α5, α7 and β2 subunits; and the retina contains α2, α3, α4, α6, α7, α8, β3, β4, and β2 subunits. α7 subunits are not shown there. (Modified from Gotti & Clementi, 2004).

2.8 nAChRs cellular localization and their function

Nicotinic transmission mediated by postsynaptic nAChRs occurs in autonomic ganglia, within the spinal cord at the motoneuron- Renshaw cell synapse and on cochlear hair cells (reviewed by Role & Berg, 1996). Within the brain, many neurons can generate fast inward nicotinic currents, but physiological studies show that fast synaptic transmission is not usually mediated by nAChRs (Role & Berg, 1996). Some exceptions are the nucleus ambiguous (Zhang *et al.,* 1993) and the dorsal motor nucleus of vagus, the medial vestibular nucleus and substantia nigra neurons (Clarke *et al.,* 1987; Ito *et al.,* 1989; Phelan & Gallagher, 1992), where nicotinic transmission has been documented. Also, direct nicotinic transmission has been observed in the developing visual cortex (Roerig *et al.,* 1997) and in GABAergic interneurons of the hippocampus (Alkondon *et al.,* 1998). The scarcity of nicotinic transmission may be partly due to the difficulties in studying central cholinergic synapses, which are widely diffuse. The cholinergic innervation is also diffuse and could be damaged upon brain slice preparation, which is a commonly used experimental model.

As a result, brain nAChRs are preferentially expressed presynaptically (Wonnacott, 1997; Gotti & Clementi, 2004), where they modulate neurotransmitter release. nAChRs can enhance spontaneous and evoked ACh, glutamate, noradrenalin, dopamine, GABA and serotonin release (reviewed by Role & Berg, 1996). A single neuron type can be modulated by as many as three nAChRs types (Alkondon & Albuquerque, 2004).

Nicotinic receptors can also modulate neurotransmitter release at peri-terminal locations. nAChRs activation may initiate Na^+ mediated axonal membrane depolarization, which in turn activates Ca^{2+} entry through voltage gated channels. The action is blocked by tetrodotoxin (Lena *et al.,* 1993). Moreover, strategically located nAChRs might enable activation of only specific portions of the cellular compartments.

Therefore, brain nAChRs seem to modulate, rather than mediate direct nicotinic transmission.

2.9 nAChR desensitization and upregulation

Desensitization is a transient loss of receptor biological response following prolonged or repetitive agonist application. Muscle nAChR desensitization was first described by Katz and Thesleff (1957). The onset of desensitization is time, agonist concentration and type, and nAChR subunit type dependent (Katz & Thesleff, 1957; Giniatullin *et al.,* 2005). The α7 containing receptors desensitize rapidly (in milliseconds), while non- α7 receptors desensitize slowly (in seconds) (Giniatullin *et al.,* 2005).

A complex relationship exists between agonist concentration and nAChR desensitization. Desensitization could be classified as "classical desensitization" and "high-affinity desensitization" (Giniatullin *et al.,* 2005). When medium to high (μM to mM) agonist concentration is applied, nAChRs are first activated and then desensitize with subsequent recovery after agonist removal. This is the "classical desensitization" that usually develops in tens of milliseconds. During the "high-affinity desensitization", low (nM) agonist concentrations can induce desensitization even without prior activation. It is a slow process, taking seconds to minutes, and is likely to be generated during chronic exposure of agonist. Both types of desensitization are nAChR subunit and agonist dependent. Desensitization is accompanied by an affinity shift and a structural change at the ACh binding sites (Fenster *et al.,* 1997).

Desensitization is a plastic process, rapidly adapting to changes in neuronal activity. It can be modulated by substance P, Ca^{2+}, phosphorylation and other factors (Giniatullin *et al.,* 2005). Desensitization, induced by low concentrations of nicotine, is variable among neurons: even two adjacent neurons in the same brain slice could be desensitized by a different degree (Wang & Sun, 2005).

The recovery from desensitization is also both nAChR subunit type and agonist dependent (Giniatullin *et al.,* 2005).

Another feature upon prolonged agonist exposure is nAChRs upregulation. This is in contrast with other receptor types, when prolonged agonist exposure decreases the number of receptors. Upregulation of nAChRs dependends on the length of agonist exposure and upon the nature of agonist itself (Peterson & Nordberg, 2000). The change in nAChR number seems to be both due to enhanced transcription level and due to post-transcriptional mechanisms, hitherto there is no consensus on the main mechanism of unregulation (reviewed by Wang & Sun, 2005). Agonist application could increase mRNA levels (Bencherif *et al.,* 1995; Garrido *et al.,* 2001) or could reduce turnover rate of already existing receptors (Wang *et al.,* 1998). Recently it was shown (Sallette *et al.,* 2005), that nicotine enhances nAChR maturation, which normally is an inefficient process.

As brain nAChRs enhance release of various neurotransmitters, desensitized receptors would change the amount of neurotransmitter released. Therefore, nAChR desensitization and upregulation could influence synaptic transmission at a single synapse and even at local neuronal circuits. Selective desensitization of one receptor subtype, when the other subtypes remain active, may play a significant role in changing the plasticity of particular brain

networks. Desensitization also plays a role in tobacco addiction and in mental disorders, where nAChRs are involved. Besides that, desensitized nAChRs facilitate muscarinic ACh receptors, increasing their affinity to agonists (Wang & Sun, 2004). Eventually, since nAChRs are found widely diffused and extrasynaptically, and there should be a range of concentrations over which low levels of agonist can continuously open nAChR channels, a role of nAChRs for non-synaptic transmission was proposed (Lester, 2004). nAChRs might detect ambient levels of ACh and may participate in an alternative form of chemical transmission— volume transmission.

2.10 nAChR role in normal brain function and mental disorders

The functional role of nAChRs could be determined by genetically engineered knock-out (Ko) or knock-in (Kin) animals. nAChRs are not essential for survival and execution of basic behaviours, but they are important for the fine control of sophisticated and complex behaviours, where they are tuning a particular function, rather that executing it. It was found that nicotinic transmission participates in many cognitive processes (reviewed by Gotti & Clementi, 2004). Nicotine administration improves performances in various tasks, including spatial and associative learning, working memory, attention and cognition. nAChRs contribute to neuronal protection and the maintenance of cognitive performances during aging (Messi *et al.,* 1997; Gotti & Clementi, 2004; Nakamizo *et al.,* 2005). Adequate nAChRs activation during development of the nervous system is essential for the anatomical and functional maturation of cerebral neuronal circuits, visual system and other areas (Champtiaux & Changeux, 2002; Goti & Clementi, 2004). nAChRs are involved in the organization of sleep, as they control the rhythms of breathing and arousal during sleep (Cohen *et al.,* 2002; Lena *et al.,* 2004; Gotti & Clementi, 2004). Moreover, nAChRs are involved in drug reinforcement. Nicotine is able to modulate dopaminergic system by increasing dopamine (DA) release in the mesolimbic dopamine system (Corrigall *et al.,* 1994; Picciotto & Corrigall, 2002; Gotti & Clementi, 2004). By regulating dopamine release, and, therefore, reinforcement, nAChRs are also important for the addictive properties of nicotine.

Besides the above-mentioned effects, nAChRs play a role in a wide variety of diseases affecting the nervous system and non-neuronal tissues. These diseases could be classified into three groups: age-related degenerative diseases, age-dependent disorders and age-independent disorders. Age-related degenerative diseases are the most severe ones and they affect

cholinergic pathways in the brain: the nucleus basalis of Meynert undergoes different degrees of degeneration and cortical CAT activity is decreased (reviewed in Clementi *et al.,* 2000).

Degenerative diseases are:

1) **Alzheimer's disease (AD).** During AD, the number of nAChRs is decreased in the absence of a general decrease in the number of neurons. The most affected areas are the neocortex, hippocampus, presubiculum and various thalamic nuclei. Individual nAChR subunits are affected in a different way (reviewed in Clementi *et al.,* 2000; Gotti & Clementi, 2004). Another feature, relating AD and nAChRs, is β-amyloid protein (β-AP). β-AP plaques, found in AD patients, are related to the neurodegeneration. They are severely neurotoxic and disrupt cholinergic neurotransmission even at low concentrations. Early treatment with nAChR agonists or AChE inhibitors could have positive effect on the disease. Nicotine or AChE inhibitors improve cognitive processes, which persist over time.

2) **Parkinson's disease (PD).** The relevant pathology of this disease is the loss of dopaminergic neurons in the nigro-striatal pathway. α6β3β2 and α4β2 nAChR subtypes in striatum are responsible for the release of dopamine (Quik & Kulak, 2002; Champtiaux *at el.,* 2003); experimental rodent and monkey models of PD show a selective decrease in the number of α6-, α4- and β2-containing receptors (Zoli *et al.,* 2002; Quik & Kulak, 2002; Champtiaux *at el.,* 2003). However, nicotine treatment for PD has led to controversial results, with little improvement in cognitive or motor systems (Kelton *et al.,* 2000).

The age-dependent disorders, where nAChRs play a role, are the following:

1) **Tourette syndrome.** This is an inherited neurological disorder with onset in childhood, characterized by the presence of multiple physical (motor) tics and at least one vocal (phonic) tic. The most common tics are inappropriate vocalizations, eye blinking, coughing, throat clearing, sniffing, and facial movements; they could be transient or chronic. Even if there is no evidence of the direct involvement of nAChRs in this syndrome, nicotine administration significantly improves the motor disorder and other symptoms, perhaps by modulating DA release from striatal and limbic cortical areas (reviewed by Gotti & Clementi, 2004).

2) **Autism,** which is a severe developmental disorder that becomes noticeable in the early childhood, is characterized by severely impaired social relations and communication, planning and attention, and by restrictive, odd and stereotyped behaviour. Abnormalities in the brain cholinergic system have been observed, including decreased number of α4β2 nAChRs in the

parietal cortex and cerebellum and increased α7 levels in the cerebellum (Perry *et al.,* 2001; Lee *et al.,* 2002; Martin-Ruiz *et al.,* 2004).

3) **Attention-deficit hyperactivity disorder (ADHD).** ADHD is an inheritable multigenic psychiatric disorder of childhood characterized by difficulties to concentrate on a task, hyperactivity and hyperactivity-impulsive symptoms. Even no genetic evidence of nAChR involvement has been reported, several observations suggest that nAChRs could be involved in this disease: ADHD is associated with early smoking and maternal smoking is a risk factor (Leonard *et al.*, 2001).

4) Schizophrenia. It is a psychiatric disorder characterized by impairment in the perception or expression of reality, and the onset of symptoms manifests in young adulthood. Schizophrenic patients are reported to have α7 receptor deficit, while heteromeric receptor involvement is doubtful (reviewed by Gotti & Clementi, 2004). Smoking is prevalent among schizophrenic patients, but it remains unclear if it is a cause or a consequence of the disease.

The age-independent disorders are the following ones:

1) **Epilepsy and febrile convulsions**. Autosomal dominant nocturnal frontal lobe epilepsy (epilepsy that causes clusters of brief, frequent and violent seizures during sleep) is a genetic disease with abnormalities located in chromosome 20q13.2–q13.3, which contains the gene encoding also the α4 nicotinic subunit (Phillips *et al.,* 1995). Mutations lead to increased sensitivity to ACh and possibly a change in Ca^{2+} permeability, thus facilitating the synchronization of the spontaneous oscillations in the thalamo-cortical circuits and generating seizures. α7 receptors are also involved in seizure control (Marks *et al.,* 1989). Thus, both heteromeric and homomeric nAChR subtypes are important in the control of brain excitability and nAChR antagonists have antiepilectic activity as well (Loscher *et al.*, 2003).

2) **Depression and anxiety.** Smoking cessation is associated with depression in individuals who have a history of depression. Nicotine has been reported to be antidepressive and mood stabilizer in humans (Shytle *et al.*, 2002 a, b) and a number of antidepressants are antinicotinic agents (Fryer & Lukas, 1999). In experimental animals, nAChRs are involved in both anxiolytic and anxiogenic effects of nicotine (reviewed by Picciotto *et al.,* 2002). Thus, even if studies are too preliminary, they suggest that nAChRs can modulate the pathways involved in depression and anxiety.

2.11 nAChRs on hypoglossal motoneurons

Since nAChRs are chiefly located on presynaptic endings or even axon fibres (Gotti & Clementi, 2004), it is often difficult to investigate them functionally and to compare their properties with any postsynaptic nAChRs. However, in the mammalian brainstem the overwhelming majority of neurons in the nucleus hypoglossus are motoneurons that natively express nAChRs also present within the local network (Zaninetti *et al.*, 1999; Chamberlin *et al.*, 2002; Robinson *et al.*, 2002; Shao & Feldman, 2005). The precise composition of nAChRs of HMs and surrounding network remain incompletely understood. For instance, autoradiographic (Zaninetti *et al.*, 1999) and electrophysiological (Chamberlin *et al.*, 2002; Shao & Feldman, 2005) studies do not support the presence of α7 receptors, while a recent immunocytochemical report shows their abundant expression (Dehkordi *et al.*, 2005). Hence, the hypoglossal nucleus and the local networks is a good model system for studying simultaneously how pre- and postsynaptic nAChRs can operate.

3. Hypoglossal nucleus: a model for studying nAChR function

The hypoglossal nucleus (XII cranial nucleus) is located in the medulla oblongata close to the midline immediately beneath the base of the fourth ventricle (Fig. 9). It innervates lingual musculature that is composed of intrinsic and extrinsic muscles. The extrinsic muscles have clear bone attachment, and include hypoglossus, styloglossus, geniohyloid and genioglossus muscles, whose activity control protrusion, retraction and elevation of the tongue. Intrinsic muscles are not attached to the bone and are located within the body of the tongue. They are composed of vertical, transversal, superior and inferior longitudinal muscles, whose alter the shape of the tongue. In rat, ventrolateral subdivision of XII nucleus innervates the tongue protractor muscles, dorsal part innervates retractor muscles, and the motoneurons of the middle third of the XII nucleus innervate tongue intrinsic muscle (Aldes, 1995; McClung & Goldberg, 1999; McClung & Goldberg, 2000; Sokoloff, 2000). Such XII nerve organization allows the fine control of various tongue movements, including mastication, sucking, swallowing, controlling respiration and others oral behaviours (Lowe, 1980).

At least 90 % of neurons within the hypoglossal nucleus are motoneurons, while the remaining ones are interneurons (Viana *et al.*, 1990). Hypoglossal motoneurons (HMs) are large (25-50 μm) multipolar cells, whereas interneurons are smaller (10-20 μm), round to oval shaped neurons. Motoneurons spread their dendrites extensively within the XII nucleus and the neighboring reticular formation, while the interneurons have few dendritic processes and are

located at the ventrolateral or dorsolateral borders of the nucleus. The HMs are organized myotopically within the hypoglossal nucleus. Axons of the HMs exit the hypoglossal nucleus, penetrate the *dura mater* and coalesces to form the hypoglossal nerve (XII cranial nerve) in the hypoglossal canal (Fig. 9). The XII nerve then runs to the floor of the mouth, where its fibers are distributed to intrinsic and extrinsic muscles of the tongue.

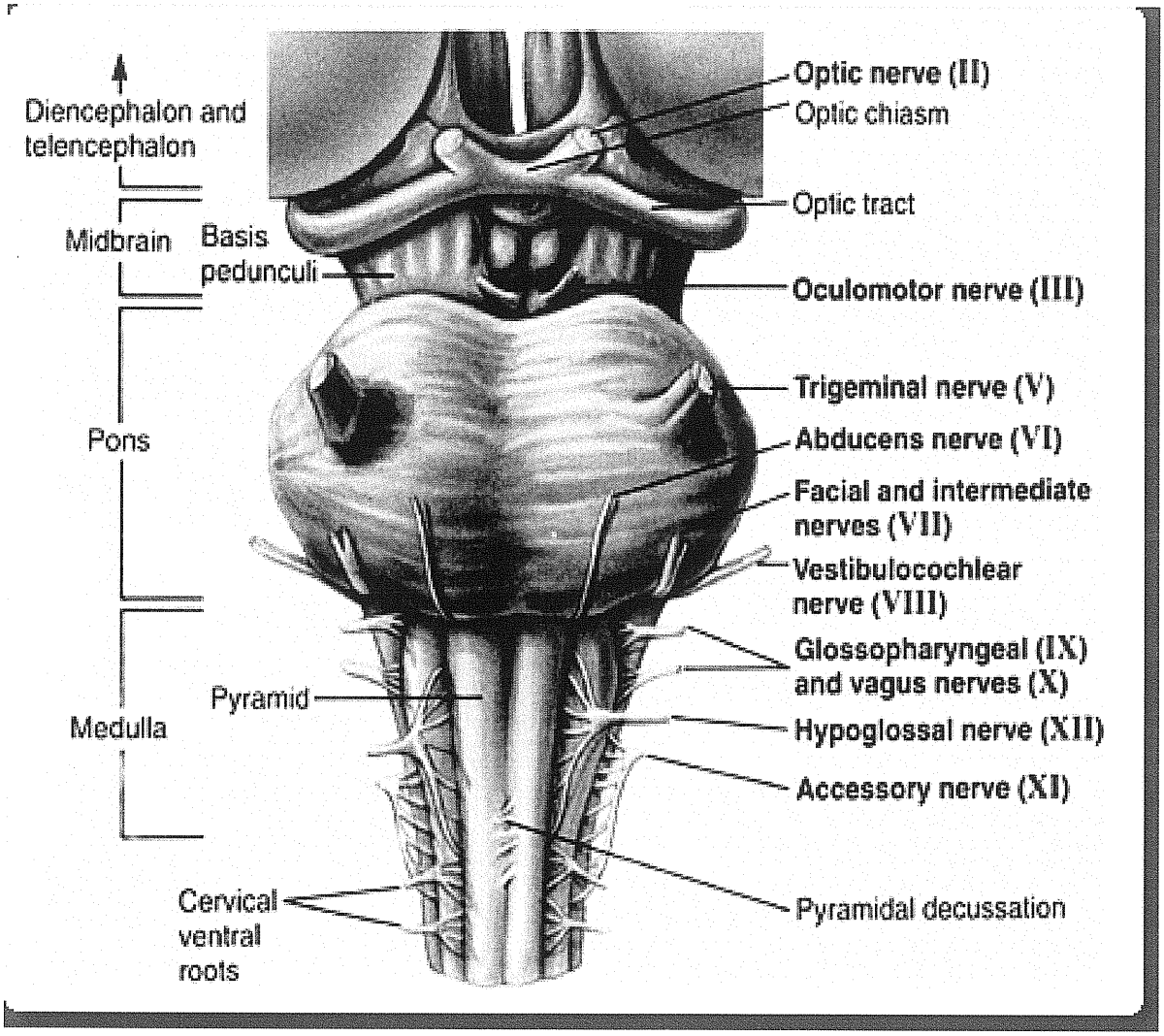

Fig. 9. The front view of human brainstem. The brainstem is composed of three major divisions: medulla, pons, and midbrain, whose give the rise to cranial nerves. Hypoglossal nerve (XII cranial nerve) originates in the medulla. (From Kandel *et al.,* 1991).

The XII nucleus receives innervation from reticular formation, other brainstem centers and higher centers of the brain (Borke *et al.,* 1983; Dobbins & Feldman, 1995). The primary source of the inputs to the XII nucleus arises from the caudal reticular formation immediately ventral to the nucleus of the solitary tract (NTS), which was termed dorsal medullary reticular column

(DMRC; Cunningham & Sawchenko, 2000; Fig. 10). Projections from the DMRC are largely bilateral, distributed to both dorsal and ventral subdivisions of XII nucleus, and, therefore, can simultaneously innervate both tongue protractor and retractor muscles (Cunningham & Sawchenko, 2000). It was shown that protractor vs. retractor HMs receive inputs from DMRC, which are overlapping, although partially segregated (Dobbins & Feldman, 1995; Fay & Norgren, 1997). This arrangment shows an independent, albeit coordinated activation of antagonist muscles of the tongue. It has been suggested that the XII nucleus is sparsely innervatated from NTS, although retrograde labeling never demonstrated labeled cells in the NTS. Human XII nucleus receives cortico-nuclear fibers from the pre-central gyrus of both cerebral hemispheres; however, no direct cortical connections to orofacial motor nuclei, including the XII nucleus, have been shown in rats (Travers & Norgren, 1983). Thus, voluntary motor commands in rat must pass through various relay stations.

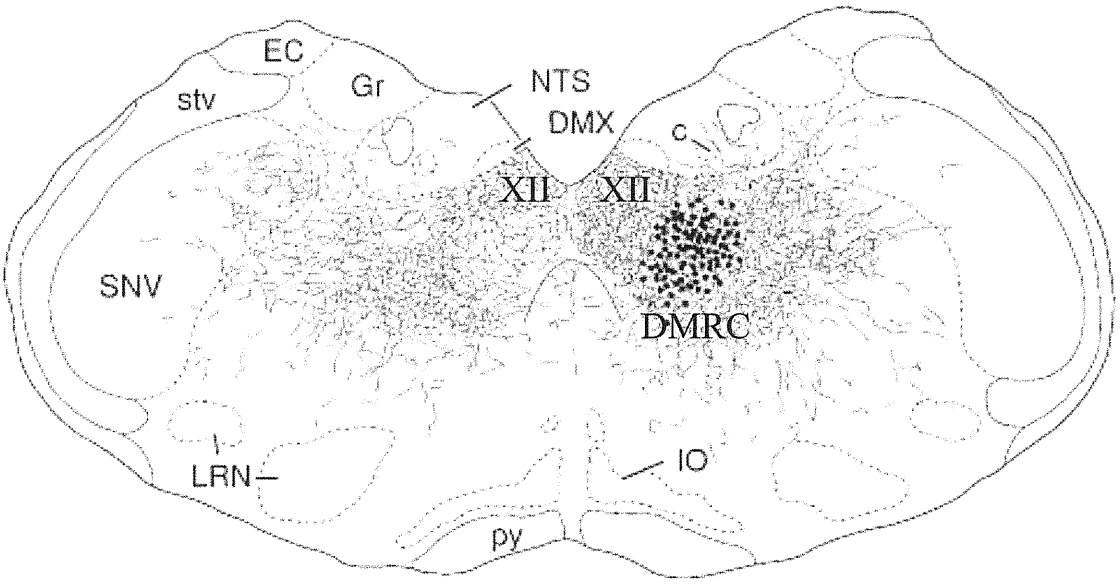

Fig. 10. Schematic representation of XII nucleus innervation. Anterograde labeling shows that hypoglossal nuclei (XII) receive inputs from dorsomedial reticular column (DMRC), where labeling dye was injected. DMRC innervates both contralateral and ipsilateral XII nuclei. Abbreviations: NTS, nucleus tractus solitarius; DMX, dorsal motor nucleus of the vagus nerve; Gr, gracile nucleus; EC, external cuneate nucleus; stv, spinal tract of the trigeminal nucleus; SNV, spinal trigeminal nucleus; LRN, lateral reticular nucleus; py, pyramidal tract; IO, inferior olive. (Modified from Cunningham & Sawchenko, 2000).

Excitatory premotor neurons in the XII nucleus are glutamatergic, while the inhibitory ones are GABAergic and glycinergic (Rekling *et al.,* 2000). *In vitro* recordings from neonatal rats show that HMs express both NMDA and non-NMDA receptors at synaptic sites (O'Brien *et al.,* 1997). However, *in vivo* recording from adult rats (Ouardouz & Durand, 1994) and recordings from HM embryonic organotypic cultures (Launey *et al.,* 1999) suggest that NMDA receptors are not directly involved in synaptic transmission, and could be located either extrasynaptically or at silent synapses. The neurotransmitters GABA and glycine operate by activating Cl^- channels. GABA receptors mainly belong to $GABA_A$ class and are reversibly blocked by bicuculline, while glycine receptors are blocked by strychnine (Barnard *et al.,* 1993; Kuhse *et al.,* 1995). On brainstem motoneurons, $GABA_A$ and glycine receptors are present on the same neuron, and HMs receive both GABAergic and glycinergic synaptic inputs (O'Brien & Berger, 1999). On hypoglossal motoneurons, however, Cl^- mediated synaptic transmission is mainly due to glycine rather than GABA (Donato & Nistri, 2000).

Hypoglossal motoneurons are among the most strongly damaged neurons in amyotrophic lateral sclerosis (Krieger *et al.,* 1994; Lips & Keller, 1999). Amyotrophic lateral sclerosis (ALS), resulting from loss of motoneurons in the brain and spinal cord, is the most common form of motoneuron disease, which comprises a group of unrelated progressive neurodegenerative disorders characterized by paralysis and early death. In particular, the bulbar form of ALS produces slurred speech and difficulties in mastication, swallowing and eating. The bulbar form of ALS manifests severe degeneration of brainstem motoneurons, although some motor nuclei are more vulnerable than others (Rowland & Shneider, 2001). It was suggested that HM vulnerability could be due to their characteristic intracellular Ca^{2+} homeostasis (Ladewig *et al.,* 2003), expression of Ca^{2+} permeable AMPA channels (Del Cano *et al.,* 1999), or impaired glutamate uptake (Sharifullina & Nistri, 2006). To date, riluzole is the only drug licensed for the ALS clinical treatment (Meininger *et al.,* 2000), even if it has modest beneficial effects because it can only slow down disease progression temporarily (Miller *et al.,* 2007).

4. The action of riluzole on motoneurons

Riluzole has also been suggested for treating spinal cord (Schwartz & Fehlings, 2002) and brain injury (Wahl & Stutzmann, 1999), severe mood disorders (Coderre *et al.,* 2007), Huntington's disease (Wu *et al.,* 2006) and epilepsy (Farber *et al.,* 2002). The action of riluzole was first shown to be due to block of glutamatergic neurotransmission (Kretschmer *et al.,* 1998). More recently, the action of riluzole has been attributed to powerful block of the persistent sodium current (Del Negro *et al.*, 2005; Miles *et al.*, 2005; Harvey *et al.*, 2006; Theiss *et al.*, 2007), which appears essential for prolonged rhythmic discharges (Darbon *et al.*, 2004; Cramer *et al.*, 2007; van Drongelen *et al.*, 2006; Zhong *et al.*, 2007). Thus, riluzole has multiple effects, which I will overview in the following sections.

4.1 Presynaptic effects

4.1.1 The action of riluzole on glutamatergic neurotransmission

Riluzole (2-amino-6-trifluoromethoxybenzothiazol) was first proposed to inhibit the release of glutamate (Mantz *et al.*, 1992; Zona *et al.*, 2002; Martin *et al.*, 1993; Coderre *et al.*, 2007), whose levels are found raised (due to impaired transport) in many ALS patients (Cleveland & Rothstein, 2001). Riluzole can block the release of glutamate both *in vivo* and *in vitro*. Both basal glutamate release and release evoked by neuronal activation were affected by riluzole (Hubert & Doble, 1989; Cheramy *et al.,* 1992; Martin *et al.,* 1993; Hubert *et al.,* 1994). The mechanism of action of riluzole is not well understood. The effect of riluzole persists in the presence of TTX (Hubert & Doble, 1989; Martin *et al.,* 1993; Hubert *et al.,* 1994), although riluzole is ineffective on mEPSCs occurring at very low frequency (Tazerart *et al.*, 2007). The data with TTX points to a process directly controlling glutamate release. The inhibition of excitatory amino acid release could be blocked by pretreatment of the cells with pertussis toxin, suggesting that riluzole may interact with a G-protein-driven mechanism (Doble *et al.,* 1992; Hubert *et al.,* 1994). However, it is not known whether the mechanism is independent or operates together with other mechanisms, including postsynaptic ones. In rat cultured granule cells (Hubert *et al.,* 1994) it was found, that, besides G-protein-dependent pathway, riluzole acted on voltage-dependent sodium channels: these two mechanism were independent and operated synergistically. In conclusion, it seems that presynaptically riluzole could inhibit glutamate release via a G-protein-dependent signal transduction pathway (reviewed by Doble, 1996) and the mechanism most probably is exerted synergically with other postsynaptic factors.

4.2 Postsynaptic effects

4.2.1 The action of riluzole on sodium currents

On motoneurons, the persistent inward current (PIC) is composed of persistent sodium current (I_{NaP}) and/or persistent calcium current (I_{CaP}), that integrate synaptic inputs (Crill, 1996; Russo & Housgaard, 1999). Brainstem (Powers & Binder, 2003; Moritz *et al.,* 2007) and spinal motoneurons (Harvey *et al.*, 2006; Theiss *et al.*, 2007) express I_{NaP}, which can be evoked by injecting slow triangular voltage commands. Under voltage clamp conditions, I_{NaP} activation leads to a region of a negative slope conductance, while in current clamp conditions I_{NaP} activation is followed by a repetitive firing (Fig. 11). The negative slope conductance and/or repetitive firing can be blocked by riluzole (5-20 μM) in motoneurons (Del Negro *et al.*, 2005; Miles *et al.*, 2005; Harvey *et al.*, 2006; Theiss *et al.*, 2007) as well as in neocortical network (van Drogelen *et al.,* 2006), cultured cortical neurons (Zona *et al.,* 1998), vibrissa system neurons (Cramer *et al.,* 2007), mesencephalic trigeminal neurons (Kang *et al.,* 2007), supratrigeminal area interneurons (Hsiao *et al.,* 2007) and other neurons. Under current clamp conditions, I_{NaP} contributes to the frequency-current (F/I) relation (Bennett *et al.,* 1998; Lee & Heckman, 1998), firing rate acceleration (Hounsgaard *et al.,* 1988; Lee & Heckman, 1998), bistable discharge behaviour (Hounsgaard *et al.,* 1988; Lee & Heckman, 1998), amplification of synaptic currents (Lee & Heckman, 1998; Power & Binder, 2000), and repetitive firing (Kuo *et al.,* 2006; Harvey *et al.,* 2006; Tazerart *et al.,* 2007).

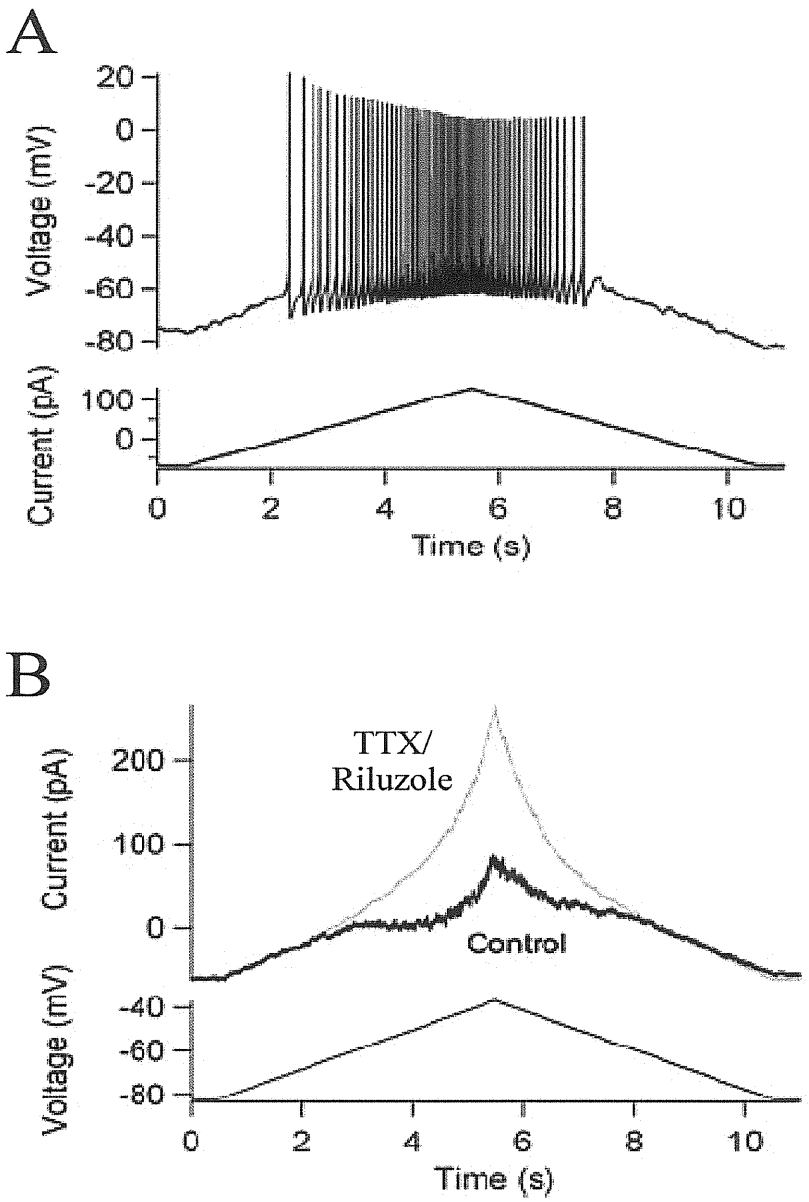

Fig. 11. I_{NaP} activation under current- and voltage clamp conditions. (A) When the I_{NaP} activation threshold was reached under current clamp recording, the cell responded to a slow-depolarizing current ramp (bottom trace) with sustained repetitive firing (top trace). (B) Under voltage clamp conditions, a slow-depolarizing voltage-ramp command (bottom trace) induced a negative slope region (top trace), which could be blocked by TTX (1 μM) or by riluzole (5-20 μM). Adapted from Kuo *et al.,* 2006.

The fast sodium current is important for a generation of an action potential and is not blocked by riluzole applied at low μM concentrations (Kuo *et al.,* 2006; Harvey *et al.,* 2006; Tazerart *et al.,* 2007). Thus, while the repetitive firing could be inhibited by riluzole, the single action potential is not affected and could be produced upon injection of a DC current (Fig. 12).

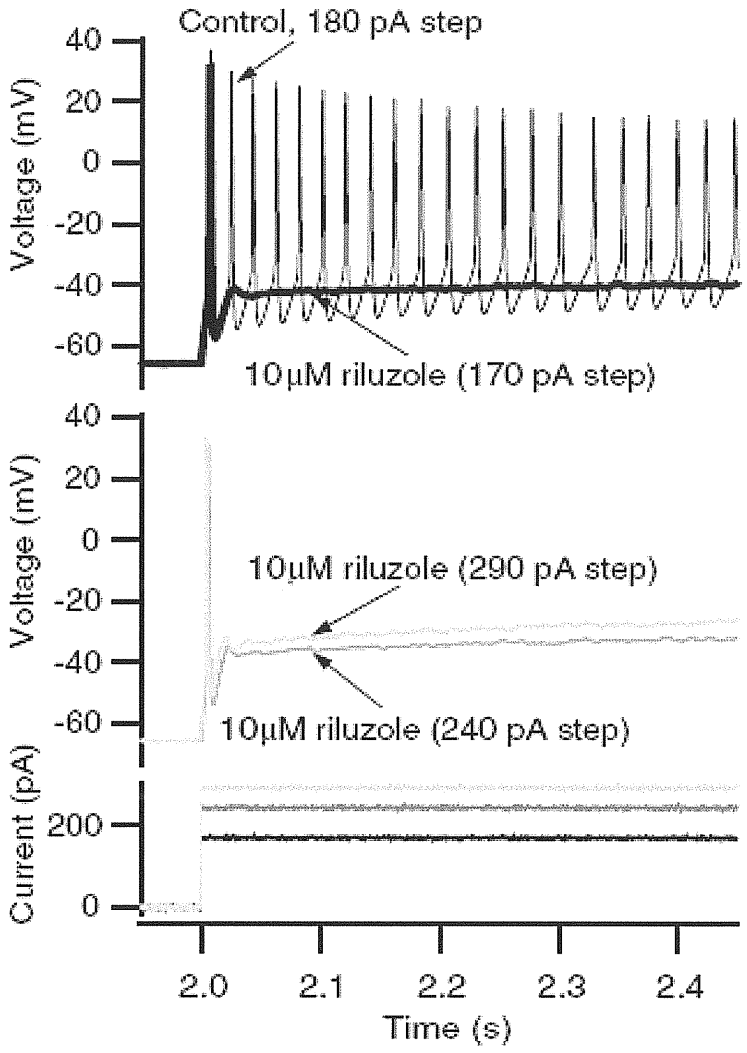

Fig. 12. Effect of riluzole on persistent and fast sodium currents. In control conditions, repetitive firing (top panel, grey trace) was observed to a current step injection (bottom panel, black trace). Riluzole (10 µM) blocked repetitive firing, while the first spike remained (top panel, black trace). Increasing the DC current amplitude (bottom panel, grey traces) did not restore firing (middle panel). (From Kuo *et al.,* 2006).

Since I_{NaP} appears important for prolonged rhythmic discharges (Darbon *et al.*, 2004; Cramer *et al.*, 2007; van Drongelen *et al.*, 2006; Zhong *et al.*, 2007), its inhibition by riluzole might disrupt rhythmic patterns of motoneurons. I_{NaP} is, however, unnecessary for motoneuron bursting evoked by brainstem preBotzinger neurons (Pace *et al.,* 2007 a, b). One recent study shows that low doses of riluzole, besides blocking or having no effect on the rhythmic pattern, can even induce oscillations in cultured spinal networks (Yvon *et al.*, 2007).

4.2.2 Multiple postsynaptic effects of riluzole

Several studies show that riluzole could inhibit currents evoked by NMDA and kainate (Debono *et al.,* 1993, Mantz, 1996; Centonze *et al.,* 1998). However, radioligand binding studies show that riluzole does not bind AMPA, kainate, NMDA nor metabotropic glutamate receptors (Doble, 1996; Peluffo *et al.* 1997; Kretschmer *et al.,* 1998). The previous reports of riluzole interaction with excitatory amino acid receptors may be explained by an indirect mechanism (Kretschmer *et al.,* 1998). The currents may be inhibited indirectly, via a G-protein coupled receptor mechanism, which could block or decrease the NMDA mediated responses (Kretschmer *et al.,* 1998).

In addition to its action on persistent sodium currents, riluzole inhibits both high- and low-voltage-activated calcium currents in cortical, dorsal root ganglion neurons and neuroendocrine cells (Huang *et al.*, 1997; Siniscalchi *et al.*, 1997; Stefani *et al.*, 1997; Beltran-Parrazal & Charles, 2003). The drug can also blocks potassium conductances (Zona *et al.*, 1998; Duprat *et al.*, 2000; Cao *et al.*, 2002; Ahn *et al.*, 2005). In addition, riluzole may interact with $GABA_A$ and glycine receptors (Umemiya & Berger, 1995; Mohammadi *et al.*, 2001; He *et al.*, 2002).

4.3 Neuroprotective action of riluzole

Riluzole is important for neuroprotection both *in vitro* and *in vivo. In vitro* excitotoxicity can be produced by exposing the cells to depolarizing agents in the incubation medium, such as the excitatory amino acids AMPA, NMDA, kainate or the sodium channel activator veratridine (Malgouris *et al.,* 1989; Estevez *et al.,* 1995). The resulting cell necrosis can be assessed both histologically and by measuring the efflux of the cytosolic marker lactate dehydrogenase (LDH). Riluzole rescued the cells from NMDA and veratridine produced excitotoxicity (Malgouris *et al.,* 1989; Estevez *et al.,* 1995). The neuroprotective effect of riluzole against NMDA was abolished by pretreating the slices with pertussis toxin (Malgouris *et al.,* 1989). This suggests that neuroprotection might be mediated by a G-protein-dependent mechanism.

Riluzole alone or in a combination with other neuroprotective drugs, could enhance the survival and reinnervating capacity of injured motoneurons (Mu *et al.,* 2000; Nogradi & Vrbova, 2001; Bergerot *et al.*, 2004; Nogradi *et al.,* 2007). Riluzole was shown to rescue damaged motoneurons and regenerate their axons up to 10 days after injury (Nogradi *et al.,* 2007). Several studies demonstrate that riluzole could promote survival of motoneurons by stimulating trophic activity and/or new neurotrophic factor synthesis of astrocytes (Peluffo *et al.,* 1997; Mituza *et al.,* 2001).

One further neuroprotective action of riluzole is increased glutamate uptake (Azbill *et al.,* 2000; Frizzo *et al.,* 2004). The effect is biphasic and dose dependent, since low, up to 10 μM, doses of riluzole enhances glutamate uptake, while higher doses depress it (Samuel *et al.,* 1992; Azbill *et al.,* 2000; Frizzo *et al.,* 2004). The increase of glutamate uptake depends on Gs proteins, sensitive to cholera toxin (CTX), since CTX inhibited the effects of riluzole (Azbill *et al.,* 2000). The same study shows, that PKA and PKC are not involved in the glutamate uptake regulation by riluzole since inhibition of PKA or PKC had no effect on the ability of riluzole to increase glutamate uptake (Azbill *et al.,* 2000).

Riluzole is also neuroprotective *in vivo* in several animal models of neuronal injury, known to involve excitotoxic mechanisms, such as experimentally induced cerebral ischemia. These animal models of stroke involve excitotoxic neuronal loss, following massive release of glutamate in the ischemic area (Meldrum & Garthwaite, 1990). When ischemia is induced experimentally, riluzole reduces the volume of damaged ischemic area and preventes necrosis (Malgouris *et al.,* 1989; Pratt *et al.,* 1992). Furthermore, riluzole is neuroprotective in models of basal ganglia degeneration, where selective dopaminergic neurons are affected (Boireau *et al.,* 1994 a, b; Benazzouz *et al.,* 1995). In rats, mice and monkeys riluzole administration can reverse the decrease in striatal dopamine levels (Boireau *et al.,* 1994 a, b; Benazzouz *et al.,* 1995).

Thus, riluzole is an important neuroprotective agent. Although clinical data are currently available only for ALS, its neuroprotective profile in experimental animals suggests that it may be of use in other neurologic conditions, such as spinal cord injury, stroke or basal ganglia disease.

AIMS OF THE STUDY

The scientific questions I have studied during my thesis project are the following ones:

1. What kind of nAChRs are present in the XII nucleus of the neonatal rat?

2. nAChR role in neuronal network activity and rhythmicity within XII nucleus.

3. Pre- and postsynaptic nAChR involvement in oscillatory patterns.

4. Cellular and network mechanism for the oscillatory activity in the XII nucleus.

5. The mechanism of the action of riluzole on hypoglossal motoneurons.

6. Synaptic transmission changes induced by riluzole.

METHODS

1. Slice preparation

All experiments were carried out in accordance with the regulations of the Italian Animal Welfare act (DL 27/1/92 n. 116) following the European Community directives no. 86/609 93/88 (Italian Ministry of Health authorization for the local animal care facility in Trieste, D 69/98-B), and approved by the local authority veterinary service.

Neonatal (0-5 day old, P0-P5) Wistar rats were anaesthetized with i.p. urethane (2 g/kg body weight) and decapitated. Brainstem was quickly dissected within ice-cold oxygenated (95 % O_2/ 5 % CO_2) physiological solution. Cooling of the preparation was of particular importance because it declined the rate of physiological processes and, therefore, minimized the slice damage from anoxia. A vibrating tissue slicer (Vibracut, FTB, Weinheim, Germany) was used to cut 200-350 μm thick slices. For this purpose, the dissected brainstem, containing medulla and pons, was fixed onto an agar block (4 % in 0.9 % NaCl), and shaped to keep the tissue immobile in the correct orientation (caudal part upwards). Then the agar block was glued to the stage of the vibro-slicer, immersed in ice-cold, oxygenated physiological saline and the slices were cut.

Slices were first transferred to an incubation chamber, containing the same physiological saline, and were kept there for 40 minutes at 32 °C. Then the incubation chamber was left in a room temperature for one hour. This incubation period allowed us to have stable recordings. After the recovering period single brainstem slices were transferred to a small recording chamber. There they were held in place by a fine nylon net glued to a horse-shaped platinum wire. Slices were continuously perfused with oxygenated recording solution (2-3 ml/min).

Hypoglossal motoneurons (HMs) were identified within the XII nucleus (Fig. 13A) with a Zeiss microscope connected to an infrared video camera. Under x40 magnification single neuron somata (20-40 μm in diameter) were clearly visible (Fig. 13B) and ready for patch clamp recording.

For a XII nerve recording, the brainstem was dissected in order to preserve maximally intact and long hypoglossal nerves. Only one slice (350 μm thick) was cut from a single brainstem.

A

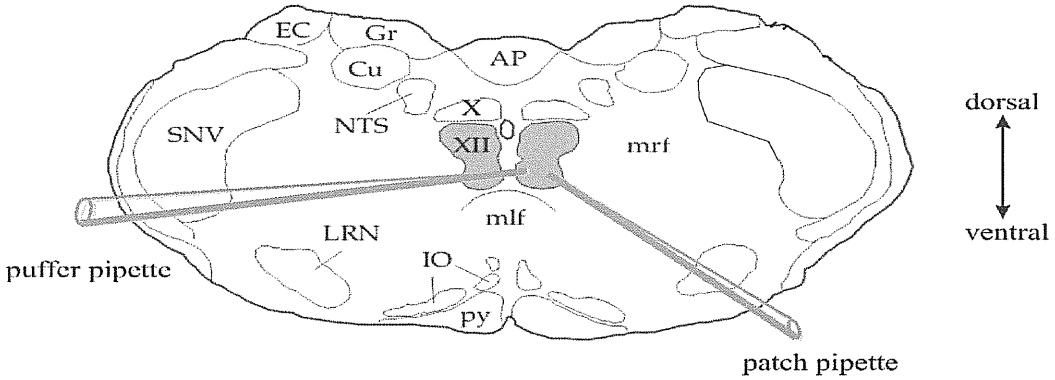

B

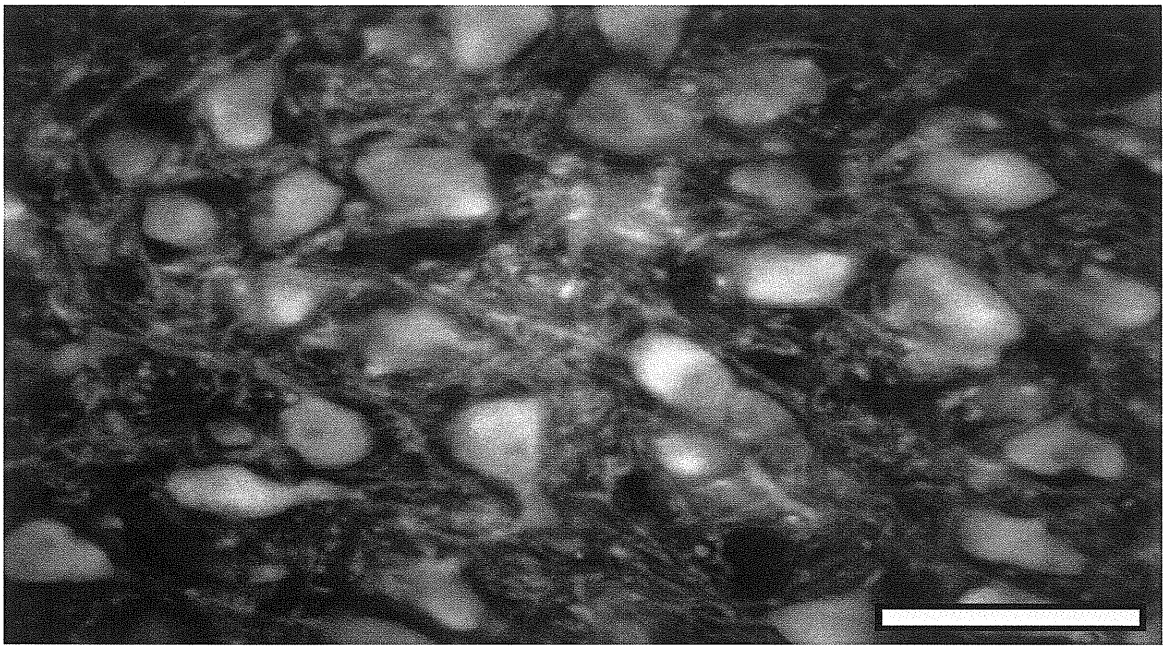

Fig. 13. Hypoglossal motoneuron identification within the brainstem slice. (A) Schematic representation of a brainstem slice. Recordings were done via patch pipette, while some drugs were applied locally via puffer pipette. The following structures can be identified: AP, area postrema; Cu, cuneate nucleus; EC, external cuneate nucleus; Gr, gracile nucleus; IO, inferior olive; LRN, lateralreticular nucleus; mlf, medial longitudinal fasciculus; mrf, medullary reticular formation; NTS, nucleus of the tractus solitarius; SNV, spinal trigeminal nucleus; py, pyramidal tract; X, vagal nucleus; XII, hypoglossal nucleus. (B) Single motoneurons are easily identified within the XII nucleus. Immunostaining of brainstem slices (x40 magnification) with antibodies against α7 nAChR subunits. Scale bar = 50 μm.

2. Solutions and drugs

2.1 Slice preparation and maintenance

The solution for slice cutting and maintenance contained (in mM): NaCl 130, KCl 3, NaH_2PO_4 1.5, $CaCl_2$ 1.5, $MgCl_2$ 1, $NaHCO_3$ 25, glucose 15 (pH 7.4; 300-320 mOsm). All the time the solution was oxygenated with 95 % O_2/ 5 % CO_2 gas mixture.

2.2 Voltage and current clamp recordings

For voltage clamp experiments, patch pipettes were filled with intracellular solution containing (in mM): CsCl 130, NaCl 5, $MgCl_2$ 2, $CaCl_2$ 1, HEPES 10, BAPTA 10, ATP-Mg 2, sucrose 2 (pH 7.2, 280-300 mOsm). Intracellular CsCl, that minimized the leak outward current of the recorded cell, was used more often than KCl to enable larger changes in holding potential (Vh) under voltage clamp. For current clamp experiment 130 mM KCl always replaced CsCl. In some experiments QX-314 (300 μM) was added to the pipette solution to block voltage activated Na^+ currents and the slow inward rectifier I_h (Perkins & Wong, 1995; Marchetti *et al.* 2002).

2.3 Liquid junction potential

In current clamp mode membrane potential values for the liquid junction potential (Vj) between external and internal solutions were corrected off-line after the experiment (Neher, 1992). Vj was calculated with Clampex 9.2 software. For our solutions, the liquid junction potential was of 3.5 mV. In voltage clamp mode, it was about zero mV and no correction was applied.

2.4 Drug application

Drugs were applied in two different ways: either bath-applied via extracellular solution superfused at 2-3 ml/min or via fast, local pressure pulses. For a bath-application, a minimum of 5-10 min passed to reach apparent equilibrium conditions before any recording was made. For the local pressure pulses, a thin-walled glass micropipette was pulled in the same way as a patch pipette using a two stage puller 3P-A, List Medical, Germany. The pipette was filled with 2 mM nicotine, diluted in the external recording solution. The puffer pipette was positioned approximately 10-50 μm away from the soma of the recorded cell. The pipette was connected to a Pneumatic Picopump (WPI, Sarasota, Fl, USA) that delivered 4-8 psi pressure

pulses, the duration of which ranged from 10 ms to 60 s. The pipette position, the puffer pulse pressure and duration were adjusted for every cell in order to record the largest response of the cell and to avoid disrupting the patch at the same time. The pressure pulses were delivered at preset intervals of 1 min to allow nAChR recovery from desensitization pulses. Full details of the analysis of responses evoked by puffer applied agonists to HMs have been published (Di Angelantonio & Nistri, 2001; Quitadamo *et al.*, 2005; Pagnotta *et al.*, 2005).

Unless otherwise stated, all experiments were carried out in the continuous presence of bicuculline (10 μM) and strychnine (0.4 μM) in the bathing solution to block GABA and glycine-mediated transmission (Donato & Nistri, 2000; Marchetti *et al.*, 2002) in order to study glutamatergic transmission in isolation.

2.5 Drugs used

The following drugs were used: D-amino-phosphonovaleriate (APV), 6-cyano-7-nitroquinoxaline-2,3-dione (CNQX), N-(2.6-dimethylphenylcarbamoylmethyl) triethylammonium bromide (QX-314), and methyllycaconitine citrate (MLA) purchased from Tocris (Bristol, UK); acetylcholine chloride, atropine sulphate salt, ethyl-[*m*-hydroxyphenil]-dimethylammonium chloride (edrophonium), bicuculline methiodide (bicuculline), dihydro-β-erythroidine hydrobromide (DHβE), (RS)-1-aminoindan-1,5-dicarboxylic acid (AIDA), nicotine tartrate (nicotine), carbenoxolone disodium salt (carbenoxolone) and strychnine hydrochloride (strychnine), 2-amino- 6-trifluoromethoxybenzothiazole (riluzole), cadmium chloride and manganese chloride from Sigma (Milan, Italy). Tetrodotoxin (TTX) was obtained from Latoxan (Valence, France).

3. Electrophysiological recordings

3.1 Patch clamp recording

The conventional whole-cell patch clamp technique (Hamill *et al.*, 1981) was employed. All recordings were performed at room temperature. HMs, visualized within the nucleus hypoglosssus with an infrared video camera, were patch-clamped in voltage and current clamp modes. The Digidata 1322A data acquisition system with Clampex 9.2 software (Axon Instruments, Molecular Devices Corporation, Sunnywale, CA, USA) was used for the data acquisition. Data were stored in a PC and analyzed off-line.

For voltage clamp recording, an L/M-EPC-7 patch-clamp amplifier (List Medical, Germany) was used. Cells were usually held at –60 to –65 mV holding potential (Vh) to minimize the

leak current at rest. Series resistance (5-25 MΩ) was routinely monitored without any compensation. Recordings were filtered at 3 kHz, sampled at 10 kHz and stored in a PC. A small heat-polished pipette, pulled from thin-walled borosilicate glass capillaries with a two-stage puller (3P-A, List Medical, Germany) was used to make the seal. The pipette with a series resistance of 3-5 MΩ was positioned close to the cell membrane, continuously blowing the air through the pipette interior in order to keep it clean. Then gentle suction, applied to the pipette interior, led to increase in series resistance until 1-5 GΩ. After the giga-seal formation, an additional suction applied to the pipette interior led to the membrane rupture and access to the cell interior.

For current clamp recording, an Axoclamp 2B amplifier (Axon Instruments, Molecular Devices Corporation, Sunnywale, CA, USA) was utilized. We have used a different amplifier since compensation of pipette resistance was not available with the previous one. Moreover, it has been shown that most amplifiers designed for voltage clamp experiments give distortions to fast occurring events like action potentials (Magistretti *et al.,* 1996). For current clamp mode the bridge was routinely balanced. The junction potential was corrected off-line after every experiment. The pipette had 3-10 MΩ series resistance and was made in a similar manner as for voltage clamp recordings.

3.2 Nerve recording

Motoneuronal population activity was recorded from the XII nerve roots using suction electrodes. The electrodes were made from thin-walled borosilicate glass capillaries with a two-stage puller (3P-A, List Medical, Germany). Their internal diameter was adjusted to adequately fit the nerve root inside the electrode and they were filled with an external recording solution. The nerve activity was amplified using an L/M-EPC-7 patch-clamp (List Medical, Germany) and DAM 50 (WPI, Sarasota, Fl, USA) amplifiers. The data were filtered at 3 kHz, sampled at 10 kHz and stored in a PC.

4. Immunofluorescence experiments

Experiments were carried out as previously reported (Pagnotta *et al.*, 2005). Microtome-cut sections (40 μm thick) of brainstem were treated with a blocking solution (5 % bovine serum albumin, 4 % fetal calf serum, 0.1 % Triton X-100 in phosphate buffer saline; pH 7.4) for at least 60 min at room temperature. From each rostro-caudally sectioned rat brainstem about forty sections containing the hypoglossal nucleus were cut. Eight slices per animal (one every

five slices) were analyzed for staining with one of the nAChR antibodies; neurons immunoreactive for the nicotinic subunits were counted. Slices were incubated overnight at 4°C with antibodies against α7, β2 or α4 nAChR subunits (diluted 1:100, Santa Cruz Biotechnology) in the same blocking buffer at 4°C. The secondary antibodies used were AlexaFluor 488 and 594 (1:500 dilution; Molecular Probes, Invitrogen, San Giuliano Milanese, Italy) for 2 h at room temperature. Slices were mounted with Vectarshield (Vector Laboratories, Burlingame CA, USA) to avoid photobleaching and visualized under UV microscopy. Immunofluorescence measurements were obtained with ImagePro software (Hamamatsu Srl, Arese, Italy). Slices stained with only the secondary antibody showed no immunostaining. Likewise, slices of non-neuronal tissues like kidney or liver also shown no immunoreactivity when processed with antibodes against α7, β2 and α4 nAChR subunits. Furthermore, using the current α7 or β2 antibodies, we found no staining in hippocampal slices of knock-out mice lacking either the α7 gene (generous gift by Drs. E. Aztiria and L. Domenici, SISSA, Trieste) or the β2 gene (generous gift by Prof. M. Zoli, University of Modena and Reggio Emilia, Italy), respectively.

5. Data analysis

Cell input resistance (Rin) was calculated by measuring the current response to 10 mV hyperpolarizing steps from Vh (Pagnotta *et al.*, 2005; Quitadamo *et al.*, 2005). Spontaneous and miniature EPSCs (sEPSCs and mEPSCs) were detected using the software Clampfit 9.2 (Axon Instruments, Molecular Devices, Sunnyvale, CA, USA). The oscillations were discriminated from sEPSCs based on the following characteristics: oscillations had very limited dependence on cell holding potential, stereotypic amplitude and duration, often resembling spikelets (Long *et al.*, 2004; Sharifullina *et al.*, 2005) propagated via electrical coupling within the network. The oscillation amplitude was measured as the voltage difference between a peak and a through in voltage clamp mode. The period was measured as the time difference from a peak to a peak. For each measurement, at least 30 cycles were averaged. The coefficient of variation (standard deviation/mean, CV) was expressed as a percentage value. In order to quantify oscillation frequency changes over time, the oscillatory trace was divided into 30 s epochs, taking as control the value at the onset of oscillations. The oscillation frequency in each epoch was then expressed as a fraction of the value found during the first epoch.

In triangular voltage clamp commands (ramps), the voltage-activated inward current was extracted by subtracting the passive leak current, extrapolated from linear regression fits to the

I-V curve at membrane voltages between -80 and -60 mV (Fig. 14). The deflection starting point was considered as a voltage-activated inward current threshold, and the maximal current was reached at the holding potential when the deflection was the largest. The inward current area was measured as a whole area below the trace baseline after a leak correction.

Action potential amplitude was calculated from the first spike fired to a given input as the difference between peak (overshoot) and baseline membrane potential. Action potential maximum rate of rise was measured at the peak of the first derivative of the local spike voltage trace with respect to time.

SigmaStat 3.1 software (Jandel Scientific, San Rafael, CA, USA) and KyPlot 2.0 (Qualest Co., www.qualest.co.jp) were used for statistical analysis. SigmaPlot 9.0 software (Jandel Scientific, San Rafael, CA, USA) and the CorelDraw 13 (Vector Capital, San Francisco, CA, USA) software packages were used for graphical data representation. Results were expressed as a mean ± S.E.M.; n refers to the number of cells. Statistical significance was assessed with the Student's paired or unpaired *t*-test, applied only to parametric raw data. For non-parametric data, Wilcoxon Sign Rank rest for paired data or Wilcoxon Mann-Whitney test for unpaired data were applied. Two groups of data were considered statistically different if $P < 0.05$. Kolmogorov-Smirnov test was used for probability distributions.

For imunofluoresce experiment analysis ImagePro software (Hamamatsu srl, Arese, Italy) software was used.

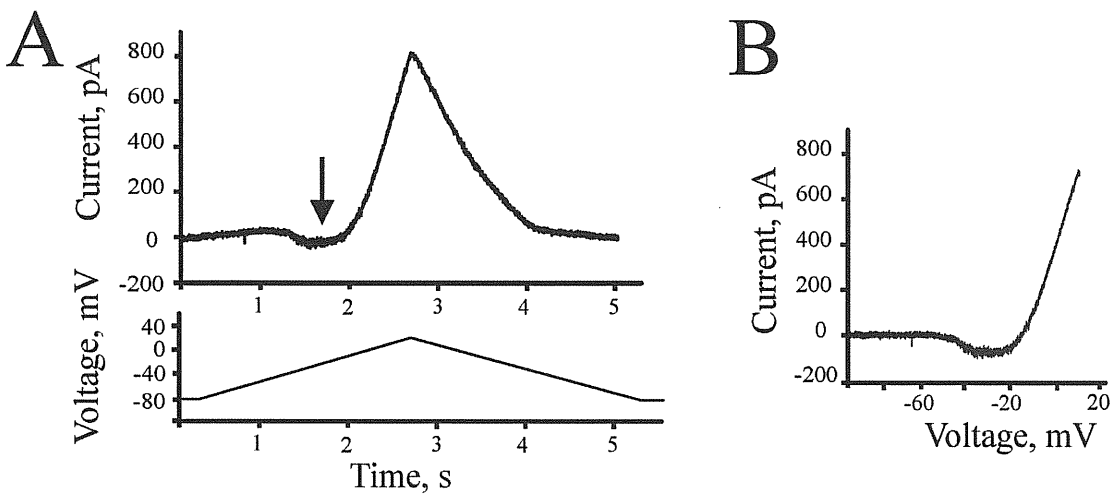

Fig. 14. The triangular voltage clamp command (ramp) protocol to measure persistent inward current. (A) The membrane holding potential was changed from -80 mV to 20 mV with a speed of 42 mV/s (bottom panel). Top panel shows the cell's response. The negative deflection reveals an inward current, while the positive current shows an outward current. The arrow shows persistent inward current (PIC). (B) Persistent inward current after leak subtraction. . Data in (A) and (B) are from the same cell.

RESULTS

1. nAChR subunit composition in the brainstem

Brain nicotinic acetylcholine receptors (nAChRs) are made up by either five homomeric α7 subunits or heteromeric α/β subunits, the latter mainly of $(\alpha4)_2(\beta2)_3$ composition (Gotti & Clementi, 2004). Since nAChRs are chiefly located on presynaptic endings or even axon fibres (Gotti & Clementi, 2004), it is often difficult to investigate their expression and functions directly. However, in the mammalian brainstem the overwhelming majority of neurons in the nucleus hypoglossus are motoneurons (HMs) that natively express nAChRs which are also present within the local network (Zaninetti *et al.*, 1999; Chamberlin *et al.*, 2002; Robinson *et al.*, 2002; Shao & Feldman, 2000). The nAChR composition and the effects of nicotine on nAChRs of HMs remain incompletely understood. Autoradiographic (Zaninetti *et al.*, 1999) and electrophysiological (Chamberlin *et al.*, 2002; Shao & Feldman, 2000) studies do not support the presence of α7 receptors, while immunocytochemical studies show their abundant expression (Dehkordi *et al.*, 2005). Recent electrophysiological studies in our lab have revealed the presence of α7 and β2 nAChR subunits. Finally, there is scanty information on how nAChR activity influences synaptic transmission on HMs. Thus, my first goal was to determine subunits composition of nAChRs, expressed on hypoglossal motoneurons.

Slices (40 μm width) were treated with a blocking buffer at least 60 min, then they were incubated with a primary antibody overnight and later with a secondary antibody for two ours. After wash out of the secondary antibody, slices were visualized under UV microscopy. Immunoreactive staining revealed the presence of α4, α7 and β2 nAChR subunits (Fig. 15A). nAChRs were present on cell bodies, fibers and fine processes (Fig. 15A, lower panels and Fig. 15B). Likewise, slices of non-neuronal tissues like kidney or liver showed no immunoreactivity when processed with antibodies against α7, β2 and α4 nAChR subunits. Furthermore, using the current α7 or β2 antibodies, it was found no staining in hippocampal slices of knock-out mice lacking either the α7 gene (generous gift by Drs. E. Aztiria and L. Domenici, SISSA, Trieste) or the β2 gene (generous gift by Prof. M. Zoli, University of Modena and Reggio Emilia, Italy), respectively.

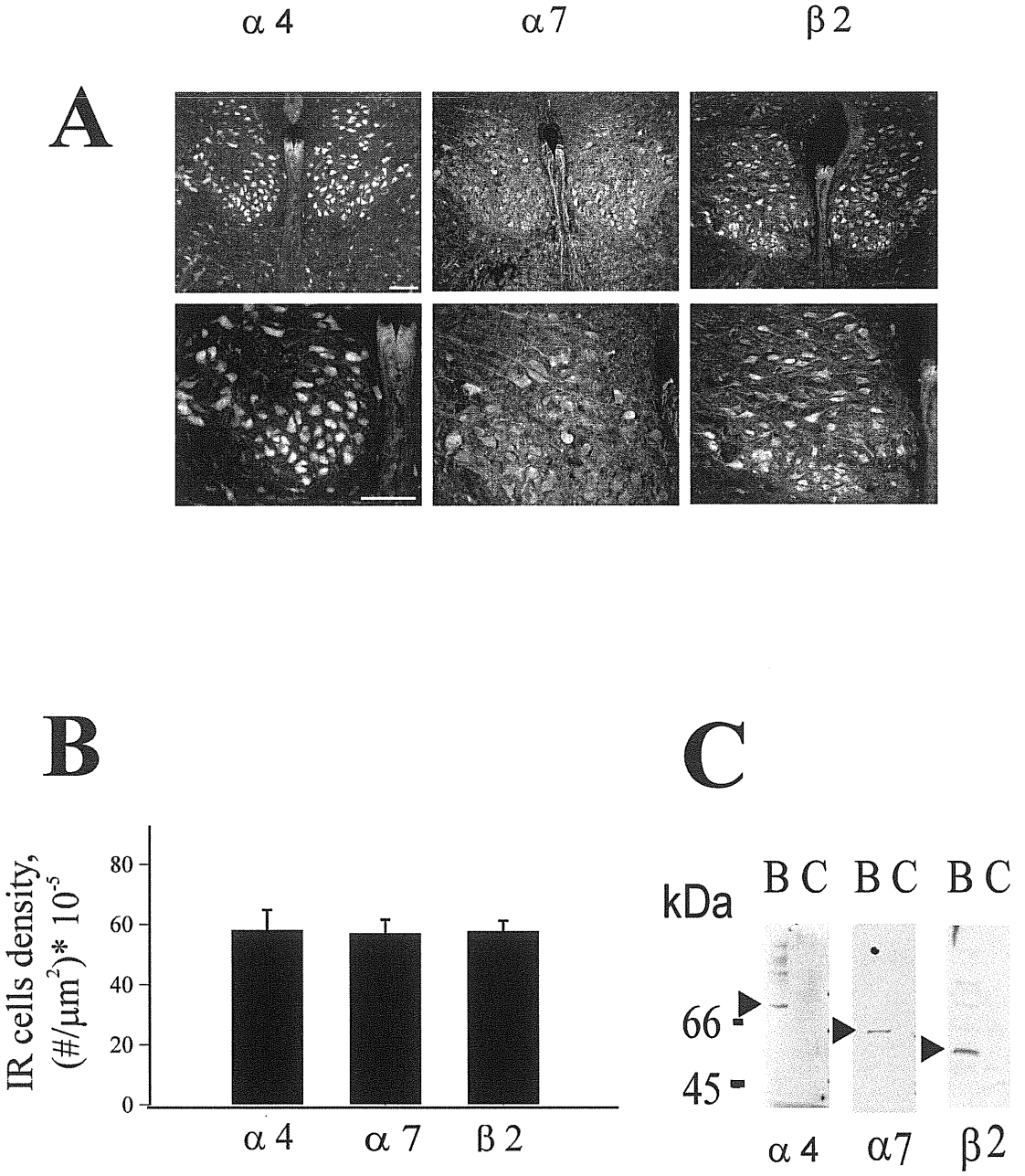

Fig. 15. Immunohistochemistry of nAChRs in the nucleus hypoglossus. (A) Immunostaining of brainstem slices (x10 and x20 magnification for top and bottom rows, respectively) with antibodies against α4, α7 or β2 nAChR subunits reveals reactivity in HMs. Scale bar = 100 μm. (B) Bar charts of the density of immunoreactive cells in the hypoglossal nucleus for each type of nAChR subunit. (C) Western immunoblot of α4, α7 or β2 nAChR subunits. Lane b refers to brainstem samples while lane c refers to kidney samples used as a negative control.

As motoneurons comprise about 90 % of all neurons in the nucleus hypoglossus, all immunoreactive cells were counted. Since slices were cut along the rostro-caudal axis from the hypoglossal nucleus, they could contain a different number of neurons. To quantify the number of motoneurons in various sections, large cells (20-40 μm somatic diameter) immunoreactive for any nAChR subunit were counted and divided by the area of the nucleus hypoglossus in the same slice (Fig. 15B). The density of neurons immunoreactive to α4, β2 or α7 was found to be very similar. In general, immunoreactive cells were more numerous in the caudal end than in the rostral end of the nucleus. The mean area of nucleus hypoglossus in the examined histochemical sections was 122,104 ± 3,530 μm^2 (62 slices from 13 P4-P5 animals).

Western immunoblotting experiments of lysates derived from P3 rat brainstem, performed in our lab by Dr. E. Fabretti, further supported these findings. As shown in Fig. 15C (lanes B), a single immunoreactive band corresponding to the expected molecular weight of the α4, α7, or β2 nAChR subunits in the rat was observed. In particular, the anti-α4 antibody recognized a band of 70 kDa, the anti-α7 displayed a band of 57 kDa, and the anti-β2 antibody recognized a band at approximately 50 kDa in full support of previous studies performed on rat brain tissue (Arroyo-Jimenez *et al.*, 1999; Jones *et al.*, 2001; De Simone *et al.*, 2005). Western blots of comparable amount of protein extracts from rat kidney, used as negative control, showed no signal (Fig. 15C, lanes c).

2. Brainstem nAChR function at a single cell level

2.1 Postsynaptic nAChR action on glutamatergic transmission

In our lab it was shown (Quitadamo *et al.*, 2005) that there is no tonically active, fast nicotinic synaptic transmission in the brainstem slice preparation. After glutamatergic, GABAergic and glycinergic synaptic transmission block with CNQX (20 μM), APV (50 μM), bicuculline (10 μM) and strychnine (0.4 μM), there were no spontaneous synaptic events (Quitadamo *et al.*, 2005). During my thesis project, I have decided to investigate in more detail if activation by endogenous ACh of nAChRs could have any role on glutamatergic transmission. Therefore, experiments were done in the continuous presence of bicuculline (10 μM) and strychnine (0.4 μM) to block GABAergic and glycinergic synaptic transmission, respectively. Under these conditions, spontaneous excitatory postsynaptic current (sEPSC) amplitude on average was -23.5 ± 1.9 pA and the frequency was 0.33 ± 0.06 Hz (data from five cells). TTX (1 μM) was applied to isolate synaptic terminal activity, so that miniature glutamatergic synaptic events

(mEPSC) could be recorded. In these conditions mEPSC amplitude was -20.5 ± 2.1 pA and the frequency was 0.25 ± 0.04 Hz (data from the same five cells). The decrease in amplitude and frequency was statistically significant (P = 0.001 for amplitude and P = 0.03 for frequency, n = 5). We wondered if blocking acetyl cholinesterase (AChE) activity with edrophonium (20 μM) could boost cholinergic activity and help to unmask cholinergic events. However, as shown in Fig. 16, edrophonium did not have any effect on mEPSC amplitude on frequency. After edrophonium application, mEPSC amplitude became -17.8 ± 1.6 pA (P = 0.38, n = 5, Fig. 16), and the frequency was 0.31 ± 0.04 Hz, which did not reach statistically significant difference (P = 0.1, n = 4, Fig. 16). The current baseline was not affected by edrophonium application.

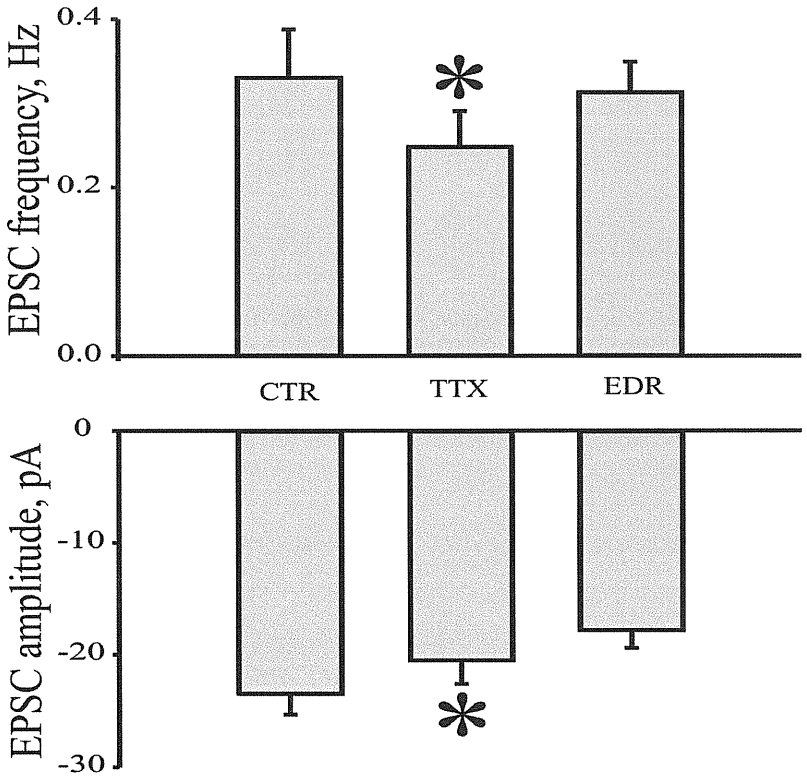

Fig. 16. Edrophonium effect on glutamate release. In control saline sEPSC amplitude was -23.5 ± 1.9 pA and the frequency was 0.33 ± 0.06 Hz, n = 5. After TTX (1 μM) application, mEPSC amplitude decreased to -20.5 ± 2.1 pA, and the frequency became 0.25 ± 0.04 Hz, which was statistically different (P = 0.001 for the amplitude and P = 0.03 for the frequency, n = 5). Edrophonium (EDR, 20 μM) in the presence of TTX did not change mEPSC amplitude or frequency (-17.8 ± 1.6 pA and 0.31 ± 0.04 Hz, n = 4). The asterisk indicates statistically significant results (P < 0.05) between control saline and TTX saline.

2.2 nAChR action on GABAergic transmission

Anatomical studies have shown that nAChRs are often expressed at GABAergic synapses, both presynaptically and postsynaptically (Fabian-Fine *et al.*, 2001; Kawai *et al.*, 2002; Zago *et al.*, 2006). nAChRs cocluster with $GABA_A$ receptors on hippocampal interneurons (Liu *et al.*, 2001; Kawai *et al.*, 2002) and on chick ciliary ganglion neurons (Wilson Horch & Sargent, 1995; *Shoop et al.*, 1999). Recently it was shown that nAChRs downregulate postsynaptic GABAergic currents (Wanaverbecq *et al.*, 2007; Zhang & Berg, 2007). At presynaptic level, nAChRs slightly increase GABA release, but the overall effect of nAChRs is dominated by postsynaptic depression of GABAergic signaling (Wanaverbecq *et al.*, 2007). Thus, I have tested if nAChRs, besides acting on glutamatergic transmission, can regulate GABAergic transmission on hypoglossal motoneurons.

I have applied nicotine (10 μM) in the presence of CNQX (20 μM), APV (50 μM) and strychnine (0.4 μM) to block AMPA, NMDA and glycine receptors, respectively. Since the depression of GABAergic neurotransmission was abolished by chelating intracellular Ca^{2+} and attenuated by inhibitors of protein kinase C (PKC) (Wanaverbecq *et al.*, 2007), instead of 10 mM, I have used 1 mM EGTA in the intracellular solution to provide mild buffering of calcium. Before nicotine application, sIPSC frequency was 0.1 ± 0.03 Hz and after 5-6 min of application, the frequency increased to 0.22 ±0.09 Hz ($P = 0.01$, $n = 4$). sIPSC amplitude in control saline was -25.23 ± 2.1 pA and after nicotine application it became -30.14 ± 3.2 pA. ($n = 4$). However, the effect was not statistically significant ($P = 0.22$, $n = 4$). The increase in sIPSC frequency suggests a presynaptic action of nAChRs, without a postsynaptic depressant action. To validate this notion, I have made a recording when intracellular pipette contained 10 mM EGTA. Glutamatergic neurotransmission was blocked by CNQX and APV, as described previously. In control saline, sIPSC frequency was 1.43 ± 0.19 Hz and the amplitude was -52.8 ± 4 pA ($n = 3$). Nicotine (10 μM) application did not change the frequency (0.95 ± 0.06 Hz, $P = 0.19$, $n = 3$) nor amplitude (-57.4 ± 4.6 pA, $P = 0.49$, $n = 3$). Thus, on HMs, nAChR activation presynaptically upregulated GABA release and did not affect postsynaptic GABAergic neurotransmission.

3. Brainstem nAChR evoked oscillations at network level

3.1 Nicotine induced oscillatory activity in HMs

I have investigated nAChR action on glutamatergic neurotransmission. Even if boosting cholinergic activity with edrophonium did not affect glutamatergic transmission at a single cell level, a previous study in our lab has showed that exogenous nicotine (0.5 μM) application first facilitated glutamatergic transmission on motoneurons and later depressed it through receptor desensitization (Quitadamo *et al.*, 2005). These effects were, however, detected at nicotine doses much lower than the ones necessary for saturating the α4β2 and α7 classes of nAChRs (Chavez-Noriega *et al.*, 1997). We wondered if more intense nicotinic activation could introduce additional changes in motoneuron excitability. To this end, I applied 10 μM nicotine concentration to the brainstem slices.

Fig. 17A shows that, under voltage clamp configuration (Vh = -65 mV), after 1.5-2 min delay from the start of application, nicotine produced an inward current that was accompanied by oscillatory activity indicated by a star (see expanded timescale in Fig. 17B, left trace). Membrane oscillations required continuous application of nicotine, because they disappeared after nicotine washout (Fig. 17B, right trace). Nevertheless, not all HMs generated oscillations after nicotine (10 μM) application: the occurrence of this phenomenon did not depend on the recording conditions because there was no significant difference between the fraction of oscillating HMs (39 % of 249 cells) recorded with intracellular Cs^+ and the fraction of oscillating HMs (23 % of 17 cells) recorded with intracellular K^+. This observation suggests that, even when the HM leak conductance was minimized by intracellular Cs^+, there was no increased likelihood of detecting oscillations.

The oscillation frequency was in the range of 3-13 Hz (mean = 5.6 ± 0 .3 Hz for a sample of 32 HMs) with high degree of regularity because its coefficient of variation (CV) was 9.6 ± 0.9 %. Each oscillatory cycle consisted of a slower outward current and a faster inward current with peak-to-peak oscillation amplitude of 70.5 ± 5.1 pA. Figure 17C (note much faster timescale) compares (for the same HM) glutamatergic spontaneous excitatory postsynaptic currents (sEPSCs) before and during nicotine application with similar onset and decay (rise time 1.4 ± 0.1 ms, decay time 5.0 ± 0.5 ms before nicotine versus 1.6 ± 0.1 ms and 6.4 ± 0.6 ms in the presence of nicotine; n = 15). In the presence of nicotine, sEPSC amplitude was slightly increased (-20.3 ± 1.1 pA before nicotine versus -23.0 ± 1.1 in the presence of nicotine; P = 0.01, n = 42). Oscillatory activity could also be produced with 5 μM (n = 2) or 20 μM (n = 2) nicotine concentration without change in the oscillation characteristics. Thus, once a certain

network level of activity was achieved, oscillations emerged with similar characteristics and abruptly disappeared when the network excitability presumably fell below threshold. The stereotypic nature of oscillations suggested them to be all-or-none signals electrically propagated within a functionally connected network.

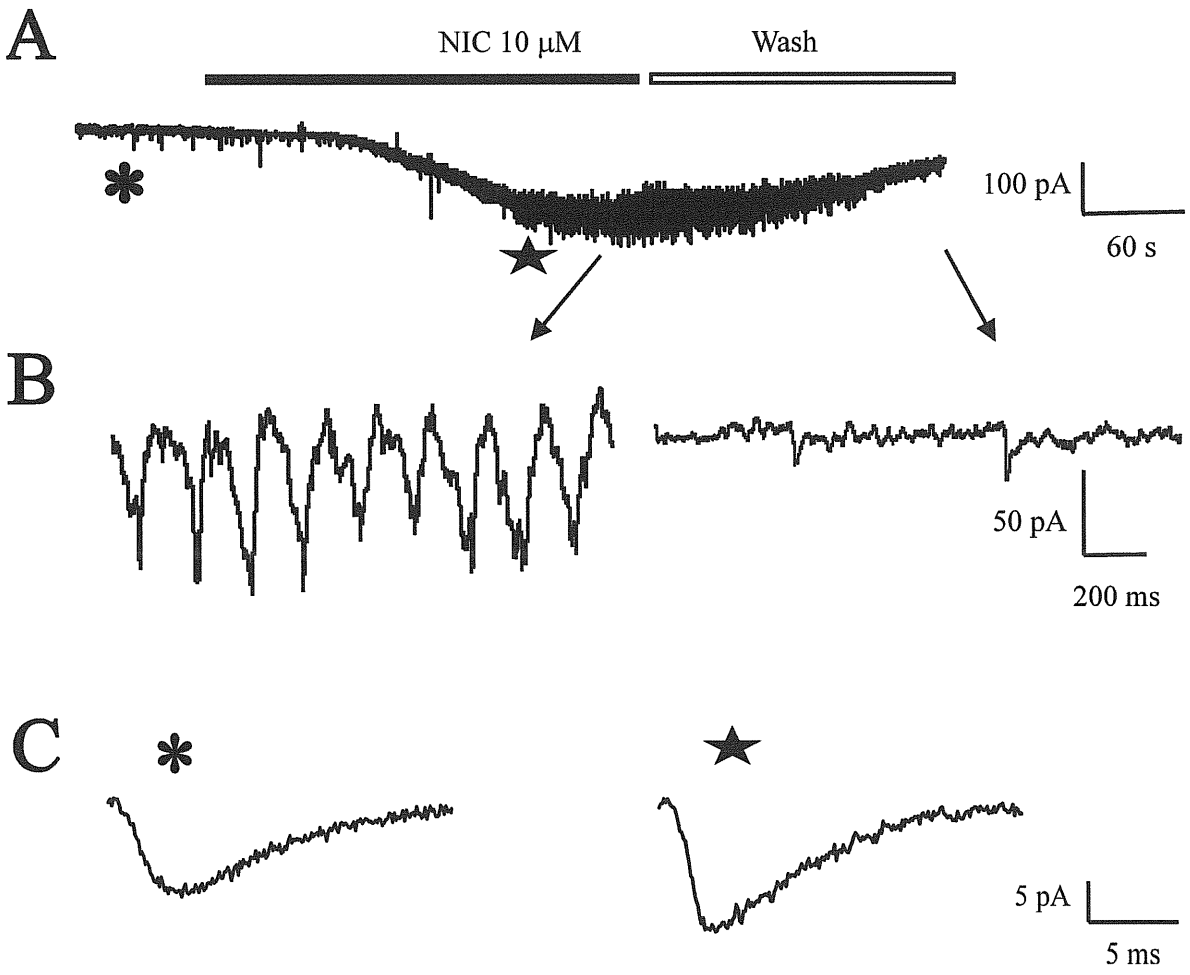

Fig. 17. Nicotine (10 μM) application produced oscillatory activity on HM. (A) Example of nicotine effect on a motoneuron recorded under voltage clamp conditions in the presence of strychnine (0.4 μM) and bicuculline (10 μM). Nicotine produced an inward current and oscillatory activity, which disappeared after nicotine washout. (B) Faster time-base trace shows characteristics of oscillations (left), and their disappearance after nicotine washout (right). (C) Spontaneous postsynaptic currents (sEPSCs; average of 30 events) possess the same kinetics before (left; asterisk) and after (right; star) nicotine application. All data are from the same cell.

3.2 Time course of oscillatory activity

Because the oscillation frequency placed these responses in the theta frequency range of electrical oscillations typically associated with a range of behavioral activities (Smith & Denny, 1990; Tarasiuk & Sica, 1997; Funk & Parkis, 2002; Hasselmo, 2005), it seemed interesting to explore their properties. First, I investigated for how long they could last and whether they changed their characteristics during continuous application of nicotine. Fig. 18A shows a typical example of sustained oscillations in the continuous presence of 10 μM nicotine. After 1-1.5 min nicotine administration, the inward current was suddenly accompanied by intense oscillatory activity which persisted for 8.5 min, and then vanished. Fig. 18A also indicates a slow decline in the inward current after the disappearance of oscillations. On average, oscillatory activity lasted for 8.3 ± 0.6 min (n = 12). In order to quantify oscillation frequency changes over time, I divided the oscillatory trace into 30 s epochs starting from the onset of the oscillations and expressed them as a fraction of the value found during the first epoch. Bottom traces of Fig. 18A show that, at the end of the oscillatory activity the frequency of oscillations was similar to the one at the start (Fig. 18B).

I also measured spontaneous synaptic activity and expressed its frequency with respect to the value before nicotine application. Fig. 18C shows a plot of the oscillation frequency versus the sEPSC frequency (n = 5). The data are best fitted with linear regression (R = 0.64), indicating a high degree of correlation between such events.

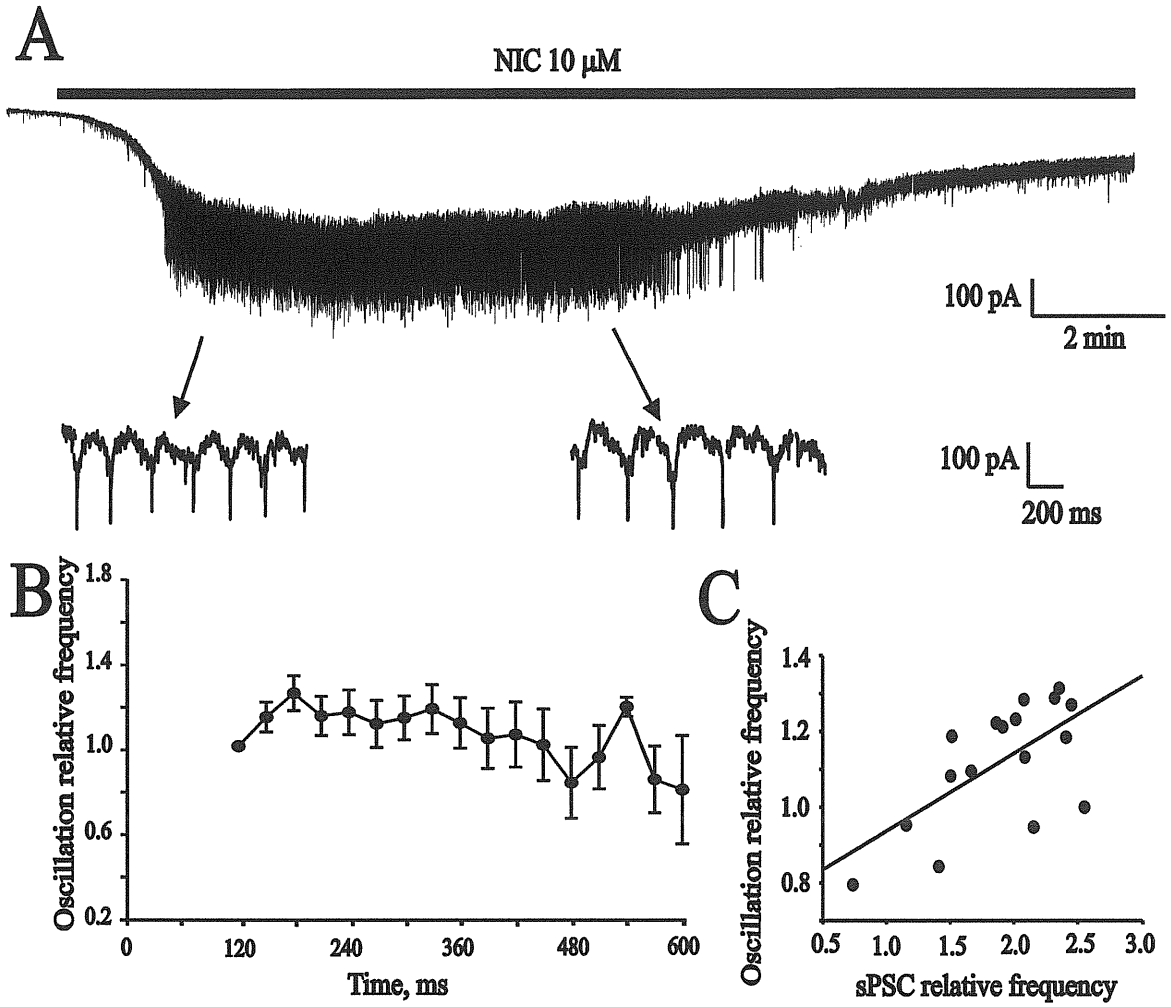

Fig. 18. Time profile of oscillatory activity. (A) Bath-applied nicotine (10 μM) produced an oscillatory behavior which spontaneously vanished after 9 min. Oscillatory patterns showed similar characteristics at the beginning (see faster time base trace indicated by arrow on the left) and at the end (right) of the rhythm. (B) Plot of oscillation fractional frequency versus time. The oscillatory trace was divided into 30 s epochs, starting from the onset of oscillations. The frequency in the first epoch was taken as 1, and the frequency of the following epochs was expressed as a fraction of the value found in the first epoch. The Figure indicates maximal value after 60 s from nicotine application with subsequent, modest decreases. Same HM as in A. (C) Plot of oscillation frequency versus sEPSC frequency for 5 HMs. Straight line has a correlation coefficient (R) = 0.64, indicating good data correlation.

3.3 Single HM properties and their contribution to oscillatory behavior

It was important to find out if oscillating HMs possessed special intrinsic properties that changed following nicotine application. Table 2 summarizes such data. In control solution, oscillating HMs had significantly (P = 0.04) lower input resistance than non-oscillating HMs, while sEPSC frequency and amplitude were similar. On oscillating HMs, 10 μM nicotine induced an inward current twice as large as on non-oscillating HMs (P = 0.0017). On oscillating cells, nicotine doubled the sEPSC frequency (P = 0.00036) and slightly but significantly enhanced the amplitude of sEPSCs (P = 0.01). On non-oscillating cells, the frequency of sEPSCs was unchanged, while the amplitude decreased (P = 0.002).

Experiments were done with slices from P0-P5 animals. Only in one case oscillatory activity was observed at P0, as the incidence of detecting oscillations was the highest at P3 (30 %) and P4 (33 %; n = 39 HMs). Once oscillations were produced, their characteristics did not depend on animal age. Oscillatory HMs could be found in each sub-region of the hypoglossal nucleus (dorsal, ventral, central or lateral to the forth ventricle) as well as through the rostro-caudal axis of the XII nucleus.

Table 2. HM properties in the presence of nicotine. NIC = nicotine (10 μM). n = 37 for oscillating and n = 24 for non-oscillating HMs.

	Oscillating HMs	Non-oscillating HMs	
Inward current, pA	-111 ± 10	-52 ± 6	**P = 0.0017**
Rin, MΩ			
Before NIC	199 ± 23	297 ± 43	**P = 0.04**
In NIC solution	211 ± 28	251 ± 23	
sEPSC frequency, Hz			
Before NIC	0.31 ± 0.03	0.33 ± 0.05	
In NIC solution	0.61 ± 0.08	0.31 ± 0.04	
	P = 0.00036		
sEPSC amplitude, pA			
Before NIC	-20.3 ± 1.1	-23.1 ± 0.9	
In NIC solution	-23 ± 1.1	-19.1 ± 0.9	
	P = 0.01	**P = 0.002**	

3.4 Oscillatory activity dependence on network properties

The stereotyped, repeated nature of oscillatory behavior raised the question about its origin and underlying mechanisms. To find out if oscillations were generated by network activity or were intrinsic to the recorded HM, we explored their voltage sensitivity. Without nicotine application, oscillations could never be evoked by merely changing the Vh of a single HM (n=8) or by elevating extracellular K^+ to 7 mM (n = 5). Once nicotine induced oscillations and the inward current reached an apparent steady-state level, the HM Vh was changed from –90 to +80 mV. One representative experiment is shown in Fig. 19A, in which 30 cycles of activity were averaged at different Vh: the period of oscillations was essentially unchanged, while their amplitude was partially changed. Fig. 19B demonstrates the independence of inter-event interval from Vh (n = 6), whereas Fig. 19C shows the limited dependence of oscillation amplitude on Vh (same 6 cells) as oscillations persisted even at very positive values (+80 mV).

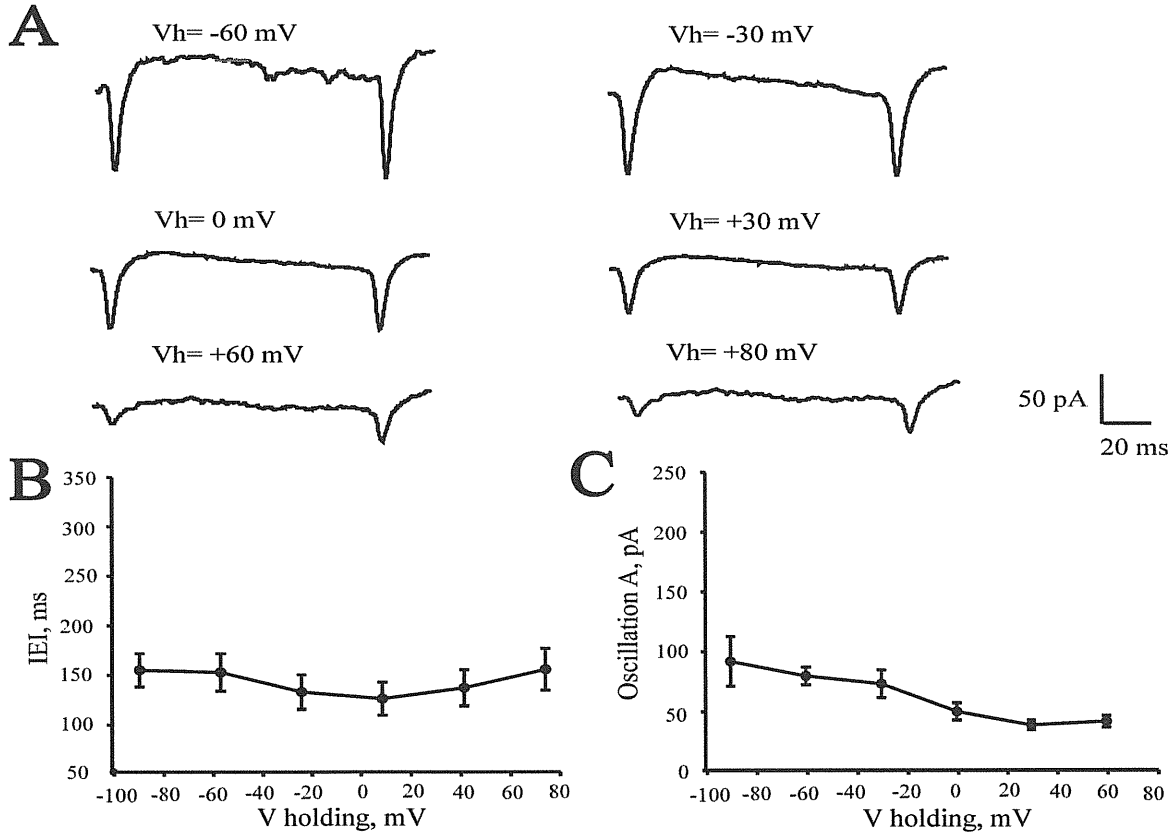

Fig. 19. Voltage dependence of oscillatory activity. (A) In voltage clamp experiments, oscillation period and amplitude were not dependent on holding potential in the range from -60 mV to 80 mV. Traces were averaged of 30 responses for each indicated holding potential. (B) Plot of oscillation inter-event interval (ISI) versus holding potential values in the range from -90 mV to 70 mV for six HMs. Note similar values at all recorded potentials. (C) Plot of oscillation amplitude versus holding potential values in the range from -90 mV to 70 mV for the same cells shown in B. Note limited decrease in oscillation amplitude at potentials less negative than -20 mV.

3.5 nAChR subtype contribution to oscillatory activity

Since HMs possess α7 (Dehkordi *et al.*, 2005 and my data) as well as α4β2 (Zaninetti *et al.*, 1999; Chamberlin *et al.*, 2002 and my data) nAChR subtypes, I tested if both of these nAChR subtypes are involved in the oscillatory rhythm. I first tested if α4β2 nAChR subtypes were involved in oscillatory patterns. As soon as oscillations appeared, I applied 0.5 μM DHβE, a selective antagonist of the α4β2 subtype (Harvey & Luetje, 1996). Figure 20A shows a representative example of such an experiment. Once nicotine had evoked oscillatory activity, 0.5 μM DHβE blocked oscillations within 3.7 ± 0.9 min, a time significantly faster than the normal duration of oscillations ($P = 0.004$, $n = 5$, see Fig. 20A, bottom traces for fast timebase records). To check for the contribution by α7 nAChRs, I used 5 nM MLA, a selective antagonist of this receptor subtype (Palma *et al.*, 1996; Bergmeier *et al.*, 1999; Davies *et al.*, 1999). Figure 20B shows an example of MLA-induced block of nicotine-evoked oscillations after 2.5-3 min. On average, MLA blocked oscillations after 2.5 ± 0.5 min ($n = 4$), a value significantly smaller than control ($P = 0.001$). It is noteworthy that there was no difference in the time taken by each antagonist to block oscillations. Both antagonists inhibited the nicotine-induced inward current (26 ± 11 % of control after applying DHβE, $n = 5$, and 46 ± 24 % after MLA application, $n = 4$). These data show that nAChRs needed continuous activation in order to maintain oscillatory behavior in HMs.

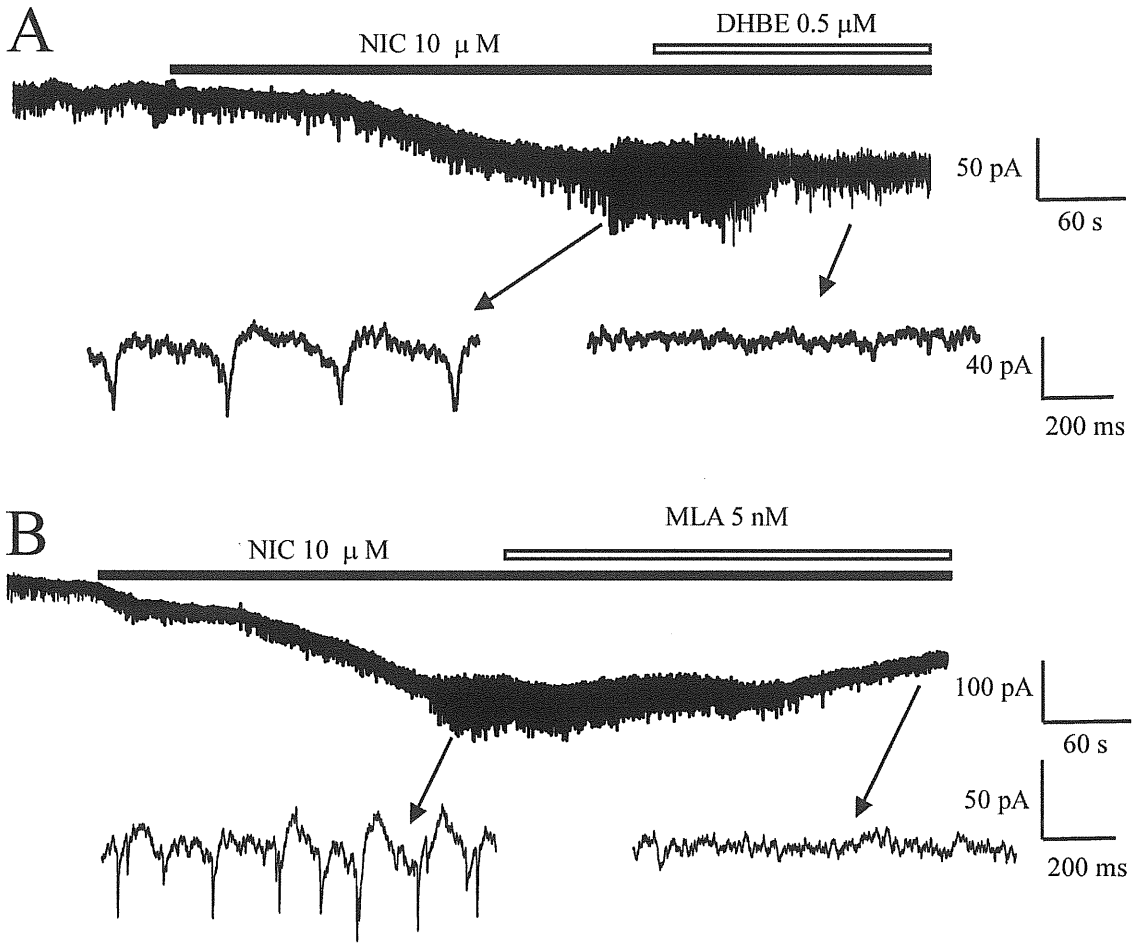

Fig. 20. Nicotinic receptor activation was required for oscillations. (A) Oscillatory activity evoked by nicotine (applied as shown by the filled bar) was blocked by 0.5 μM dihydro-β-erythroidine (DHβE; applied as indicated by the open bar), a selective α4β2 nAChR subtype blocker. Faster time base records are shown before (lower panel, left) and after (lower panel, right) DHβE application. (B) Methyllicaconitine (MLA; 5 nM), a selective blocker of α7 nAChRs, abolished oscillatory activity. Expanded time scale recordings before (lower panel, left) and after (lower panel, right) MLA application are also shown.

3.6 Desensitization of HMs and network nAChRs

Neuronal nAChRs undergo desensitization following application of nicotine (Paradiso & Steinbach, 2003; Zhang *et al.*, 2004; Giniatullin *et al.*, 2005; Quitadamo *et al.*, 2005). Since the oscillatory activity of HMs lasted on average >8 min and required continuous nicotine administration, these results implied that at least part of the nAChR population remained active. This novel result prompted me to test if such slow-desensitizing nAChRs were located on HMs or within the premotoneuronal network. In keeping with our previous report (Quitadamo *et al.*, 2005), I used a puffer pipette to apply nicotine mainly to the HM somatic nAChRs, while bath-applied nicotine presumably bound HM as well as more remote, network nAChRs.

In a representative experiment depicted in Fig. 21A, puffer-applied nicotine (arrows) produced transient oscillatory behavior, which quickly disappeared (this behavior was observed in two out of 6 HMs). After nicotine (10 μM) was added to the extracellular solution (horizontal filled bar in Fig. 21A), persistent oscillatory activity appeared. While oscillations and the steady inward current were apparently stable, responses to brief nicotine pulses were largely attenuated. Figure 21B summarizes the nicotine effects for the cell depicted in Fig 21A. Oscillation frequency, sEPSC frequency and the amplitude of nAChR responses to nicotine puffers were measured at 30 s epochs and expressed as relative values with respect to those before bath-application of nicotine (indicated by the shaded area). It took 60 s for bath-applied nicotine to produce an oscillatory behavior, whose frequency then decreased slightly and suddenly vanished in coincidence with the return of the sEPSC frequency to control. Conversely, nAChRs, located on HMs, desensitized quickly, as their responses to puffers of nicotine diminished shortly after the start of nicotine bath-application (2 min later it was only 40 % of control; Fig. 21B). Hence, at a time when HM nAChRs were largely desensitized, network nAChRs presumably involved in boosting sEPSC frequency and triggering oscillatory behavior remained active.

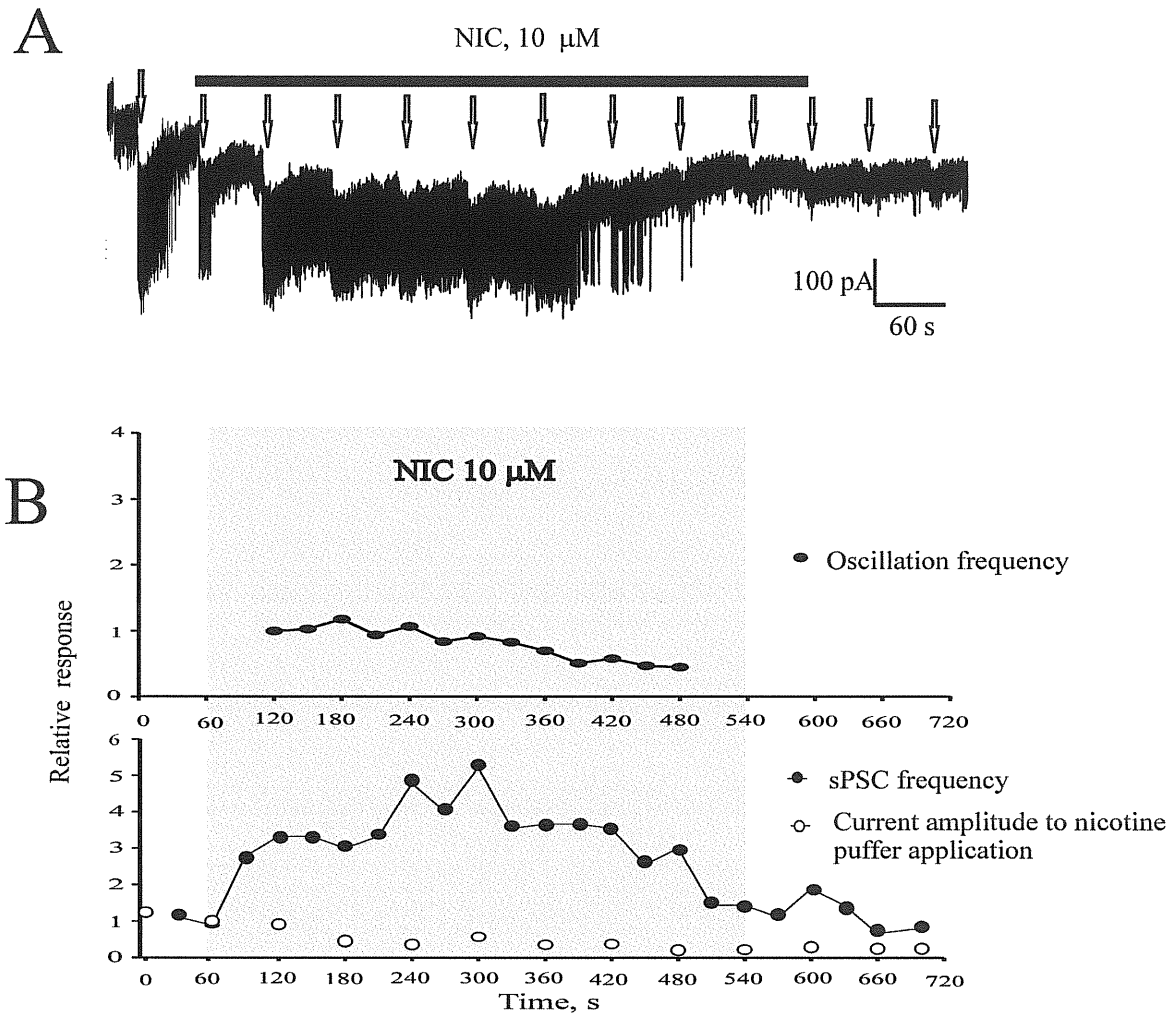

Fig. 21. Time-course of desensitization of nicotinic receptors, located on motoneurons and within the premotoneuronal network. (A) Puffer pulses (50 ms, arrows) of nicotine (2 mM) produced inward currents from HM. When nicotine (10 μM) was applied continuously via the bathing solution, oscillatory activity appeared while responses to puffer pulses became very small (20 % of control). (B) Summary plots of oscillation frequency (top panel), sEPSC frequency and response amplitude to nicotine puffer application (bottom panel). Shaded area indicates the time of 10 μM nicotine bath-application. Oscillations appeared after 30 s from nicotine application with slow decrease in their frequency. Currents produced by nicotine puffer applications were largely inhibited before oscillations stop. Thus, motoneuron nicotinic receptors desensitized rapidly and were not responsible for oscillatory behavior maintenance. The sEPSC frequency (an index of premotoneuronal network nAChR activation) increased 3-5 times after nicotine bath-application. The time when sEPSC frequency returned to its control level closely correlated with the time when oscillations stopped. Thus, loss of oscillations was associated with network nAChR desensitization. Frequency values were obtained by analyzing 30-s consecutive epochs. All values were normalized to control. Same cell as in A.

3.7 Pharmacology of oscillatory behavior

3.7.1 Glutamate receptor and synaptic activity involvement in the rhythm

Application of 1 μM TTX via the bathing solution blocked oscillatory activity within 2.7 ± 0.7 min, while, in the absence of TTX, oscillations lasted 8.3 ± 0.6 min (P = 0.002, n = 4, Fig. 22). The depression of sEPSCs by TTX indicated that spontaneous glutamatergic currents were events predominantly dependent on network synaptic activity rather than originating in a single cell. The inward current produced by nicotine was also diminished (58 ± 13 % of control) by TTX. Lower traces in Fig. 22 show, on a faster time scale, that the regular rhythmic activity disappeared after TTX application.

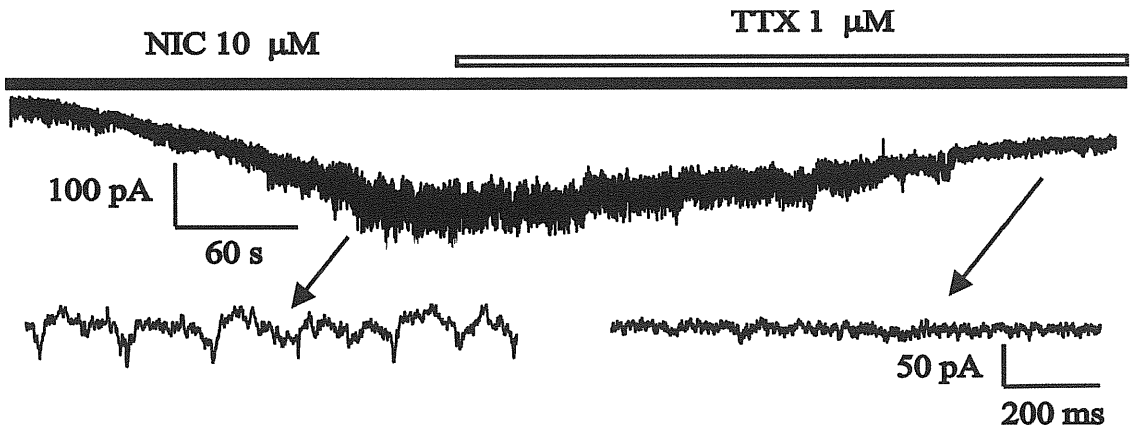

Fig. 22. Synaptic activity role in the oscillations. Nicotine induced oscillations were blocked by the selective Na^+ channel blocker TTX (1 μM). In lower panel, faster time course traces show rhythmic oscillatory activity (left) and its disruption by TTX (right).

I next tested the glutamate receptor contribution to the oscillatory activity. Figure 23 shows that AMPA/kainate receptors were required for this activity because the antagonist CNQX (20 μM) blocked oscillatory patterns within 5 ± 0.4 min (P = 0.048, n = 6). After the arrest of oscillations, the remaining inward current was not significantly reduced.

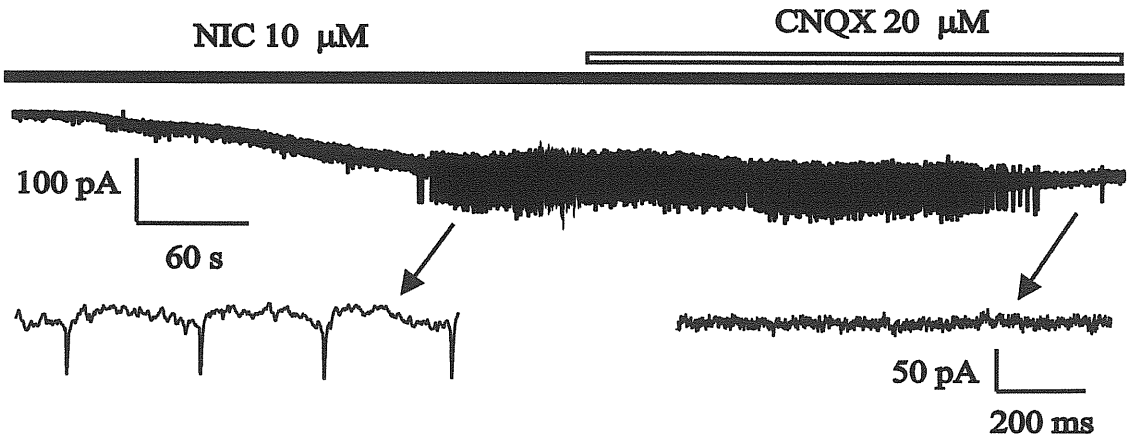

Fig. 23. AMPA receptor involvement in the oscillatory rhythm. Nicotine produced an inward current with oscillatory activity that, after 4 min, was suppressed by 20 μM CNQX, a blocker of AMPA/ kainate receptors. Expanded time scale shows rhythmic activity (lower panel, left), which was arrested after CNQX application (lower panel, right).

I also investigated the NMDA receptor involvement in this phenomenon. After application of APV (50 μM), a selective NMDA receptor antagonist, the nicotine-evoked oscillations disappeared with similar timecourse regardless of the presence of APV (8.6 ± 0.6 min in the presence of APV versus 8.3 ± 0.6 min in control, n = 4). In this case, the nicotine-evoked inward current gradually decreased together with slowing down of oscillation period (80% of control) and amplitude (62% of control; see Fig. 24 lower panel, central for records taken at 4.7 min). Further fall (60% for period and 42% for amplitude) was observed 7.8 min later (Fig. 24 lower panel, right) before a full arrest of oscillations (> 8 min). In the absence of pharmacological antagonists, oscillation persisted >8 min without changing their characteristics (Fig. 18 left and right). In 3 out of 4 cells, APV attenuated oscillatory activity without complete suppression, while in one cell APV had no effect. Hence, oscillatory activity required continuous activation of CNQX-sensitive receptors and was modulated, in part, by APV-sensitive receptors.

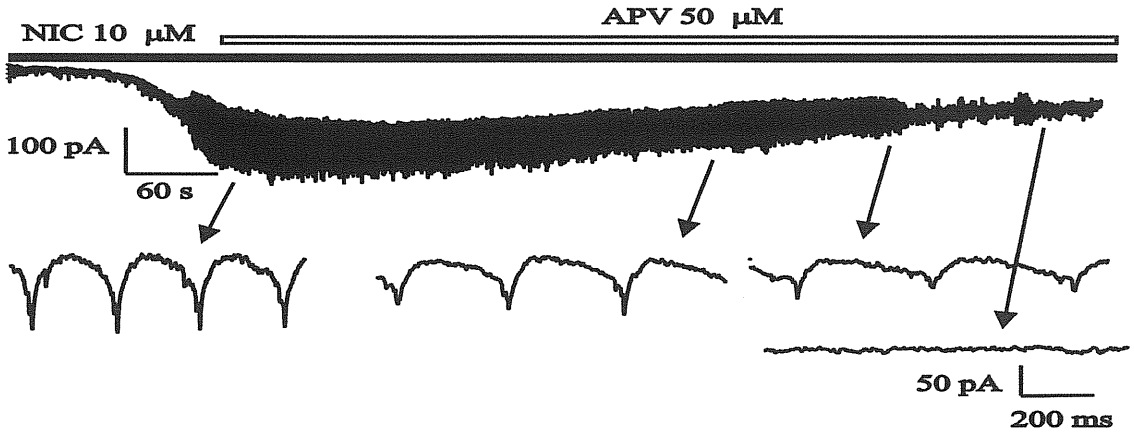

Fig. 24. NMDA receptor role in the oscillatory behaviour. Nicotine produced oscillations were modulated by 50 μM APV, NMDA receptors blocker, application. In this cell the oscillations lasted about 8 min; the time which was compatible with a spontaneous oscillation stop. Lower panels show that APV continuously decreased oscillation period and amplitude until full suppression.

As metabotropic glutamate subtype 1 receptors of group I (mGluR1s) are functionally expressed in the developing XII nucleus (Hay *et al.*, 1999; Nistri *et al.*, 2006) and their activation can produce theta frequency oscillations (Sharifullina *et al.*, 2005), it seemed likely that they could play an important role even in the nicotine-induced oscillatory activity. To this end, I used AIDA, a selective mGluR1 antagonist (Pellicciari *et al.*, 1995; Sharifullina *et al.*, 2005). Figure 25 shows that 300 μM AIDA blocked the oscillatory behavior within 2.3 ± 0.4 min (see also Fig. 25 lower panel, left and right traces; n = 3), which was significantly faster than the spontaneous oscillation arrest (P = 0.004, n = 3).

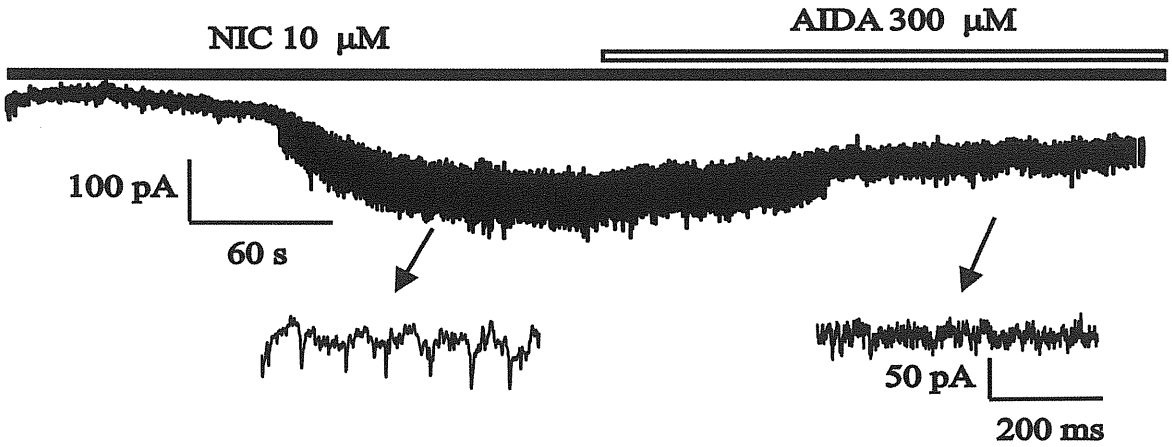

Fig. 25. mGluR involvement in the oscillatory rhythm. AIDA (300 μM), a blocker of mGluR1s, inhibited oscillatory behavior. Recordings on a faster time scale represent rhythmic activity (lower panel, left) abolished after 2.5 min of AIDA application (lower panel, right).

3.7.2 Synaptic inhibition role in oscillatory behavior

We wondered if oscillations could also be induced in more physiological conditions, namely without blocking glycinergic and GABAergic transmission. Omission of strychnine and bicuculline from the extracellular solution led to increased amplitude and frequency of sIPSCs. Large sIPSCs are known to be generated by network-dependent release of GABA and glycine (Donato & Nistri, 2000). Despite intact synaptic inhibition, oscillations still could be induced by 10 μM nicotine as indicated by a typical example in Fig. 26. In standard saline solution, large sIPSCs were detected (-52 ± 2 pA on average) at high frequency (3.9 Hz) as shown in Fig. 26 (lower panel, left). After 2 min delay, nicotine induced an inward current with oscillatory activity (Fig. 26 lower panel, right) analogous to the one observed when inhibition was pharmacologically blocked. In extracellular solution with intact synaptic inhibition, nicotine produced oscillatory behavior in 17 % HMs (n = 17). Neither the time course of oscillatory behavior development (3.6 ± 0.5 min without inhibition versus 2.2 ± 0.5 min with inhibition) nor oscillation temporal characteristics (inter-event interval = 210 ± 10.5 ms with intact inhibition versus 177 ± 20 ms without inhibition; CV = 10 ± 2 % with inhibition versus 9.65 ± 1 % without inhibition, n = 36) were affected by a synaptic inhibition. Thus, inhibition block was not a prerequisite for detecting oscillations; it rather increased the probability of detecting them. Since inhibitory receptor antagonists optimized the experimental conditions to analyze oscillatory behavior uncontaminated by large synaptic inhibitory events, most data were collected under such experimental conditions.

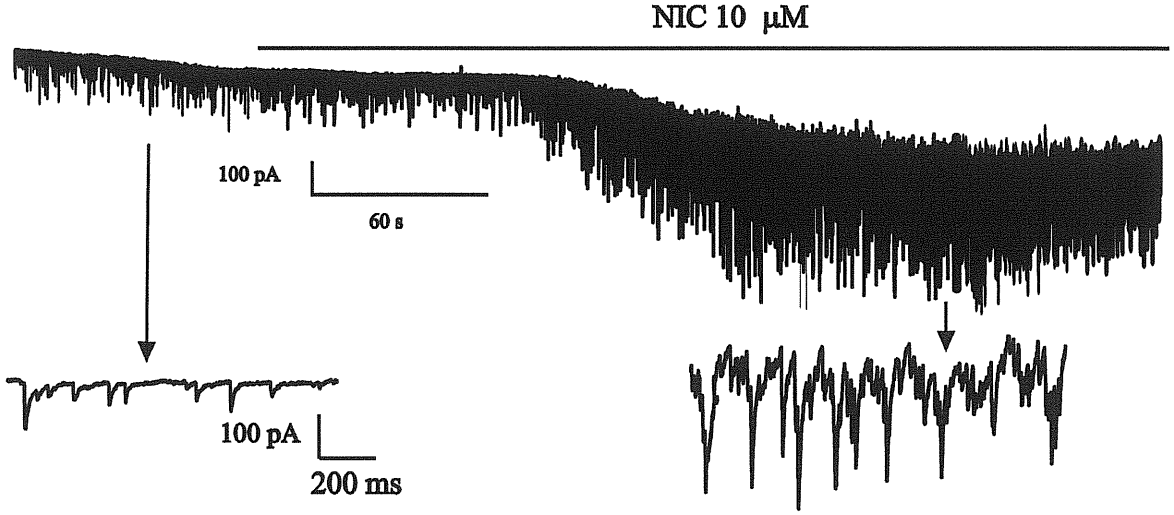

Fig. 26. Role of synaptic inhibition in oscillatory behavior. Nicotine could produce oscillations in motoneurons with intact synaptic inhibition. Example shows that, when strychnine and bicuculline were omitted from the saline solution, the HM possesses high spontaneous activity composed of excitatory and inhibitory sIPSCs (lower panel, left). Bath-applied nicotine induced rhythmic oscillatory behavior, mixed with spontaneous activity (lower panel, right).

3.7.3 Electrical coupling between oscillating HMs

Previous studies have shown electrical coupling among brainstem motoneurons (Mazza *et al.*, 1992; Rekling *et al.*, 2000). Since electrical coupling is functionally important for oscillatory activity in certain brain areas (Galarreta & Hestrin, 1999; Landisman *et al.*, 2002; LeBeau *et al.*, 2003) including the nucleus hypoglossus (Sharifullina *et al.*, 2005), it was important to ascertain the role of electrical coupling in the nicotine-dependent oscillatory activity. For this purpose, I used, as a pharmacological tool, the gap junction blocker carbenoxolone (100 μM) that was previously demonstrated in our lab to be an effective inhibitor of gap junction-mediated electrical coupling among HMs (Sharifullina *et al.*, 2005). Indeed, as soon as oscillations developed, bath-application of carbenoxolone (100 μM) increased the period (201 ± 15 %, n = 4; P < 0.001) and attenuated amplitude (64 ± 10 %, n = 4, P < 0.001) of oscillations within 8 min (Fig. 27, left and central). In three HMs, oscillations were fully suppressed in less than 8 min exposure to carbenoxolone.

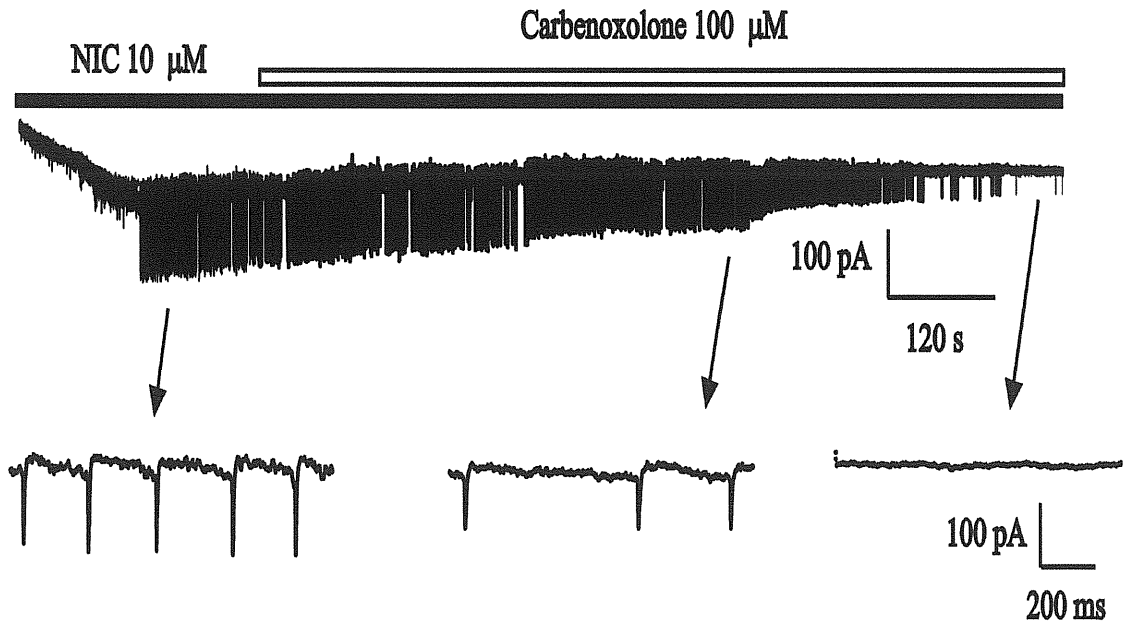

Fig. 27. Role of electrical coupling in oscillatory behavior. The gap junction blocker carbenoxolone (100 μM) depressed oscillatory behavior. Periodic oscillations (lower panel, left) became sporadic after carbenoxolone application, their amplitude and frequency decreased (lower panel, centre), until they finally disappeared (lower panel, right).

It was, however, noteworthy that carbenoxolone *per se* did not significantly change the excitability of single HMs. In fact, in current clamp experiments, the threshold for action potential firing was -47 ± 1 mV in control conditions and -48 ± 3 mV after 10 min application of carbenoxolone, respectively (P = 0.89, n = 6, Fig. 28). Likewise, the number of spikes produced by the same DC current pulse (10-80 pA range), injected at fixed amplitude into each cell, was 9 ± 1 in control solution and 9 ± 2 after 10 min application of carbenoxolone (P = 0.64, n = 4; Fig. 28). These data demonstrated lack of effect by carbenoxolone on neuronal excitability.

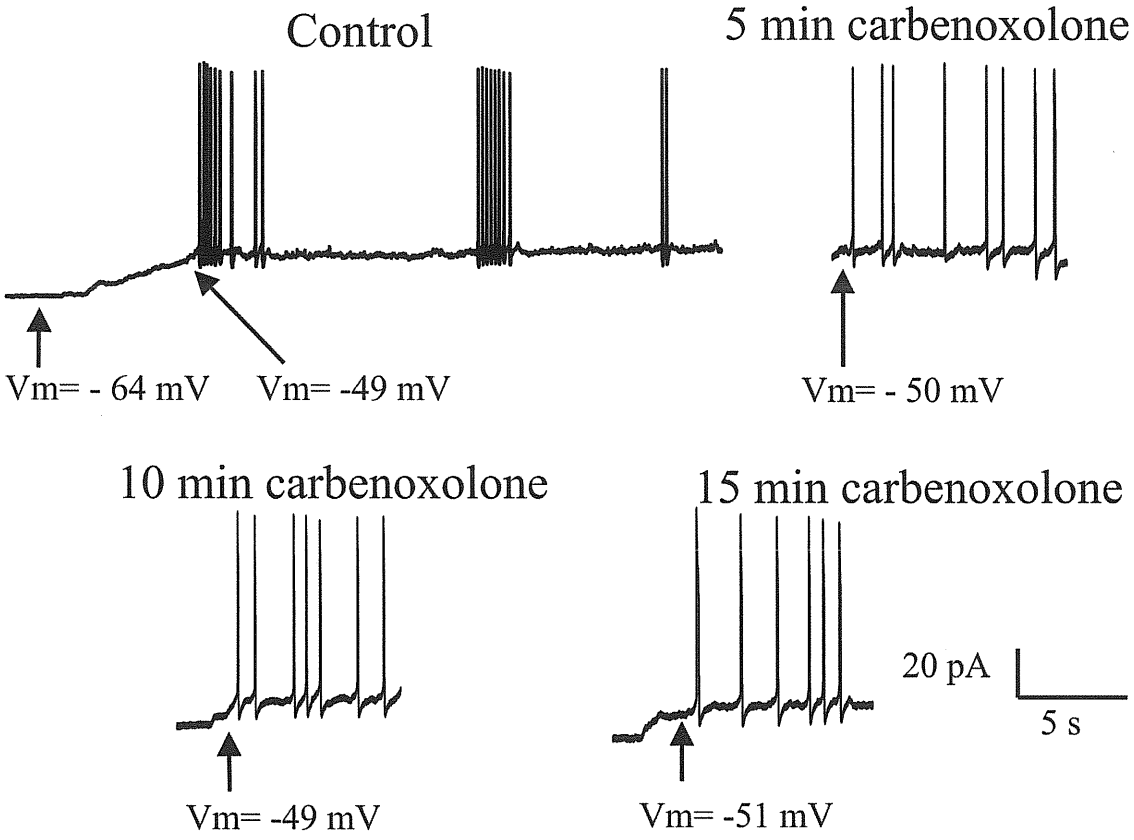

Fig. 28. Carbenoxolone lack of action on HM excitability. Under current clamp conditions, a motoneuron was depolarized from -64 to -49 mV by injecting current (25 pA) to start action potential firing. On the same cell, repeating this test in the presence of carbenoxolone (100 μM) at different times from the start of the application, the same voltage threshold value for action potential generation was observed, indicating that this drug did not change motoneuronal excitability.

3.7.4 Persistent inward current involvement in the oscillations

Since persistent sodium current (PIC) seems to be necessary for prolonged rhythmic discharges (Darbon *et al.*, 2004; Cramer *et al.*, 2007; van Drongelen *et al.*, 2006; Zhong *et al.*, 2007), its inhibition by riluzole might disrupt collective behaviour of motoneurons. I_{NaP} is, however, not essential for rhythm generation by brainstem preBotzinger neurons (Pace *et al.*, 2007 a, b). Thus, we raised a question about PIC role in nicotine-induced oscillations in HMs. Recent data shows, that PICs, evoked by depolarization of brainstem (Powers & Binder, 2003; Moritz *et al.*, 2007) or spinal motoneurons (Harvey *et al.*, 2006; Theiss *et al.*, 2007), are composed of I_{NaP} and could be blocked by riluzole (Del Negro *et al.*, 2005; Miles *et al.*, 2005; Harvey *et al.*, 2006; Theiss *et al.*, 2007).

Thus, I have tested riluzole (10 μM) action on PICs and the rhythmic discharges. PICs, which can be expressed by the soma of HMs (Moritz et al., 2007), contribute to integration of motoneuron signals for patterned output (Brownstone, 2007), and are mediated by sustained influx of Na^+ and/or Ca^{2+} (Crill, 1996; Russo & Housgaard, 1999). Since riluzole was reported to inhibit PICs (Del Negro *et al.*, 2005; Miles *et al.*, 2005; Harvey *et al.*, 2006; Theiss *et al.*, 2007), we first monitored PICs of neonatal rat HMs to find out where they were sensitive to riluzole, and how their presence was temporally related to nicotine-evoked oscillations. Averaged PIC amplitude in control conditions did not differ between oscillating (300 ± 35 pA; n = 10) and non-oscillating cells (391 ± 73 pA, P = 0.275, n = 11). Nicotine did not change PIC amplitude in oscillating cells (270 ± 42 pA after 5 min nicotine application, while oscillations were present, P = 0.3; n = 11) as well as in non-oscillating cells (396 ± 90 pA after 5 min nicotine application, P = 0.19; n = 10).

However, under voltage clamp conditions, in six out of seven cells nicotine-induced oscillations were blocked by riluzole (10 μM) and the steady inward current evoked by nicotine was decreased from 325 ± 80 pA to 160 ± 25 pA (P = 0.03, n = 7). On average, in the presence of riluzole, oscillations lasted significantly less than their normal time course (187 ± 40 s, n = 5, vs 497 ± 37 s, n = 10; P < 0.001). In the remaining cell, oscillation period and amplitude were merely attenuated (10.2 ± 0.5 Hz frequency and 87 ± 5 pA amplitude in control vs 3.1 ± 0.25 Hz frequency and 40 ± 2 pA amplitude after 8 min riluzole application).

This discrepancy prompted us to investigate riluzole action on HMs in more details.

4. Electrophysiological effects of riluzole on HMs

4.1 Riluzole action on nicotine-induced oscillations

The mechanism of action of riluzole is complex and not fully clear. It was first proposed to inhibit the release of glutamate (Mantz *et al.*, 1992; Zona *et al.*, 2002; Martin *et al.*, 1993; Coderre *et al.*, 2007), which, at high extracellular concentrations, produces excitotoxic damage (Azbill *et al.*, 2000; Dunlop *et al.*, 2003). Recently it was used to inhibit PIC at similar concentrations (Darbon *et al.,* 2004; Del Negro *et al.*, 2005; Miles *et al.*, 2005; Harvey *et al.*, 2006; Theiss *et al.*, 2007).

To reveal riluzole action on both glutamate release and PICs at the same time, I have done the following experiments. I applied nicotine (10 μM) and, when oscillatory behavior appeared, I applied riluzole (10 μM). Every 20 s I was recording PICs by injecting triangular voltage commands (Powers & Binder, 2003; Li & Bennett, 2003; Harvey *et al.,* 2006) which for routine experiments were set at the rate of 42 mV/s. The voltage-activated inward current were obtained after subtracting the passive leak current (see Methods). PICs were expressed as fractional responses taking as control the values before nicotine application. During 20 s epochs, oscillation and sEPSC frequency was measured. The oscillation frequency in each epoch was then expressed as a fraction of the value found during the first epoch. sEPSC frequency was expressed as a fraction of the value found before nicotine application.

Fig. 29A shows that, when riluzole (10 μM) was added to the bathing solution (indicated by the open bar) after applying nicotine (10 μM), the PIC amplitude was soon decreased to a stable level (after 120 s it was down to 30 % of control), while oscillations continued and lasted 60 s longer. On the other hand, the sEPSC frequency (an index of network-dependent glutamate release) gradually decreased during riluzole application from its peak value evoked by nicotine (filled triangles; Fig. 29B). As long as sEPSC frequency remained above control, electrical oscillations persisted. These data suggest that riluzole had a complex action on nicotine-evoked oscillations, which were differentially related to PICs and sEPSC frequency. Further experiments were done to investigate separately the basic dynamics of PICs, their sensitivity to riluzole and riluzole effect on glutamate release.

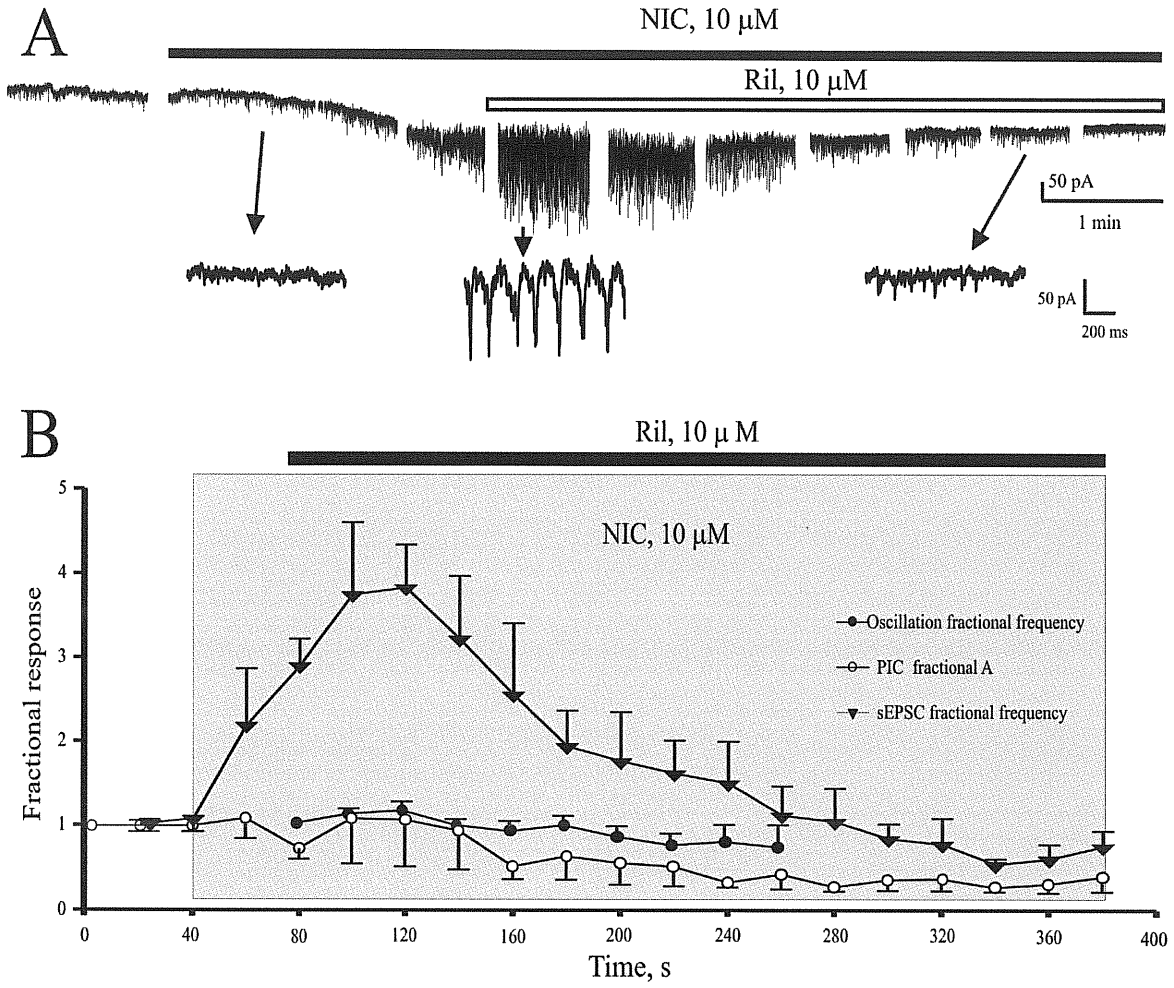

Fig. 29. Time-course of the oscillation frequency, sEPSC frequency and PIC amplitude changes during nicotine and riluzole application. (A) Sample traces of rhythmic oscillations evoked by bath-applied nicotine (10 μM, black bar) and blocked by riluzole application (10 μM, open bar). PIC amplitude was measured at 20 s intervals by applying voltage ramps that correspond to the gaps in the record. Faster time-scale shows rhythmic oscillatory behaviour (bottom panel, centre) blocked by riluzole (bottom panel, right). (B) Averaged data (from five cells) expressed as fractional values of those before nicotine (10 μM) application. The shaded area indicates nicotine application, while the black bar indicates riluzole (10 μM) application. Oscillations appeared after 40 s from nicotine application; they slowly decreased in frequency first and, then, were fully arrested after 180 s riluzole treatment. PIC amplitude decreased more than twice after 80 s in the presence of riluzole and remained at similar values until the end of the experiment. sEPSC relative frequency increased 2-4 times soon after nicotine application and was gradually decreasing with riluzole application. When sEPSC frequency fell to control value, oscillations stopped.

4.2 Persistent inward currents (PICs) of neonatal rat HMs

4.2.1 Properties of PICs of neonatal rat HMs

Before testing riluzole action on PICs of HMs, I determined the basic PIC properties and their pharmacological features. PICs were produced by injecting triangular voltage commands at three different rates (42 mV/s, Fig. 30A; 20 mV/s, Fig. 30B; 6.7 mV/s, Fig. 30C) in voltage clamp mode. Up to -55 mV, the current response was linear and shallow, indicating high input resistance. At values positive to -55 mV, all traces demonstrated the presence of a typical PIC that lasted from 0.8 (Fig. 30A) to 6 s (Fig. 30C) between -55 mV and -5 mV, beyond which PICs disappeared together with the onset of large outward currents. When the membrane potential was repolarized at similar speed, no resurgent currents were present in these examples (Fig. 30A, B and C).

The PIC dependence on the ramp rate is quantified in Table 3, demonstrating that the fastest speed was accompanied by the largest PIC amplitude (though with the smallest area). The threshold for PIC activation did not, however, depend on the ramp rate, while the PIC amplitude reached its maximal value at more depolarized potential for 42 mV/s ramp speed than for 6.7 mV/s ramp speed. Nevertheless, once PICs were activated, they could last several seconds as shown with the slowest ramp protocol (Fig. 30C).When I tested the faster ramp rate of 80 mV/s, it was difficult to clamp neurons because of unclamped fast sodium spikes (not shown). Because the 42 mV/s ramp speed was adequate to clamp HMs without substantial PIC inactivation, it was thereafter used for further tests.

Fig. 30D shows the current/voltage relation of PICs after leak current subtraction for each rate of membrane depolarization. At 42 mV/s ramp speed, all 59 HMs tested had PICs of 214 ± 23 pA average amplitude, 229 ± 47 s·pA area, and activation threshold at -57 ± 1 mV (see example in Fig. 30D, filled arrow), while reaching maximal size (see example in Fig. 30D, open arrow) at -32 ± 2 mV membrane potential (initial Vm was -65 ± 0.5 mV).

An inward current during the descending ramp phase, indicating a resurgent current (Moritz *et al.*, 2007), was found only in 3 out of 59 neurons tested. Its amplitude was 143 ± 42 pA, always smaller than the one during the ascending phase (245 ± 38 pA in these 3 neurons). The sparse incidence (5 %) of neurons with PICs on the descending ramp prevented further statistical analysis even though values for PIC area, activation potential and peak were included in the range of corresponding values obtained for the ascending phase of the protocol.

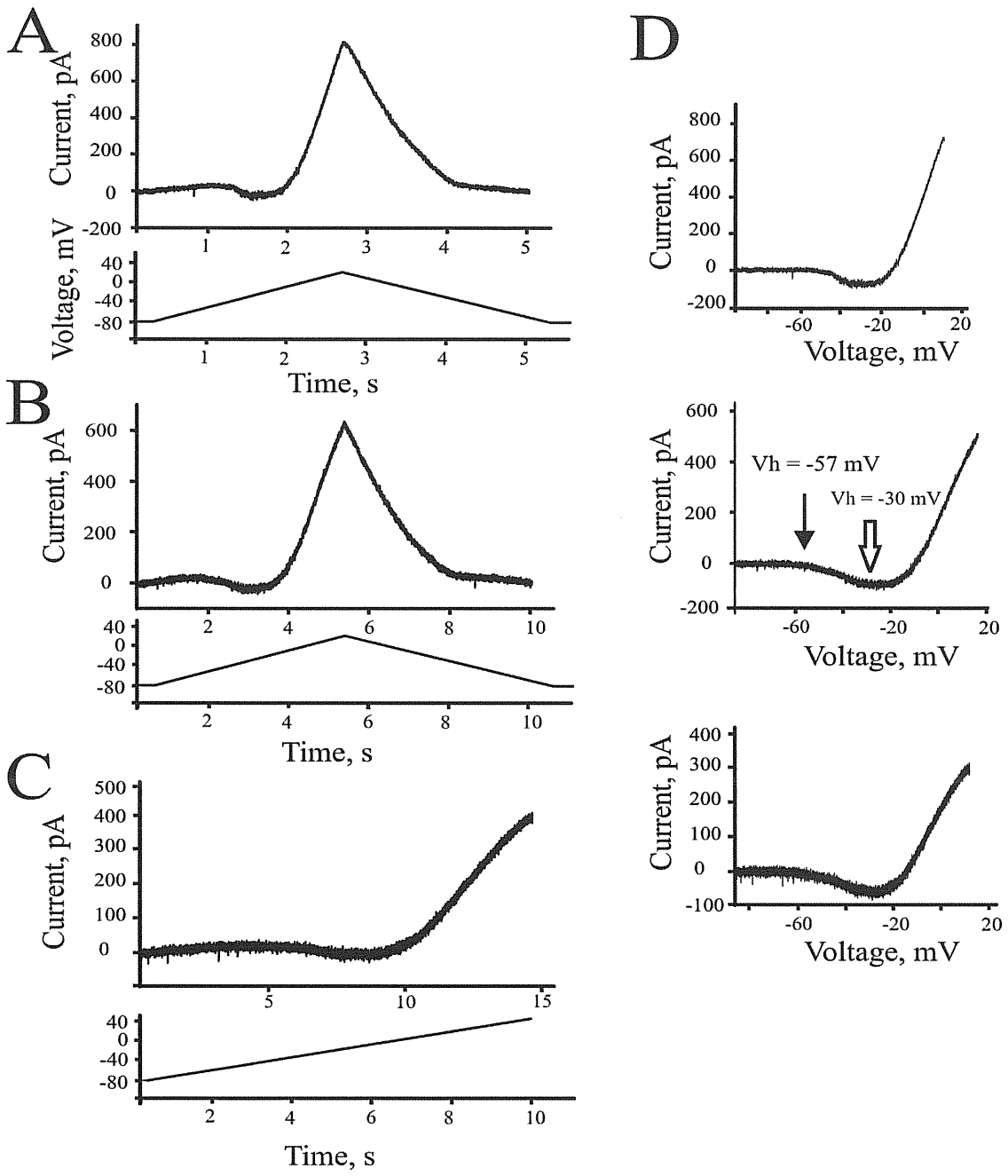

Fig. 30. PIC dependence on voltage command speed. Sample records of PICs induced by 42 mV/s (A), 20 mV/s (B) or 6.7 mV/s (C). PIC amplitude was the largest at 42 mV/s (A), while PIC area was the wider at 7 mV/s (C). No resurgent current was present on the descending phase of the ramp protocol. Note that persistent outward currents overcame PICs at more depolarized holding potential values. Injected voltage clamp commands are shown below each record. (D) I-V relation after leak current subtraction for corresponding tests shown in A-C. Threshold for PIC activation was -57 mV (middle panel, filled arrow) and did not depend on the ramp speed. The maximal inward current was at -30 mV (middle panel, open arrow).
Table 3. PIC properties depend on ramp depolarization speed. PIC = persistent inward current. Stars indicate statistically significant data. n = 10.

Table 3. Comparison of persistent inward current (PIC) amplitude, area, threshold and holding potential (Vh) at different voltage command speed.

Ramp speed	42 mV/s	20 mV/s	7 mV/s	42 vs. 7 mV/s
PIC ampl., pA	180 ± 20*	140 ± 20	130 ± 25*	**P = 0.001**
PIC area, s·pA	140.1 ± 19*	200.2 ± 30	563 ± 125*	**P = 0.005**
PIC threshold, mV	-56.7 ± 1	-54.4 ± 1	-52.8 ± 1	
Vh for max PIC, mV	-32.1 ± 2*	-38.2 ± 1	-39 ± 1*	**P = 0.005**

4.2.2 Pharmacological characteristics of persistent Na^+ and Ca^{2+} currents

I_{NaP}, which is sensitive to riluzole, is one component of the global PIC, mediated by Na^+ and/or Ca^{2+} (Crill, 1996; Russo & Housgaard, 1999). However, riluzole has also been reported to block potassium (Zona *et al.*, 1998; Duprat *et al.*, 2000; Cao *et al.*, 2002; Ahn *et al.*, 2005) and calcium (Huang *et al.*, 1997; Siniscalchi *et al.*, 1997; Stefani *et al.*, 1997; Beltran-Parrazal & Charles, 2003) conductances. In addition, riluzole interacts with $GABA_A$ and glycine receptors (Umemiya & Berger, 1995; Mohammadi *et al.*, 2001; He *et al.*, 2002), and can even induce oscillations in cultured spinal networks (Yvon *et al.*, 2007). Since persistent sodium (Darbon *et al.*, 2004; Cramer *et al.*, 2007; van Drongelen *et al.*, 2006; Zhong *et al.*, 2007) and persistent calcium currents (I_{CaP}, Pace *et al.*, 2007 a, b) appear necessary for prolonged rhythmic discharges, I have checked the pharmacological action of riluzole on both PIC components.

While I_{NaP} is reported to be more sensitive to low concentrations of TTX than the fast Na^+ current (Harvey *et al.*, 2005; van Drongelen *et al.*, 2006), stronger pharmacological separation between these Na^+ conductances is thought to be possible with riluzole (Feldman & del Negro, 2006; Pace *et al.*, 2007a). Hence, I first studied the relative contribution of I_{NaP} to the global PIC current and then examined whether 10 μM riluzole could be used as a selective inhibitor of I_{NaP} on neonatal rat HMs.

Fig. 31A shows how PIC had a component blocked by TTX (1 μM; filled arrow), leaving a residual inward current fully abolished by subsequent application of the inorganic Ca^{2+} channel blocker Mn^{2+} (2 mM; open arrow). In accordance with previous studies (Crill, 1996; Russo & Hounsgaard, 1999), I assumed that the TTX-sensitive component represented I_{NaP}, while the Mn^{2+}-sensitive component represented I_{CaP}. In order to measure I_{NaP} in isolation, I applied Mn^{2+} to inhibit I_{CaP} and then subtracted the leak current. With this procedure, the average I_{NaP} had 71 ± 28 pA amplitude and 340 ± 240 s·pA area (6 tests from three HMs; Fig. 31B). It was activated at -56 mV (filled arrow in Fig. 31B) and reached its maximum at -34 mV holding potential value, which was not significantly different from the control global PIC. I_{NaP} comprised 40 % of the global PIC amplitude and 55 % of the PIC area (Fig. 32). Similar results were obtained with the I_{CaP} blocker Cd^{2+} (400 μM): in fact, after leak subtraction, the Cd^{2+}-resistant current had 86 ± 36 pA amplitude, corresponding to 37 % of PIC amplitude (n = 6).

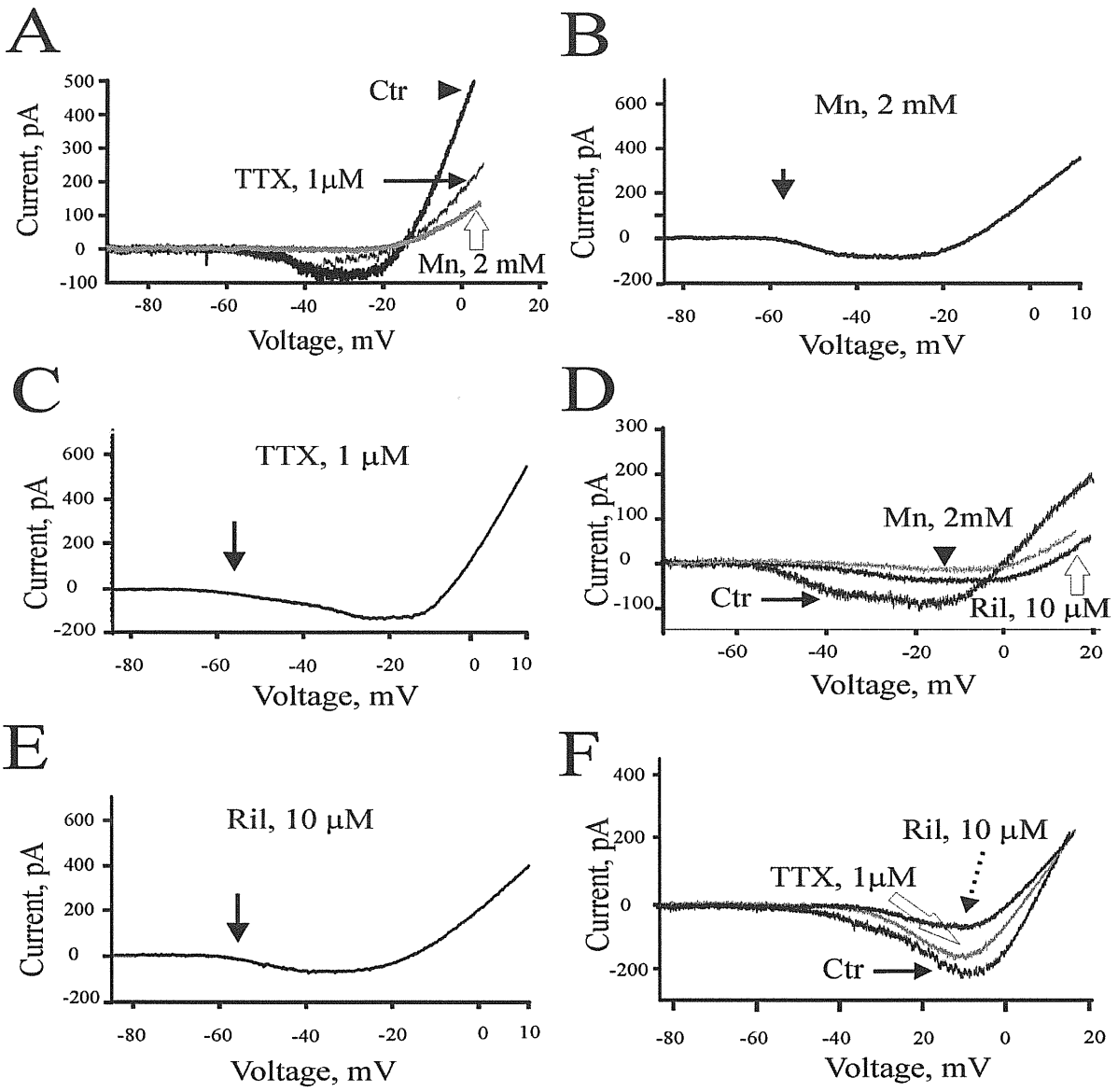

Fig. 31. Pharmacological characteristics of PICs. (A) Sample record of total PIC (black arrowhead) composed of the persistent sodium current (I_{NaP}) blocked by 1 μM TTX (filled arrow), and of the persistent calcium current (I_{CaP}), blocked by 2 mM Mn^{2+} (open arrow). Voltage ramp speed in this subsequent example was 42 mV/s. (B) Averaged (leak-subtracted) I_{NaP} current isolated after I_{CaP} block with 2mM Mn^{2+}, n = 4 traces. I_{NaP} was activated at -56 mV holding potential (filled arrow). (C) Averaged (leak-subtracted) I_{CaP} current isolated after I_{NaP} block with 1 μM TTX. I_{CaP} was activated at more depolarized value (filled arrow) and had shape different from isolated I_{NaP}. n = 10 traces. (D) Example of total PIC (filled arrow) inhibited by 10 μM riluzole (open arrow). The residual PIC was then blocked by 2 mM Mn^{2+} (black arrowhead). (E) Averaged (leak-subtracted) current left after 10 μM riluzole application. It was activated at -55 mV (black arrow) and had a different shape from averaged I_{NaP} shown in C, n = 6 traces. (F) Example of total PIC (black arrow) partly blocked by 1 μM TTX (open arrow), and further reduced by 10 μM riluzole (dotted arrow).

In a separate set of experiments, I applied 1 μM TTX to pharmacologically isolate I_{CaP}. Fig. 31C shows that, after leak subtraction, the average I_{CaP} had an amplitude of 136 ± 65 pA and an area of 52 ± 32 s·pA (n = 5). I_{CaP} was activated at -46 ± 4 mV (filled arrow in Fig. 31C) and reached maximum at -16 ± 4 mV holding potential. I_{CaP} comprised 44 % of the total PIC amplitude and 36 % of total area (Fig. 32). Co-application of TTX and Mn^{2+} fully suppressed the appearance of PICs (see example in Fig. 31A), indicating absence of other voltage activated inward currents. Summary data from TTX and Mn^{2+} tests enabled to calculate that 50 % PIC amplitude and 60 % of PIC area was due to I_{NaP}, with the remaining components due to I_{CaP} (n = 14).

The action of 10 μM riluzole (open arrow) is exemplified in Fig. 31D, in which it largely decreased the global PIC (filled arrow), leaving a residual current abolished by 2 mM Mn^{2+} (arrowhead). Fig. 31E demonstrates that the average PIC after riluzole application had an amplitude of 46 ± 11 pA and an area of 42 ± 15 s·pA (n = 5). It was activated at -55 ± 4 mV (filled arrow) and peaked at -26 ± 4 mV. Comparison of average traces in Fig. 31C and E shows that the PIC remaining after riluzole application was different from the one left after TTX application. On average, as indicated in Fig. 32, the PIC depression by riluzole was more intense that the one by the maximally effective concentration of TTX.

Further experiments were carried out to quantify any current component with differential sensitivity to TTX and riluzole: thus, I first applied 1 μM TTX, and then 10 μM riluzole to find out if TTX could fully occlude the action of riluzole on PICs. Fig. 31F shows that, even after TTX application (open arrow), riluzole could still block the residual component of PIC (dotted arrow). On average, after TTX application, riluzole could still inhibit PIC amplitude by 30 ± 10 % (nonparametric Wilcoxon test, $P < 0.05$, n = 7). These data suggest that riluzole, besides its block of I_{NaP}, could partly inhibit other inward conductances such as I_{CaP}.

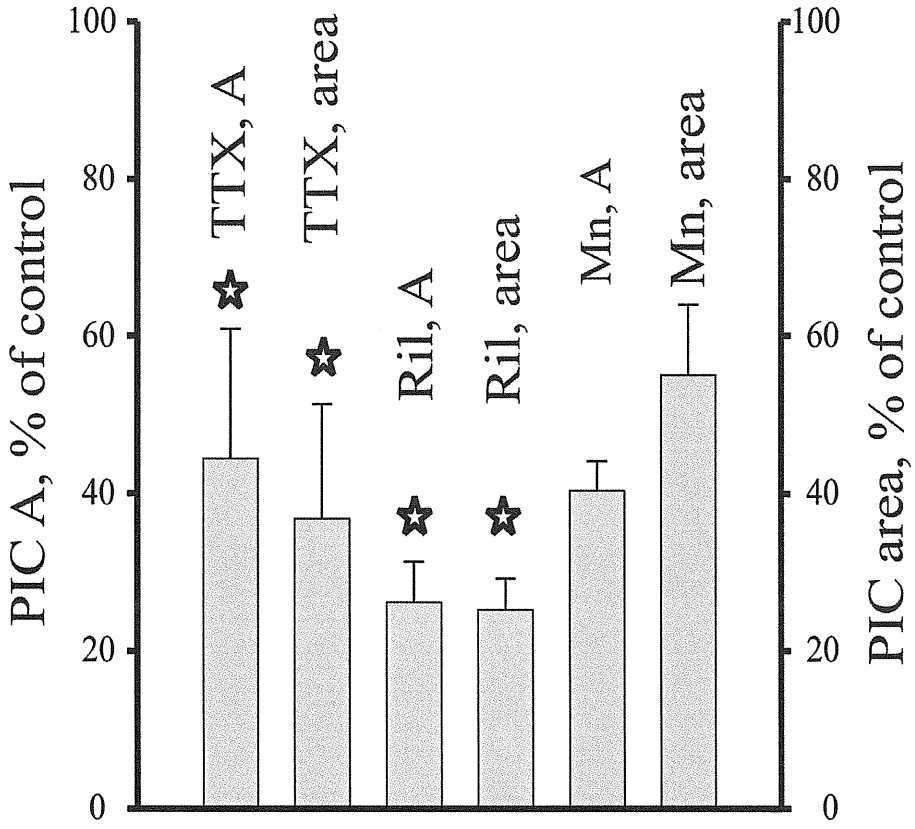

Fig. 32. Relative contribution by I_{NaP} and I_{CaP} to PIC. PIC amplitude (A, left) and area (right) were differentially depressed by TTX (1 μM), Mn^{2+} (2 mM) or riluzole (10 μM). The residual PIC amplitude and area after each drug application are shown as percent of control. Five cells were recorded with TTX or riluzole, and three cells were recorded with Mn^{2+}. Stars represent statistically different values from the control (non-parametric Wilcoxon test, $P < 0.05$).

4.3 Riluzole changed the firing properties of HMs

Since PICs confer repetitive firing properties to motoneurons (Crill, 1996; Russo & Housgaard 1999; Kuo *et al.*, 2006; Harvey *et al.*, 2006; Theiss *et al.*, 2007), I explored how the PIC blocking ability of riluzole could be translated into changes in firing activity of rat HMs in current clamp mode. Fig. 33A shows an example of responses evoked by a 0.2 pA/s current clamp command before and after applying 10 μM riluzole. In control conditions, the neuron started firing after 4.83 s (Fig. 33A, left trace). After applying riluzole for 2 min, the cell started firing at 5.5 s (Fig. 33A, center trace) and stopped 4.5 min later (Fig. 33A, right trace), demonstrating strong reduction in excitability. Only one cell out of five was insensitive to riluzole, as in the other four cells firing stopped after 217 ± 54 s. When the riluzole concentration was 20 μM, all cells (9/9) stopped firing 247 ± 40 s later. Nevertheless, to limit the dose-dependent non-specific effects of riluzole (Darbon *et al.*, 2004; Kuo *et al.*, 2006; Cramer *et al.*, 2007; Yvon *et al.*, 2007), further experiments were done with 10 μM riluzole.

With relatively slow ramp depolarizations, the fast Na^+ current undergoes voltage dependent inactivation (Enomoto *et al.*, 2006; Magistretti *et al.*, 2006; Kuo *et al.*, 2006). Thus, to investigate the interplay between the fast Na^+ current and I_{NaP} for generating rapid firing as well as repetitive spiking (Crill, 1996; Enomoto *et al.*, 2006; Kuo *et al.*, 2006; Magistretti *et al.*, 2006; van Drongelen *et al.*, 2006), we next used instantaneous current pulses to induce firing. Current steps (0.01-0.08 pA) injected into HMs evoked firing as exemplified in Fig. 33B (0.03 pA current pulse applied before and after 10 μM riluzole). In the presence of riluzole, repetitive firing (for control conditions see Fig. 33B, left trace) was decreased after 5.5 min (Fig. 33B, center trace) and lost after 7 min (Fig. 33B, right trace) even though the first action potential persisted with similar amplitude (79 ± 4 mV in control conditions vs. 76 ± 6 mV after 10 min riluzole application, $P = 0.44$, $n = 4$). The maximal rate of rise of the action potential (which is a very sensitive index of activation of the fast Na^+ conductance; Eccles, 1957) was also unchanged (100 ± 28 mV/s in control conditions vs. 92.4 ± 31 mV/s after 10 min riluzole application, $P = 0.39$, $n = 4$). Thus, in the presence of riluzole, HMs lost their ability to generate trains of action potentials, although single spikes were still inducible.

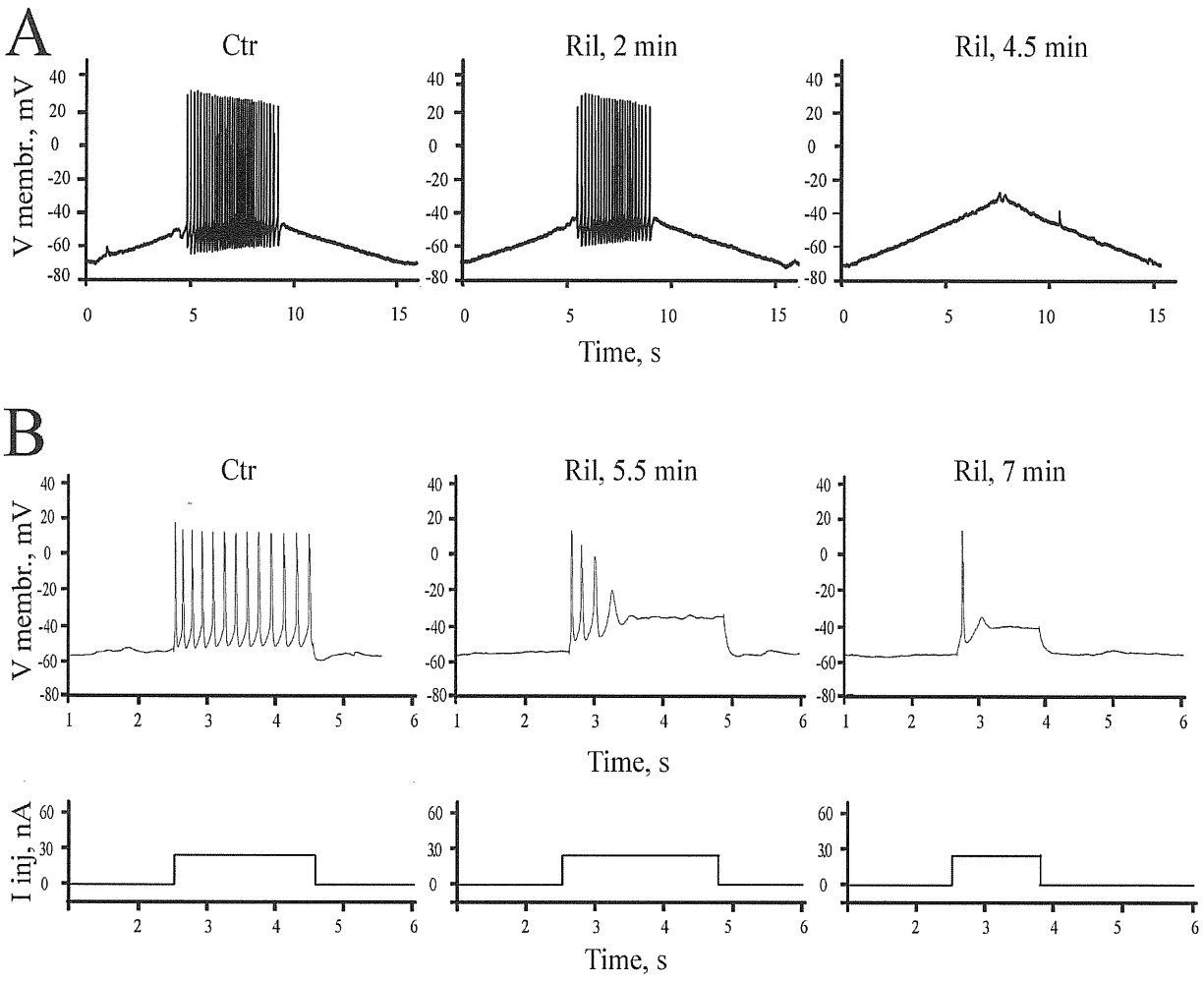

Fig. 33. Current clamp recording of spike activity before and after 10 μM riluzole treatment. (A) In control conditions (0.13 nA/s current injection) HM started firing after 4.83 s. After 2 min riluzole (10 μM) administration, HM started firing after 5.5 s. After 4.5 min riluzole application, the neuron stopped firing. (B) In control conditions (left trace), HM fired 13 action potentials (AP) when 30 nA depolarizing current step was injected (see bottom panels for scheme of injected DC amplitude and duration). After 5.5 min riluzole treatment (middle trace), only 4 spikes were present, and after 7 min riluzole treatment (right) only 1 spike was left.

4.4 Riluzole inhibited glutamate release

The effect of 10 μM riluzole on glutamate synaptic release was studied by measuring the properties of miniature glutamatergic currents (mEPSCs) of rat HMs in the presence of 1 μM TTX. In eight out of fourteen cells, mEPSC frequency decreased (P = 0.01) from 0.26 ± 0.06 Hz to 0.06 ± 0.02 Hz after 5 min riluzole treatment. Fig. 34A shows an example of cumulative probability distribution of the mEPSC inter-event interval: after riluzole application (open symbols), the plot was shifted to the right, indicating a much lower probability of observing synaptic events. On riluzole sensitive cells the mEPSC amplitude was moderately, yet significantly (P = 0.033), decreased from -27.75 ±2.9 pA to -25.3±2.5 pA (Fig. 34B, n = 8).

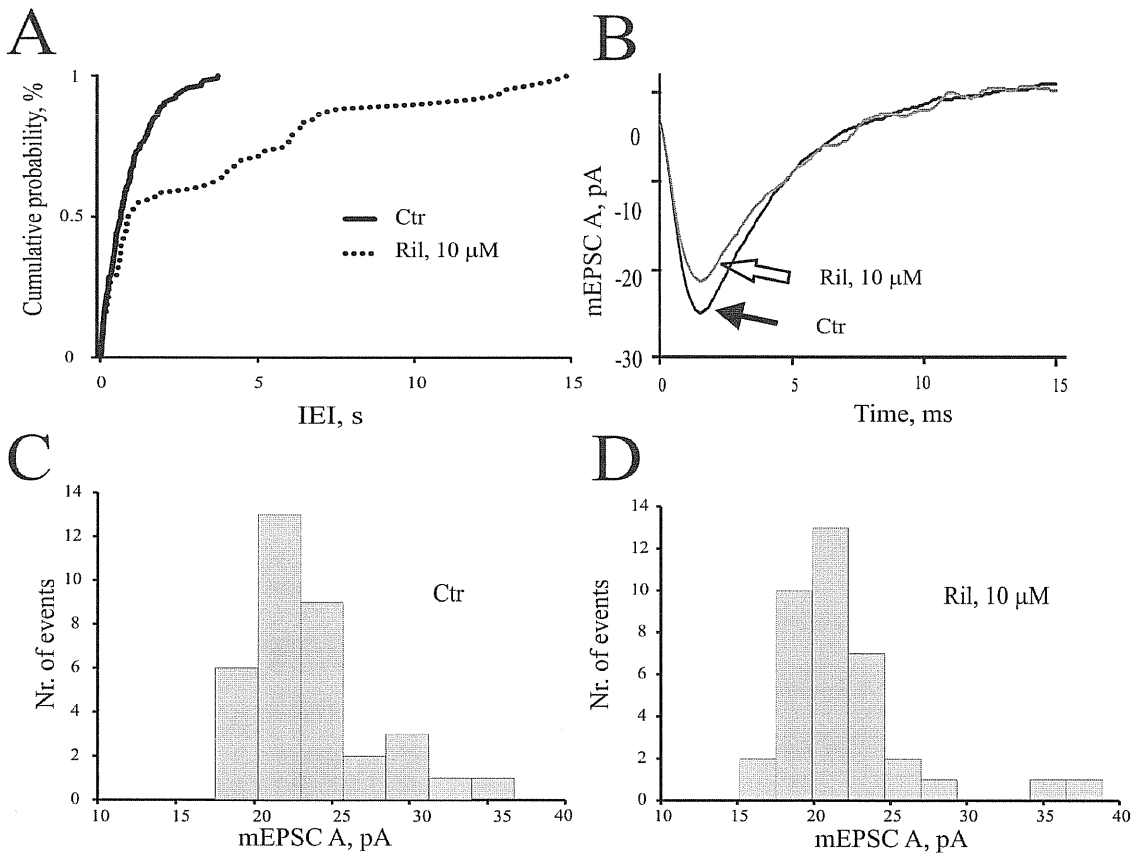

Fig. 34. mEPSC frequency and amplitude changes after riluzole application. (A) Plot of cumulative probability distribution for inter-event-interval (IEI) of mEPSC that was shifted to the right by 10 μM riluzole (black dots). (B) Averaged mEPSC amplitude before (filled arrow, average of 65 events) and after (open arrow, average of 20 events) 10 μM riluzole application. Riluzole slightly decreased mEPSC amplitude. Data in A and B are from the same cell. C and D Histograms show mEPSC amplitude distribution before and after riluzole (10 μM) application, respectively. All events were equally sensitive to riluzole, regardless of their size.

The example of the cell in Fig. 34C and D show that riluzole did not alter the distribution of mEPSC amplitudes, indicating that all events were sensitive to riluzole, regardless of their size. Time constant values for onset and decay (τ_{on} and τ_{off}, respectively) were decreased after riluzole application for the riluzole sensitive cells (see example in Fig. 34B and Table 4) without significant change for riluzole insensitive HMs. In other six cells, the mEPSC frequency (control = 0.12 ± 0.02 Hz) was not changed (P = 0 .23) after riluzole application (0.11 ± 0.02 Hz), nor was the mEPSC amplitude (Table 4). Riluzole per se did not change the HM input resistance (290 ± 100 MΩ of riluzole sensitive cells and 320 ± 120 MΩ of riluzole insensitive ones; P = 0.4, n = 14).

Table 4. Glutamatergic events in the presence of riluzole. Ril = 10 μM riluzole application for 4-5 min. n = 8 for riluzole sensitive and n = 6 for riluzole insensitive cells. τ values refer to the monoexponential time constant for the onset (on) and decay (off) of miniature currents.

	Riluzole sensitive HMs	Riluzole insensitive HMs
mEPSC amply, pA		
Before Ril	-27.75 ± 2.9	-29.8 ± 3.3
After Ril	-25.3 ± 2.5	-28.7 ± 3.2
	P = 0.033	
mEPSC frequency, Hz		
Before Ril	0.26 ± 0.06	0.12 ± 0.02
After Ril	0.06 ± 0.02	0.11 ± 0.02
	P = 0.01	
τ_{on}, ms		
Before Ril	1.39 ± 0.2	0.99 ± 0.2
After Ril	0.8 ± 0.1	1.25 ± 0.3
	P = 0.051	
τ_{off}, ms		
Before Ril	3.8 ± 0.7	5.86 ± 1.1
After Ril	3.01 ± 0.7	5.01 ± 1.2
	P = 0.004	

Since riluzole insensitive cells had lower mEPSC control frequency, I investigated whether the depressant action of riluzole was dependent on the initial release rate of glutamate. Thus, on a separate batch of HMs, I elevated the extracellular K^+ concentration from 3 to 20 mM to increase mEPSC frequency which rose from 0.25 ± 0.04 Hz to 1.63 ± 0.57 Hz (P = 0.05; n = 6; Fig. 35). Upon return to 3 mM K^+, in 5 out of 6 cells the mEPSC frequency was not significantly changed by riluzole (0.25 ± 0.04 Hz before riluzole and 0.21 ± 0.08 Hz after

riluzole, P = 0.52). When riluzole was later tested on mEPSC frequency in 20 mM K^+, a depressant action now emerged (from 1.63 ± 0.57 Hz to 0.81 ± 0.33 Hz; P = 0.04; n = 5; Fig. 35). In the remaining cell, mEPSC frequency was not affected by riluzole even in 20 mM K^+ (0.35 Hz in control conditions vs. 0.36 Hz after riluzole treatment). Thus, on most HMs, glutamate release inhibition by riluzole could be demonstrated when the mEPSC frequency was elevated.

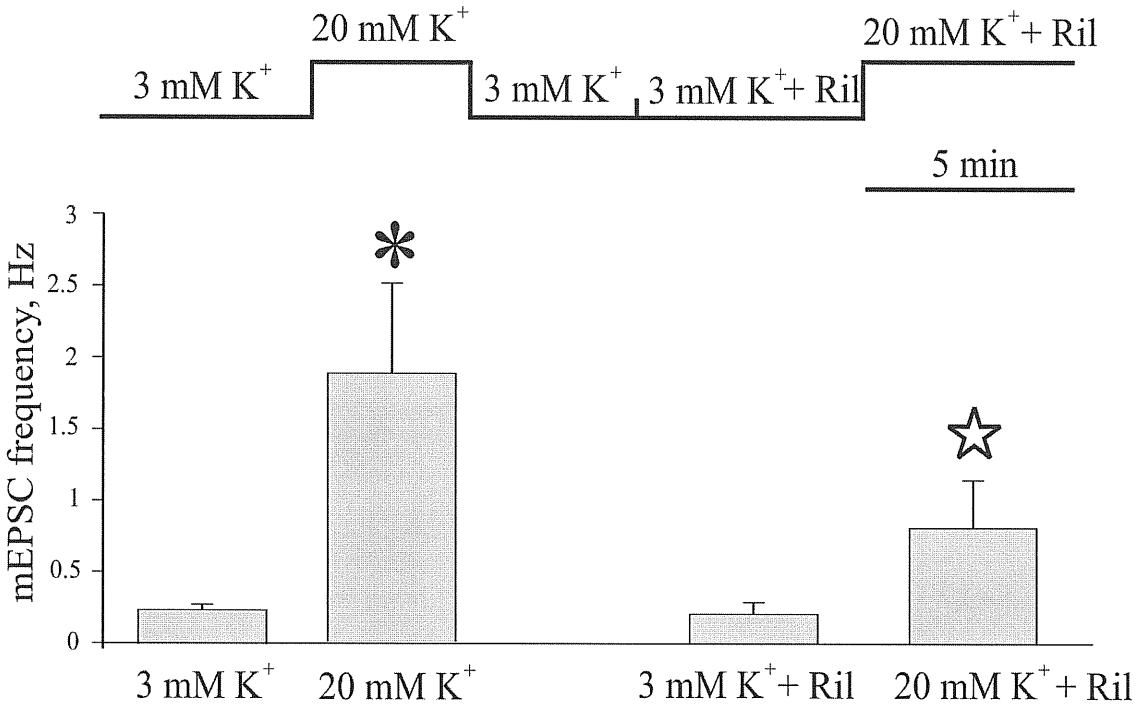

Fig. 35. Riluzole-evoked depression of glutamate release. The scheme of the experimental protocol is shown in the upper panel. mEPSC frequency was first recorded in 3 mM extracellular K^+, and then in 20 mM K^+ concentration. After return to standard solution, riluzole (10 μM) was added to 3 mM K^+ and, later, to 20 mM K^+ solution. Lower panel shows average mEPSC frequency. An asterisk indicates statistically significant difference between data at 3 mM and 20 mM K^+ (P = 0.05, n = 6); a star indicates statistically significant results between 20 mM K^+ versus 20 mM K^+ plus riluzole (P = 0.04, n = 5). All experiments were run in the continuous presence of 1 μM TTX.

5. Mechanism of action of riluzole on glutamate release

What is the mechanism of riluzole to induce glutamate release inhibition? Riluzole is reported to inhibit excitatory synaptic transmission (Mantz *et al.*, 1992; Zona *et al.*, 2002; Martin *et al.*, 2003; Coderre *et al.*, 2007), but the mechanism remains unclear. Since the effect of riluzole persists in the presence of TTX (Cheramy *et al.,* 1992; Hubert & Doble, 1989; Martin *et al.,* 1993; Hubert *et al.,* 1994, and our present data), it points to a process directly controlling glutamate release.

5.1 Loss of postsynaptic nAChRs function on glutamate release

A previous report from our lab showed how nicotinic receptor activity positively controls synaptic release of glutamate in basal or stimulated conditions (Quitadamo *et al.*, 2005). This process might be a target for the depressant action of riluzole that in high concentrations (≥100 μM) can block nicotinic receptors (Mohammadi *et al.*, 2002). Therefore , I tested if riluzole might inhibit nicotinic receptor-mediated currents activated by brief (100-900 ms) puffer applications of nicotine to HMs (Pagnotta *et al.*, 2005; Quitadamo *et al.*, 2005; Lamanauskas & Nistri, 2006). As shown in Fig. 36, the inward current amplitude produced by nicotine remained unchanged following application of 1 μM TTX (91.2 ± 60 pA in control vs 115.63 ± 95 pA after TTX treatment, P = 0.56) or 10 μM riluzole (115.63 ± 95 pA in TTX solution vs. 95.67 ± 83 pA after riluzole application, P = 0.26; n = 3). These data make unlikely antagonism of nicotinic receptors by riluzole.

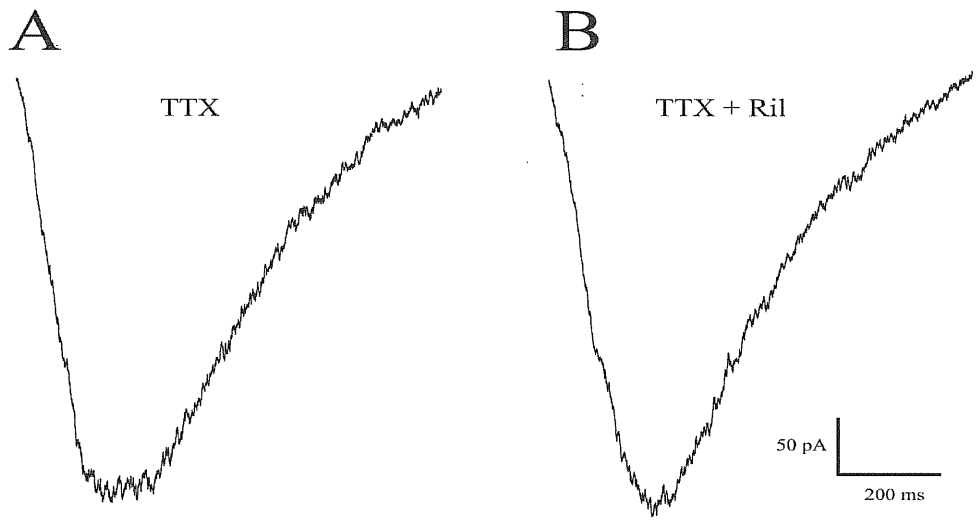

Fig. 36. Lack of riluzole effect on HM nicotinic receptors. Sample records of HM inward currents evoked by nicotine puffer application and unchanged by riluzole (10 μM). Experiment were done in the presence of 1 μM TTX.

5.2 Presynaptic NMDA receptor control of glutamate release

Recent observations show that endogenously released glutamate can enhance further glutamate release through presynaptic NMDA receptor activation (Engelman & MacDermott, 2004).

I have checked if, in the brainstem, riluzole could act via presynaptic NMDA receptors to modulate glutamate release. Because the riluzole action depended on the on-going release activity, experiments were run in 20 mM extracellular K^+ to maximize detection of mEPSCs. In the presence of 1 μM TTX, I applied the NMDA receptor blocker APV (50 μM) first and, after 5-6 min, riluzole (10 μM), using the protocol schematized in Fig. 37A. In the presence of APV, there was fall in mEPSC frequency and amplitude (Fig. 37A). This was associated with a rightward shift in the cumulative probability plot (Fig. 37B) indicating low occurrence of miniature events. Further application of riluzole could not block mEPSC frequency or amplitude (Fig. 37A and B).

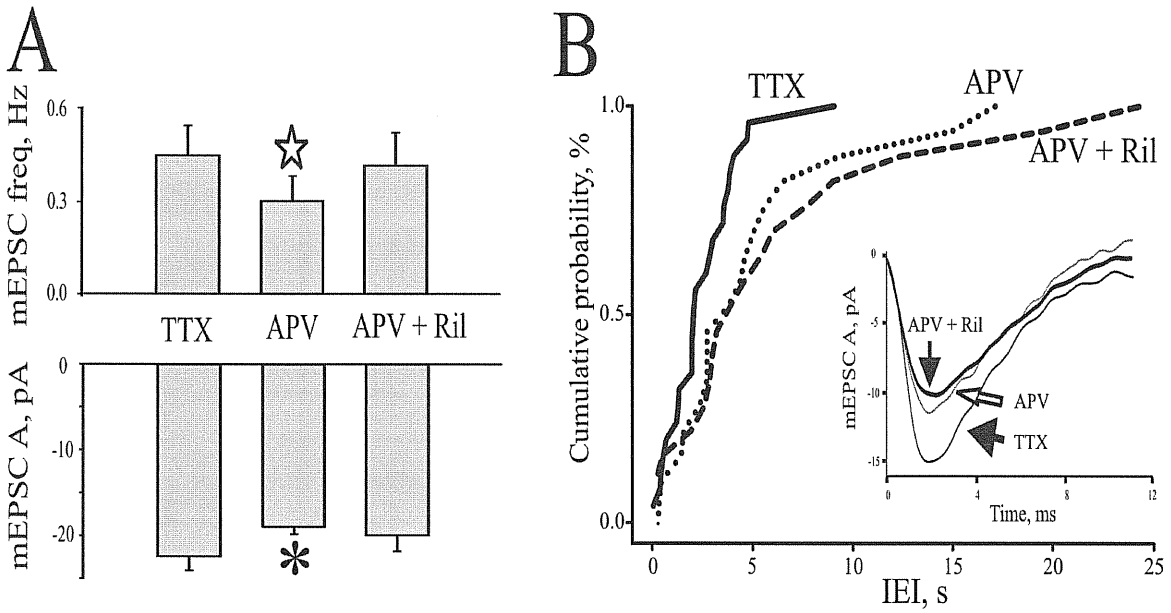

Fig. 37. Riluzole action on glutamate release is occluded by APV. (A) In the presence of TTX (1 μM), APV (50 μM) decreased mEPSC frequency from 0.45 ± 0.1 Hz to 0.3 ± 0.08 Hz, $P < 0.05$, $n = 6$. Further riluzole (10 μM) application did not affect mEPSC frequency. APV also decreased mEPSC amplitude from -22.43 ± 1.6 pA to -19 ± 0.8 HpA($P < 0.05$, $n = 7$), which was not further affected by riluzole. (B) Plot of cumulative probability distribution of IEI (see legend to Fig. 6) shifted to the right by 50 μM APV (dotted line). Riluzole (10 μM, dashed line) did not produce any further effect. Inset shows average mEPSC amplitudes in control (filled arrow), 50 μM APV (open arrow) and after 10 μM riluzole application (arrowhead). APV decreased mEPSC amplitude, while subsequently-applied riluzole had no further action. Traces were averaged from 40-100 events. All data in (B) are from the same cell.

These data suggest that riluzole was depressing glutamatergic transmission via presynaptic NMDA receptors as long as the latter were functionally active. To validate this notion, experiments were run in reverse order so that 10 μM riluzole was applied first, and 50 μM APV later always in the presence of 1 μM TTX and 20 mM K^+. As shown in Fig. 38A, riluzole decreased mEPSC frequency, an effect which was not further diminished by APV. Fig. 38A shows that there was no change in mEPSC amplitude with riluzole or riluzole plus APV. Riluzole shifted to the right a cumulative probability plot (Fig. 38B), while adding APV had no further action (Fig. 38A and B). The data suggests that presynaptic NMDA receptors were upregulating glutamate release onto hypoglossal motoneurons, an action that could be disrupted by riluzole.

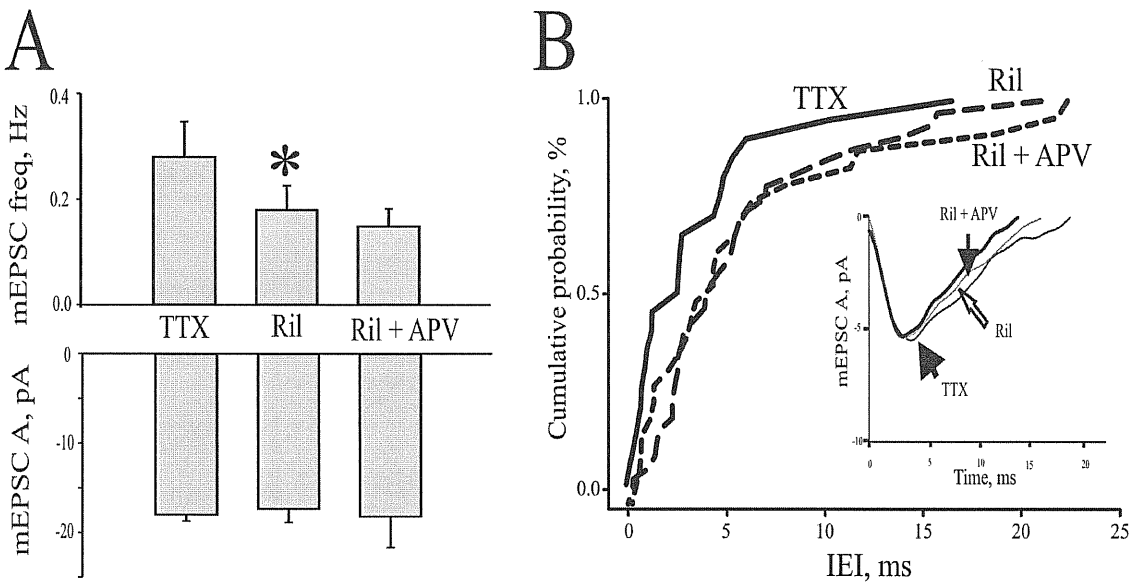

Fig. 38. APV action on glutamate release occlusion by riluzole. (A) In the presence of TTX (1 μM), riluzole (10 μM) decreased mEPSC frequency from 0.28 ± 0.07 Hz to 0.18 ± 0.05 Hz, $P < 0.05$, $n = 5$. Further APV (50 μM) application had no effect on mEPSC frequency, $n = 4$. Neither riluzole nor APV affected mEPSC amplitude, $n = 4$. (B) Plot of cumulative probability distribution of IEI shifted to the right by 10 μM riluzole (long dashes). Further APV application did not change probability distribution (short dashes). Inset shows average mEPSC amplitude, when riluzole (10 μM) was applied first. Riluzole (opened arrow) slightly decreased mEPSC amplitude (filled arrow), while APV (arrowhead), applied later, had no effect on mEPSC amplitude. The traces were averages from 20-40 events. All data in (B) are from the same cell. All experiments were done in 20 mM extracellular K^+ to increase mEPSC frequency to optimize the action of riluzole. A star shows statistically significant results ($P < 0.05$) from 6 out of 7 cells, while an asterisk indicates statistically significant results for all seven cells.

Could riluzole act by direct modulation of NMDA receptors? Radioligand binding studies show that riluzole does not bind to NMDA, AMPA, kainate, or metabotropic glutamate receptors (Peluffo *et al.*, 1997; Doble, 1996; Kretschmer *et al.*, 1998). It is known that NMDA receptors can be regulated by G protein-coupled receptors (Koles *et al.*, 2001; Marino & Conn, 2002; MacDonald *et al.,* 2007). G protein-coupled receptors can exert their action on NMDA receptors either directly binding them or via serine-threonine kinases, including protein kinase C (PKC) (Lu *et al.*, 1999; MacDonald *et al.,* 2007). It has been shown that in cultured cortical cells riluzole can directly bind PKC and inhibit its activity (Noh *et al.,* 2000). Therefore, I tested if the PKC pathway for NMDA receptor regulation was involved in HMs. I applied chelerythrin (2.5 μM), a selective PKC blocker, in the presence of TTX (1 μM) and 20 mM K^+. After 6-8 min of application, chelerythrin decreased mEPSC frequency and amplitude in all five cells tested (Fig. 39A). Cumulative probability distribution plot shows a rightward shift in inter-event interval (Fig. 39B). mEPSC amplitude was decreased after chelerythrin and riluzole treatment without affecting event kinetics (Fig. 39C). The data suggest that riluzole regulated NMDA receptors via protein kinase C and presynaptic NMDA receptors facilitated glutamate release.

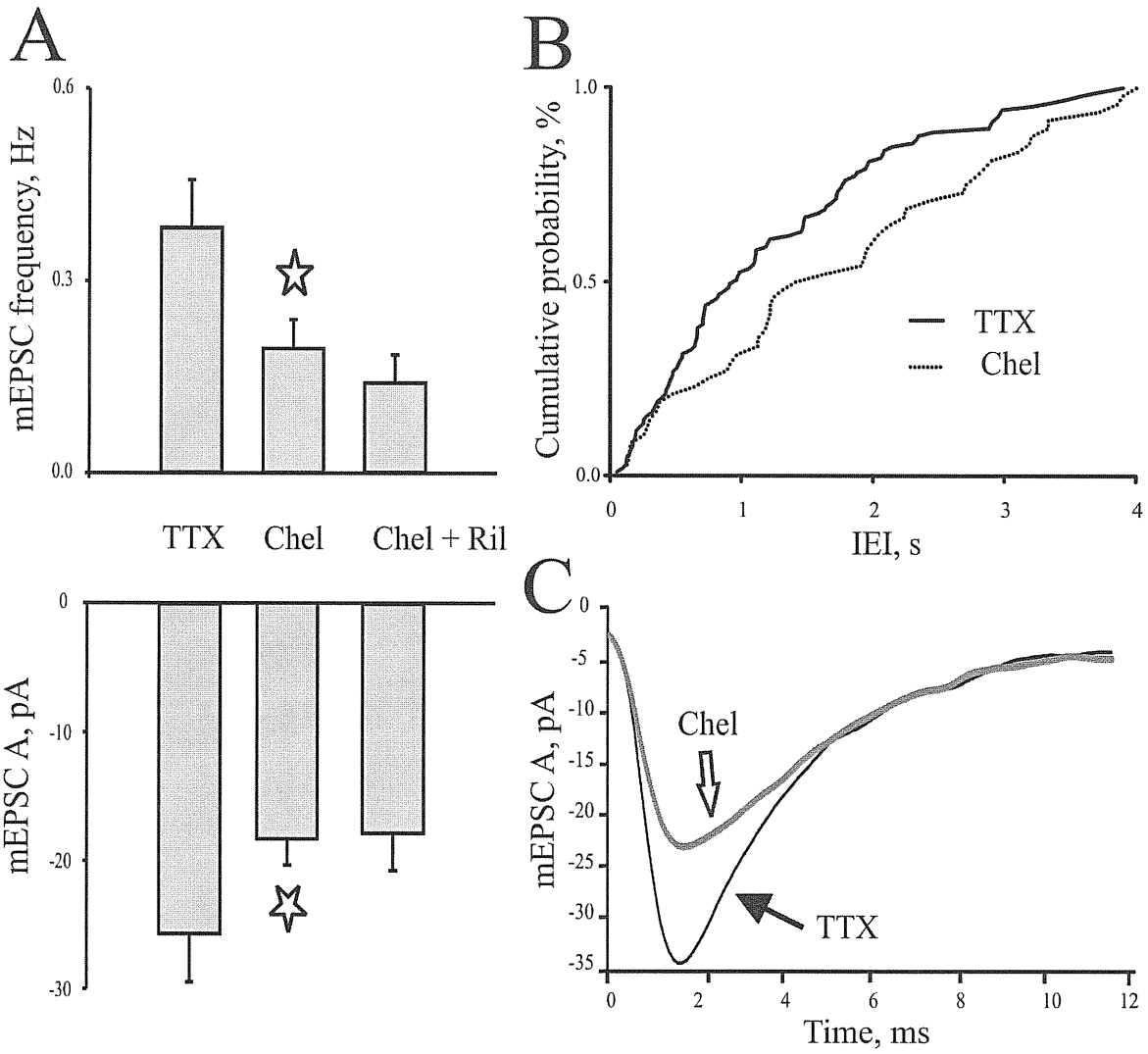

Fig. 39. Chelerythrin action on mEPSCs. (A) In the presence of TTX (1 μM), chelerythrin (2.5 μM) decreased mEPSC frequency (from 0.43 ± 0.06 Hz to 0.2 ± 0.04 Hz, P = 0.03, n = 7) and amplitude (from -25.7 ± 3.8 pA to -20.55 ± 3.1 pA, P = 0.05, n = 7). Further riluzole (10 μM) application did not affect mEPSC frequency or amplitude (B) Plot of cumulative probability distribution of IEI shifted to the right by 2.5 μM chelerythrin treatment. Data from 100 and 40 events. (C) mEPSC averaged amplitudes before and after chelerythrin (2.5 μM) application in the presence of TTX (1 μM). The traces were averaged from 30 and 50 events. Data in (B) and (C) are from the same cell. The experiments were done in 20 mM extracellular K^+. A star shows statistically significant results ($P < 0.05$, n = 5).

6. Functional significance of HM oscillatory behavior

6.1 Current clamp recordings

Previous experiments were done in voltage clamp to keep the holding potential fixed and to investigate electrical currents produced by nicotine. To find out whether oscillations evoked by nicotine had an influence on the ability of HMs to fire action potentials, I have performed current clamp experiments. Figure 40 shows a typical experiment in which 10 μM nicotine produced theta frequency oscillations. From an initial resting potential of –63 mV, nicotine depolarized the cell to –54 mV when oscillations (254 ± 10 ms period) appeared with spikes regularly occurring at the peak of each cycle (Fig. 40 lower panel, left). Injecting intracellular current (30 pA) further depolarized (-30 mV) the neuron to speed up firing (33 %) which remained coincident with the peak of oscillations (period = 180 ± 8 ms; Fig. 40 lower panel, middle). Conversely, by applying hyperpolarizing current (-40 pA) to take the membrane potential to -72 mV (Fig. 40 lower panel, right), firing was suppressed while oscillations persisted (period of 282 ± 15 ms).

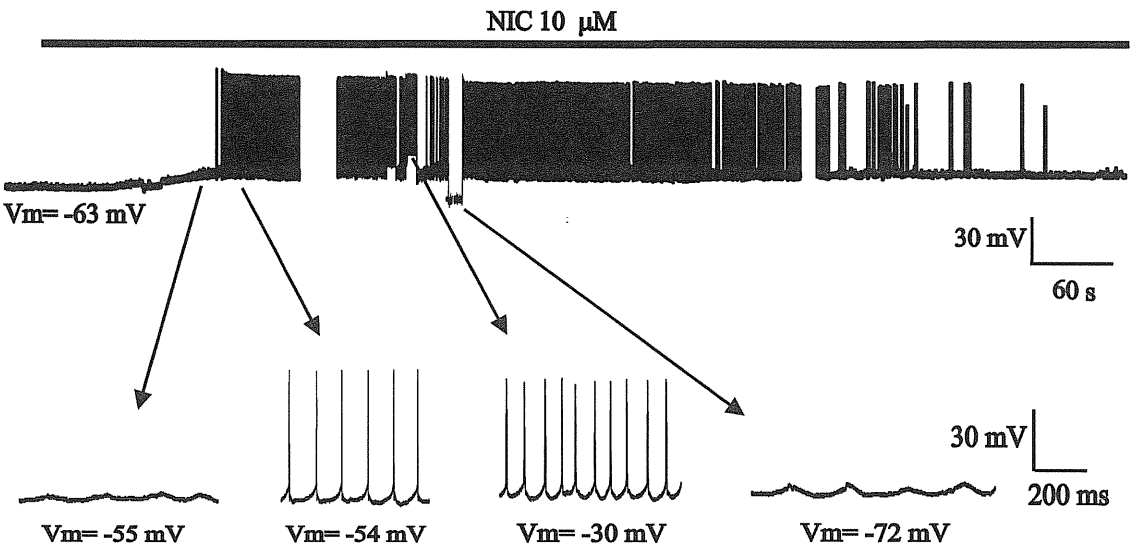

Fig. 40. HM firing characteristics under current clamp conditions during oscillatory behavior. HM membrane potential was -63 mV at the beginning of recording. Nicotine application depolarized the HM to -54 mV and evoked oscillatory activity (lower panel, left). Action potentials occured regularly and always at the peak of an oscillation. When the HM was depolarized to -30 mV by injecting +30 pA DC, the firing frequency increased and remained regular (lower panel, centre). During -40 pA DC injection, the membrane potential became -72 mV, and spiking stopped while oscillations persisted (lower panel, right). Protocols for measuring I-V curves were run during record gaps.

These observations suggest that dynamic changes in HM membrane potential could partly modulate the frequency of oscillations, even though these events remained locked in with spike generation. The simplest hypothesis is that HM voltage-activated currents could shape the oscillatory behavior. This issue was tested by applying the sodium current and I_h blocker QX-314 (300 µM) via the intracellular solution (Perkins & Wong, 1995; Marchetti *et al*, 2002). In the presence of QX-314, at the membrane potential between –40 mV and 10 mV, the oscillation frequency was independent from holding potential as shown by the plot in Fig. 41A (n = 3).

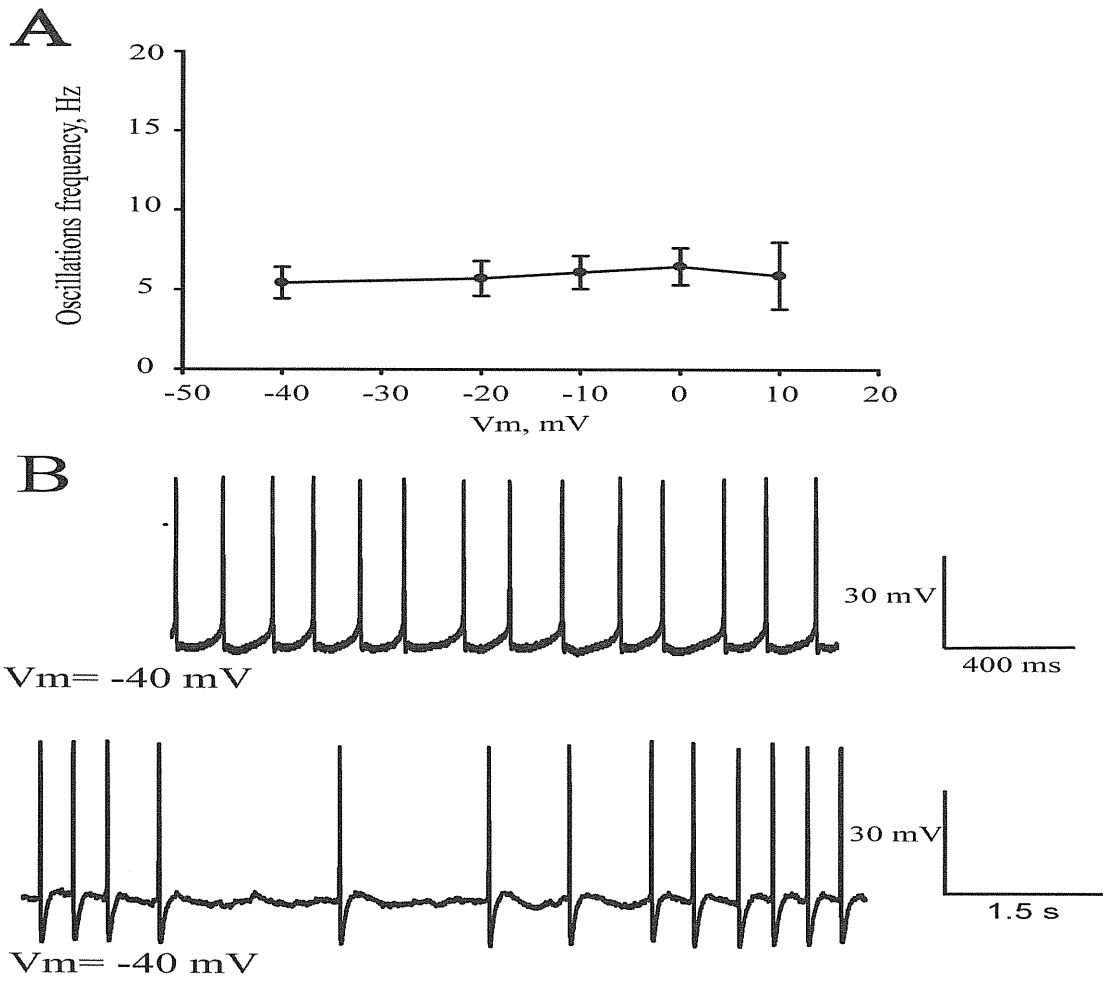

Fig. 41. HM firing behavior in the presence and in the absence of oscillations in current clamp conditions. (A) Plot of oscillation frequency versus membrane potential (Vm) values demonstrates event independence of Vm. The intracellular solution contained the Na^+ and I_h current blocker QX-314 (300 µM) in order to prevent HM firing (n = 3). (B) Example of two HMs recorded in the presence of nicotine (10 µM) at the same membrane potential (-40 mV). The cell above generated oscillations with regular spikes always at the peak of an oscillation. Conversely, the cell shown in the bottom record did not generate oscillations and fired randomly.

In current clamp experiments run on 24 HMs, 37.5 % of them oscillated after nicotine application with average frequency of 6.6 ± 0.8 Hz (n = 9). Oscillations made firing regular as the CV value of the inter spike interval was 15 ± 1 % (n = 9) in the presence of oscillations (see example in Fig. 41B, upper panel), while non-oscillating HMs generated irregular firing (CV = 68 ± 17 % for their inter spike interval; n = 10, Fig. 41B, lower panel).

Before nicotine application, oscillating and non-oscillating cells had comparable membrane potential (-62 ± 1 mV for non-oscillating cells, n = 10, versus -62 ± 1 mV, n = 9, for oscillating cells). Nicotine (10 μM) depolarized oscillating cells to -37 ± 5 mV (n = 10), and non-oscillating cells to -51 ± 2 mV (P = 0.02; n = 12). After nicotine administration, there was, however, no difference in firing threshold between these two groups of neuron (-46 ± 3 mV, n = 9 for oscillating cells versus -50 ± 5 mV, n = 3 for non-oscillating cells).

While the spiking modality became regular because of oscillations, other neuronal firing characteristics were altered by nicotine regardless the presence of oscillations. Hence, the probability of firing increased in oscillating as well as in non-oscillating cells, so that data were pooled together. Before nicotine administration, the probability of firing was 0.08 ± 0.06 and became 1 ± 0 in the presence of nicotine for the same amount of injected current (P=0.0002; n = 5).

I next examined the input/output properties of HMs by injecting DC current steps and measuring the corresponding firing rates. Figure 42A demonstrates one such experiment with an oscillating neuron. I measured the instantaneous firing frequency (Lape & Nistri, 2000; Pagnotta *et al.,* 2005) caused by 30 pA DC current. In all experimental conditions (control, nicotine and washout) firing reached steady state after the first two spikes, indicating fast adaptation (Lape & Nistri, 2000). Thus, the neuron preserved its ability to transduce depolarization into output signals over a similar time-course, although the output frequency was higher after nicotine administration. Figure 42B shows standard F/I (frequency/injected current) plots for five oscillating neurons: in the presence of nicotine, the plot was shifted upwards to the left, confirming increased firing frequency. Nevertheless, the slope of the plot indicating the averaged gain function of the HM was unchanged (0.36 ± 0.04 before nicotine application versus 0.36 ± 0.03 in the presence of nicotine).

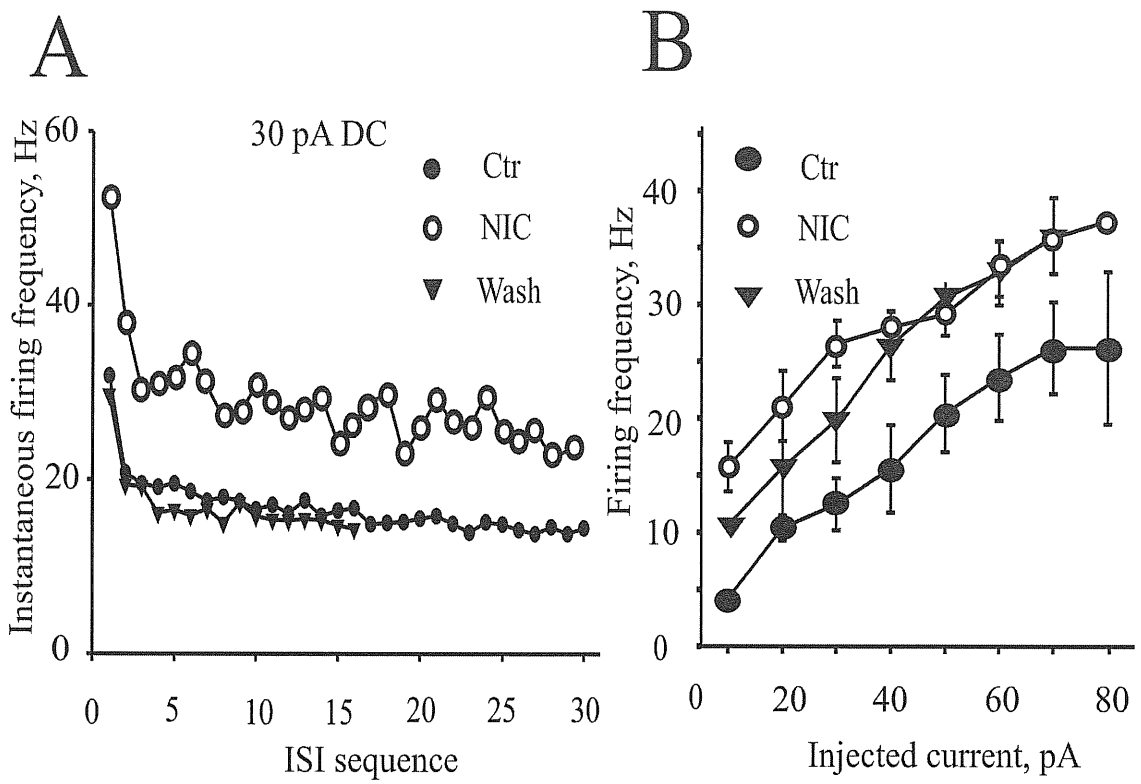

Fig. 42. HM responses to injected current before and after nicotine application in the presence of oscillations. (A) Plot shows that the instantaneous firing frequency for injected DC current (30 pA) into an oscillating HM was increased after nicotine (10 μM) application. The effect was fully reversible on washout. Note that the instantaneous firing frequency reached steady state after the second spike because of rapid adaptation. (B) On 5 oscillating HMs, nicotine shifted the frequency-current relation (F/I curve) to the left, thus increasing HM excitability. The slope of F/I curve was unchanged (0.36 ± 0.04 in control conditions vs. 0.36 ± 0.03 after nicotine application) indicating equivalent motoneuron gain function. Firing frequency was measured at steady state. The slope of F/I curve was measured for each injected current value and then averaged.

For a non-oscillating HM during 30 pA DC current injection, steady firing frequency was also achieved after the first two spikes and remained higher in the presence of nicotine (Fig. 43A). For a group of non-oscillating HMs (n = 4), the F/I curve was shifted upwards to the left by nicotine application without change in its slope (0.44 ± 0.02 before nicotine application versus 0.46 ± 0.07 in the presence of nicotine; Fig. 43B). In oscillating neurons, firing frequency increased by 84 % for all injected current values (n = 5), while in non-oscillating neurons the firing frequency increased by 42 % (n = 4), which was not statistically significant.

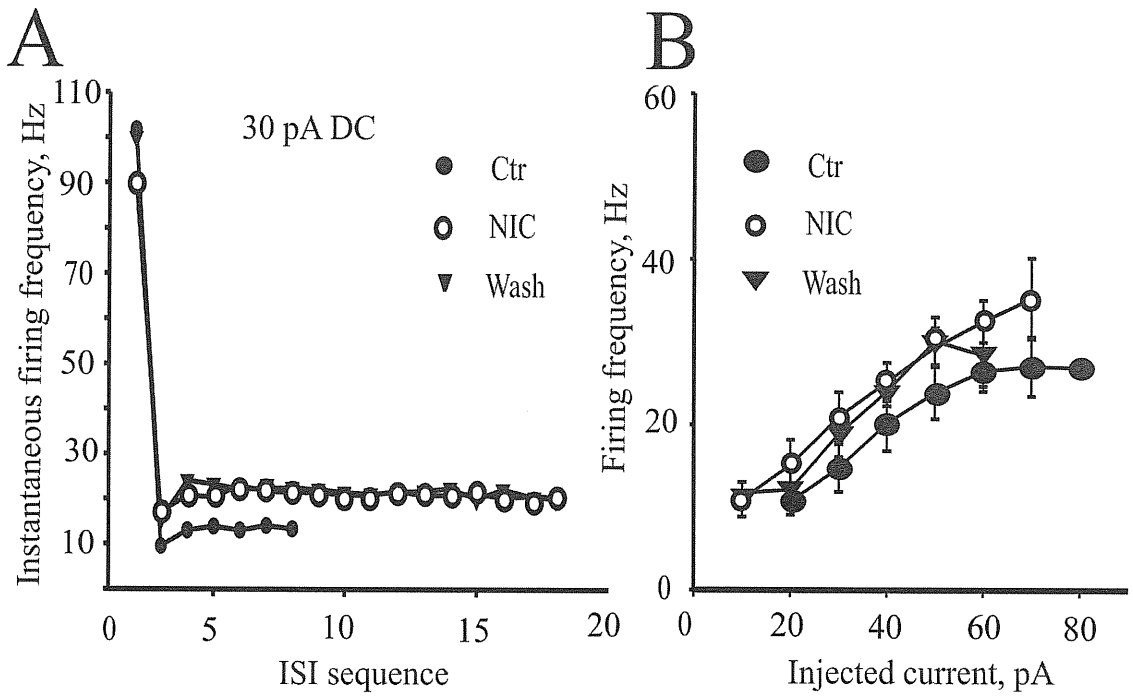

Fig. 43. HM responses to injected current before and after nicotine application in the absence of oscillations. (A) In a non-oscillating motoneuron, the instantaneous firing frequency for injected 30 pA DC was increased after nicotine (10 μM) application. (B) The F/I relation of non-oscillating neurons was shifted to the left after nicotine (10 μM) application, while the slope of these plots remains the same (0.44 ± 0.02 before nicotine administration and 0.47 ± 0.07 after it; n = 4 cells).

Thus, nicotine increased neuronal excitability in all cells, irrespective of whether they did or did not show oscillatory behavior. When oscillations were present, they transformed disperse neuronal spiking to the regular theta frequency spiking.

6.2 Nerve recording

Since upon nAChR activation only about 40 % of HMs showed oscillatory behavior in both voltage and current clamp, I also explored the oscillatory output of the hypoglossal nucleus during nicotine application. In general, oscillations might be local events within the XII nucleus or, conversely, might involve a percentage of cells large enough to influence motor output to the tongue. HMs innervate the tongue musculature and are, therefore, involved in several motor functions of the tongue (Lowe, 1980). Thus, I recorded spike activity from the XII nerve, namely the sum of firing HMs. Even with a slice preparation, rhythmic activity recorded from the XII nerve could be produced upon nicotine (10 μM) application. The oscillatory activity was observed in 6 out of 10 preparations. The oscillatory behavior was

complex and, unlike that observed with HM voltage- or current clamp recording, was composed of several different activities. Upon nicotine application, 3 out of 10 nerves showed a rhythmic pattern of 0.7 ± 0.26 Hz frequency, 2 nerves showed a rhythmic pattern of 5.94 ± 1.4 Hz frequency and one nerve demonstrated both types of activities (Fig. 44). The slow rhythm on average lasted 210 ± 91 s (n = 4), while the theta frequency rhythm lasted 285 ± 53 s. Co-existence of fast and slow rhythmic outputs is demonstrated with the example shown in Fig. 44. In this nerve, depicted in Fig. 44A, the slow rhythm was the first to appear after 1.5 min of nicotine application (Fig. 44B, upper panel, left). After 3.5 min it was then replaced by the theta frequency rhythm (Fig. 44B, lower panel, left), that lasted 0.5 min, when spikes vanished, but oscillations remained (Fig. 44B, upper panel, right). Eventually, after 2.5 min, the oscillations stopped (Fig. 44B, lower panel, right). I have also observed that during the theta frequency rhythm on each peak of the oscillatory cycle there were four (n = 2 preparations) or one spike (n = 1 preparation). Thus, nicotine- induced oscillatory activity coud be transmitted to the tongue musculature via the XII nerve. These last data suggest that the rhythmic activity had a large-scale effect on motor output.

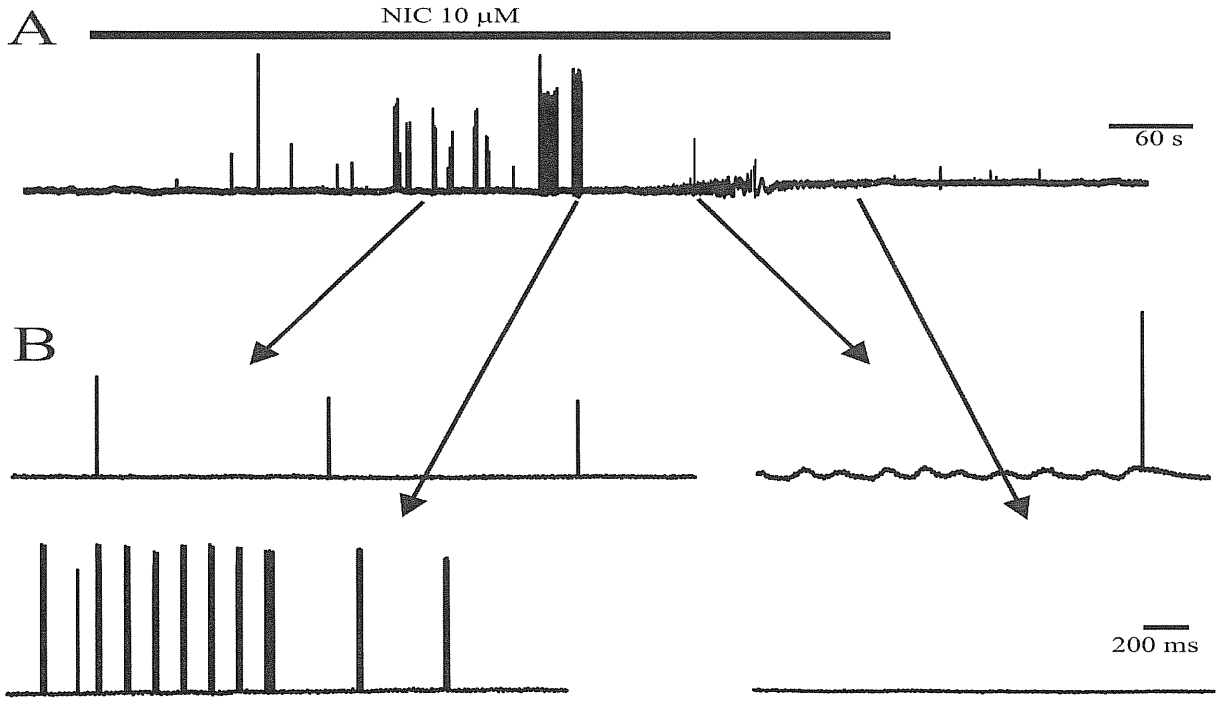

Fig. 44. XII nerve recording of oscillatory activity upon nicotine application. (A) Nicotine (10 μM, indicated by black bar) produced a complex oscillatory behavior, which lasted 6.5 min in this cell. (B) At the beginning of nicotine application, a slow (0.31 ± 0.16 Hz for this cell) rhythm appeared (upper panel, left). This rhythm was replaced by the theta frequency rhythm (6.13 ± 0.12 Hz for this cell, lower panel, left). The latter rhythm lasted 0.5 min, when spiking disappeared, but the oscillations remained (5.6 ± 0.15 Hz, upper panel, right). At the end of the recording oscillations spontaneously vanished (lower panel, right).

DISCUSSION

1. nAChRs of HMs: subunit composition and function

Nicotinic acetylcholine receptors are widely distributed in the brain (Gotti & Clementi, 2004) including the hypoglossal nucleus (Wonnacott, 1997; Zaninetti *et al.*, 1999; Dehkordi *et al.*, 2005; Quitadamo *et al.*, 2005) in which the main subtypes of nAChR belong to the α2β4 and α7 classes. Nevertheless, there are only a few cases when direct nicotinic transmission in the brain has been reported: for instance, in the nucleus ambiguous (Zhang *et al.*, 1993), on GABAergic interneurons in the hippocampus (Alkondon *et al.*, 1998), on hypothalamic supraoptic neurons (Hatton & Yang, 2002), and in the developing visual cortex (Roerig *et al.*, 1997). Since nAChRs are chiefly located on presynaptic endings or even axon fibres (Gotti & Clementi, 2004), it is often difficult to investigate them functionally and to compare their properties with any postsynaptic nAChRs. However, in the mammalian brainstem the overwhelming majority of neurons in the nucleus hypoglossus are motoneurons (HMs) that natively express nAChRs also present within the local network (Zaninetti *et al.*, 1999; Chamberlin *et al.*, 2002; Robinson *et al.*, 2002; Shao & Feldman, 2000). Hence, the nucleus hypoglossus offers the advantage of studying simultaneously how pre- and postsynaptic nAChRs operate.

The nAChR composition of HMs is not completely identified. While previous studies show presence of α4β2 receptors, the expression of α7 receptors has not been reported by either autoradiographic (Zaninetti *et al.*, 1999) or electrophysiological (Chamberlin *et al.*, 2002; Shao & Feldman, 2000) studies. Nevertheless, more recent immunocytochemical data have indicated their substantial expression in the adult rat brainstem (Dehkordi *et al.*, 2005) in accordance with our study of neonatal tissue. Recent electrophysiological studies in our lab (Quitadamo *et al.*, 2005) have revealed the presence of functional α7 and β2 nAChR subunits. Immunohistochemistry and Western immunoblot data show that HMs express α4, α7 and β2 nAChR subunits. All three nAChR subunit types were abundantly expressed on motoneuron somata and fibres. However, antibodies are against nAChR intracellular epitopes, thus unsuitable for detailed mapping of their cell topography. Immunoreactive cells to each nAChR subunit were expressed along all rostro-caudal axis of XII nucleus, even if they were more numerous in the caudal end than in the rostral end of the nucleus. At P0-P5, there was no age dependence for nAChR expression.

We propose that HM nAChRs of neonatal rats are made up by homomeric α7 and heteromeric $(\alpha4)_2(\beta2)_3$ subunits and they are present throughout the XII nucleus.

Our lab has shown (Quitadamo *et al.,* 2005) that there is no tonically active, fast nicotinic synaptic transmission on HMs in the brainstem slice preparation. I have done experiments to find out if presynaptic nAChRs could have any effect on glutamatergic or GABAergic neurotransmission. Endogenously released acetylcholine normally is cleared away from the synaptic cleft by acetylcholinesterase (see Introduction). To boost endogenous cholinergic signaling, I used edrophonium, an acetylcholinesterase blocker. Experiments were done in the continuous presence of TTX to block synaptic inputs. Edrophonium induced no change in mEPSC frequency, amplitude or current baseline.

There are several mechanisms, which could account for the nicotinic action of ACh as a modulator of synaptic transmission at pre- and/or postsynaptic level. For example, activation of nAChRs leads to increased Ca^{2+} influx and neuronal depolarization. Calcium influx through nAChRs could result in a cascade of metabotropic functions, including modulation of transmitter release, changes in enzyme activity and gene transcription (Alkondon *et al.,* 2000; Fisher & Dani, 2000). In hippocampus, Ca^{2+} influx activates calmodulin, which can presynaptically enhance glutamate release or postsynaptically modulate neuron responsiveness (Fisher & Dani, 2000). The amplitude and duration of the postsynaptic Ca^{2+} increase are important factors in determining whether long-term depression, long-term potentiation, or neither arises from synaptic activity (Bear, 1995; Nicoll & Malenka, 1995). Coincident activation of nAChRs and NMDARs could increase postsynaptic Ca^{2+} level above the threshold for long-term potentiation. Conversely, activation of nAChRs prior to activation of NMDARs could reduce the responsiveness of NMDARs, resulting in long-term depression (Fisher & Dani, 2000).

On CA1 interneurons of rat hippocampus, α7 nAChR activation could modulate GABAergic transmission and have multiple postsynaptic effects (Alkondon *et al.,* 2000). Presynaptically, nAChR activation increases Ca^{2+} influx, depolarizes neurons and, therefore, modulates GABA release, inducing synaptic plasticity. Postsynaptically, desensitized nAChRs could inhibit spike generation and, therefore, alter the rate of rhythmic discharges. Alternatively, postsynaptic nAChRs activation could initiate spike generation and affect inhibition, disinhibition or rhythm generation. In a population of interneurons, nAChRs desensitization curtailed the spike activity, while in other neurons nAChR activation inactivated Na^{+} channels, which was the main reason for synaptic transmission inhibition (Alkondon *et al.,* 2000).

Previous studies in our lab had shown that nicotine treatment upregulated glutamate release, and application of nAChR blockers could decrease glutamatergic events on HMs (Quitadamo *et al.,* 2005). In my experimental model, neither nAChRs on HMs nor presynaptic nAChRs modified glutamatergic or GABAergic neurotransmission upon elevation of endogenous ACh level. Previous data from our lab have shown that nAChRs of HMs, in the continuous presence of acetylcholine or nicotine, desensitize with a time constant of approximately 200 ms (Quitadamo *et al.,* 2005). We propose that nAChRs, found in hypoglossal nucleus, desensitize quickly and do not influence glutamatergic or GABAergic neurotransmission at a single cell level, which is in agreement with studies of other nAChRs in the brain (for review see Quick & Lester, 2002).

2. nAChR role on GABAergic transmission on HMs

Anatomical studies have shown that nAChRs often occur at GABAergic synapses, both presynaptically and postsynaptically (Fabian-Fine *et al.*, 2001; Kawai *et al.*, 2002; Zago *et al.*, 2006). Within the nucleus hypoglossus, nAChR action on GABAergic neurotransmission is not known. My data show that presynaptic nAChRs upregulated GABAergic neurotransmission within the nucleus hypoglossus, increasing sEPSC frequency. This is consistent with other studies, where presynaptic nAChRs were showed to upregulate GABAergic neurotransmission (Alkondon *et al.,* 1997; Zhu & Chiappinelli, 1999; Wang *et al.,* 2003; Wanaverbecq *et al.,* 2007).

nAChRs can cocluster with $GABA_A$ receptors on postsynaptic membranes of hippocampal interneurons (Liu *et al.,* 2001; Kawai *et al.*, 2002) and chick ciliary ganglion neurons (Wilson Horch & Sargent, 1995; *Shoop et al.,* 1999).

Recently it was shown that postsynaptic nAChRs downregulate GABAergic currents (Wanaverbecq *et al.,* 2007; Zhang & Berg, 2007). The mechanism is intracellular Ca^{2+} - and PKC dependent. Several mechanisms have been proposed to cause the dynamic regulation of $GABA_A$ receptors by protein kinases and phosphorylases, leading to altered phosphorylation status of $GABA_A$ receptors and/or internalization (Kittler & Moss, 2003; Luscher & Keller, 2004). If the main effect of nAChRs is to promote the internalization of receptors, the fact that the effect is slow and reversible suggests that this occurs against a background of constitutive cycling of receptors at the synapse. The effect of α7 nAChR agonists on postsynaptic GABAergic signaling via activation of PKC is similar to that of exogenous activation of TrkB receptors, serotonin receptors and muscarinic receptors, suggesting substantial convergence of

signaling (Wanaverbecq *et al.,* 2007). However, while chelating intracellular Ca^{2+} abolished the depression of GABAergic currents, PKC inhibitors only attenuated the depression (Wanaverbecq *et al.,* 2007), suggesting that other pathways may also contribute to $GABA_A$ receptor regulation. In chick ciliary ganglion neurons, inhibitors of both Ca^{2+}–calmodulin-dependent protein kinase II (CaMKII) and mitogen-activated protein kinase (MAPK) were required to block completely the α7-nAChR effects on GABA-induced currents (Zhang & Berg, 2007). The later finding also raises the possibility that the two pathways may operate in parallel.

My data show that, within the hypoglossal nucleus, nAChRs do not influence postsynaptic GABA responses. Therefore, the main action of nAChRs on GABAergic neurotransmission was presynaptic facilitation of GABA release. The effect was calcium dependent, because chelating intracellular Ca^{2+} with 10 mM EGTA abolished the facilitating effect of nAChRs.

3. Brainstem network nAChRs and their function

3.1 Premotoneuronal nAChR activation evoked oscillatory behavior in HMs

Even if nAChRs are ion channels with a high Ca^{2+} permeability (Fucile, 2004), the main effect of nAChRs activation is known to be modulatory, as nicotine facilitates presynaptic release of various neurotransmitters, including glutamate (McGehee & Role, 1996; Gray *et al.*, 1996; Girod *et al.,* 2000; Giniatullin *et al.,* 2005). Our previous data showed that nicotine facilitated glutamatergic inputs to motoneurons of the XII cranial nucleus (Quitadamo *et al.,* 2005). In general, ultrastructural analysis shows that cholinergic nerve terminals are usually scattered and do not make contact with postsynaptic densities, even if they are equipped for vesicular release (Vizi & Kiss, 1998; Descarries & Meckawar, 2000). Thus, cholinergic signaling might be expected to be expressed via diffused, network-dependent mechanisms.

Our lab had shown that a low (0.5 μM) concentration of nicotine first facilitated glutamatergic transmission on HMs and later depressed it through receptor desensitization (Quitadamo *et al.,* 2005). When 0.1 μM nicotine was used, only depression of synaptic transmission occurred, in keeping with the suggestion that nAChRs can be desensitized without prior activation (Paradiso & Steinbach, 2003). To activate a wide variety of nAChRs within the XII nucleus, I used 10 μM nicotine. Such nicotine concentration enhanced glutamatergic transmission, which produced theta frequency rhythmic discharges in 40 % of HMs. This oscillatory activity required sustained nAChR activation, because it rapidly waned after nicotine washout. Because DHβE or MLA (applied at nAChR subtype selective concentrations; Harvey & Luetje, 1996;

Palma *et al.*, 1996; Bergmeier *et al.*, 1999; Davies *et al.*, 1999) blocked nicotine-evoked oscillations, it appears that synergic activation of both receptor classes was necessary for oscillation production. The electrophysiological characteristics of oscillations were rather similar to those induced by application of a metabotropic glutamate receptor agonist (Sharifullina *et al.*, 2005; Nistri *et al.*, 2006): thus, oscillations had very limited dependence on HM potential, and stereotypic characteristics of amplitude and duration, resembling spikelets (Long *et al.*, 2004; Sharifullina *et al.*, 2005) propagated via electrical coupling within the network as further discussed below. This suggestion appears more likely than implying that oscillations were synaptic events of remote location on motoneurons and, thus, outside the voltage clamp ability of the patch electrode. In fact, glutamatergic synaptic events can be readily reversed at positive holding potential (Sharifullina *et al.*, 2005) and display kinetics distinct from those of oscillatory currents. Furthermore, intracellular application of QX-314 failed to block oscillations, a finding also in favor of their network origin. It is interesting to mention that, under current clamp conditions in the presence of QX-314, the oscillation period was voltage independent, whereas, in the absence of QX-314, membrane depolarization accelerated the oscillatory period, indicating that voltage-dependent conductances, though not rhythmogenic *per se*, could, however, shape the oscillation characteristics.

Although oscillations could be distinguished from glutamatergic events, there was a tight correlation between oscillation frequency and synaptic event frequency, suggesting that a large facilitation of excitatory synaptic transmission at network level accompanied the onset of oscillations. The simplest interpretation is that oscillations were the electrophysiological expression of rhythmic discharges from functionally coupled HMs activated by enhanced synaptic inputs.

3.2 Nicotine-induced oscillatory behaviour was an emergent property

In other brain areas, the role of nAChRs in theta rhythmic activity is controversial: some studies have reported activation of nAChRs to block (Bland & Colom, 1988; Steriade, 1993; Mansvelder *et al.,* 2006), or slowdown oscillations (Kadoya *et al.*, 1994; Lindgren *et al.*, 1999). Other studies have indicated no effect (Konopacki *et al.,* 1988; Konopacki & Golebiewski, 1992), or even an enhancement *in vivo* (Bringmann, 1997; Siok *et al.,* 2006) or in vitro (Song *et al.,* 2005). By eliciting stronger activation of nAChRs with a higher dose (10 μM) of nicotine as employed in other studies (Robinson *et al.,* 2002; Giocomo & Hasselmo,

2005; Song *et al.,* 2005), the present study provides evidence that network nAChRs can induce theta frequency rhythms.

Hence, while single HMs did not express pacemaker properties that enabled them to generate intrinsic oscillations, intense nAChR activity could functionally bind HMs together so that rhythmic behavior appeared. This phenomenon belongs to the class of so-called emergent properties of neurons (Faingold, 2004; Feldman & Del Negro, 2006) which could not be deduced at single cell level, but could be manifested when the network excitability reached a critical threshold in the presence of efficient neuronal wiring (see Fig. 3).

To the best of our knowledge, our report is the first demonstration that nAChR activation could actually induce theta frequency rhythm in the CNS.

3.3 Rhythmic oscillations required sustained nAChR activity

Oscillations were never observed spontaneously; even when a single HM was depolarized by current injection or the extracellular K^+ concentration was elevated to 7 mM. While oscillating HMs had larger input resistance than non-oscillating ones, other properties (sEPSC frequency and amplitude, resting membrane potential, firing threshold) were the same. Since our experimental protocols included block of glycinergic and GABA-ergic synapses and there is no direct cholinergic neurotransmission on HMs (Quitadamo *et al.*, 2005), it was possible to restrict our analysis of the origin of oscillations to glutamatergic transmission.

While previous studies have shown that brainstem nAChRs desensitize in the continuous presence of nicotine (Chamberlin *et al.,* 2002; Quitadamo *et al.*, 2005), the process of desensitization depends on various factors like receptor structure, agonist concentration and duration of application (Lester, 2004; Giniatullin *et al.*, 2005). We observed that the oscillatory behavior evoked by nicotine persisted for many minutes and required sustained receptor activation as shown by its block following application of receptor antagonists. This realization prompted us to consider the possibility that network nAChRs desensitized at slower rate than motoneuron receptors. This hypothesis could be experimentally tested by comparing, during a long application of bath-applied nicotine, responses to nicotine pulses applied to HMs, with changes in glutamatergic event frequency, and network-dependent oscillations. HM nAChRs underwent fast desensitization and were not crucial for oscillatory behavior. Conversely, network receptors supporting enhanced glutamatergic frequency remained active for at least 8 min. This time-course correlated well with the oscillation duration. On neurons in culture, nAChRs can still generate responses, albeit of smaller amplitude, after a prolonged application

of nicotine (Sokolova *et al.*, 2005), confirming that certain receptors can remain functional for an extended time. The different desensitization properties of pre- and postsynaptic nAChRs (despite similar structure) are not easily explained. Desensitization is regulated by intracellular factors, such as phosphorylation by different protein kinases (Huganir *et al.,* 1986), whose distribution and efficiency might differ between pre- and postsynaptic sites.

3.4 Oscillatory behavior required both chemical and electrical transmission

Since mere network depolarization with high K^+ could not induce oscillations, it seems likely that nicotine-sensitive nAChRs were strategically placed on certain glutamatergic neurons rather than on virtually all network elements.

AMPA receptor activity was necessary for oscillatory activity, because CNQX, a selective AMPA/kainate receptor antagonist, blocked it. NMDA receptors minimally contributed to oscillations, because the NMDA receptor antagonist APV could not reliably arrest them, it attenuated oscillatory activity without complete suppression. Since group I metabotropic glutamate receptors (mGluR1s) are largely expressed in the developing hypoglossal nucleus (Hay *et al.*, 1999; Nistri *et al.*, 2006) and their activation can induce theta rhythms (Sharifullina *et al.*, 2005), it was not surprising that these receptors were also involved in present oscillatory behavior, as indicated by the block evoked by the selective antagonist AIDA.

Previous studies have identified electrical coupling between brainstem motoneurons under *in vitro* and *in vivo* conditions (Mazza *et al.*, 1992; Rekling *et al.*, 2000). Indeed, it has been suggested that electrical coupling is responsible for oscillatory activity, so that only coupled HMs can oscillate (Sharifullina *et al.*, 2005; Nistri *et al.*, 2006). In the present study, electrical coupling was also apparently involved in oscillatory behavior because carbenoxolone, a selective gap junction blocker, attenuated or even suppressed oscillations. Because of the action of this drug is often slow (Sharifullina *et al.,* 2005), it is possible that, had longer recordings be possible, oscillatory behavior would have been systematically blocked. It is noteworthy that electrical coupling among premotoneurons may have also been one important contributor to the oscillatory activity in analogy with recent results obtained from electrically coupled interneurons within the motor network of the spinal cord (Hinckley & Ziskind-Conhaim, 2006).

The contribution of gap junctions to nicotine-induced oscillations was further corroborated by the observation that oscillations comprised spikelets and burstlets (Long *et al.*, 2004;

Sharifullina *et al.*, 2005). These phenomena are typical of electrical coupling and reflect single cell or cell cluster firing, respectively, once network excitability had been adequately raised.

3.5 Synaptic inhibition was not required for oscillatory behaviour

Many models for rhythmogenesis require synaptic inhibition (Grillner *et al.*, 1991; Dale, 1995; Roberts *et al.*, 1995; Richter & Spyer, 2001). Nevertheless, HM rhythmic activity can be generated even without synaptic inhibition in young animals (Sharifullina *et al.*, 2005). Likewise, block of synaptic inhibition did not prevent nicotine-induced oscillatory activity. These observations indicate that synaptic inhibition was not directly participating in rhythm generation, while it had a permissible role in controlling the number of oscillating HMs.

3.6 Persistent inward current was not necessary for the oscillations

PIC, composed of I_{NaP} and $I_{CaP,}$ appears to be important for prolonged rhythmic discharges (Darbon *et al.*, 2004; Cramer *et al.*, 2007; van Drongelen *et al.*, 2006; Zhong *et al.*, 2007). I_{NaP} is responsible for burst firing in spinal motoneurons (Li & Bennett, 2003; Elbasiouny *et al.*, 2006; Theiss *et al.*, 2007; Zhong *et al.,* 2007), since its inhibition by riluzole might disrupt collective excitation of motoneurons, thus protecting them from overactivity. I_{NaP} is, however, unnecessary for motoneuron bursting evoked by brainstem preBotzinger neurons (Pace *et al.*, 2007 a, b).

My data showed that while PICs were early decreased by riluzole to a stable amplitude still compatible with lower frequency oscillations, the occurrence of sEPSCs returned more slowly to control value that coincided with the disappearance of oscillations. The simplest interpretation is that enhanced glutamatergic transmission was essential to generate oscillations which could emerge even with halved (or less than halved) PICs. Thus, PICs could contribute to oscillatory patterns without being crucial for them, in analogy with data from brainstem respiratory neurons (Pace *et al.*, 2007 a, b). Indeed, the data showed how TTX arrested oscillations probably because it had the widespread effect of preventing network propagation of fast action potentials as well as repetitive firing supported by PICs.

One alternative possibility is that the time lag between PIC depression and loss of oscillations was due to slow activation of a process leading to delayed inhibition of oscillations. This hypothesis, however, contrasts with the early suppression of oscillations by glutamate receptor blockers (Lamanauskas & Nistri, 2006) which do not interfere with motoneuron persistent inward currents (Harvey *et al.*, 2006; Kuo *et al.*, 2006; Theiss *et al.*, 2007). Furthermore,

oscillating and non-oscillating HMs had similar PICs whose amplitude was unchanged by nicotine. Thus, on HMs, the main generator for the oscillations was increased glutamatergic transmission, whereas I_{NaP} played a modulatory role in setting oscillations. Since HMs can produce a range of rhythmic motor patterns (Nistri *et al.*, 2006), our data do not exclude that PICs can be essential to support bursting at other frequencies or patterned discharges induced by other mechanisms.

3.7 Functional role of oscillations

Current clamp experiments helped to understand the input/output function of HMs during oscillations. Following application of nicotine, spikes appeared at the peak of an oscillation. Because of the tight association between action potentials and oscillations, the consequence was that oscillations paced neuronal firing to theta frequency range. Under these conditions, neuronal firing became a high-fidelity mechanism to convert depolarizing signals to a reliable output to muscle fibres.

Furthermore, the administration of nicotine ensued that all recorded HMs could still fire at higher frequency with their time-dependent adaptation. Hence, the slope of the F/I curve was not significantly changed, indicating no alteration in the motoneuron gain. The electrophysiological consequence of nicotine application were, on the one hand, constraint of firing rates when oscillations were present, and, on the other hand, preserved ability to transduce large depolarizations into adapted firing behavior. This bimodal operation of HMs during application of nicotine outlined a large safety margin of HM function as fidelity of spiking at low rates did not preclude the possibility of generating stronger outputs when necessary. This process may allow HMs to express a wide range of tongue movements in accordance with very different patterns of behavior.

XII nerve recording revealed that oscillations were not a local phenomenon within the nucleus hypoglossus, but oscillations were transmitted from the nucleus to the effector muscles. HMs innervate the tongue musculature and are, therefore, involved in several motor functions of the tongue, including sucking, mastication, chewing and respiration (Lowe, 1980). The nerve recording represented summated activity of many spiking HMs. Even in a thin slice preparation (350 μm), the rhythmic activity within the nerve could be produced upon nicotine (10 μM) application. For the breathing command generation, XII nucleus is believed to play a passive role, collecting inputs from higher brain centers, such as preBotC complex, where the rhythm is generated, and sending an output to the tongue musculature (Feldman & Del Negro,

2006; Pace *et al.*, 2007 a, b). However, in our lab it was shown (Sharifullina *et al.*, 2005), that XII nucleus *per se* could be rhythmogenic. In that study, theta frequency oscillations were generated by metabotropic glutamate receptor activation. The present study showed that rhythmic behaviour could be induced in the XII nucleus by increased levels of endogenous glutamate. Glutamate release was enhanced by presynaptic nAChR activation. The rhythm could transform the HM input to the tongue musculature, thus shaping tongue movements into a regular pattern, which could exert several motor functions.

In summary, the realization that brainstem nAChRs represent a resource for facilitating release of endogenous glutamate to enhance motor output might outline novel strategies to treat the severe dysphagia which accompanies certain neurodegenerative disorders (von Lewinski & Keller, 2005).

4. Electrophysiological effects of riluzole on HMs

4.1 Riluzole depressed I_{NaP} and I_{CaP}

On motoneurons, I_{NaP} is one component of the persistent inward current (PIC) mediated by Na^+ and/or Ca^{2+} to integrate synaptic inputs (Crill, 1996; Russo & Housgaard, 1999). Since I_{NaP} appears to be important for prolonged rhythmic discharges (Darbon *et al.*, 2004; Cramer *et al.*, 2007; van Drongelen *et al.*, 2006; Zhong *et al.*, 2007), its inhibition might disrupt collective excitation of motoneurons. I_{NaP} is, however, unnecessary for motoneuron bursting evoked by brainstem preBotzinger neurons (Pace *et al.*, 2007 a, b). Consequently, we wondered if I_{NaP} is involved in oscillations of HMs produced by nicotine (Lamanauskas & Nistri, 2006). Recently it was shown that the persistent sodium current could be blocked by riluzole (I_{NaP}; Del Negro *et al.*, 2005; Miles *et al.*, 2005; Harvey *et al.*, 2006; Theiss *et al.*, 2007) evoked by depolarization of brainstem (Powers & Binder, 2003; Moritz *et al.*, 2007) or spinal motoneurons (Harvey *et al.*, 2006; Theiss *et al.*, 2007). Therefore, my first approach was to employ riluzole to block I_{NaP} to find out how this conductance is involved in oscillations. Consequently, I had to evaluate the selectivity of riluzole to block persistent inward currents.

PIC amplitude and area (demonstrated with slow voltage ramps to inactivate fast currents) depended on ramp speed and slowly inactivated on a time scale of several seconds, in agreement with data by Enomoto *et al.* (2006), Magistretti *et al.* (2006), and van Drongelen *et al.*, (2006). Despite working with neonatal cells, we found PIC values similar to the ones found in adult (Li & Bennett, 2003; Harvey *et al.*, 2006) or juvenile animals (Powers & Binder, 2003; Aracri *et al.*, 2006; Theiss *et al.*, 2007).

PICs were composed of I_{NaP} (50 % of the total PIC amplitude and 60 % of the total area) and of I_{CaP} (40 % of the total PIC amplitude and area). The activation threshold of I_{NaP} (-56 mV) and its voltage value for maximum current (-34 mV) were similar to those of other brain neurons (Darbon *et al.*, 2004; Miles *et al.*, 2005; Kuo *et al.*, 2006). I_{CaP} operating range showed more positive threshold (-46 mV) and voltage maximum (-16 mV). Since the fast Na^+ current of HMs is activated at about -45 mV (Lape & Nistri, 2001), I_{NaP} becomes active in the subthreshold region (Crill *et al.*, 1996) and can play an important role in neuronal integration and spike initiation, when I_{CaP} is not yet operative.

In the present experimental conditions, riluzole showed limited selectivity for the HM I_{NaP} as it could further depress PICs resistant to a fully effective concentration of TTX, and sensitive to Mn^{2+}. We propose that riluzole could also partly inhibit I_{CaP} which, on rat HMs, was likely to be made up by co-activation of several voltage-dependent Ca^{2+} conductances (Umemiya & Berger, 1994; Powers & Binder, 2003). Furthermore, I_{CaP} could have included I_{CAN}, a Ca^{2+} activated non-specific cationic current involved in persistent discharges (Pace *et al.* 2007 b).

The data suggests that riluzole was not a particularly selective I_{NaP} blocker, because it also depressed I_{CaP} and, therefore, the data inferring a certain role of the persistent inward currents on HMs, as the basis of the effect of riluzole, should be considered with caution.

4.2 Riluzole transformed firing properties of HMs

In current clamp conditions I could simulate burst firing by injecting slowly rising depolarizing currents which induced a cluster of action potentials at the top of the voltage trajectory. In the presence of riluzole, this firing mode was blocked presumably because riluzole suppressed I_{NaP} (and I_{CaP}) which, by operating in the subthreshold region, facilitated activation of the fast Na^+ conductance and supported repeated spiking above threshold (Schwindt & Crill, 1980). When HMs were depolarized by step current commands, fast spikes were resistant to riluzole, while repeated firing vanished.

The present results lead us to propose that oscillations could continue for some time even when long bursting was inhibited by riluzole, because fast action potentials triggered by nicotine-stimulated glutamatergic excitatory transmission could still propagate and recruit electrically-coupled HMs (Lamanauskas & Nistri, 2006).

4.3 Depression by riluzole of glutamatergic transmission

While riluzole is known to inhibit excitatory synaptic transmission (Mantz *et al.*, 1992; Martin *et al.*, 19933; Zona *et al.*, 2002; Coderre *et al.*, 2007), its mechanism of action is unknown. Since the effect of riluzole persists in the presence of TTX (Cheramy et al., 1992; Hubert & Doble, 1989; Martin et al., 1993; Hubert et al., 1994, and our present data), it points to a process directly controlling glutamate release.

The present study provides several new elements helpful to understand the action of riluzole. First, by measuring mEPSCs, I restricted the analysis to the local control of glutamate release without influences from network dependent activity. Second, I observed that the effect of riluzole was directed to synaptic transmission occurring at relatively high releasing rates. This result shows that riluzole was not indiscriminately depressing synaptic transmission, but it targeted those synapses which were particularly active. The data are consistent with a recent report on spinal motoneurons that found riluzole ineffective on mEPSCs occurring at low frequency (Prakriya & Mennerick, 2000; Tazerart *et al.*, 2007). Thus, my observations have interesting implications for the use of riluzole to treat overactive and potentially excitotoxic glutamatergic transmission. Third, riluzole reduced not only the frequency but also (slightly) the amplitude of mEPSCs. Although smaller event amplitude could be due to antagonism of postsynaptic receptors, previous reports show that riluzole does not bind any glutamate receptor type (Doble, 1996; Peluffo *et al.*, 1997; Kretschmer *et al.*, 1998). Since a modest reduction in glutamatergic event amplitude may have presynaptic origin (Quitadamo *et al.*, 2005), this interpretation accords with the observed decrease in event frequency without change in event distribution.

5. Presynaptic NMDA receptor control of glutamate release

5.1 Presynaptic NMDA receptors upregulated glutamate release

Several studies indicate that glutamate release may be positively regulated by presynaptic NMDA receptors (reviewed by Engelman & MacDermott, 2004), although there are no available data for HMs or other brainstem motoneurons. My present data show that the selective NMDA receptor antagonist APV depressed mEPSCs and prevented the effect of a subsequent application of riluzole, while the initial mEPSC decrease elicited by riluzole was not affected by later addition of APV. Although a brain slice preparation with its unavoidable severance/damage of afferent fibers is not ideally suited to quantify the contribution of presynaptic receptors, the current results suggest that NMDA receptor activity presumably

stimulated by ambient glutamate (originating from neurons and glia) positively contributed to glutamate release. This notion is consistent with former studies of cortical and hippocampal neurons (Yang *et al.*, 2006; Le Meur *et al.,* 2007) where presynaptic NMDA receptors may be activated by ambient glutamate despite the presence of 1 mM Mg^{2+}. When NMDA receptors contain the NR2D subunit, they show poor sensitivity to Mg^{2+} (Monyer *et al.*, 1994). Because abundant NR2D expression has been found in the nucleus hypoglossus (Paarmann *et al.*, 2000), this property may ensure sustained activation to promote glutamate release.

5.2 Riluzole action on presynaptic NMDA receptors

What is the mechanism of action of riluzole on glutamate release? Riluzole did not depress postsynaptic nicotinic responses. It does not seem that nAChRs could regulate glutamate release when the synaptic transmission is blocked. Radioligand binding studies show that riluzole does not bind NMDA, AMPA, kainate, or metabotropic glutamate receptors (Doble, 1996; Peluffo *et al.*, 1997; Kretschmer *et al.*, 1998). Nevertheless, the function of NMDA receptors can be highly regulated by G protein-coupled receptors (Koles *et al.*, 2001; Marino & Conn, 2002; MacDonald *et al.,* 2007) operating through PKC (Lu *et al.*, 1999; MacDonald *et al.,* 2007). The G-protein coupled receptor regulation of NMDA receptors is schematically demonstrated in Fig. 45.

In accordance with the finding, that riluzole is a direct enzyme inhibitor of PKC (Noh *et al.,* 2000), I observed mutual occlusion between the effect of the PKC blocker chelerythrine and the one of riluzole. We, therefore, propose that, in the rat nucleus hypoglossus, PKC activity facilitates presynaptic NMDA receptors to favour glutamate release. When glutamate release is increased to critical level, either via metabotropic glutamate receptors (Sharifullina *et al.,* 2005), glutamate uptake inhibition (Sharifullina & Nistri, 2006) or by presynaptic nAChR activation (my present data), oscillatory behavior could be produced. The main target of riluzole to attenuate excitatory transmission seemed to be PKC.

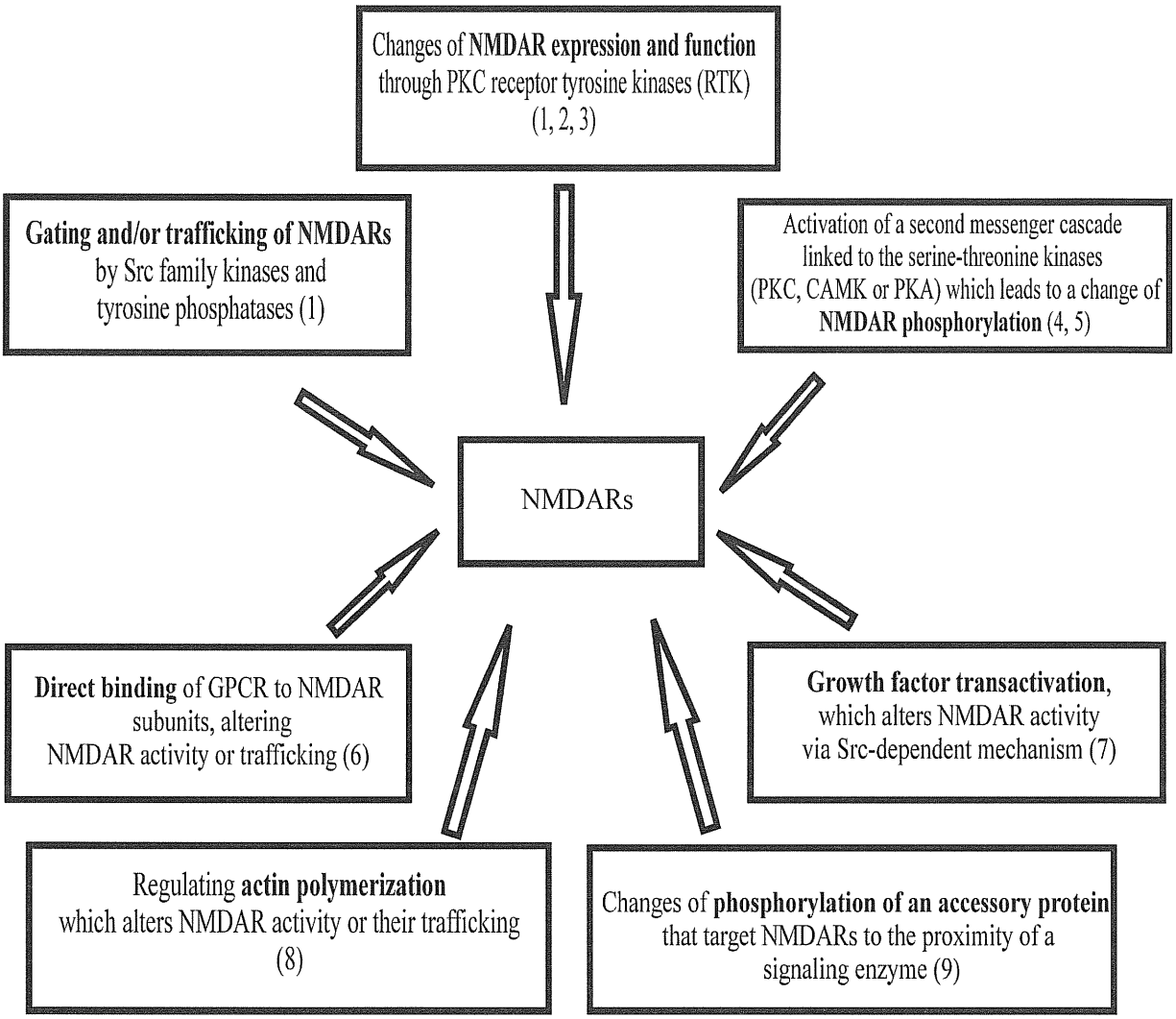

Fig. 45. A scheme of NMDA receptor modification by G-protein coupled receptors. The data are taken from: 1- MacDonald *et al.,* 2007; 2- Della *et al.,* 1999; 3- Kotecha *et al.,* 2002; 4- Kotecha & MacDonald, 2003; 5- Perez-Otano & Ehlers, 2005; 6- Lee & Liu, 2004; 7- Shah & Catt, 2004; 8- Lei *et al.,* 2001; 9- Westphal *et al.,* 1999.

5.3 Functional implications of riluzole use for clinical treatment

The multiple effects produced by riluzole on ionic currents and synaptic transmission can help to understand why this drug might be clinically useful in a variety in brain disorders which implicate deranged or enhanced glutamatergic transmission. Because riluzole limited spike bursting without changing single action potentials, its action is surmised to be primarily directed to block neuronal overactivity.

The same argument may be applied to the use-dependent inhibition by riluzole of glutamatergic transmission. The latter finding, however, disclosed two interesting phenomena related to presynaptic control of glutamate release, namely the role of NMDA receptors and their regulation by PKC activity. PKC can regulate both the presynaptic release of glutamate, as well as the function of postsynaptic NMDA and AMPA receptors (MacDonald *et al.,* 2001). NMDA receptor regulation by PKC was observed in CA1 pyramidal neurons of the hippocampus, where NMDAR activity could be enhanced or depressed, depending on the pathway, through which PKC was activated (Lu *et al.,* 1999; MacDonald *et al.,* 2001). In Xenopus oocytes, mGluR1 potentiates NMDA channel activity by increase in channel open probability and by recruitment of new channels to the plasma membrane; the mechanism was intracellular Ca^{2+} and PKC dependent (Lan *et al.,* 2001; Skeberdis *et al.,* 2001). G-protein coupled receptors can activate a second messenger cascade, linked to the serine-threonine kinases, which leads to a change in phosphorylation of NMDAR subunits (Kotecha & MacDonald, 2003). These observations open a wide horizon of NMDA receptor regulation via a large number of G-protein coupled effectors that operate via PKC as long as the presynaptic glutamatergic terminals express the appropriate metabotropic receptors. On the other hand, this realization also carries potentially useful fallbacks in terms of pharmacological modulation of glutamate release. In particular, former attempts to prevent or limit excitoxicity with NMDA receptor antagonists have been very unhelpful in man because of the psychotomimetic action of certain antagonists (Svensson, 2000). One can hypothesize that pharmacological tools directed to inhibit PKC can be interesting alternatives to dampen NMDA receptor function and associated glutamate release, especially if the precise identity of the involved PKC is revealed and the molecular targets of PKC on NMDA receptors (MacDonald *et al.,* 2007) become fully understood and accessible to modulation by molecular biology approaches.

6. Conclusions

The present study was able to achieve the following results:

1) Immunohistochemical and Western immunoblot data showed that nAChRs of the XII nucleus of neonatal rat were composed of α4, α7 and β2 subunits. They were abundantly expressed on motoneuron somata, fibres and along all rostro-caudal axis of the XII nucleus. Their expression was not age dependent during the first five days after the birth.
The present study and the previous studies in our lab (Quitadamo *et al.,* 2005) showed that nAChRs of the XII nucleus can be readily blocked by selective antagonists of the α7 and β2 receptor subtypes. Since the vast majority of nAChRs in the brain are composed of homomeric α7 and heteromeric $(\alpha4)_2(\beta2)_3$ subunits, we propose that HM nAChRs of neonatal rats are made up by functional homomeric α7 and heteromeric $(\alpha4)_2(\beta2)_3$ subunits.

2) Presynaptic nAChRs upregulated GABAergic neurotransmission within the hypoglossal nucleus. The facilitation of GABA release was calcium dependent and could be blocked by chelating intracellular calcium. On the postsynaptic site of action, nAChRs did not influence GABA responses, whose amplitude and kinetics remained unchanged. We propose that nAChRs, found in the hypoglossal nucleus, desensitize quickly and do not influence GABAergic neurotransmission postsynaptically. Therefore, the overall action of nAChRs on GABAergic neurotransmission was presynaptic facilitation of GABA release.

3) Nicotine (10 μM) activated premotoneuronal network nAChRs, which enhanced glutamatergic transmission and produced theta frequency rhythmic behaviour in 40 % of HMs. The oscillations resembled those induced by exogenous application of a metabotropic glutamate receptor agonist (Sharifullina *et al.*, 2005; Nistri *et al.*, 2006): they had very limited dependence on HM potential and stereotypic characteristics of amplitude and duration, resembling spikelets, propagated via electrical coupling (Long *et al.*, 2004).
While single HMs did not express pacemaker properties that would enable them to generate intrinsic oscillations, intense nAChR activity could functionally bind HMs together so that rhythmic behavior appeared. This phenomenon belongs to the class of so-called emergent properties of neurons (Faingold, 2004; Feldman & Del Negro, 2006) which could not be deduced at single cell level, but could be manifested as a collective behaviour that results in the presence of efficient neuronal wiring.

In other brain areas, the role of nAChRs in the rhythmic activity is controversial. nAChR activation could block or slowdown the rhythm, could have no effect or even enhance it *in vivo* and *in vitro*. However, it has never been shown that nAChR activation itself could induce the oscillatory pattern. Thus, the present study provides the first evidence that ample nAChR activation can induce theta frequency rhythm in the CNS.

4) The oscillatory behavior evoked by nicotine persisted for at least eight minutes and required sustained nAChR activation, since nicotine washout or application of receptor antagonists abolished the rhythm. nAChRs, present on HMs, desensitized quickly and were not involved in the oscillatory behaviour. Premotoneuronal network nAChRs, on the other hand, desensitized at slower rate and remained active for several minutes, as long as oscillations were present. Both receptor type activity, $\alpha 7$ and $(\alpha 4)_2(\beta 2)_3$, was required for the oscillatory activity, since the pharmacological block of each one of them abolished the rhythm. Thus, while nAChRs of HMs desensitized quickly and did not play a role in the oscillations, premotoneuronal network nAChRs were responsible for increased glutamate levels and, therefore, for the oscillatory behaviour.

5) Since I_{NaP} is responsible for burst firing in spinal motoneurons (Li & Bennett, 1993; Elbasiouny *et al.*, 2006; Theiss *et al.*, 2007; Zhong *et al.*, 2007, but is unnecessary for bursting evoked by brainstem preBotzinger neurons (Pace *et al.*, 2007 a, b), I checked out if I_{NaP} was involved in the oscillatory rhythm in the hypoglossal nucleus. The data showed that I_{NaP} was quickly decreased by riluzole to a stable amplitude still compatible with lower frequency oscillations and, therefore, I_{NaP} could contribute to oscillatory patterns without being crucial for them, in analogy with data from brainstem respiratory neurons (Pace *et al.*, 2007 a, b).
The main mechanism for the rhythm was enhanced glutamatergic transmission induced by presynaptic nAChR activity. TTX arrested oscillations probably because it had the widespread effect of preventing network propagation of fast action potentials as well as repetitive firing supported by PICs. AMPA and mGluR1s responded to the elevated level of glutamate and, thus, were required for the oscillatory activity, while the NMDA receptors minimally contributed to oscillations.
Electrical coupling was also apparently involved in oscillatory behavior because carbenoxolone, a selective gap junction blocker, attenuated or even suppressed oscillations. In addition, oscillations comprised spikelets and burstlets, which are typical of electrical coupling

and reflect single cell or cell cluster firing, respectively, once network excitability had been adequately raised (Long *et al.*, 2004; Sharifullina *et al.*, 2005).
Synaptic inhibition was not directly participating in rhythm generation, while it had a permissible role in controlling the amount of oscillating HMs.

6) Riluzole could have diverse mechanisms of action: it can inhibit the release of glutamate (Mantz *et al.*, 1992; Zona *et al.*, 2002; Martin *et al.*, 1993; Coderre *et al.*, 2007), block the persistent sodium current (Del Negro *et al.*, 2005; Miles *et al.*, 2005; Harvey *et al.*, 2006; Theiss *et al.*, 2007), potassium (Zona *et al.*, 1998; Duprat *et al.*, 2000; Cao *et al.*, 2002; Ahn *et al.*, 2005) and calcium (Huang *et al.*, 1997; Siniscalchi *et al.*, 1997; Stefani *et al.*, 1997; Beltran-Parrazal & Charles, 2003) conductances and can even induce oscillations in cultured spinal networks (Yvon *et al.,* 2007). Thus, my aim was to investigate the action of riluzole on HMs, in particular, keeping in mind its action on I_{NaP}.
In the present experimental conditions, riluzole showed limited selectivity for the I_{NaP} as it also depressed I_{CaP}. Therefore, the data concerning the selectivity of riluzole action on the persistent sodium current on HMs should be considered with caution. Even if HMs retained the ability to fire single action potential, riluzole transformed repetitive firing properties of HMs.

7) An unexpected finding was that riluzole inhibited glutamate release in the presence of TTX. The mechanism of action of riluzole could not be direct since radioligand binding studies show that riluzole does not bind NMDA, AMPA, kainate, or metabotropic glutamate receptors (Doble, 1996; Peluffo *et al.*, 1997; Kretschmer *et al.*, 1998). In addition, riluzole did not appear to work via inhibition of NAChRs.
I found that the riluzole inhibition of glutamate release was prevented by NMDA receptor or PKC inhibitors (APV and chelerythrin, respectively). Keeping in mind that presynaptic NMDA receptors can positively regulate glutamate release (Engelman & MacDermott, 2004), and that NMDA receptors are upregulated by PKC (MacDonald *et al.,* 2007), we propose that, in the rat nucleus hypoglossus, PKC activity facilitates presynaptic NMDA receptors, which, in turn, facilitate glutamate release.

REFERENCE LIST

Ahn HS, Choi JS, Choi BH, Kim MJ, Rhie DJ, Yoon SH, Jo YH, Kim MS, Sung KW & Hahn SJ (2005) Inhibition of the cloned delayed rectifier K^+ channels, Kv1.5 and Kv3.1, by riluzole. *Neurosci,* **133**, 1007–1019.

Aldes LD (1995) Subcompartmental organization of the ventral (protrusor) compartment in the hypoglossal nucleus of the rat. *J Comp Neurol,* **353**, 89-108.

Alkondon M, Braga MF, Pereira EF, Maelicke A, Albuquerque EX (2000) alpha7 nicotinic acetylcholine receptors and modulation of gabaergic synaptic transmission in the hippocampus. *Eur J Pharmacol,* **393**, 59-67.

Alkondon M, Pereira EF, Barbosa CT, Albuquerque EX (1997) Neuronal nicotinic acetylcholine receptor activation modulates gamma-aminobutyric acid release from CA1 neurons of rat hippocampal slices. *J Pharmacol Exp Ther,* **283**, 1396-1411.

Alkondon M, Pereira EF, Albuquerque EX(1998) alpha-bungarotoxin- and methyllycaconitine-sensitive nicotinic receptors mediate fast synaptic transmission in interneurons of rat hippocampal slices. *Brain Res,* **810**, 257-263.

Alkondon M, Albuquerque EX (2004) The nicotinic acetylcholine receptor subtypes and their function in the hippocampus and cerebral cortex. *Prog Brain Res,* **145**, 109-120.

Altevogt BM & Paul DL (2004) Four classes of intercellular channels between glial cells in the CNS. *J Neurosci,* **24**, 4313-4323.

Alvarez-Maubecin V, Garcia-Hernandez F, Williams JT & Van Bockstaele EJ (2000) Functional coupling between neurons and glia. *J Neurosci,* **20**, 4091-4098.

Anand R & Lindstrom J (1992) Chromosomal localization of seven neuronal nicotinic acetylcholine receptor subunit genes in humans. *Genomics*, **13,** 962-967.

Aracri P, Colombo E, Mantegazza M, Scalmani P, Curia G, Avanzini G & Franceschetti S (2006) Layer-specific properties of the persistent sodium current in sensorimotor cortex. *J Neurophysiol,* **95,** 3460-3468.

Arroyo-Jimenez MM, Bourgeois JP, Marubio LM, Le Sourd AM, Ottersen OP, Rinvik E, Fairen A & Changeux JP (1999) Ultrastructural localization of the α4-subunit of the neuronal acetylcholine nicotinic receptor in the rat substantia nigra. *J Neurosci*, **19**, 6475-6487.

Azam L, Winzer-Serhan UH, Chen Y, Leslie FM (2002) Expression of neuronal nicotinic acetylcholine receptor subunit mRNAs within midbrain dopamine neurons. *J Comp Neurol,* **444**, 260-274.

Azbill RD, Mu X & Springer JE (2000) Riluzole increases high-affinity glutamate uptake in rat spinal cord synaptosomes. *Brain Res,* **871,** 175-180.

Ballantyne D, Andrzejewski M, Muckenhoff K & Scheid P (2004) Rhythms, synchrony and electrical coupling in the Locus coeruleus. *Respir Physiol Neurobiol,* **143**, 199-214.

Barnard EA, Sutherland M, Zaman S, Matsumoto M, Nayeem N, Green T, Darlison MG & Bateson AN (1993) Multiplicity, structure, and function in $GABA_A$ receptors. *Ann N Y Acad Sci.,* **707**, 116-125.

Bate L. & Gardiner M (1999) Expert Reviews in Molecular Medicine, Cambridge University Press.

Bear MF (1995) Mechanism for a sliding synaptic modification threshold. *Neuron,* **15**, 1–4

Beltran-Parrazal L & Charles A (2003) Riluzole inhibits spontaneous Ca^{2+} signaling in neuroendocrine cells by activation of K^+ channels and inhibition of Na^+ channels. *Br J Pharmacol,* **140,** 881-888.

Benazzouz A, Boraud T, Dubedat P, Boireau A, Stutzmann JM & Gross C (1995) Riluzole prevents MPTP-induced parkinsonism in the rhesus monkey: a pilot study. *Eur J Pharmacol,* **284**, 299-307.

Bencherif M, Fowler K, Lukas RJ & Lippiello PM. (1995) Mechanisms of up-regulation of neuronal nicotinic acetylcholine receptors in clonal cell lines and primary cultures of fetal rat brain. *J Pharmacol Exp Ther,* **275**, 987-994.

Bennett DJ, Hultborn H, Fedirchuk B & Gorassini M (1998) Synaptic activation of plateaus in hindlimb motoneurons of decerebrate cats. *J Neurophysiol,* **80**, 2023-2037.

Bennett MV & Zukin RS (2004) Electrical coupling and neuronal synchronization in the mammalian brain. *Neuron,* **41**, 495-511.

Bergerot A, Shortland PJ, Anand P, Hunt SP & Carlstedt T (2004) Co-treatment with riluzole and GDNF is necessary for functional recovery after ventral root avulsion injury. *Exp Neurol,* **187**, 359-366.

Berger H (1929) Uber das Elektroenkephalogram des Menschen. *Arch Psychiatr Nervenkrankh.*

Bergmeier SC, Lapinsky DJ, Free RB & McKay DB (1999) Ring E analogs of methyllycaconitine (MLA) as novel nicotinic antagonists. *Bioorg Med Chem Lett*, **9**, 2263-2266.

Bevan MD, Magill PJ, Terman D, Bolam JP & Wilson CJ (2002) Move to the rhythm: oscillations in the subthalamic nucleus-external globus pallidus network. *Trends Neurosci,* **25**, 525-531.

Bland BH & Colom LV (1988) Responses of phasic and tonic hippocampal theta-on cells to cholinergics: differential effects of muscarinic and nicotinic activation. *Brain Res,* **440**, 167–171.

Boireau A, Dubedat P, Bordier F, Peny C, Miquet JM, Durand G, Meunier M & Doble A (1994, a) Riluzole and experimental parkinsonism: antagonism of MPTP-induced decrease in central dopamine levels in mice. *Neuroreport,* **5,** 2657-2660.

Boireau A, Miquet JM, Dubedat P, Meunier M & Doble A (1994, b) Riluzole and experimental parkinsonism: partial antagonism of MPP(+)-induced increase in striatal extracellular dopamine in rats in vivo. *Neuroreport,* **5**, 2157-2160.

Borke RC, Nau ME & Ringler RL (1983) Brain stem afferents of hypoglossal neurons in the rat. *Brain Res*, **269**, 47-55.

Botros SM & Bruce EN (1990) Neural network implementation of a three-phase model of respiratory rhythm generation. *Biol Cybern,* **63,** 143-153.

Brecht M, Schneider M, Sakmann B & Margrie TW (2004) Whisker movements evoked by stimulation of single pyramidal cells in rat motor cortex. *Nature,* **427**, 704-710.

Breese CR, Adams C, Logel J, Drebing C, Rollins Y, Barnhart M, Sullivan B, Demasters BK, Freedman R & Leonard S (1997) Comparison of the regional expression of nicotinic acetylcholine receptor alpha7 mRNA and [125I]-alpha-bungarotoxin binding in human postmortem brain. *J Comp Neurol,* **387**, 385-398.

Brejc K, van Dijk WJ, Klaassen RV, Schuurmans M, van Der Oost J, Smit AB & Sixma TK (2001) Crystal structure of an ACh-binding protein reveals the ligand-binding domain of nicotinic receptors. *Nature,* **411**, 269-276.

Bringmann A (1997) Nicotine affects the occipital theta rhythm after lesion of the pedunculopontine tegmental nucleus in rats. *Neuropsychobiology,* 35, 102–107.

Brown TG (1911) The intrinsic factors in the act of progression in the mammal. *Proc R Soc Lond Biol,* **84**, 308- 319.

Brownstone RM (2007) Take Your PIC: Motoneuronal Persistent Inward Currents May Be Somatic as Well as Dendritic. *J Neurophysiol*, **98**, 579-580.

Buccafusco JJ, Letchworth SR, Bencherif M & Lippiello PM (2005) Long-lasting cognitive improvement with nicotinic receptor agonists: mechanisms of pharmacokinetic-pharmacodynamic discordance. *Trends Pharmacol Sci,* **26**, 352–360.

Buschges A, Wikström MA, Grillner S & El Manira A (2000) Roles of high voltage-activated calcium channel subtypes in a vertebrate spinal locomotor network. *J Neurophysiol*, **84**, 2758-2766.

Butt SJ, Harris-Warrick RM & Kiehn O (2002) Firing properties of identified interneuron populations in the mammalian hindlimb central pattern generator. *J Neurosc.,* **22**, 9961-9971.

Buzsaki G (2002) Theta oscillations in the hippocampus. *Neuron*, **33**, 325-340.

Cao YJ, Dreixler JC, Couey JJ & Houamed KM (2002) Modulation of recombinant and native neuronal SK channels by the neuroprotective drug riluzole. *Eur J Pharmacol,* **449**, 47–54.

Centonze D, Calabresi P, Pisani A, Marinelli S, Marfia GA & Bernardi G (1998) Electrophysiology of the neuroprotective agent riluzole on striatal spiny neurons. *Neuropharmacology*, **37**, 1063-1070.

Chamberlin NL, Bocciaro CM, Greene NW & Feldman JL (2002) Nicotinic excitation of rat hypoglossal motoneurons. *Neuroscience,* **115,** 861-870.

Champtiaux N & Changeux JP (2002) Knock-out and knock-in mice to investigate the role of nicotinic receptors in the central nervous system. *Curr Drug Targets CNS Neurol Disord,* **1**, 319-330.

Champtiaux N, Gotti C, Cordero-Erausquin M, David DJ, Przybylski C, Lena C, Clementi F, Moretti M, Rossi FM, Le Novere N, McIntosh JM, Gardier AM & Changeux JP (2003) Subunit composition of functional nicotinic receptors in dopaminergic neurons investigated with knock-out mice. *J Neurosci,* **23**, 7820-7829.

Changeux JP & Edelstein SJ (1998) Allosteric receptors after 30 years. *Neuron,* **21,** 959-980.

Charnet P, Labarca C, Cohen BN, Davidson N, Lester HA & Pilar G (1992) Pharmacological and kinetic properties of alpha 4 beta 2 neuronal nicotinic acetylcholine receptors expressed in Xenopus oocytes. *J Physiol,* **450**, 375-394.

Chavez-Noriega LE, Crona JH, Washburn MS, Urrutia A, Elliott KJ & Johnson EC (1997) Pharmacological characterization of recombinant human neuronal nicotinic acetylcholine receptors h-alpha2-beta2, h-alpha2-beta4, h-alpha3-beta2, h-alpha3-beta4, h-alpha4-beta2, h-alpha4-beta4 and h-alpha7 expressed in Xenopus oocytes. *J Pharmacol Exp Ther,* **280**, 346-356.

Cheramy A, Barbeito L, Godeheu G & Glowinski J (1992) Riluzole inhibits the release of glutamate in the caudate nucleus of the cat in vivo. *Neurosci Len,* **147,** 209-212.

Christianson JC &. Green WN (2004) Regulation of nicotinic receptor expression by the ubiquitin-proteasome system. *EMBO J,* **23**, 4156–4165.

Clarke PBS, Hommer DW, Pert A & Skirboll LR (1987) Innervation of substantia nigra neurons by cholinergic afferents from the pedunculopontine nucleus in rats: neuroanatomical and electrophysiological evidence. *Neuroscience,* **23**, 1011–1020.

Clementi F, Court J & Perry E (2000) Involvement of neuronal nicotinic receptors in disease. In: Clementi F, Forsanati D & Gotti C (Eds.), Handbook of Experimental Pharmacology, Vol. Neuronal nicotinic Receptors, Springer, Berlin.

Cleveland DW & Rothstein JD (2001) From charcot to lou gehrig: deciphering selective motor neuron death in ALS. *Nature Reviews Neuroscience,* **2**, 806-819.

Cobb SR, Bulters DO & Davies CH (2000) Coincident activation of mGluRs and mAChRs imposes theta frequency patterning on synchronised network activity in the hippocampal CA3 region. *Neuropharmacology*, **39**, 1933-1942.

Coderre TJ, Kumar N, Lefebvre CD & Yu JS (2007) A comparison of the glutamate release inhibition and anti-allodynic effects of gabapentin, lamotrigine, and riluzole in a model of neuropathic pain. *J Neurochem,* **100,** 1289-1299.

Cohen G, Han ZY, Grailhe R, Gallego J, Gaultier C, Changeux JP & Lagercrantz H (2002) beta2 nicotinic acetylcholine receptor subunit modulates protective responses to stress: A receptor basis for sleep-disordered breathing after nicotine exposure. *Pnas*, **99**, 13272-13277.

Collins DR, Pelletier JG & Pare D (2001) Slow and fast (gamma) neuronal oscillations in the perirhinal cortex and lateral amygdala. *J Neurophysiol,* **85**, 1661-1672.

Connelly CA, Dobbins EG & Feldman JL (1992) Pre-Botzinger complex in cats: respiratory neuronal discharge patterns. *Brain Res,* **590**, 337-340.

Conroy WG & Berg DK (1995) Neurons can maintain multiple classes of nicotinic acetylcholine receptors distinguished by different subunit compositions. *J Bio Chem,* **270**, 4424-4431.

Cooper ST & Millar NS (1997) Host cell-specific folding and assembly of the neuronal nicotinic acetylcholine receptor alpha7 subunit. *J Neurochem,* **68**, 2140–2151.

Corrigall WA, Coen KM & Adamson KL (1994) Self-administered nicotine activates the mesolimbic dopamine system through the ventral tegmental area. *Brain Res,* **653**, 278-284.

Corringer PJ, Sallette J & Changeux JP (2006) Nicotine enhances intracellular nicotinic receptor maturation: a novel mechanism of neural plasticity? *J Physiol Paris,* **99**, 162-171.

Cramer NP, Li Y & Keller A (2007) The whisking rhythm generator: a novel mammalian network for the generation of movement. *J Neurophysiol,* **97,** 2148-2158.

Crill WE (1996) Persistent sodium current in mammalian central neurons. *Annu Rev Physiol,* **58**, 349-362.

Crunelli V, Toth TI, Cope DW, Blethyn K & Hughes SW (2005) The 'window' T-type calcium current in brain dynamics of different behavioural states. *J Physiol*, **562**, 121-129.

Cunningham ET Jr, Sawchenko PE (2000) Dorsal medullary pathways subserving oromotor reflexes in the rat: implications for the central neural control of swallowing. *J Comp Neurol,* **417**, 448-466.

Dale N (1995) Experimentally derived model for the locomotor pattern generator in the Xenopus embryo. *J Physiol,* **489**, 489-510.

Darbon P, Yvon C, Legrand JC & Streit J (2004) INaP underlies intrinsic spiking and rhythm generation in networks of cultured rat spinal cord neurons. *Eur J Neurosci,* **20,** 976-988.

Darsow T Booker TK, Pina-Crespo JC & Heinemann SF (2005) Exocytic trafficking is required for nicotine-induced upregulation of alpha4beta2 nicotinic acetylcholine receptors. *J Biol Chem*, **280**, 18311–18320.

Davies AR, Hardick DJ, Blagbrough IS, Potter BV, Wolstenholme AJ & Wonnacott S (1999) Characterisation of the binding of [^{3}H]methyllycaconitine: a new radioligand for labelling α7-type neuronal nicotinic acetylcholine receptors. *Neuropharmacology*, **38**, 679-690.

De Simone R, Ajmone-Cat MA, Carnevale D & Minghetti L (2005) Activation of α7 nicotinic acetylcholine receptor by nicotine selectively up-regulates cyclooxygenase-2 and prostaglandin E2 in rat microglial cultures. *J Neuroinflammation*, **2,** 4.

Debono MW, Le Guern J, Canton T, Doble A & Pradier L (1993) Inhibition by riluzole of electrophysiological responses mediated by rat kainate and NMDA receptors expressed in Xenopus oocytes. *Eur J Pharmacol,* **235,** 283-289.

Dehkordi O, Millis RM, Dennis GC, Coleman BR, Johnson SM, Changizi L & Trouth OC (2005) α-7 and α-4 nicotinic receptor subunit immunoreactivity in genioglossus muscle motoneurons. *Respir Physiol Neurobiol*, **145**, 153-161.

Del Negro CA, Morgado-Valle C, Hayes JA, Mackay DD, Pace RW, Crowder EA & Feldman JL (2005) Sodium and calcium current-mediated pacemaker neurons and respiratory rhythm generation. *J Neurosci,* 25, 446-53.

D'Angelo E, Nieus T, Maffei A, Armano S, Rossi P, Taglietti V, Fontana A & Naldi G (2001) Theta-frequency bursting and resonance in cerebellar granule cells: experimental evidence and modeling of a slow k+-dependent mechanism. *J Neurosci,* **21**, 759-770.

Del Cano GG, Millan LM, Gerrikagoitia I, Sarasa M & Matute C (1999) Ionotropic glutamate receptor subunit distribution on hypoglossal motoneuronal pools in the rat. *J Neurocytol,* **28**, 455-468.

Del Negro CA, Hsiao CF & Chandler SH (1999) Outward currents influencing bursting dynamics in guinea pig trigeminal motoneurons. *J Neurophysiol,* **81**, 1478-1485.

Della Rocca GJ, Maudsley S, Daaka Y, Lefkowitz RJ & Luttrell LM (1999) Pleiotropic coupling of G protein-coupled receptors to the mitogen-activated protein kinase cascade. Role of focal adhesions and receptor tyrosine kinases. *J Biol Chem,* **274**, 13978-13984.

Descarries L & Mechawar N (2000) Ultrastructural evidence for diffuse transmission by monoamine and acetylcholine neurons of the central nervous system. *Prog Brain Res,* **125**, 27–47.

Di Angelantonio S & Nistri A (2001) Calibration of agonist concentrations applied by pressure pulses or via rapid solution exchanger. *J Neurosci Methods,* **110**, 155-161.

Dobbins EG & Feldman JL (1995) Differential innervation of protruder and retractor muscles of the tongue in rat. *J Comp Neurol,* **357**, 376-394.

Doble A (1996) Excitatory amino acid receptors and neurodegeneration. *Therapie*, **50**, 319-337.

Doble A, Hubert JP & Blanchard JC (1992) Pertussis toxin pretreatment abolishes the inhibitory effect of riluzole and carbachol on aspartate art ate release from cerebellar granule cells. *Neurosci Lett*, **140**, 251-254.

Donato R & Nistri A (2000) Relative contribution by GABA or glycine to Cl^--mediated synaptic transmission on rat hypoglossal motoneurons in vitro. *J Neurophysiol,* **84,** 2715-2724.

Drachman DA (2005) Do we have brain to spare? *Neurology,* **64**, 2004-2005.

Draguhn A, Traub RD, Schmitz D & Jefferys JG (1998) Electrical coupling underlies high-frequency oscillations in the hippocampus in vitro. *Nature,* **394**, 189-192.

Dunlop J, McIlvain BH, She Y & Howland DS (2003) Impaired spinal cord glutamate transport capacity and reduced sensitivity to riluzole in a transgenic superoxide dismutase mutant rat model of amyotrophic lateral sclerosis. *J Neurosci,* **23**, 1688-1696.

Duprat F, Lesage F, Patel AJ, Fink M, Romey G & Lazdunski M (2000) The neuroprotective agent riluzole activates the two P domain K^+ channels TREK-1 and TRAAK. *Mol Pharmacol.* **57**, 906 –912.

Eccles JC (1957) The physiology of nerve cells. Johns Hopkins Press, Baltimore. p. 38-41.

El Manira A & Bussieres N (1997) Calcium channel subtypes in lamprey sensory and motor neurons. *J Neurophysiol,* **78**, 1334-1340.

Ellgaard L & Helenius A (2003) Quality control in the endoplasmic reticulum. *Nat Rev Mol Cell Biol,* **4**, 181–191.

Elbasiouny SM, Bennett DJ & Mushahwar VK (2006) Simulation of Ca^{2+} persistent inward currents in spinal motoneurones: mode of activation and integration of synaptic inputs. *J Physiol,* **570**, 355-374.

Elgoyhen AB, Johnson DS, Boulter J, Vetter DE, Heinemann S. (1994) Alpha 9: an acetylcholine receptor with novel pharmacological properties expressed in rat cochlear hair cells. *Cell,* **79**, 705-715.

Engelman HS & MacDermott AB (2004) Presynaptic ionotropic receptors and control of transmitter release. *Nat Rev Neurosci,* **5**, 135-145.

Enomoto A, Han JM, Hsiao CF, Wu N & Chandler SH (2006) Participation of sodium currents in burst generation and control of membrane excitability in mesencephalic trigeminal neurons. *J Neurosci,* **26,** 3412-3422.

Estevez AG, Stutzmann JM & Barbeito L (1995) Protective effect of riluzole on excitatory amino acid-mediated neurotoxicity in motoneuron-enriched cultures. *Eur J Pharmacol,* **280**, 47-53.

Fabian-Fine R, Skehel P, Errington ML, Davies HA, Sher E, Stewart MG & Fine A (2001) Ultrastructural distribution of the 7 nicotinic acetylcholine receptor subunit in rat hippocampus. *J Neurosci,* **21**, 7993– 8003.

Farber NB, Jiang XP, Heinkel C & Nemmers B (2002) Antiepileptic drugs and agents that inhibit voltage-gated sodium channels prevent NMDA antagonist neurotoxicity. *Mol Psychiatry,* **7,** 726-733.

Faingold CL (2004) Emergent properties of CNS neuronal networks as targets for pharmacology: application to anticonvulsant drug action. *Prog Neurobiol,* **72,** 55-85.

Fay RA & Norgren R (1997) Identification of rat brainstem multisynaptic connections to the oral motor nuclei using pseudorabies virus. III. Lingual muscle motor systems. *Brain Res Brain Res Rev*, **25**, 291-311.

Feldman JL & Del Negro CA (2006) Looking for inspiration: new perspectives on respiratory rhythm. *Nat Rev Neurosci*, **7**, 232-242.

Fenster CP, Rains MF, Noerager B, Quick MW & Lester RA (1997) Influence of subunit composition on desensitization of neuronal acetylcholine receptors at low concentrations of nicotine. *J Neurosci*, **17**, 5747-5759.

Ferger B & Kuschinsky K (1997) Biochemical studies support the assumption that dopamine plays a minor role in the EEG effects of nicotine. *Psychopharmacology (Berl)*, **129,** 192–196.

Fisher JL & Dani JA (2000) Nicotinic receptors on hippocampal cultures can increase synaptic glutamate currents while decreasing the NMDA-receptor component. *Neuropharmacology,* **39**, 2756-2769.

Freeman WJ (1972) Measurement of oscillatory responses to electrical stimulation in olfactory bulb of cat. *J Neurophysiol,* **35**, 762-779.

Frizzo ME, Dall'Onder LP, Dalcin KB & Souza DO (2004) Riluzole enhances glutamate uptake in rat astrocyte cultures. *Cell Mol Neurobiol,* **24**, 123-128.

Froy O & Miskin R (2007) The interrelations among feeding, circadian rhythms and ageing. *Prog Neurobiol*, **82**, 142-150.

Fryer JD & Lukas RJ (1999) Antidepressants noncompetitively inhibit nicotinic acetylcholine receptor function. *J Neurochem,* **72**, 1117–1124.

Fucile S (2004) Ca^{2+} permeability of nicotinic acetylcholine receptors. *Cell Calcium,* **35**, 1-8.

Fuentealba P, Timofeev I & Steriade M (2004) Prolonged hyperpolarizing potentials precede spindle oscillations in the thalamic reticular nucleus. *Proc Natl Acad Sci U S A,* **101**, 9816-9821.

Funk GD & Parkis MA (2002) High frequency oscillations in respiratory networks: functionally significant or phenomenological? *Respir Physiol Neurobiol*, **131,** 101-120.

Galante RJ, Kubin L, Fishman AP & Pack AI (1996) Role of chloride-mediated inhibition in respiratory rhythmogenesis in an in vitro brainstem of tadpole Rana catesbeiana. *J Physiol,* **492**, 545-558.

Galarreta M & Hestrin S (1999) A network of fast-spiking cells in the neocortex connected by electrical synapses. *Nature,* **402,** 72-75.

Garrido R, Mattson MP, Hennig B & Toborek M (2001) Nicotine protects against arachidonic-acid-induced caspase activation cytochrome c release and apoptosis of cultured spinal cord neurons. *J Neurochem,* **76,** 1395-1403.

Gibson JR, Beierlein M & Connors BW (1999) Two networks of electrically coupled inhibitory neurons in neocortex. *Nature*, **402,** 75-79.

Gillies MJ, Traub RD, LeBeau FE, Davies CH, Gloveli T, Buhl EH & Whittington MA (2002) A model of atropine-resistant theta oscillations in rat hippocampal area CA1. *J Physiol,* **543,** 779-793.

Giniatullin R, Nistri A & Yakel JL (2005) Desensitization of nicotinic ACh receptors: shaping cholinergic signaling. *Trends Neurosci,* **28**, 371-378

Giocomo LM & Hasselmo ME (2005) Nicotinic modulation of glutamatergic synaptic transmission in region CA3 of the hippocampus. *Eur J Neurosci*, **22**, 1349-1356.

Girod R, Barazangi N, McGehee D & Role LW (2000) Facilitation of glutamatergic neurotransmission by presynaptic nicotinic acetylcholine receptors. *Neuropharmacology,* **39**, 2715-2725.

Gotti C, Fornasari D & Clementi F (1997) Human neuronal nicotinic receptors. *Prog. Neurobiol.,* **53**,199-237.

Gotti C & Clementi F (2004) Neuronal nicotinic receptors: from structure to pathology. *Prog Neurobiol,* **74**, 363-396.

Grailhe R, de Carvalho LP, Paas Y, Le Poupon C, Soudant M, Bregestovski P, Changeux JP & Corringer PJ (2004) Distinct subcellular targeting of fluorescent nicotinic alpha3beta4 and serotoninergic 5–HT3A receptors in hippocampal neurons. *Eur J Neurosci,* **19**, 855–862.

Gray CM, Konig P, Engel AK & Singer W (1989) Oscillatory responses in cat visual cortex exhibit inter-columnar synchronization which reflects global stimulus properties. *Nature,* **338**, 334-337.

Gray R, Rajan AS, Radcliffe KA, Yakehiro M & Dani JA (1996) Hippocampal synaptic transmission enhanced by low concentrations of nicotine. *Nature,* **383,** 713-716.

Grenier F, Timofeev I & Steriade M (2003) Neocortical very fast oscillations (ripples, 80-200 Hz) during seizures: intracellular correlates. *J Neurophysiol*, **89**, 841-852.

Grillner S, Parker D & el Manira A (1998) Vertebrate locomotion-a lamprey perspective. *Ann N Y Acad Sci*, **860**, 1-18.

Grillner S, Wallen P, Brodin L & Lansner A (1991) Neuronal network generating locomotor behavior in lamprey: circuitry, transmitters, membrane properties, and simulation. *Annu Rev Neurosci*, **14**, 169-199.

Hajos M, Hurst RS, Hoffmann WE, Krause M, Wall TM, Higdon NR & Groppi VE (2005) The selective alpha7 nicotinic acetylcholine receptor agonist PNU-282987 [N-[(3R) -1-Azabicyclo[2.2.2]oct-3-yl]-4-chlorobenzamide hydrochloride] enhances GABAergic synaptic activity in brain slices and restores auditory gating deficits in anesthetized rats. *J Pharmacol Exp Ther*, **312**, 1213–1222.

Haller M, Mironov SL, Karschin A & Richter DW (2001) Dynamic activation of $K_{(ATP)}$ channels in rhythmically active neurons. *J Physiol*, **537,** 69-81.

Hamill OP, Marty A, Neher E, Sakmann B & Sigworth FJ (1981) Improved patch-clamp techniques for high-resolution current recording from cells and cell-free membrane patches. *Pflugers Arch,* **391**, 85-100.

Harkness PC & Millar NS (2002) Changes in conformation and subcellular distribution of α4β2 nicotinic acetylcholine receptors revealed by chronic nicotine treatment and expression of subunit chimeras. *J Neurosci*, **22**, 10172–10181.

Harris-Warrick RM (2002) Voltage-sensitive ion channels in rhythmic motor systems. *Curr Opin Neurobiol*, **12**, 646-651.

Harvey PJ, Li Y, Li X & Bennett DJ (2006) Persistent sodium currents and repetitive firing in motoneurons of the sacrocaudal spinal cord of adult rats. *J Neurophysiol,* **96**, 1141-1157.

Harvey SC & Luetje CW (1996) Determinants of competitive antagonist sensitivity on neuronal nicotinic receptor beta subunits. *J Neurosci*, **16**, 3798-3806.

Hasselmo ME (2005) What is the function of hippocampal theta rhythm? Linking behavioral data to phasic properties of field potential and unit recording data. *Hippocampus,* **15,** 936-949.

Hatton GI & Yang QZ (2002) Synaptic potentials mediated by alpha 7 nicotinic acetylcholine receptors in supraoptic nucleus. *J Neurosci*, **22**, 29-37.

Hay M, McKenzie H, Lindsley K, Dietz N, Bradley SR, Conn PJ & Hasser EM (1999) Heterogeneity of metabotropic glutamate receptors in autonomic cell groups of the medulla oblongata of the rat. *J Comp Neurol,* **403,** 486-501.

He Y, Benz A, Fu T, Wang M, Covey DF, Zorumski CF & Mennerick S (2002) Neuroprotective agent riluzole potentiates postsynaptic $GABA_A$ receptor function. *Neuropharmacology,* **42,** 199-209.

Hinckley CA & Ziskind-Conhaim L (2006) Electrical coupling between locomotor-related excitatory interneurons in the mammalian spinal cord. *J Neurosci*, 26, 8477- 8483.

Hoffmann WE, Schaeffer E & Hajos M (2005) Auditory gating in rat entorhinal cortex, medial septum and hippocampus: modeling dysfunctional information processing associated with schizophrenia. *Soc Neurosci Abstr*, 1023.

Hounsgaard J, Hultborn H, Jespersen B & Kiehn O (1988) Bistability of alpha-motoneurones in the decerebrate cat and in the acute spinal cat after intravenous 5-hydroxytryptophan. *J Physiol,* **405**, 345-367.

Hsiao CF, Gougar K, Asai J & Chandler SH (2007) Intrinsic membrane properties and morphological characteristics of interneurons in the rat supratrigeminal region. *J Neurosci Res,* In press.

Huang CS, Song JH, Nagata K, Yeh JZ & Narahashi T (1997) Effects of the neuroprotective agent riluzole on the high voltage-activated calcium channels of rat dorsal root ganglion neurons. *J Pharmacol Exp Ther,* **282,** 1280-1290.

Hubert JP, Delumeau JC, Glowinski J, Premont J & Doble A (1994) Antagonism by riluzole of entry of calcium evoked by NMDA and veratridine in rat cultured granule cells: evidence for a dual mechanism of action. *Br J Pharmacol,* **113,** 261-267.

Hubert JP & Doble A (1989). Ibotenic acid stimulated Image-(3H)-aspartate release from cultured cerebellar granule cells. *Neurosci Lett,* **96**, 345–350.

Huganir RL, Delcour AH, Greengard P & Hess GP (1986) Phosphorylation of the nicotinic acetylcholine receptor regulates its rate of desensitization. *Nature,* **321**, 774-776.

Itier V & Bertrand D (2001) Neuronal nicotinic receptors: from protein structure to function. *FEBS Lett,* **504,** 118-125.

Ito C, Fukuda A, Nabekura J & Oomura Y (1989) Acetylcholine causes nicotinic depolarization in rat dorsal motor nucleus of the vagus *in vitro*. *Brain Res,* **503,** 44–48.

Jones IW, Bolam JP & Wonnacott S (2001) Presynaptic localisation of the nicotinic acetylcholine receptor β2 subunit immunoreactivity in rat nigrostriatal dopaminergic neurones. *JComp Neurol,* **439**, 235-247.

Jope R (1979) High affinity choline transport and acetylCoA production in brain and their roles in the regulation of acetylcholine synthesis. *Brain Res,* **180,** 313-344.

Kadoya C, Domino EF & Matsuoka S (1994) Relationship of electroencephalographic and cardiovascular changes to plasma nicotine levels in tobacco smokers. *Clin Pharmacol Ther,* **55**, 370–377.

Kandel ER, Schwartz JE, Jessel TM (2000) Principles of neural science, 4th edition. New York, McGraw-Hill. p 235.

Kang Y, Saito M, Sato H, Toyoda H, Maeda Y, Hirai T & Bae YC (2007) Involvement of persistent Na^+ current in spike initiation in primary sensory neurons of the rat mesencephalic trigeminal nucleus. *J Neurophysiol,* **97**, 2385-2393.

Katz B & Miledi R (1977) Transmitter leakage from motor nerve endings. *Proc R Soc London,* **196**, 59-72.

Katz B & Thesleff S (1957) A study of the desensitization produced by acetylcholine at the motor end-plate. *J Physiol,* **138**, 63-80.

Kawai H, Zago W & Berg DK (2002) Nicotinic 7 receptor clusters on hippocampal GABAergic neurons: regulation by synaptic activity and neurotrophins. *J Neurosci,* **22**, 7903–7912.

Kelton MC, Kahn HJ, Conrath CL& & Newhouse PA (2000) The effects of nicotine on Parkinson's disease. *Brain Cogn,* **43**, 274-282.

Kiehn O, Tresch MC, Kjaerulff O & Harris-Warrick RM (2000) The transformation of cellular properties into coordinated motor patterns in the neonatal rat spinal cord. *Brain Res Bull,* **53,** 649-659.

Kitagawa H, Takenouchi T, Azuma R, Wesnes KA, Kramer WG, Clody DE & Burnett AL (2003) Safety, pharmacokinetics, and effects on cognitive function of multiple doses of GTS-21 in healthy, male volunteers. *Neuropsychopharmacology,* **28**, 542–551.

Kittler JT & Moss SJ (2003) Modulation of GABAA receptor activity by phosphorylation and receptor trafficking: implications for the efficacy of synaptic inhibition. *Curr Opin Neurobiol,* **13**, 341–347.

Khiroug SS, Harkness PC, Lamb PW, Sudweeks SN, Khiroug L, Millar NS & Yakel JL (2002) Rat nicotinic ACh receptor alpha7 and beta2 subunits co-assemble to form functional heteromeric nicotinic receptor channels. *J Physiol,* **540**, 425-434.

Koles L, Wirkner K & Illes P (2001) Modulation of Ionotropic Glutamate Receptor Channels. *Neurochemical Research,* **26,** 925–932.

Konopacki J, Bland BH & Roth SH (1988) Evidence that activation of *in vitro* hippocampal theta rhythm only involves muscarinic receptors. *Brain Res*, **455**, 110–114.

Konopacki J & Golebiewski H (1992) Theta rhythms in the rat medial entorhinal cortex *in vitro*: evidence for involvement of muscarinic receptors. *Neurosci Lett*, **141**, 93–96.

Koshiya N & Smith JC (1999) Neuronal pacemaker for breathing visualized in vitro. *Nature,* **400**, 360–363.

Kotecha SA & MacDonald JF (2003) Signaling molecules and receptor transduction cascades that regulate NMDA receptor-mediated synaptic transmission. *Int Rev Neurobiol.* **54**, 51-106.

Kotecha SA, Oak JN, Jackson MF, Perez Y, Orser BA, Van Tol HH & MacDonald JF (2002) A D2 class dopamine receptor transactivates a receptor tyrosine kinase to inhibit NMDA receptor transmission. *Neuron,* **35**, 1111-1122.

Kretschmer BD, Kratzer U & Schmidt WJ (1998) Riluzole, a glutamate release inhibitor, and motor behaviour. *Naunyn Schmiedebergs Arch Pharmacol,* **358,** 181-190.

Krieger C, Jones K, Kim SU & Eisen AA (1994) The role of intracellular free calcium in motor neuron disease. *J Neurol Sci,* **124**, 27-32.

Kuhse J, Betz H & Kirsch J (1995) The inhibitory glycine receptor: architecture, synaptic localization and molecular pathology of a postsynaptic ion-channel complex. *Curr Opin Neurobiol,* **5**, 318-323.

Kuo JJ, Lee RH, Zhang L & Heckman CJ (2006) Essential role of the persistent sodium current in spike initiation during slowly rising inputs in mouse spinal neurones. *J Physiol,* **574**, 819-834.

Ladewig T, Kloppenburg P, Lalley PM, Zipfel WR, Webb WW & Keller BU (2003) Spatial profiles of store-dependent calcium release in motoneurones of the nucleus hypoglossus from newborn mouse. *J Physiol,* **547**, 775-787.

Lamanauskas N & Nistri A (2006) Persistent rhythmic oscillations induced by nicotine on neonatal rat hypoglossal motoneurons in vitro. *Eur J Neurosci,* **24,** 2543-2556.

Lan JY, Skeberdis VA, Jover T, Grooms SY, Lin Y, Araneda RC, Zheng X, Bennett MV & Zukin RS (2001) Protein kinase C modulates NMDA receptor trafficking and gating. *Nat Neurosci,* **4,** 382-390.

Landisman CE, Long MA, Beierlein M, Deans MR, Paul DL & Connors BW (2002) Electrical synapses in the thalamic reticular nucleus. *J Neurosci,* **22,** 1002-1009.

Lape R & Nistri A (2000) Current and voltage clamp studies of the spike medium afterhyperpolarization of hypoglossal motoneurons in a rat brain stem slice preparation. *J Neurophysiol,* **83,** 2987-95.

Launey T, Ivanov A, Kapus G, Ferrand N, Tarnawa I & Gueritaud JP (1999) Excitatory amino acids and synaptic transmission in embryonic rat brainstem motoneurons in organotypic culture. *Eur J Neurosci,* **11**, 1324-1334.

Laurent G, Wehr M & Davidowitz H (1996) Temporal representations of odors in an olfactory network. *J Neurosci,* **16**, 3837-3847.

Le Meur K, Galante M, Angulo MC & Audinat E (2007) Tonic activation of NMDA receptors by ambient glutamate of non-synaptic origin in the rat hippocampus. *J Physiol,* **580**, 373-383.

Le Novere N & Changeux JP (1995) Molecular evolution of the nicotinic acetylcholine receptor: an example of multigene family in excitable cells. *J Mol Evol,* **40**, 155-172.

Le Novere N, Zoli M & Changeux JP (1996) Neuronal nicotinic receptor alpha 6 subunit mRNA is selectively concentrated in catecholaminergic nuclei of the rat brain. *Eur J Neurosci,* **8**, 2428-2439.

LeBeau FE, Traub RD, Monyer H, Whittington MA & Buhl EH (2003) The role of electrical signaling via gap junctions in the generation of fast network oscillations. *Brain Res Bull,* **62,** 3-13.

Lee FJ & Liu F (2004) Direct interactions between NMDA and D1 receptors: a tale of tails. *Biochem Soc Trans.* **32**, 1032-1036.

Lee RH & and Heckman CJ (1998) Bistability in spinal motoneurons in vivo: systematic variations in rhythmic firing patterns. *J Neurophysiol,* **80**, 572-582.

Lee M, Martin-Ruiz C, Graham A, Court J, Jaros E, Perry R, Iversen P, Bauman M & Perry E (2002) Nicotinic receptor abnormalities in the cerebellar cortex in autism. *Brain,* **125**, 1483-1495.

Lei S, Czerwinska E, Czerwinski W, Walsh MP & MacDonald JF (2001) Regulation of NMDA receptor activity by F-actin and myosin light chain kinase. *J Neurosci,* **21,** 8464-8472.
Lena C, Changeux JP & Mulle C (1993) Evidence for "preterminal" nicotinic receptors on GABAergic axons in the rat interpeduncular nucleus. *J Neurosci,* **13**, 2680-2688.

Lena C, Popa D, Grailhe R, Escourrou P, Changeux JP & Adrien J (2004) Beta2-containing nicotinic receptors contribute to the organization of sleep and regulate putative micro-arousals in mice. *J Neurosci,* **24**, 5711-5718.

Leonard S, Adler LE, Benhammou K, Berger R, Breese CR, Drebing C, Gault J, Lee MJ, Logel J, Olincy A, Ross RG, Stevens K, Sullivan B, Vianzon R, Virnich DE, Waldo M, Walton K & Freedman R (2001) Smoking and mental illness. *Pharmacol Biochem Behav,* **70**, 561-570.

Lester RAJ (2004) Activation and desensitization of heteromeric neuronal nicotinic receptors: implications for non-synaptic transmission. *Bioorg Med Chem Lett,* **14**, 1897-1900.

Leung LW & Yim CY (1991) Intrinsic membrane potential oscillations in hippocampal neurons in vitro. *Brain Res,* **553**, 261-274.

Leung LS & Yim CY (1993) Rhythmic delta-frequency activities in the nucleus accumbens of anesthetized and freely moving rats. *Can J Physiol Pharmacol,* **71**, 311-320.

Li Y & Bennett DJ (2003) Persistent sodium and calcium currents cause plateau potentials in motoneurons of chronic spinal rats. *J Neurophysiol,* **90,** 857-869.

Li Z & Hatton GI (1996) Oscillatory bursting of phasically firing rat supraoptic neurones in low-Ca^{2+} medium: Na^{+} influx, cytosolic Ca2+ and gap junctions. *J Physiol*, **496**, 379-394.

Lindgren M, Molander L, Verbaan C, Lunell E & Rosen I (1999) Electroencephalographic effects of intravenous nicotine— a dose–response study. *Psychopharmacology (Berl),* **145**, 342–350.

Lindstrom J (1997) Nicotinic acetylcholine receptors in health and disease. *Mol Neurobiol,* **15**, 193-222.

Lips MB & Keller BU (1999) Activity-related calcium dynamics in motoneurons of the nucleus hypoglossus from mouse. *J Neurophysiol,* **82,** 2936-2946.

Liu Y, Ford B, Mann MA & Fischbach GD (2001) Neuregulins increase alpha7 nicotinic acetylcholine receptors and enhance excitatory synaptic transmission in GABAergic interneurons of the hippocampus. *J Neurosci,* **21**, 5660-5669.

Llinas R & Ribary U (1993) Coherent 40-Hz oscillation characterizes dream state in humans. *Proc Natl Acad Sci U S A,* **90**, 2078-2081.

Llinas R & Yarom Y (1986) Oscillatory properties of guinea-pig inferior olivary neurones and their pharmacological modulation: an in vitro study. *J Physiol*, **376**, 163-182.

Long MA, Deans MR, Paul DL & Connors BW (2002) Rhythmicity without synchrony in the electrically uncoupled inferior olive. *J Neurosci*, **22**, 10898-10905.

Long MA, Landisman CE & Connors BW (2004) Small clusters of electrically coupled neurons generate synchronous rhythms in the thalamic reticular nucleus. *J Neurosci,* **24**, 341-349.

Loscher W, Potschka H, Wlaz P, Danysz W & Parsons CG (2003) Are neuronal nicotinic receptors a target for antiepileptic drug development? Studies in different seizure models in mice and rats. *Eur J Pharmacol,* **466,** 99–111.

Lowe AA (1980) The neural regulation of tongue movements. *Prog Neurobiol,* **15,** 295-344.

Lu WY, Xiong ZG, Lei S, Orser BA, Dudek E, Browning MD & MacDonald JF (1999) G-protein-coupled receptors act via protein kinase C and Src to regulate NMDA receptors. *Nat Neurosci,* **2,** 331-338.

Luscher B & Keller CA (2004) Regulation of GABAA receptor trafficking, channel activity, and functional plasticity of inhibitory synapses. *Pharmacol Ther,* **102**, 195–221.

Lustig LR & Peng H (2002) Chromosome location and characterization of the human nicotinic acetylcholine receptor subunit alpha (alpha) 9 (CHRNA9) gene. *Cytogenet Genome Res,* **98**, 154-159.

Lustig LR (2006) Nicotinic acetylcholine receptor structure and function in the efferent auditory system. *Anat Rec A Discov Mol Cell Evol Biol,* **288**, 424-434.

MacDonald JF, Jackson MF & Beazely MA (2007) G protein-coupled receptors control NMDARs and metaplasticity in the hippocampus. *Biochim Biophys Acta,* **1768,** 941-951.

MacDonald JF, Kotecha SA, Lu WY & Jackson MF (2001) Convergence of PKC-dependent kinase signal cascades on NMDA receptors. *Curr Drug Targets,* **2**, 299-312.

Magistretti J, Castelli L, Forti L & D'Angelo E (2006) Kinetic and functional analysis of transient, persistent and resurgent sodium currents in rat cerebellar granule cells in situ: an electrophysiological and modelling study. *J Physiol,* **573,** 83-106.

Malgouris C, Bardot F, Daniel M, Pellis F, Rataud J, Uzan A, Blanchard JC & Laduron PM (1989) Riluzole, a novel antiglutamate, prevents memory loss and hippocampal neuronal damage in ischemic gerbils. *J Neurosci,* **9**, 3720-3727.

Mansvelder HD, Aerde KI, Couey JJ & Brussaard AB (2006) Nicotinic modulation of neuronal networks: from receptors to cognition. *Psychopharmacology*, 184, 292–305.

Mantz J (1996) Riluzole. *CNS drug rev,* **2**, 40-51.

Mantz J, Cheramy A, Thierry AM, Glowinski J & Desmonts JM (1992) Anesthetic properties of riluzole (54274 RP), a new inhibitor of glutamate neurotransmission. *Anesthesiology,* **76,** 844-848.

Mao D, Yasuda RP, Fan H, Wolfe BB & Kellar KJ (2006) Heterogeneity of Nicotinic Cholinergic Receptors in Rat Superior Cervical and Nodose Ganglia. *Mol Pharmacol,* **70**, 1693-1639.

Marks MJ, Stitzel JA & Collins AC (1989) Genetic influences on nicotine responses, *Pharmacol Biochem Behav,* **33**, 667–678.

Marchetti C, Pagnotta S, Donato R & Nistri A (2002) Inhibition of spinal or hypoglossal motoneurons of the newborn rat by glycine or GABA. *Eur J Neurosci*, **15**, 975-983.

Margiotta JF & Gurantz D (1989) Changes in the number, function, and regulation of nicotinic acetylcholine receptors during neuronal development. *Dev Biol,* **135**, 326-339.

Marino MJ & Conn PJ (2002) Direct and indirect modulation of the N-methyl D-aspartate receptor. *Curr Drug Targets CNS Neurol Disord,* **1**, 1-16.

Marritt AM, Cox BC, Yasuda RP, McIntosh JM, Xiao Y, Wolfe BB & Kellar KJ (2005) Nicotinic cholinergic receptors in the rat retina: simple and mixed heteromeric subtypes. *Mol Pharmacol,* **68**, 1656-1668.

Martin D, Thompson MA & Nadler JV (1993) The neuroprotective agent riluzole inhibits release of glutamate and aspartate from slices of hippocampal area CA1. *Eur J Pharmacol,* **250,** 473-476.

Martin-Ruiz CM, Lee M, Perry RH, Baumann M, Court JA & Perry EK (2004) Molecular analysis of nicotinic receptor expression in autism. *Brain Res Mol Brain Res,* **123**, 81-90.

Martina M, Vida I & Jonas P (2000) Distal initiation and active propagation of action potentials in interneuron dendrites. *Science*, **287**, 295-300.

Mazza E, Nunez-Abades PA, Spielmann JM & Cameron WE (1992) Anatomical and electrotonic coupling in developing genioglossal motoneurons of the rat. *Brain Res,* **598,** 127-137.

McClung JR & Goldberg SJ (1999) Organization of motoneurons in the dorsal hypoglossal nucleus that innervate the retrusor muscles of the tongue in the rat. *Anat Rec,* **254**, 222-230.

McClung JR & Goldberg SJ (2000) Functional anatomy of the hypoglossal innervated muscles of the rat tongue: a model for elongation and protrusion of the mammalian tongue. *Anat Rec*, **260**, 378-386.

McGehee DS & Role LW (1996) Presynaptic ionotropic receptors. *Curr Opin Neurobiol*, **6**, 342-349.

Meininger V, Lacomblez L & Salachas F (2000) What has changed with riluzole? *J Neurol,* **247**, 19-22.

Meldrum B & Garthwaite J (1990) Excitatory amino acid neurotoxicits and neurodegenerative disease. *Trends Pharmacol Sc.,* **11,** 379-387.

Merlie JP & Lindstrom J (1983) Assembly in vivo of mouse muscle acetylcholine receptor: identification of an alpha subunit species that may be an assembly intermediate. *Cell*, **34,** 747–757.

Messi ML, Renganathan M, Grigorenko E & Delbono O (1997) Activation of alpha7 nicotinic acetylcholine receptor promotes survival of spinal cord motoneurons. *FEBS Lett,* **411,** 32-38.

Miles GB, Dai Y & Brownstone RM (2005) Mechanisms underlying the early phase of spike frequency adaptation in mouse spinal motoneurones. *J Physiol,* **566,** 519-532.

Millar NS (2003) Assembly and subunit diversity of nicotinic acetylcholine receptors. *Biochem Soc Trans,* **31**, 869-874.

Miller RG, Mitchell JD, Lyon M & Moore DH (2007) Riluzole for amyotrophic lateral sclerosis (ALS)/ motor neuron disease (MND). *Cochrane Database Syst Rev*, **24**, CD001447.

Miltner WH, Braun C, Arnold M, Witte H & Taub E (1999) Coherence of gamma-band EEG activity as a basis for associative learning. *Nature,* **397**, 434-436.

Mizuta I, Ohta M, Ohta K, Nishimura M, Mizuta E & Kuno S (2001) Riluzole stimulates nerve growth factor, brain-derived neurotrophic factor and glial cell line-derived neurotrophic factor synthesis in cultured mouse astrocytes. *Neurosci Lett,* **310**, 117-120.

Mohammadi B, Krampfl K, Moschref H, Dengler R & Bufler J (2001) Interaction of the neuroprotective drug riluzole with $GABA_A$ and glycine receptor channels. *Eur J Pharmacol*, **415,** 135-140.

Mohammadi B, Lang N, Dengler R & Bufler J (2002) Interaction of high concentrations of riluzole with recombinant skeletal muscle sodium channels and adult-type nicotinic receptor channels. *Muscle Nerve,* **26**, 539-545.

Monyer H, Burnashev N, Laurie DJ, Sakmann B & Seeburg PH (1994) Developmental and regional expression in the rat brain and functional properties of four NMDA receptors. *Neuron,* **12,** 529 –540.

Morello JP, Salahpour A, Laperriere A, Bernier V, Arthus MF, Lonergan M, Petaja-Repo U, Angers S, Morin D, Bichet DG & Bouvier M (2000) Pharmacological chaperones rescue cell-surface expression and function of misfolded V2 vasopressin receptor mutants. *J Clin Invest,* **105**, 887–895.

Moritz AT, Newkirk G, Powers RK & Binder MD (2007) Facilitation of Somatic Calcium Channels Can Evoke Prolonged Tail Currents in Rat Hypoglossal Motoneurons. *J Neurophysiol*, **98**, 1042-1047.

Mu X, Azbill RD & Springer JE (2000) Riluzole and methylprednisolone combined treatment improves functional recovery in traumatic spinal cord injury. *J Neurotrauma,* **17**, 773-780.

Murthy VN, Fetz EE. (1996) Oscillatory activity in sensorimotor cortex of awake monkeys: synchronization of local field potentials and relation to behavior. J Neurophysiol., 76(6):3949-67.

Nakamizo T, Kawamata J, Yamashita H, Kanki R, Kihara T, Sawada H, Akaike A & Shimohama S (2005) Stimulation of nicotinic acetylcholine receptors protects motor neurons. *Biochem Biophys Res Commun,* **330**, 1285-1289.

Nashmi R, Dickinson ME, McKinney S, Jareb M, Labarca C, Fraser SE & Lester HA (2003) Assembly of alpha4beta2 nicotinic acetylcholine receptors assessed with functional fluorescently labeled subunits: effects of localization, trafficking, and nicotine-induced upregulation in clonal mammalian cells and in cultured midbrain neurons. *J Neurosci,* **23**, 11554–11567.

Nelson ME, Kuryatov A, Choi CH, Zhou Y & Lindstrom J (2003) Alternate stoichiometries of alpha4beta2 nicotinic acetylcholine receptors. *Mol Pharmacol,* **63**, 332-341.

Nicholls JG, Martin AR & Wallace BG (1992) From Neuron to Brain, 3rd edition. Sunderland, MA Sinauer Associates, p. 279.

Nicoll RA & Malenka RC (1995) Contrasting properties of two forms of long-term potentiation in the hippocampus. *Nature,* **377**, 115–118.

Nistri A, Ostroumov K, Sharifullina E & Taccola G (2006) Tuning and playing a motor rhythm: how metabotropic glutamate receptors orchestrate generation of motor patterns in the mammalian central nervous system. *J Physiol,* **572,** 323-334.

Noh KM, Hwang JY, Shin HC & Koh JY (2000) A novel neuroprotective mechanism of riluzole: direct inhibition of protein kinase C. *Neurobiol Dis,* **7,** 375-783.

Nogradi A, Szabo A, Pinter S, Vrbova G (2007) Delayed riluzole treatment is able to rescue injured rat spinal motoneurons. *Neuroscience,* **144**, 431-438.

Nogradi A & Vrbova G (2001) The effect of riluzole treatment in rats on the survival of injured adult and grafted embryonic motoneurons. *Eur J Neurosci,* **13**, 113-118.

O'Brien JA & Berger AJ (1999) Cotransmission of GABA and glycine to brain stem motoneurons. *J Neurophysiol*, **82**, 1638-1641.

O'Brien JA, Isaacson JS & Berger AJ (1997) NMDA and non-NMDA receptors are co-localized at excitatory synapses of rat hypoglossal motoneurons. *Neurosci Lett*, **227**, 5-8.

Ogilvie MD, Gottschalk A, Anders K, Richter DW & Pack AI (1992) A network model of respiratory rhythmogenesis. *Am J Physiol*, **263**, 962-975.

Onimaru H, Arata A & Homma I (1995) Intrinsic burst generation of preinspiratory neurons in the medulla of brainstem-spinal cord preparations isolated from newborn rats. *Exp Brain Res*, **106**, 57-68.

Ouardouz M & Durand J (1994) Involvement of AMPA receptors in trigeminal post-synaptic potentials recorded in rat abducens motoneurons in vivo. *Eur J Neurosci,* **6**, 1662-1668.

Paarmann I, Frermann D, Keller BU & Hollmann M (2000). Expression of 15 glutamate receptor subunits and various splice variants in tissue slices and single neurons of brainstem nuclei and potential functional implications. *J Neurochem,* **74**, 1335-1345.

Pace RW, Mackay DD, Feldman JL & Del Negro CA (2007, a) Role of persistent sodium current in mouse preBotzinger Complex neurons and respiratory rhythm generation. *J Physiol,* **580**, 485-496.

Pace RW, Mackay DD, Feldman JL & Del Negro CA (2007, b) Inspiratory bursts in the preBotzinger Complex depend on a calcium-activated nonspecific cationic current linked to glutamate receptors. *J Physiol,* **580**, 485-496

Pagnotta SE, Lape R, Quitadamo C & Nistri A (2005) Pre- and postsynaptic modulation of glycinergic and GABAergic transmission by muscarinic receptors on rat hypoglossal motoneurons in vitro. *Neuroscience*, **130,** 783-795.

Palma E, Bertrand S, Binzoni T & Bertrand D (1996) Neuronal nicotinic α7 receptor expressed in Xenopus oocytes presents five putative binding sites for methyllycaconitine. *J Physiol,* **491,** 151-161.

Papke RL, Boulter J, Patrick J & Heinemann S. (1989) Single-channel currents of rat neuronal nicotinic acetylcholine receptors expressed in Xenopus oocytes. *Neuron,* **3**, 589-596.

Paradiso KG & Steinbach JH (2003) Nicotine is highly effective at producing desensitization of rat α4β2 neuronal nicotinic receptors. *J Physiol,* **553**, 857-871.

Peinado A, Yuste R & Katz LC (1993) Extensive dye coupling between rat neocortical neurons during the period of circuit formation. *Neuron*, **10**, 103–114

Pellicciari R, Luneia R, Costantino G, Marinozzi M, Natalini B, Jakobsen P, Kanstrup A, Lombardi G, Moroni F & Thomsen C (1995) 1-Aminoindan-1,5-dicarboxylic acid: a novel antagonist at phospholipase C-linked metabotropic glutamate receptors. *J Med Chem,* **38,** 3717-3719.

Peluffo H, Estevez A, Barbeito L &. Stutzmann JM (1997) Riluzole promotes survival of rat motoneurones in vitro by stimulating trophic activity produced by spinal astrocytes monolayers. *Neurosci Lett,* **228**, 207–211.

Pena F, Parkis MA, Tryba AK & Ramirez JM (2004) Differential contribution of pacemaker properties to the generation of respiratory rhythms during normoxia and hypoxia. *Neuron,* **43**, 105–117.

Pena F & Ramirez JM (2002) Endogenous activation of serotonin-2A receptors is required for respiratory rhythm generation in vitro. *J Neurosci,* **22**, 11055-11064.

Perez-Otano I & Ehlers MD (2005) Homeostatic plasticity and NMDA receptor trafficking. *Trends Neurosci,* **28**, 229-238

Perkins KL & Wong RK (1995) Intracellular QX-314 blocks the hyperpolarization-activated inward current Iq in hippocampal CA1 pyramidal cells. *J Neurophysiol,* **73**, 911-915.

Perry EK, Lee ML, Martin-Ruiz CM, Court JA, Volsen SG, Merrit J, Folly E, Iversen PE, Bauman ML, Perry RH & Wenk GL (2001) Cholinergic activity in autism: abnormalities in the cerebral cortex and basal forebrain. *Am J Psychiatr,* **158**, 1058–1066.

Peterson EL (1983) Generation and coordination of heartbeat timing oscillation in the medicinal leech. I. Oscillation in isolated ganglia. *J Neurophysiol,* **49**, 611-626.

Paterson D & Nordberg A (2000) Neuronal nicotinic receptors in the human brain. *Prog Neurobiol*, **61**, 75-111.

Phelan KD & Gallagher JP (1992) Direct muscarinic and nicotinic receptor-mediated excitation of rat medial vestibular nucleus neurons *in vitro*. *Synapse,* **10**, 349–358.

Phillips HA, Scheffer IE, Berkovic SF, Hollway GE, Sutherland GR & Mulley JC (1995) Localization of a gene for autosomal dominant nocturnal frontal lobe epilepsy to chromosome 20q 13.2. *Nat Genet*, **10**, 117–118.

Picciotto MR, Caldarone BJ, Brunzell DH, Zachariou V, Stevens TR &. King SL (2001) Neuronal nicotinic acetylcholine receptor subunit knockout mice: physiological and behavioral phenotypes and possible clinical implications. *Pharmacology & Therapeutics*, **92,** 89– 108.

Picciotto MR & Corrigall WA (2002) Neuronal systems underlying behaviors related to nicotine addiction: neural circuits and molecular genetics. *J Neurosci,* **22**, 3338-3341.

Picciotto MR, Brunzell DH & Caldarone BJ (2002) Effect of nicotine and nicotinic receptors on anxiety and depression. *Neuroreport,* **13**, 1097–1106.

Poth K, Nutter TJ, Cuevas J, Parker MJ, Adams DJ & Luetje CW (1997) Heterogeneity of nicotinic receptor class and subunit mRNA expression among individual parasympathetic neurons from rat intracardiac ganglia. *J Neurosci,* **17**, 586-596.

Powers RK & Binder MD (2003) Persistent sodium and calcium currents in rat hypoglossal motoneurons. *J Neurophysiol*, **89,** 615-624.

Prakriya M & Mennerick S (2000) Selective Depression of Low–Release Probability Excitatory Synapses by Sodium Channel Blockers. *Neuron*, **26,** 671–682.

Pratt J, Rataud J, Bardot F, Roux M, Blanchard JC, Laduron PM & Stutzmann JM (1992) Neuroprotective actions of riluzole in rodent models of global and focal cerebral ischaemia. *Neurosci Lett*, **140**, 225-230.

Prinz AA, Billimoria CP & Marder E (2003) Alternative to hand-tuning conductance-based models: construction and analysis of databases of model neurons. *J Neurophysiol,* **90**, 3998-4015.

Quik M & Kulak JM (2002) Nicotine and nicotinic receptors; relevance to Parkinson's disease. *Neurotoxicology,* **23**, 581-594.

Quick MW & Lester RA (2002) Desensitization of neuronal nicotinic receptors. *J Neurobiol,* **53**, 457-478.

Quitadamo C, Fabbretti E, Lamanauskas N & Nistri A (2005) Activation and desensitization of neuronal nicotinic receptors modulate glutamatergic transmission on neonatal rat hypoglossal motoneurons. *Eur J Neurosci*, **22**, 2723- 2734.

Radek RJ (1993) Effects of nicotine on cortical high voltage spindles in rats. *Brain Res,* **625**, 23–28

Ramirez JM & Richter DW (1996) The neuronal mechanisms of respiratory rhythm generation. *Curr Opin Neurobiol*, **6**, 817-825.

Ramirez JM, Telgkamp P, Elsen FP, Quellmalz UJ & Richter DW (1997) Respiratory rhythm generation in mammals: synaptic and membrane properties. *Respir Physiol*, **110**, 71-85.

Ramirez JM, Tryba AK & Pena F (2004) Pacemaker neurons and neuronal networks: an integrative view. *Curr Opin Neurobiol*, **14**, 665-674.

Ramirez JM & Viemari JC (2005) Determinants of inspiratory activity. *Respir Physiol Neurobiol,* **147**, 145-157.

Rekling JC, Shao XM & Feldman JL (2000) Electrical coupling and excitatory synaptic transmission between rhythmogenic respiratory neurons in the preBotzinger complex. *J Neurosci,* **20,** RC113.

Richter DW & Spyer KM (2001) Studying rhythmogenesis of breathing: comparison of in vivo and in vitro models. *Trends Neurosci,* **24**, 464-472.

Riekkinen P Jr, Riekkinen M & Sirvio J (1993) Effects of nicotine on neocortical electrical activity in rats. *J Pharmacol Exp Ther,* **267**, 776–784.

Roberts A & Tunstall MJ (1990) Mutual Re-excitation with Post-Inhibitory Rebound: A Simulation Study on the Mechanisms for Locomotor Rhythm Generation in the Spinal Cord of Xenopus Embryos. *Eur J Neurosci,* **2**, 11-23.

Roberts A, Tunstall MJ & Wolf E (1995) Properties of networks controlling locomotion and significance of voltage dependency of NMDA channels: simulation study of rhythm generation sustained by positive feedback. *J Neurophysiol,* **73**, 485-495.

Robinson DM, Peebles KC, Kwok H, Adams BM, Clarke LL, Woollard GA & Funk GD (2002) Prenatal nicotine exposure increases apnoea and reduces nicotinic potentiation of hypoglossal inspiratory output in mice. *J Physiol,* **538,** 957-973.

Rodriguez E, George N, Lachaux JP, Martinerie J, Renault B & Varela FJ (1999) Perception's shadow: long-distance synchronization of human brain activity. *Nature*, **397**, 430-433.

Roerig B, Nelson DA & Katz LC (1997) Fast synaptic signaling by nicotinic acetylcholine and serotonin 5-HT3 receptors in developing visual cortex. *J Neurosci,* **17**, 8353-6832.

Role LW & Berg DK (1996) Nicotinic receptors in the development and modulation of CNS synapses. *Neuron,* **16**, 1077-1085.

Rosenberg MM, Blitzblau RC, Olsen DP & Jacob MH (2002) Regulatory mechanisms that govern nicotinic synapse formation in neurons. *J Neurobiol,* **53,** 542-555.

Rowland LP & Shneider NA (2001) Amyotrophic lateral sclerosis. *N Engl J Med,* **344**, 1688-1700.

Russo RE & Hounsgaard J (1999) Dynamics of intrinsic electrophysiological properties in spinal cord neurones. *Prog Biophys Mol Biol*, **72**, 329-365.

Sallette J, Pons S, Devillers-Thiery A, Soudant M, Prado de Carvalho L, Changeux JP & Corringer PJ (2005) Nicotine upregulates its own receptors through enhanced intracellular maturation. *Neuron,* **46**, 595-607.

Samuel D, Blin O, Dusticier N & Nieoullon A (1992) Effects of riluzole (2-amino-6-trifluoromethoxy benzothiazole) on striatal neurochemical markers in the rat, with special reference to the dopamine, choline, GABA and glutamate synaptosomal high affinity uptake systems. *Fundam Clin Pharmacol.* **6**, 177-184.

Sargent PB (1993) The diversity of neuronal nicotinic acetylcholine receptors. *Annu Rev Neurosci,* **16**, 403-443.

Schools GP, Zhou M & Kimelberg HK (2006) Development of gap junctions in hippocampal astrocytes: evidence that whole cell electrophysiological phenotype is an intrinsic property of the individual cell. *J Neurophysiol,* **96**, 1383-1392.

Schwartz G & Fehlings MG (2002) Secondary injury mechanisms of spinal cord trauma: a novel therapeutic approach for the management of secondary pathophysiology with the sodium channel blocker riluzole. *Prog Brain Res*, **137,** 177-190.

Schwindt P & Crill W (1980) Role of a persistent inward current in motoneuron bursting during spinal seizures. *J Neurophysiol,* **43,** 1296-1318.

Semyanov A & Kullmann DM (2001) Kainate receptor-dependent axonal depolarization and action potential initiation in interneurons. *Nat Neurosci*, **4**, 718-723.

Shah BH & Catt KJ (2004) GPCR-mediated transactivation of RTKs in the CNS: mechanisms and consequences. *Trends Neurosci,* **27**, 48-53.

Shao XM & Feldman JL (1997) Respiratory rhythm generation and synaptic inhibition of expiratory neurons in pre-Botzinger complex: differential roles of glycinergic and GABAergic neural transmission. *J Neurophysiol*, **77**, 1853-1860.

Shao XM & Feldman JL (2000). Acetylcholine modulates respiratory pattern: effects mediated by M_3-like receptors in preBotzinger complex inspiratory neurons. *J Neurophysiol,* **83,** 1243–1252.

Shao XM &Feldman JL (2005) Cholinergic neurotransmission in the preBotzinger Complex modulates excitability of inspiratory neurons and regulates respiratory rhythm. *Neuroscience,* **130**, 1069-1081.

Sharifullina E & Nistri A (2006) Glutamate uptake block triggers deadly rhythmic bursting of neonatal rat hypoglossal motoneurons. *J Physiol*, **572**, 407-423.

Sharifullina E, Ostroumov K & Nistri A (2005) Metabotropic glutamate receptor activity induces a novel oscillatory pattern in neonatal rat hypoglossal motoneurones. *J Physiol*, **563,** 139-159.

Shi WX (2005) Slow oscillatory firing: a major firing pattern of dopamine neurons in the ventral tegmental area. *J Neurophysiol*, **94**, 3516-3522.

Shoop RD, Martone ME, Yamada N, Ellisman MH & Berg DK (1999) Neuronal acetylcholine receptors with α7 subunits are concentrated on somatic spines for synaptic signaling in embryonic chick ciliary ganglia. *J Neurosci,* **19**, 692–704.

Shytle RD, Silver AA, Lukas RJ, Newman MB, Sheehan DV & Sanberg PR (2002, a) Nicotinic acetylcholine receptors as targets for antidepressants. *Mol Psychiatr,* **7**, 525–535.

Shytle RD, Silver AA, Sheehan KH, Sheehan DV & Sanberg PR (2002, b) Neuronal nicotinic receptor inhibition for treating mood disorders: preliminary controlled evidence with mecamylamine. *Depress Anxiety,* **16**, 89–92.

Singer W (1999) Neuronal synchrony: a versatile code for the definition of relations? *Neuron*, **24**, 49-65.

Singer W & Gray CM (1995) Visual feature integration and the temporal correlation hypothesis. *Annu Rev Neurosci*, **18**, 555-586.

Siniscalchi A, Bonci A, Mercuri NB & Bernardi G (1997) Effects of riluzole on rat cortical neurones: an in vitro electrophysiological study. *Br J Pharmacol,* **120,** 225-230.

Siok CL, Rogers JA, Koscis B & Hajos M (2006) Activation of α-7 acetylcholine receptors augments stimulation-induced hippocampal theta oscillation. *Eur J Neurosci*, **23**, 570–574.

Skeberdis VA, Lan J, Opitz T, Zheng X, Bennett MV & Zukin RS (2001) mGluR1-mediated potentiation of NMDA receptors involves a rise in intracellular calcium and activation of protein kinase C. *Neuropharmacology,* **40**, 856-865.

Smith A & Denny M (1990) High-frequency oscillations as indicators of neural control mechanisms in human respiration, mastication, and speech. *J Neurophysiol*, **63,** 745-758.

Smith JC, Ellenberger HH, Ballanyi K, Richter DW & Feldman JL (1991) Pre-Botzinger Complex: a brainstem region that may generate respiratory rhythm in mammals. *Science*, **254**, 726-729.

Smith MM, Lindstrom J & Merlie JP (1987) Formation of the alpha-bungarotoxin binding site and assembly of the nicotinic acetylcholine receptor subunits occur in the endoplasmic reticulum. *J Biol Chem,* **262**, 4367–4376.

Sokoloff AJ (2000) Localization and contractile properties of intrinsic longitudinal motor units of the rat tongue. *J Neurophysiol,* **84**, 827-835.

Sokolova E, Matteoni C & Nistri A (2005) Desensitization of neuronal nicotinic receptors of human neuroblastoma SH-SY5Y cells during short or long exposure to nicotine. *Br J Pharmacol*, **146**, 1087-1095.

Song C, Murray TA, Kimura R, Wakui M, Ellsworth K, Javedan SP, Marxer-Miller S, Lukas RJ & Wu J (2005) Role of alpha7-nicotinic acetylcholine receptors in tetanic stimulation-induced gamma oscillations in rat hippocampal slices. *Neuropharmacology*, **48,** 869–880.

Soteropoulos DS & Baker SN (2006) Cortico-cerebellar coherence during a precision grip task in the monkey. *J Neurophysiol,* **95**, 1194-1206.

Stefani A, Spadoni F & Bernardi G (1997) Differential inhibition by riluzole, lamotrigine, and phenytoin of sodium and calcium currents in cortical neurons: implications for neuroprotective strategies. *Exp Neurol,* **147,** 115-122.

Steriade M (1993) Cholinergic blockage of network- and intrinsically generated slow oscillations promotes waking and REM sleep activity patterns in thalamic and cortical neurons. *Prog Brain Res*, **98**, 345–355.

Steriade M (2006) Grouping of brain rhythms in corticothalamic systems. *Neuroscience,* **137**, 1087-1106.

Steriade M & Timofeev I (2003) Neuronal plasticity in thalamocortical networks during sleep and waking oscillations. *Neuron,* **37**, 563-576.

Stollberg J & Berg DK (1987). Neuronal acetylcholine receptors: fate of surface and internal pools in cell culture. *J Neurosci,* **7**, 1809–1815.

Svensson TH (2000) Dysfunctional brain dopamine systems induced by psychotomimetic NMDA-receptor antagonists and the effects of antipsychotic drugs. *Brain Res Brain Res Rev,* **31**, 320-329.

Tarasiuk A. & Sica AL (1997) Spectral features of central pattern generation in the in vitro brain stem spinal cord preparation of the newborn rat. *Brain Res Bull,* **42,** 105-110.

Tazerart S, Viemari J-C, Darbon P, Vinay L & Brocard F (2007) Contribution of persistent sodium current to locomotor pattern generation in neonatal rats. *J Neurophysiol,* **98**, 613–628.

Thoby-Brisson M & Ramirez JM (2001) Identification of two types of inspiratory pacemaker neurons in the isolated respiratory neural network of mice. *J Neurophysiol,* **86**, 104-112.

Tian GF, Peever JH & Duffin J (1999) Mutual inhibition between Botzinger-complex bulbospinal expiratory neurons detected with cross-correlation in the decerebrate rat. *Exp Brain Res*, **125**, 440-446.

Toth TI, Hughes SW & Crunelli V (1998) Analysis and biophysical interpretation of bistable behaviour in thalamocortical neurons. *Neuroscience*, **87**, 519-523.

Traub RD, Bibbig A, LeBeau FE, Buhl EH & Whittington MA (2004) Cellular mechanisms of neuronal population oscillations in the hippocampus in vitro. *Annu Rev Neurosci,* **27**, 247-278.

Traub RD & Miles R (1995) Pyramidal cell-to-inhibitory cell spike transduction explicable by active dendritic conductances in inhibitory cell. *J Comput Neurosci*, **2**, 291-298.

Traub RD, Whittington MA, Buhl EH, LeBeau FE, Bibbig A, Boyd S, Cross H & Baldeweg T (2001) A possible role for gap junctions in generation of very fast EEG oscillations preceding the onset of, and perhaps initiating, seizures. *Epilepsia*, **42**, 153-170.

Traub RD, Whittington MA, Stanford IM & Jefferys JG (1996) A mechanism for generation of long-range synchronous fast oscillations in the cortex. *Nature*, **383**, 621-624.

Travers JB & Norgren R (1983) Afferent projections to the oral motor nuclei in the rat. *J Comp Neurol,* **220**, 280-298.

Theiss RD, Kuo JJ & Heckman CJ (2007) Persistent inward currents in rat ventral horn neurones. *J Physiol,* **580**, 507-522.

Tribollet E, Bertrand D, Marguerat A & Raggenbass M (2004) Comparative distribution of nicotinic receptor subtypes during development, adulthood and aging: an autoradiographic study in the rat brain. *Neuroscience,* **124**, 405-420.

Tucek S (1978) Acetylcholine synthesis in neurons. Chapman and Hall, London.

Umemiya M & Berger AJ (1995) Inhibition by riluzole of glycinergic postsynaptic currents in rat hypoglossal motoneurones. *Br J Pharmacol,* **116,** 3227-3230.

Unwin N (1995) Acetylcholine receptor channel imaged in the open state. *Nature,* **373**, 37-43.

Vailati S, Moretti M, Longhi R, Rovati GE, Clementi F & Gotti C (2003) Developmental expression of heteromeric nicotinic receptor subtypes in chick retina. *Mol Pharmacol,* **63**, 1329-1337.

van Drongelen W, Koch H, Elsen FP, Lee HC, Mrejeru A, Doren E, Marcuccilli CJ, Hereld M, Stevens RL & Ramirez JM (2006) Role of persistent sodium current in bursting activity of mouse neocortical networks in vitro. *J Neurophysiol,* **96,** 2564-2577.

Viana F, Gibbs L & Berger AJ (1990) Double- and triple-labeling of functionally characterized central neurons projecting to peripheral targets studied in vitro. *Neuroscience,* **38**, 829-841.

Vizi ES & Kiss JP (1998) Neurochemistry and pharmacology of the major hippocampal transmitter systems: synaptic and nonsynaptic interactions. *Hippocampus*, **8**, 566–607.

Wahl F & Stutzmann JM (1999) Neuroprotective effects of riluzole in neurotrauma models: a review. *Acta Neurochir,* **73,** 103-110.

Wanaverbecq N, Semyanov A, Pavlov I, Walker MC & Kullmann DM (2007) Cholinergic axons modulate GABAergic signaling among hippocampal interneurons via postsynaptic alpha 7 nicotinic receptors. *J Neurosci,* **27**, 5683-5693.

Wang F, Gerzanich V, Wells GB, Anand R, Peng X, Keyser K & Lindstrom J (1996) Assembly of human neuronal nicotinic receptor alpha5 subunits with alpha3, beta2, and beta4 subunits. *J Biol Chem,* **271**, 17656-17665.

Wang F, Nelson ME, Kuryatov A, Olale F, Cooper J, Keyser K &. Lindstrom J (1998) Chronic nicotine treatment up-regulates human α3β2 but not α3β4 acetylcholine receptors stably transfected in human embryonic kidney cells. *J Biol Chem,* **273**, 28721–28732.

Wang H & Sun X (2005) Desensitized nicotinic receptors in brain. *Brain Res Brain Res Rev,* **48**, 420-437.

Wang J, Wang X, Irnaten M, Venkatesan P, Evans C, Baxi S & Mendelowitz D (2003) Endogenous acetylcholine and nicotine activation enhances GABAergic and glycinergic inputs to cardiac vagal neurons. *J Neurophysiol,* **89**, 2473-2481.

Weiland S, Bertrand D & Leonard S (2000) Neuronal nicotinic acetylcholine receptors: from the gene to the disease. *Behav Brain Res,* **113,** 43-56.

Westphal RS, Tavalin SJ, Lin JW, Alto NM, Fraser ID, Langeberg LK, Sheng M & Scott JD (1999) Regulation of NMDA receptors by an associated phosphatase-kinase signaling complex. *Science,* **285**, 93-96.

Wikstrom MA & El Manira A (1998) Calcium influx through N- and P/Q-type channels activates apamin-sensitive calcium-dependent potassium channels generating the late after hyperpolarization in lamprey spinal neurons. *Eur J Neurosci,* **10**, 1528-1532.

Williams JH & Kauer JA (1997) Properties of carbachol-induced oscillatory activity in rat hippocampus. *J Neurophysiol*, **78**, 2631–2640.

Williams SR, Toth TI, Turner JP, Hughes SW & Crunelli V (1997) The 'window' component of the low threshold Ca2+ current produces input signal amplification and bistability in cat and rat thalamocortical neurones. *J Physiol*, **505**, 689-705.

Wilson Horch HL & Sargent PB (1995). Perisynaptic surface distribution of multiple classes of nicotinic acetylcholine receptors on neurons in the chicken ciliary ganglion. *J Neurosci,* **15**, 7778–7795.

Wonnacott S (1997) Presynaptic nicotinic ACh receptors. *Trends Neurosci,* **20**, 92-98.

Woolf NJ (1991) Cholinergic systems in mammalian brain and spinal cord. *Prog Neurobiol,* **37**, 475-524.

Wu J, Tang T & Bezprozvanny I (2006) Evaluation of clinically relevant glutamate pathway inhibitors in in vitro model of Huntington's disease. *Neurosci Lett,* **407,** 219-223.

Yang J, Woodhall GL & Jones RS (2006) Tonic facilitation of glutamate release by presynaptic NR2B-containing NMDA receptors is increased in the entorhinal cortex of chronically epileptic rats. *J Neurosci,* **26**, 406-410.

Yvon C, Czarnecki A & Streit JJ (2007) Riluzole-induced oscillations in cultured spinal networks. *J Neurophysiol,* **97**, 3607-3620.

Zago WM, Massey KA & Berg DK (2006) Nicotinic activity stabilizes convergence of nicotinic and GABAergic synapses on filopodia of hippocampal interneurons. *Mol Cell Neurosci,* **31**, 549 –559.

Zaninetti M, Tribollet E, Bertrand D & Raggenbass M (1999) Presence of functional neuronal nicotinic acetylcholine receptors in brainstem motoneurons of the rat. *Eur J Neurosci*, **11**, 2737-2748.

Zhang J & Berg DK (2007) Reversible inhibition of GABAA receptors by alpha7-containing nicotinic receptors on the vertebrate postsynaptic neurons. *J Physiol,* **579**, 753-763.

Zhang L, Zhou FM & Dani JA (2004) Cholinergic drugs for Alzheimer's disease enhance in vitro dopamine release. *Mol Pharmacol*, **66**, 538-544.

Zhang M, Wang YT, Vyas DM, Neuman RS & Bieger D (1993) Nicotinic cholinoceptor-mediated excitatory postsynaptic potentials in rat nucleus ambiguus. *Exp Brain Res,* **96**, 83–88.

Zhong G, Masino MA & Harris-Warrick MR (2007) Persistent Sodium Currents Participate in Fictive Locomotion Generation in Neonatal Mouse Spinal Cord. *J Neurosci,* **27,** 4507– 4518.

Zhu PJ & Chiappinelli VA (1999) Nicotine modulates evoked GABAergic transmission in the brain. *J Neurophysiol,* **82**, 3041-3045.

Zigmond MJ, Bloom FE, Landis SC, Roberts JL & Squire LR (1999) Fundamental Neuroscience. Academic Press, San Diego, CA, USA, p. 243.

Zoli M, Moretti M, Zanardi A, McIntosh JM, Clementi F & Gotti C (2002) Identification of the nicotinic receptor subtypes expressed on dopaminergic terminals in the rat striatum. *J Neurosci,* **22**, 8785-8789.

Zona C, Cavalcanti S, De Sarro G, Siniscalchi A, Marchetti C, Gaetti C, Costa N, Mercuri N & Bernardi G (2002) Kainate-induced currents in rat cortical neurons in culture are modulated by riluzole. *Synapse,* **43**, 244 –251.

Zona C, Siniscalchi A, Mercuri NB & Bernardi G (1998) Riluzole interacts with voltage-activated sodium and potassium currents in cultured rat cortical neurons. *Neuroscience,* **85**, 931–938.

Zwart R & Vijverberg HP (1998) Four pharmacologically distinct subtypes of alpha4beta2 nicotinic acetylcholine receptor expressed in Xenopus laevis oocytes. *Mol Pharmacol,* **54**, 1124-1131.